Design, development and testing of user friendly, light weight and inexpensive artificial limb for trans-femoral amputees

A Thesis Submitted in Partial Fulfillment of the Requirements for the award of the Degree of

DOCTOR OF PHILOSOPHY

by

S. Arun

(Roll No. 126103030)

DEPARTMENT OF MECHANICAL ENGINEERING

INDIAN INSTITUTE OF TECHNOLOGY GUWAHATI

GUWAHATI -781039

June 2016

Department of Mechanical Engineering

Indian Institute of Technology Guwahati

Guwahati-781039, Assam, India

Certificate

It is certified that the work contained in the thesis entitled "**Design, development and testing of user friendly, light weight and inexpensive artificial limb for trans-femoral amputees"** submitted by **Mr. S. Arun (126103030)** to the Indian Institute of Technology Guwahati for the award of degree of Doctor of Philosophy has been carried out under my supervision in the department of mechanical engineering, Indian Institute of Technology Guwahati. This work has not been submitted elsewhere for the award of any other degree or diploma.

Dr. S. Kanagaraj

Associate professor

Department of Mechanical Engineering

Indian Institute of Technology Guwahati

Dedicated to all my

Teachers

Acknowledgement

I would like to express my gratitude to my supervisor Dr. S. Kanagaraj for his constructive discussion, confidence, kindness, and patience with me for all these years. I would also thank my Doctoral committee members Prof. S. K. Dwivedy, Dr. S. Senthilvelan and Prof. G. Pugazhenthi for constantly reviewing the progress of my work with valuable suggestions and to improve the quality of the thesis. I also deeply acknowledge Prof. D. Chakraborty, Prof. P. Mahanta and Prof. A. K. Dass for extending various facilities in the department of mechanical engineering during the tenure of my research work.

I wish to express my sincere thanks to the technical staff of the department of Mechanical engineering and Central instruments facility for their timely help. I am greatly indebted to Dr. Bhaskar Borgohain and Mr. Balaphrang Marbaniang from North Eastern Indira Gandhi Regional Institute of Health and Medical Sciences (NEIGRIHMS), Shillong and Mr. David, from L.G.D HI-TECH Orthotic and Prosthetic Center, Kanyakumari, for helping in carrying out the patient trial after the fixation of the developed knee joint. I also thank the technicians from Tool Room & Training Centre, Amingon, Guwahati for the fabrication of the knee joint in the needy time. I like to show special appreciation to Dr. R. Sangamesh Deepak for clarifying various doubts, while performing the dynamic analysis of the prosthetic knee joint.

The support received from Dr. V Satheeshkumar, Dr. Santhosh, A Muthuraja, Mr. SN Balaji, Dr. RS Basha, Mr. R Someshwaran, Dr. T Kannan, Dr. R Anantharaj, Dr. Subramanian, Mr. Manish Kumar, Mr. Suresh and Mr. R Vinoth kumar at different stages of my work is also acknowledged. I would like to thank my friends Dr. PS Rama

Sreekanth, N Shanmuga Priya, N Naresh Kumar, P Sridhar, R Vignesh Babu, Devarshi Kashyap, Dr. Akash Handique, Avanish Kunwar Verma, P Kishore Kumar, MA Johnney, S. Urmimala, J. Ashirbad, K. Parkavi, VM Danial, G Joshi, SS Sinha, S Hungyo, S Harichandan who made my work memorable. I also express my appreciation to K Jeevananthan, B Hazarika, M Maharana, S Ashwini, M Charan, M Broster and Ashish for their valuable support throughout my work.

I would like to thank my family particularly parents, sister, brother and brother-in-law for supporting me in the completion of this thesis in various ways. I am also thankful to S Ajith, S Abitha Rani and DS Suresh for their well wishes heartily. Their unconditional love and support inspired me to do hard work with dedication. My family has been my strength throughout these years. I especially thank my father, Mr. P. Srinivasan for inspiring for hard work, patience and teaching me Indian culture and philosophy. I don't have words to express thank my mother, S. Poomani for her love and belief without bothering what kind of science I do.

Finally, I express my sincere thanks to all who helped me in whatever form during my stay at IIT Guwahati and successful completion of this thesis.

I gratefully thank the supreme Almighty God, who has showered his/her blessings on me in various ways to make me stand for what I am today.

S. Arun

10th June, 2016 IIT Guwahati

Abstract

The above knee amputation is a surgical interference that severs the thigh segment between the hip and knee joint. Though many prosthetic devices are available in the market, which can able to generate sophisticated and versatile functional joint movements equivalent to that of human lower limb, each one of them has inherent limitations in different aspects. In order to overcome the same, an attempt was made to design and develop a light weight and user friendly artificial limb having improved functionality with affordability. Since, the knee joint imitates flexion-extension of the artificial limb and the socket plays an important role on the performance of prosthetic leg, the work is focused to overcome the limitations of the existing socket and knee joint. The knee joint was designed based on the Grashof's criterion, stance phase stability, extension bias and the maximum flexion angle. The polymeric-passive-polycentric-prosthetic knee joint having the significant advantages over conventional knee joints was developed. The stress analysis was carried out using the finite element technique and the maximum stress concentration was found to be 30 MPa as per Von-Mises theory. The position of knee joint against instantaneous time was confirmed through dynamic analysis. Based on the static and dynamic analysis, the knee joint was fabricated using nylon and it was fixed for 9 trans-femoral amputees. Later, the rehabilitation feedback was obtained from the amputees using different standards. Based on the scoring of different aspects from the rehabilitation studies, it is confirmed that the performance of prosthesis was increased in addition to improved health related quality of life of the patients. Since, the nylon has significant environmental degradation compared to other engineering polymers, the poly (methyl methacrylate) PMMA was selected as a material for the knee joint due to its attractive mechanical properties. In both cases of knee joint and socket, multi walled carbon nanotubes (MWCNT) were selected as a reinforcement in polymer matrix because of their good radical scavenging and reinforcement capability compared to other fillers. The epoxy based sandwich composites along with MWCNT reinforcement were proposed to be used as a material for the socket. The mechanical and thermophysical properties of the composites were evaluated as per ASTM/ISO standards. It was observed from the

experimental results that the flexural modulus, flexural strength, tensile strength, and Young's modulus of 0.25 wt. % of PMMA/MWCNT composite were observed to be increased by 24.1, 26.3, 32.9, and 41.9 %, respectively compared to that of pure PMMA. After 12 months of aging, the tensile strength and Young's modulus of PMMA were reduced by 12.1, and 22 %, respectively, which were limited to 3.8 and 5% by reinforcing 0.25 wt. % MWCNT with PMMA. Based on the comparison of theoretical and experimental results, the modified Halpin-Tsai model and Pukanszky model are suggested to be used to predict the modulus and strength of PMMA/MWCNT composites, respectively, up to 0.25 wt. % of reinforcement. Though the thermal conductivity and thermal diffusivity of epoxy were found to be increased with MWCNT concentration, the mechanical properties of composites were observed to be decreased beyond 0.3 wt. % of reinforcement and thus the same concentration of reinforcement in sandwich composites is suggested to fabricate the socket. The thermal diffusivity and thermal conductivity of 0.3 wt. % MWCNT reinforced sandwich composites were found to be increased by 52 and 29.8 %, respectively, compared to unreinforced sandwich composites, which is expected to decrease the temperature gradient across the thickness of the socket and it led to decrease the metabolic cost of an amputee. The increase in flexural strength of sandwich composites with 0.3 wt. % MWCNT reinforcement was observed to be 11.38 ± 1.5 % for 4-10 layers of stockinet, in comparison to that of unreinforced sandwich composites. It was observed that the increase in mechanical and thermal properties of 0.3 wt. % MWCNT reinforced sandwich composites led to the selection of one-step reduced stockinet layer and it is expected to reduce the metabolic cost of an amputee. It is inferred that the integrated effect of reduction in temperature raise inside the socket and reduction in weight of the socket and knee joint are expected to increase the comfort level of trans-femoral amputees by decreasing their metabolic cost. It is also anticipated that the newly developed light weight, durable and user-friendly knee joint is expected to make huge impact in locomotive disabled people community due to its function, performance, affordability and near sound leg gait pattern.

CONTENTS

List of Figures

Page No.

List of Tables

Page No.

Nomenclature

Symbol	Description
A_1	length of the thigh at full extension
A_2	length of the thigh at mid swing position
A_3	length of the thigh at 90° flexion
B	interfacial bonding constant (B=0 for poor bonding, B=5 for good bonding of MWCNT)
B_1	length of the shank at full extension
B_2	length of the shank at mid swing position
B_3	length of the shank at 90° flexion
C_1	sum of A1 and B1 at full extension
C_2	sum of A2 and B2 at mid swing position
C_3	sum of A3 and B3 at 90° flexion
C_4	constant
C_c	spring index of compression spring
C_m	floor clearance at mid swing position
C_n	floor clearance at 90° flexion
C_t	spring index of tension spring
D_c	mean coil diameter of compression spring
d_c	wire diameter of compression spring
d_{NTo}	outer diameter of nanotube
d_{sp}	diameter of the spring pin
D_t	mean coil diameter of spring of tension spring

d_t	wire diameter of spring of tension spring
e	free length of the extension unit GH
E_c	Young's modulus of composite
E_m	Young's modulus of matrix
E_{NT}	Young's modulus of nanotube,
f	frequency band, 9 GHz,
F_{ak}	axial component of force applied at the knee bolt by the thigh section
F_c	flexural modulus of composite
F_e	Buckling force of the knee joint
F_{er}	extension force applied by the distal limb to hold the knee in extension
F_m	flexural modulus of matrix
F_{NT}	flexural modulus of nanotube,
G	shear modulus of stainless steel
g	acceleration due to gravity
h	Plank's constant, 6.63×10-34 J.s,
H_r	external magnetic field at resonance frequency
I_1	Moment of inertia of the link 1
I_2	Moment of inertia of the link 2
I_3	Moment of inertia of the link 3
I_f	Moment of inertia of the foot
I_p	Moment of inertia of pylon
k	stiffness of the extension unit
K_c	spring stiffness of compression spring
K_t	spring stiffness of tension spring

K_w	Wahl's correction factor
l_0	length of the top link (link 0)
l_1	length of the link 1
l_{1a}	length of the link 1 including pin allowance
l_2	length of the bottom link (link 2)
l_3	length of the link 3
l_{3a}	length of the link 3 including pin allowance
l_a	length of an adapter
l_{ah}	length between A and H
l_{c1}	distance between point D and centre of mass of link 1
l_{c2}	distance between point A and centre of mass of link 2
l_{c3}	distance between point C and centre of mass of link 3
l_{cf}	distance between point A and centre of mass of foot
l_{cp}	distance between point A and centre of mass of pylon
l_{dg}	length between D and G
l_{dh}	length between D and H
l_{dl}	distance between the effective distal end and hip of the patient
l_{fi}	distance between the point f and ICR of the polycentric knee joint
l_{hi}	distance between the point H and I
l_{NT}	length of the nanotube
l_{pa}	length of the pin allowance
l_{sa}	length of spring allowance

l_{spa} length of the spring pin allowance

l_{taf} distance between the T-A line and point f

m_1 mass of the link 1

m_2 mass of the link 2

m_3 mass of the link 3

m_f mass of the foot

m_p mass of the pylon

n_c number of active coils of compression spring

n_t number of active coils of tension spring

r_p radius of the pin

T total kinetic energy of the system

T_A time taken for accelerated exposure in hours

T_N time taken for natural exposure in hours

T_i initial tension of the spring

V_{c1} velocity of the link 1 at its centre of mass

V_{c2} velocity of the link 2 at its centre of mass

V_{c3} velocity of the link 3 at its centre of mass

V_{cf} velocity of the foot at its centre of mass

V_{cp} velocity of the pylon at its centre of mass

V_{NT} volume fraction of nanotube

x_{dg} horizontal length between D and G

x_{dh} horizontal length between D and H

y_1	vertical distance between the point D to the centre of mass of link 1
y_2	vertical distance between the point D to the centre of mass of link 2
y_3	vertical distance between the point C to the centre of mass of link 3
y_{dg}	vertical length between D and G
y_{dh}	vertical length between D and H
y_f	vertical distance between the point D to the centre of mass of foot
y_p	vertical distance between the point D to the centre of mass of pylon
θ	included angle of link 1 with horizontal plane
θ_0	included angle of link 0 with horizontal plane
θ_{c2}	included angle of l_{c2} with horizontal plane
θ_{cf}	included angle of l_{cf} with horizontal plane
θ_{cp}	included angle of l_{cp} with horizontal plane
θ_d	included angle of HDA
θ_g	angle between horizontal and DG
θ_h	angle between horizontal and DH
φ	angle of the link 3 with horizontal
λ	included angle of link 2 with horizontal plane
γ	orientation factor of the nanotube
σ_c	tensile strength of composite
σ_{fc}	flexural strength of composite
σ_{fm}	flexural strength of matrix
σ_m	tensile strength of matrix

τ_i	initial shear strength of the spring
τ_s	shear strength of stainless steel
ω	electron Bhor magneton 9.27×10-24 J/T,
$\dot{\theta}$	velocity of the link 1
$\dot{\lambda}$	velocity of the link 2
$\dot{\varphi}$	velocity of the link 3
$\frac{l_{NT}}{d_{NTo}}$	aspect ratio

Chapter 1

Introduction

Human lower limb is one of the crucial parts in our body to obtain the required functional movements in order to do daily routine activities. The limbs have highly articulated and very complex structures which are able to generate sophisticated and versatile functional joint movements. The above knee amputation is a surgical interference that severs the thigh segment between the knee and hip joints. Accidental or intentional lower limb amputation is one of the major setbacks in the life of a person.

1.1. History of an artificial limb

The usage of leg prosthesis was started during the period of 5000 BC, which was confirmed from the cave-wall paintings, and it was interesting to note that the amputation done due to trauma, frostbite and leprosy carried certificates stating the reason for the loss of limb. Due to psychological pressure, the lower limb amputees preferred to die with the diseased limb, because it was difficult for them to render the previous life style including fitness to work, Friedmann et al. [1972]. Around 1500 BC, the usage of lower limb made of wood was reported in ancient Egypt, which is called as a peg leg. In 484 BC, a Persian soldier, Hegesistratus, was captured by an enemy and imprisoned by encasing in his foot. Later, he escaped by cutting off part of his foot and replaced with a wooden prosthesis, Wilson [1972]. In Peru, the usage of amputated foot was confirmed from 300 BC onwards, Friedmann et al. [1972] and they also reported that the oldest recovered prosthesis was unearthed in a tomb near Capua in 1858, which was from the Samnite wars in 300 BC. The first cup fitted with stump was evident in 50 BC at Peru. A right arm amputated soldier skeleton was unearthed in Rome, which belongs to 23 – 79 AD, where an iron hand to hold the shield was evidenced, Wilson [1972]. During the dark ages (476-1000 AD), a little advancement in prosthesis occurred, where the knight fitted with upper and lower prosthesis for holding the shield and fit in stirrup was noticed, Norton [2007]. Later in 1400,

particularly in Greek and Rome, people started to use iron, copper and wood to develop the prosthesis. This period is also known as rebirth in the history of prosthesis. During the battle of Landshut, Germany in 1508, an upper limb made of springs, leather straps and iron was used by the amputated soldiers, Norton [2007]. He also reported that French army surgeon, Ambroise Paré, who is also called as a father of modern amputation surgery and prosthetic design, developed an above knee prosthesis using leather and iron in 1536.

In 17th century, the wooden pieces and iron were used for making the prosthesis for the patients having the congenital deformity, Putti et al. [1930]. Around 18th century in US, a controlled lower limb prosthesis, known as Anglesey leg, was developed by James Potts, which was later modified by William Selpho and it led to the development of Selpho leg in 1839. Benjamin Palmer modified Selpho leg in 1846 to obtain the natural walking movement. Douglas Bly developed an anatomical leg in 1858, which was considered as one of the most complete and successful inventions ever attained in artificial limbs, Norton [2007]. In 1863, Dubois Parmlee developed an advanced prosthesis with a suction socket, polycentric knee and multi-articulated foot. At the end of US civil war in 1871, James Edward Hanger developed a Hanger limb. Later, Marcel Desoutter, a famous English Aviator, who lost his leg in an aeroplane accident, made aluminium prosthesis in 1912 with the help of his brother Charles. During World War I, Surgeon General of the Army realized that much advancement in the prosthesis field was not attained; hence the formation of the American Orthotic & Prosthetic Association (AOPA) was evolved, Norton [2007]. Later in World War II, veterans were not satisfied with the lack of technology in their devices and demanded improvement in prosthesis. Hence, the US government brokered a deal with military companies to improve the function of prosthetic devices rather than the weapons and it led to the development of advanced prosthetic devices. The development of mechanical knee joint came into light in 1975 and the improvement of the knee joint is still continuing, Campbell et al. [1977]. An improvement in prostheses is continuously being made in 21st century. The devices which are currently available are made of plastic, aluminium alloy and composite materials to provide amputees with better comfort; however the devices are much expensive.

Some of the above discussed history of the development of prostheses is summarized in Table 1.1.

Table1.1 History of the development of prostheses

Year	Prosthesis part	Materials	Reference
5000 BC	Outline of hands drawn on Cave walls	N/A	Friedmann et al. [1972]
1500 BC	Lower limb	Wood (Peg Leg)	
484 BC	Lower limb	N/A	Wilson [1972]
300 BC	Prosthesis foot	N/A	Friedmann et al. [1972]
300 BC	Lower limb prosthesis	Copper and wood	Wilson [1972]
50 BC	Cup shaped prosthesis on stump	N/A	
23-79 AD	Right arm prosthesis	Iron	Norton [2007]
Dark Ages (476-1000) AD	Knight fitted with upper prosthesis to hold a shield and lower prosthesis to fit in stirrup	N/A	
1400	Upper and lower limb prosthesis	Iron, steel, copper and wood	
1508	Right arm Upper limb	Springs, leather straps, iron	
1536	Above knee Prosthesis	Leather, iron	
16th Century	Lower limb prosthesis	iron	Putti et al. [1930]
17th Century	Congenital deformity	Wooden foot and iron pieces	

1800	Controlled lower limb prosthesis (Anglesey leg)	N/A	Norton [2007]
1839	Anglesey leg later developed to Selpho Leg	N/A	
1846	Modified selpho leg to give natural walking movement	N/A	
1858	Anatomical leg	N/A	
1863	Advanced prosthesis with a suction socket, polycentric knee and multi-articulated foot	N/A	
1871	Hanger Limb	N/A	
1912	Advanced lower limb prosthesis	Aluminium alloy	
1975	Mechanical knee joint	Aluminium alloy	Campbell [1977]
2000	Hydraulic and pneumatic based knee joint	Aluminium alloy	Nerlich et al. [2000]
2007	Microprocessor controlled prosthetic knee joint	Aluminium alloy	Au et al. [2007]

1.2. Disability statistics

Based on World disability statistics [2010] (http://www.disabled-world.com/disability/ statistics/), 10 % of the world population has some form of disability and among them, 80 % of the total disabled people has been living in developing countries. As per world population data sheet in 2011, 14.3 % of the total population has some form of disability. The number of disability was reported to be 18.5, 15, 13, 10.9, 10.7, 9.3, 8.3, 7.5, 7.2, 6.3, 5 and 4.7 % of the total population in United Kingdom, Bolivia, Ecuador, Australia, Europe, Asia, Brazil, Argentina, Africa, China, Japan and Uruguay, respectively. Among the total disability, the locomotive disability constituted 10.3 and 2.7 % in UK and Japan, respectively. As per Census bureau reports in 2010, 56.7 million out of 308.7 million people in US has been living with disability

corresponding to 19 % of the total population and among them, 10.8 % of the disabled people noted to be below the poverty line category. The number of locomotive disability was found to be 30.6 million, which is 54 % among the total disability. Based on the above information, the national limb loss information centre reported that the upper extremity amputee (UEA) and lower extremity amputee (LEA) constituted 13 and 87%, respectively, among the total locomotive disability amputation. Out of the LEA, below knee amputee (BKA) and above knee amputee (AKA) constituted 62 and 38 %, respectively, NLLIC staff [2008].

In South-East Asia, the disability range was observed to be 1.5 - 21.3 % of total population, Mont [2007]. The proportion of disabled people in India as per Census 2001 and 2011 is shown in Fig. 1.1. It was observed that 2.13 % of the total population in 2001 constituted the disabled population and it was increased to 2.21 % in 2011, and the locomotive disability was noted to be 20.2 % of total disability in India. In 2011, the number of male and female disability was reported to be 2.41 and 2.01 %, respectively, among the individual category.

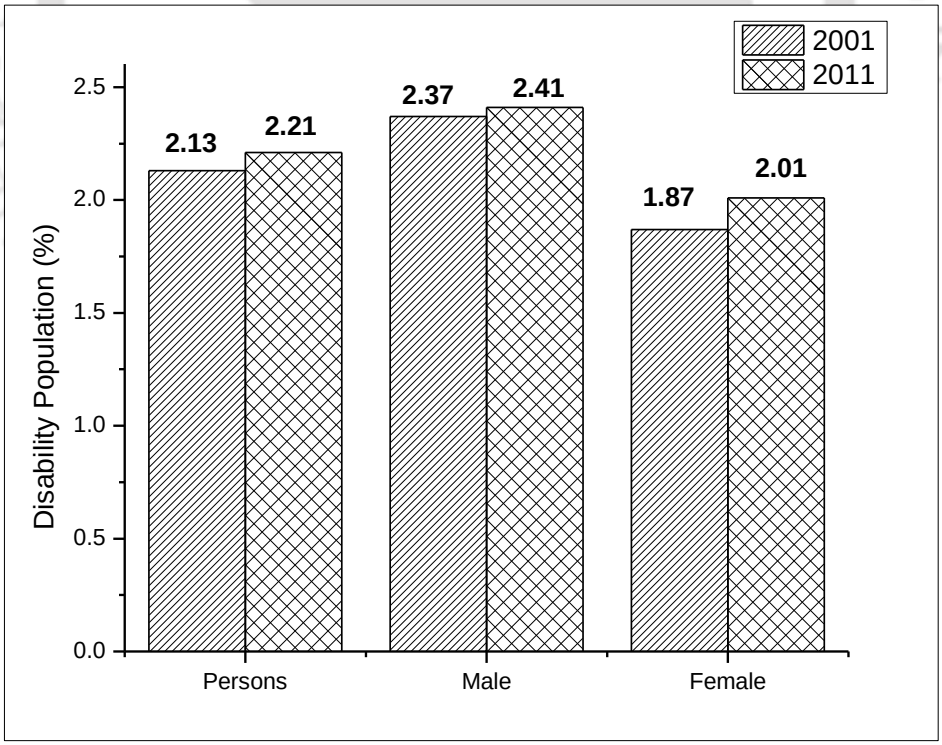

Fig. 1.1 Proportion of disabled people by sex in India: 2001-2011, Census India [2011]

Fig. 1.2 depicts the disabled population by age in India as per Census India 2011 statistics. It was noted that the disabled population was found to be increased with age group due to various reasons. For the age group of more than 60, the number of disabled population was found to be more than the national average of India and it is near about the double in case of 70 years or more and triple in case of 80 and above.

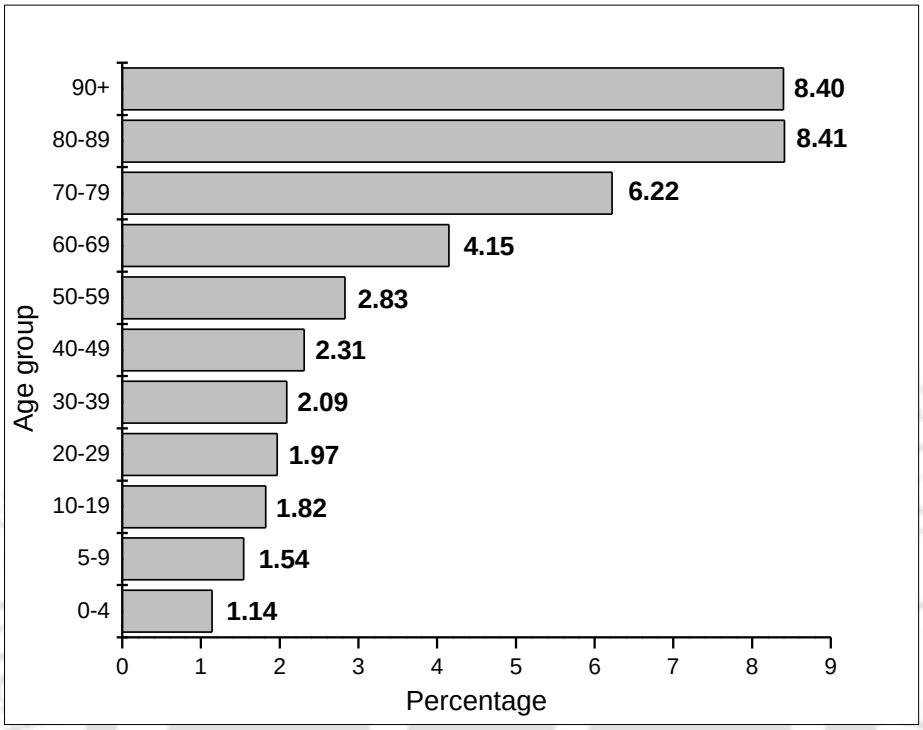

Fig. 1.2 Disabled population by age, Census India [2011]

The disability in percentage of total population and prevalence rate of disability per 1000 population in India are shown in Fig. 1.3. It was observed that the disability in Jammu & Kashmir, Sikkim, Orissa, Maharashtra, Andhra Pradesh, Lakshadweep and Puducherry was found to be above 2.51 % of total popultation, and the respective prevalence rate of disability was found to be 24 and above per 1000 population. It is also noted that the disability was found to be 1.75 % of total population or below in case of Nagaland, Mizoram, Tiripura, Meghayala, Assam, Tamilnadu, Andaman & Nicobar Islands, Chandigarh, Dadra & Nagar Haceli, Daman & Diu and NCT of Delhi, where the disability prevalence rate per 1000 people was observed to be less than 17.

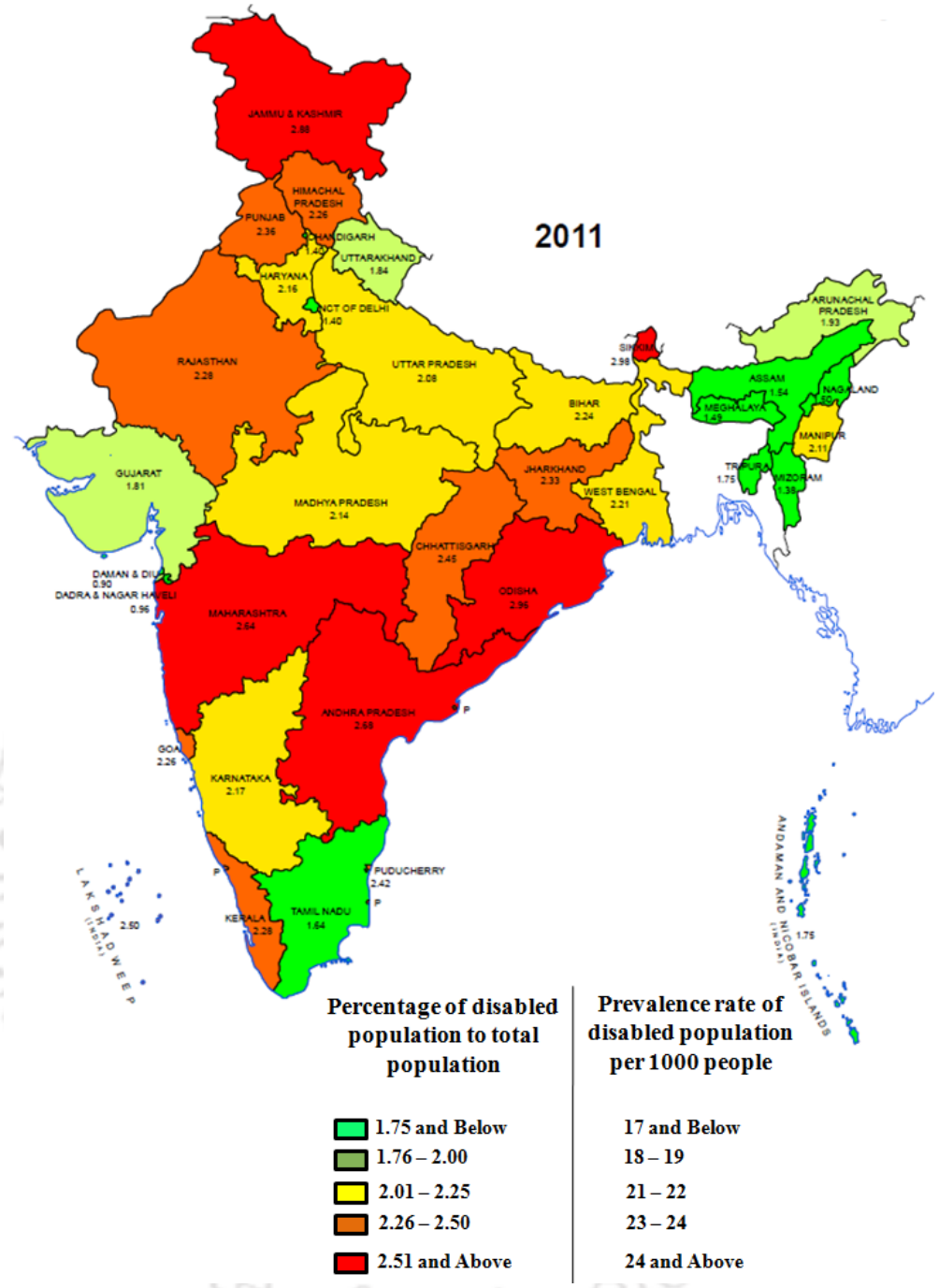

Fig. 1.3 Disability in percentage and prevalence rate of disability per 1000 people in India, Census India [2011]

The proportion of disabled population in India by the type of disability is shown in Fig. 1.4. It was reported that the disability in movement, hearing, seeing, miscellaneous, multiple disability, speech, mental retardation and mental illness was found to be 20.3, 18.9, 18.8, 18.4, 7.9, 7.5, 5.6 and 2.7 %, respectively, among the total disability, where the movement disability was noticed to be more compared to other types of disability.

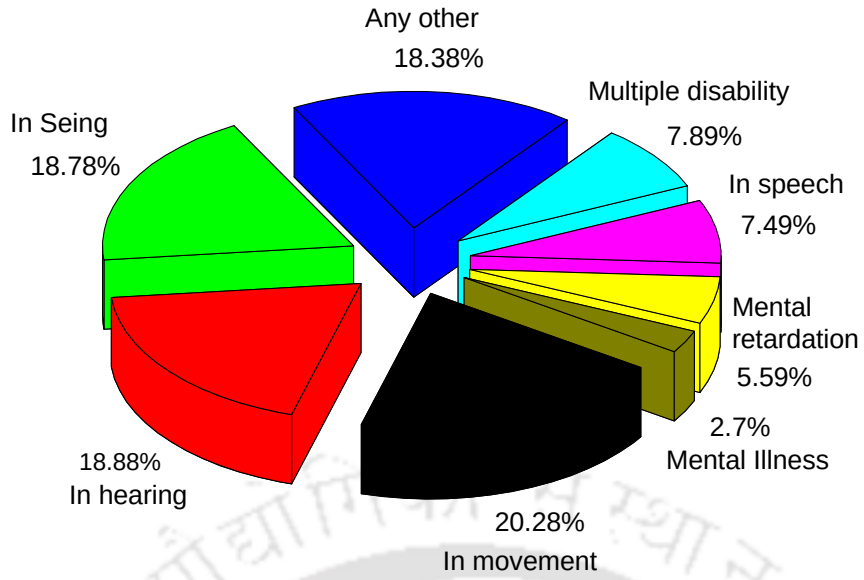

Fig. 1.4 Proportion of disabled population by the type of disability, Census India [2011]

1.3. Types of an artificial lower limb and its major parts

The artificial lower limb is classified into two types:

(i) Trans-femoral lower limb

(ii) Trans-tibial lower limb

The photographic images of trans-femoral and trans-tibial amputee fitted with their respective prosthetic devices are shown in Fig. 1.5. The major parts of the prosthetic devices are socket, knee joint, pylon and foot, which are briefly described here

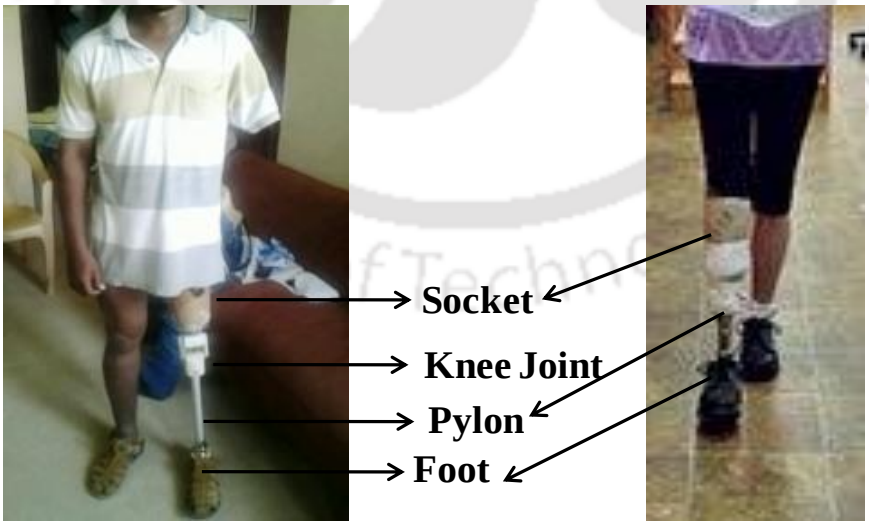

Fig. 1.5 Trans-femoral and trans-tibial amputees,
[http://minnesota.mdnews.com/articles/LocalArticle?id=40135] with prosthesis,

Socket

Socket is the only component which has direct contact with distal end of the stump and it is subjected to impact force, rotational force and shear force, which are expected to occur during the heel strike, stance phase and swing phase, respectively. The accurate fitting of the socket increases the smooth function of the prosthetic leg. Moreover, the socket is also used to judge the pain of an amputee, which in series is connected to different parts of the prosthetic device.

Knee joint

The complexity in replicating the knee mechanism of a human joint is an important task for the better function of the prosthetic leg. Prosthetic knee joint is classified into two types: single axis and polycentric knee joint. Based on the additional supporting device required to get the near sound leg gait pattern, the later is classified into passive, semi-active and active knee joint. The performance of a knee joint depends on the activity level, weight of an amputee and the residual stump length.

Pylon

Pylon transfers the vertical load caused by the weight of an amputee to the floor through a foot. Pylon is a hollow cylinder generally made of an aluminium alloy to reduce its weight.

Foot

Foot is the final component through which the load is effectively transferred to the floor. It is classified into two types: basic prosthetic foot and articulated prosthetic foot. Basic prosthetic foot is categorized into Solid Ankle Cushion Heel (SACH) foot and elastic keel foot. SACH foot is rigid and cannot bend. It consists of a rubber heel wedge and allows a little ankle movement during the initial stance phase of walking. It also provides little lateral movement in mid-stance. It has several heel heights in order to make compatible with different types of shoes. Elastic keel foot is reported to be more flexible than SACH foot. It allows the front part to move based on various walking conditions, but stay stiff and stable during the stance phase. Articulated prosthetic foot is classified into single axis foot, multi axes foot and dynamic response foot. It allows

the motion in one or more planes, quite near to the function of human foot. Single axis foot allows the foot to move up and down and it gives more stability. Multi axes foot allows the foot to move up and down and side to side, which also perform better in uneven surface. Dynamic response foot stores and releases the energy during the walking cycle. It gives a push-off in heel and a balanced gait. It increases the activity level and has split-toe design.

1.4. Problems faced by the prosthetic leg

In plain surfaces, the existing pylon and SACH foot can be used without limiting the functionality of the low activity user. However, the knee joint replicates the flexion-extension of the sound leg and the socket takes care of different forces acting on it. The problems faced by the prosthetic leg are classified into the following:

1.4.1. Problems faced in a knee joint

Above knee amputation is a surgical intervention that involves the removal of lower limb intentionally or accidentally. The lower limbs have a highly articulated and very complex structure which can able to generate sophisticated and versatile functional joint movements. The artificial prosthetic knee joint imitates the function of a human knee to achieve the flexion-extension motion of the above knee amputee. The prosthetic knee joints use various techniques to allow the leg to bend and swing.

Though a significant progress has been made with advanced prosthetic devices such as pneumatic and hydraulic swing-phase control units leading to achieve the highly functional mobility, those devices were bulkier and heavy which neglect the option of using them in children. It was also noticed that the prosthesis was more expensive and difficult to have easy maintenance. In addition, the distance travelled by the amputees to the prosthetic repair centres made them to rethink about the fixation of a prosthetic leg. Further, there are many amputees in India as well as from developing countries can't afford the prosthetic leg due to its cost.

1.4.2. Problems faced in a socket

It is an intermediate part between the residual stump and a man-made knee joint. The performance of the total prosthetic device depends on the socket system and its

inappropriate fixation induces large pain to the amputees. The factors such as friction between the socket interfaces, pressure acting on the stump, shear force and temperature raise in the socket interface can be controlled up to certain extent based on the material used for the socket. As there are many variables, which are listed below, influencing the improved performance of the socket system and the same play an important role for the total prosthetic system, a better approach is required to improve the same.

1.5. Importance of the selected problem

In this modern era, even with the development of advanced technologies, the amputees fitted with prosthetic leg were not satisfied completely. Also, retaining the previous lifestyle of an amputee is still a concern. It was evident from the literature that many amputees rejected the prostheses due to poor performance of the prosthetic devices and satisfaction level. Gailey et al. [2010] reported the reasons for the rejection of the prosthetic devices by the people with unilateral lower-limb amputation occurred during Vietnam War (VW) (1961-1973) and Operation Iraqi Freedom/Operation Enduring Freedom (OIF/OEF) conflict (2000-2008). Among 350 amputees, 178 and 172 patients were from VW and OIF/OEF, respectively, who participated in the survey. The rejection rate of prosthetic knee joints from the lower-limb amputees during VW and OIF/OEF conflict is depicted in Fig. 1.6a and b, respectively. It was observed that the rejection rate of advanced high end prosthetic knee joints was more compared to passive mechanical prosthetic knee joints. The rejection rate of high end devices due to too much fuss, too heavy and battery recharge was 83, 67 and 50 %, respectively in case of Vietnam War amputees, whereas the respective rejection in case of OIF/OEF amputees was found to be 25, 44 and 29 %. However, the rejection rate of passive mechanical knee joint by VW amputees was found to be 51, 46 and 43 % for pain, poor fit and grew out of it, respectively, which was found to be 29, 29 and 19 % in case of OIF/OEF amputees.

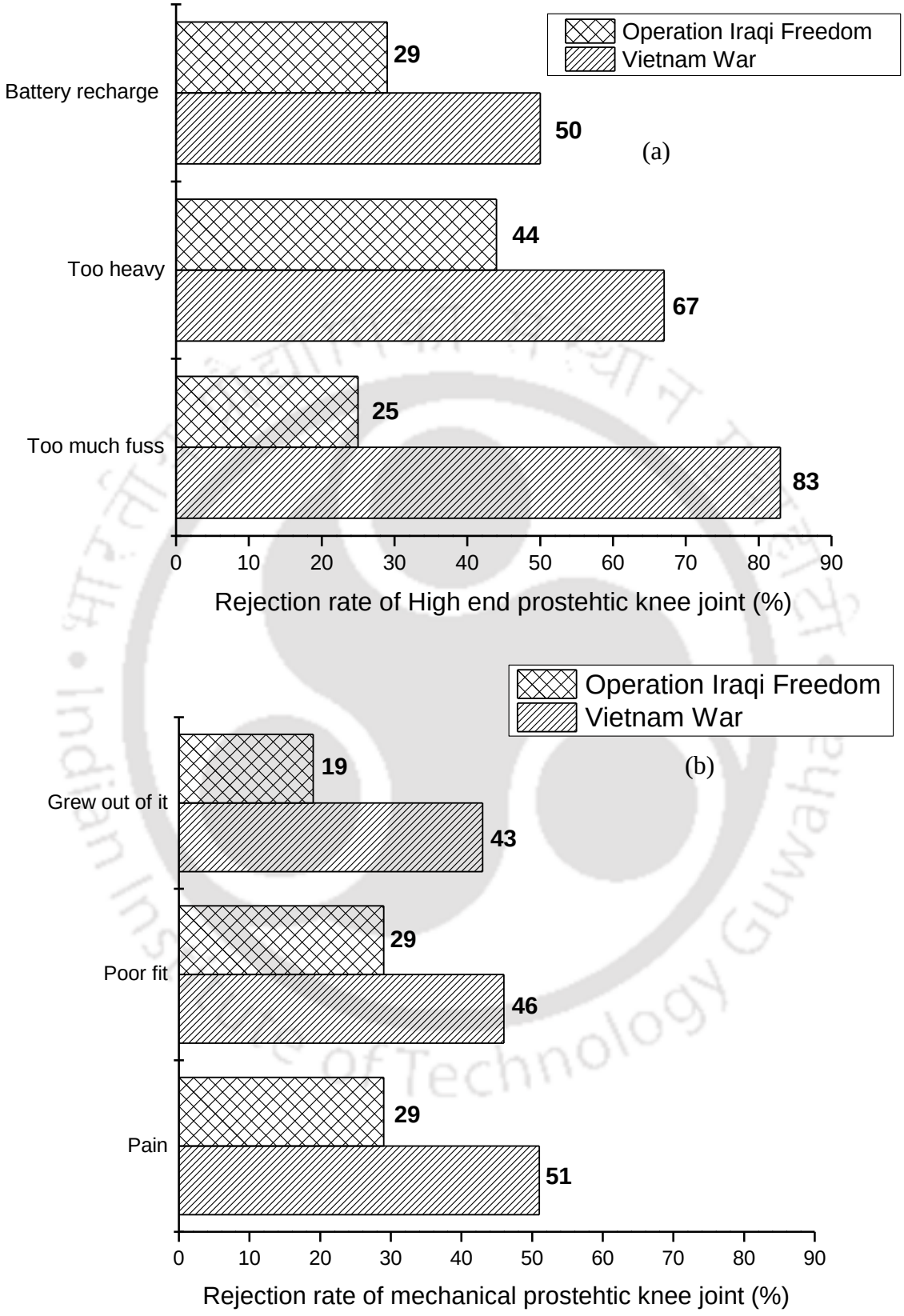

Fig. 1.6 Rejection rate of (a) high-end and (b) mechanical prosthetic knee joint, Gailey et al. [2010]

1.6. Motivation of work

Though the development period of assistive prosthetic devices is time immemorial, it is helped to come out with remarkable achievement including the invention of bionic artificial leg. However, Gailey et al. [2010] reported that the rejection rate of prosthetic leg was found to be high. The top five reasons for the rejection of prosthetic devices are cost, bulkiness, weight, pain and poor fitting. Interestingly, it was noticed that the rejection rate of high-end prosthetic knee joints was found to be 27.2 % more than that of mechanical knee joints. The increase in bulkiness and weight of the high-end prostheses led to increase the metabolic cost of an amputee. As reported by Smith et al. [2013], the metabolic cost of an amputee was increased by 12 %, if there was 100 % mass difference between the intact and the prosthetic leg. It was also noted that the weight of prosthetic knee joint contributed 67 % increase in weight of the prosthetic leg compared to other prosthetic components, (http://fillauer.eu/feet/s-a-c-h-foot). As per Arthur et al. [2001], it was accounted that the raise in 1 °C temperature inside the socket led to increase the metabolic cost of a patient by 10 %.

The total disability in the world was 14.3 % in 2011, whereas it was noted to be 10 % in 2010. Also, the 80 % of the total disability lives in developing countries. In USA, 10 % of the total disability belongs to below poverty line category. It is forecasted that the people living with loss of a limb would be more than double by 2050. The total number of persons with an amputation is expected to increase by at least 47% before 2020, Ziegler-Graham et al. [2008].

It was accounted that the cost of mechanical prosthetic knee joint, swing-phase control, stance control and other advanced mechanical or hydraulic systems starts from $15,000, whereas the computer-assisted devices are in the range of $20,000 to $30,000, McGimpsey et al. [2012]. It is also noted that the cost of a knee joint played a major role in deciding the total cost of the prosthesis, Andrysek et al. [2010]

Though the development of high end prosthetic leg has accomplished a remarkable achievement, the rejection of the same has been considerably increased. As per different statistical data, the greater number of amputees belongs to the developing countries or below poverty line, and thus the affordability of the prosthesis is still a great concern for most of the amputees because of its expensive nature. Moreover, as per forecasting

report, the number of amputees is observed to be increased steadily. Hence, the demands and challenges have kept the research activity still open for providing a permanent solution for the aforementioned problems with an uncompromising quality and increased satisfaction of the amputees. In addition to that the problems faced in a knee joint and socket such as weight, raise in temperature in the residual stump and the continuous change in the dimension of it led to the major rejection of the artificial leg. The above said problems create a huge concern in the biomedical engineering research field. Thus, an attempt is proposed to be made in the direction to develop a user-friendly, lightweight and inexpensive artificial limb for the trans-femoral amputees addressing the present and future challenges faced by them and respective medical care units.

1.7. Organization of thesis

The present thesis is organized into five chapters.

Chapter 1 gives the history of leg prosthesis with an emphasis on trans-femoral prosthesis and its importance. The significance of the selected problem, its causes, necessity and motivation to carry out the present work are also briefly described.

Chapter 2 presents a literature review in the field of design of a knee joint, composite materials proposed to be used for the knee joint, influence on the mechanical properties of composite materials against normal aging under UV rays, antioxidant activity of MWCNT, socket, composite materials in socket and finally the rehabilitation studies during the patient trial. The technical gaps present in the above referred research field were identified and discussed in the closure of literature and the objectives for the present work are framed.

Chapter 3 gives a detailed description of the techniques involved in the sample preparation, characterization of the processed samples for assessing their mechanical properties before and after the environmental aging. Sample preparation for different analytical characterization techniques, instrument specifications and the test methodology are also discussed.

Chapter 4 describes the results and elaborate discussion on the design of a passive polycentric knee joint, dynamic analysis of the knee joint, patient trial and

rehabilitation studies on the developed knee joint, role of MWCNT in enhancing the mechanical properties of knee joint material, the synergy between the matrix and reinforcement in the presence of UV rays during shelf aging, the mechanism and reasoning behind the influence of MWCNT on the aged test samples. Also, it describes the role of MWCNT in increasing the heat transfer and mechanical characteristics of the socket material and the reasons for the enhancement. The sandwich composites with and without MWCNT reinforcement were also characterized and reported.

Chapter 5 presents a gist of the overall work, prominent results obtained and salient findings from the thesis work. A conclusion note and the future direction for the further enhancement of the performance of the developed knee joint and composites are also briefed.

Chapter 2

Literature review

Prosthesis is a device used to replace a missing part of a body. A well-functioned prosthesis has the ability to bring-back independence of an amputee and it may allow the patient to participate in socio-economic activities that would be otherwise impossible. Though amputation is a failure of other reconstructive efforts, it is the start of a new chapter in patient's life, where they need to adjust the limb loss and return to normal life. From the wooden leg to the advanced bionic prosthetic leg, a prosthetic knee joint has undergone a gradual transition in improving its performance to achieve the near sound leg gait pattern. It is noted that the success of the prosthetic devices is influenced by their (i) weight and (ii) bulkiness and (a) affordability and (b) increase in metabolic cost of the patients. This chapter is divided into two sections: (i) critical review of the reports on the various designs of the knee joint to achieve the near sound leg gait pattern in addition to different materials used for the same and (ii) a detailed review on the socket and its limitations. The literature review has been broadly categorized into 4 subsections, which are as follows:

I. Review on prosthetic knee joint
II. Review on socket
III. Rehabilitation studies on leg prosthesis
IV. Gait analysis of the leg prosthesis

2.1 Review on prosthetic knee joint

The knee joint is one of the complex structures among the prosthetic components. It is a load bearing joint, which provides stability and allows mobility of the patients. A review on prosthetic knee joint was made as per the layout shown in Fig. 2.1, where the classification and kinematics of the knee joint, the factors influencing its performance, its experimental and simulation works, selection of materials for the same and its aging degradation against UV radiation were discussed in detail.

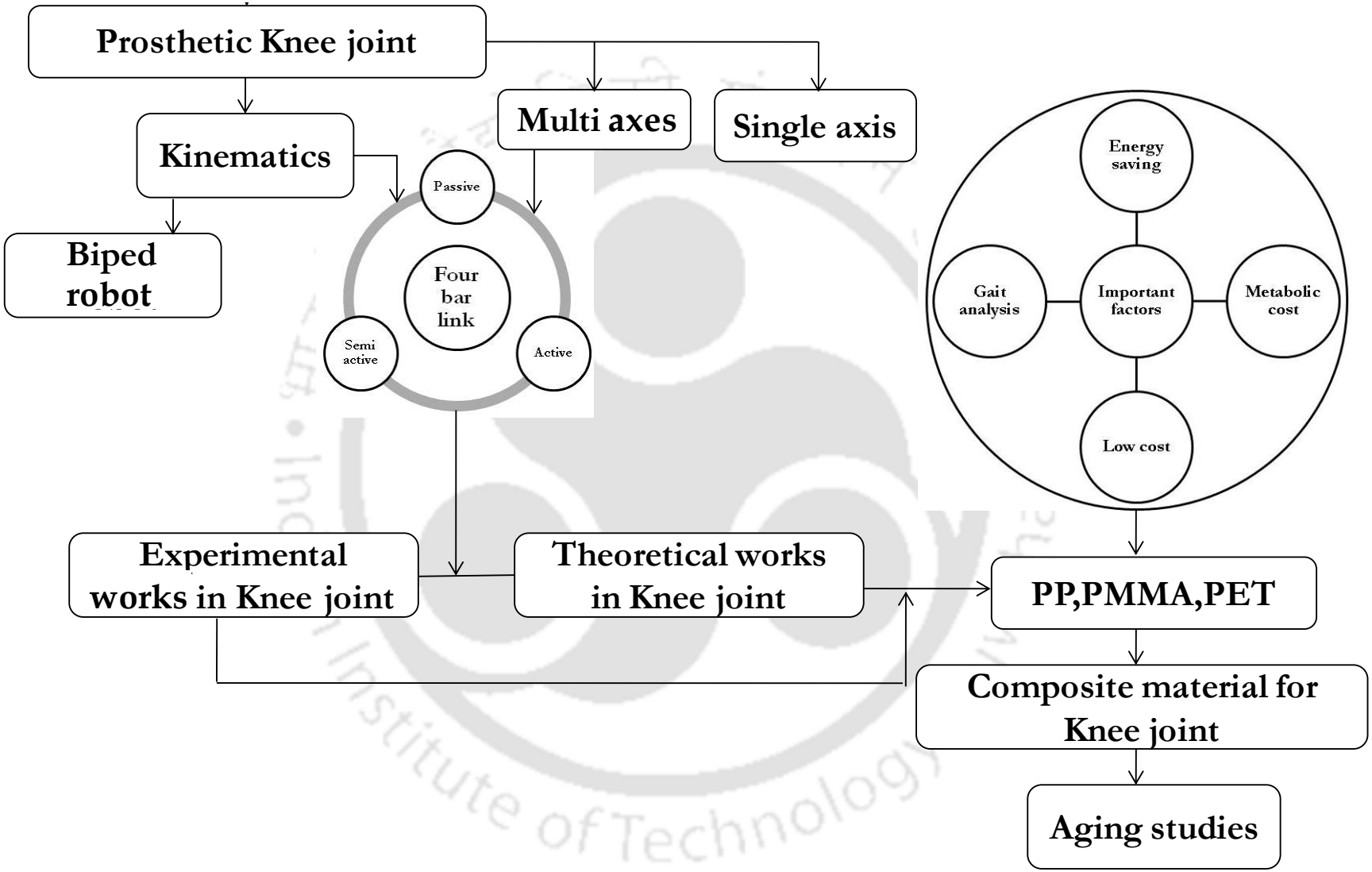

Fig. 2.1 Layout of knee prosthesis discussion

2.1.1 Types of prosthetic knee joint

Prosthesis refers to the replacement of a part of the body such as a leg, an arm, etc. The existing prosthetic knee joint is classified into two types: single axis and multi axes. In a single axis knee joint, the locking mechanism is controlled by an amputee, which is also called as a fixed knee. In case of multi axes knee joint, the locking of the knee is controlled by self weight, which also acts as a brake to prevent the bending of the knee.

2.1.2. Kinematics of the knee joint

The multi axes knee joint composed of multi-links mostly four links is used for knee mechanism, which is also called as a polycentric knee joint. The knee joint angle i.e. angle between the stump and the shank is one of the important parameters for determining the appropriate functioning of the knee joint, Xie et al. [2010]. The initiation of knee movement is achieved using muscular hip moment exerted by the residual stump in a passive polycentric knee joint. The functioning of knee joint is influenced by load line, instantaneous centre of rotation (ICR), ground reaction force (GRF) and the braking moment generated. The hip extension moment gives the forward floor reaction and the hip flexion moment contributes the backward floor reaction by varying the load line, Thorn et al. [2009]. The stability of the knee joint was evaluated using its alpha and beta stability, Greene et al. [1983], where the alpha value is posterior to the Trochanter-knee-Ankle line (T-A line). The T-A line is drawn through the ankle via centre of the pylon. In case of beta value, it should be increased to reduce the knee buckling force. Radcliffe [1994a] defined a common region called zone of voluntary stability, where ICR falls for the stability of the mechanism during the heel-contact and push-off of the prosthesis. The reduction in the hip muscular contraction for knee stabilization is called as under-stabilized knee. An amputee may not have the ability for hip muscular extension eg. insufficient muscular contraction for knee stabilization or he may not be in a position to utilize his energy due to various reasons, then the knee mechanism is required to be stabilized automatically, which can be accomplished by an active knee joint using microprocessor control, hydraulic actuators or pneumatic actuators. Asano et al. [2011] studied the kinematics of knee joint along with ICR of four-bar mechanism, where the hip moment and minimum energy required to initiate the knee mechanism were evaluated. Andrysek et al. [2005]

determined the stability of the knee joint with respect to GRF. The questionnaires study indicated that the decrease in zone of instability increased the stability of the knee joint during the stance phase. Xie et al. [2009] optimized the link length based on the selective constraints such as ICR, link length and knee joint angle. Thorn et al. [2009] compared the stability of swing phase control by 3-valve hydraulic system (Total knee 2000) and Rotary hydraulic system (3R80). It was observed that the total knee 2000 has the higher degree of overall stability than the 3R80 model. Jing et al. [2010] optimized the transmission angle, which is the acute angle between the coupler and the follower, with different constraints to improve the effective force transmission of the knee mechanism. Xie et al. [2010] studied the effective use of GRF in achieving the stability of the knee joint. The necessity of the gap between foot and ground was also evaluated to avoid the collision. It was observed that many patients tilted their body towards support leg side or drew an arc in horizontal plane during the swing phase to achieve the stability.

2.1.3 Classification of the knee joint

The knee joints are classified into three types based on the actuation of the knee mechanism: active knee joint, semi-active knee joint and passive mechanical knee joint, which are described below in detail.

2.1.3.1 Active knee joint

Kalanovic et al. [2000] used the feedback-error learning neural network to find the inverse dynamics of the trans-femoral prosthesis, where the relation for the minimum energy consumption was derived. Tan et al. [2007] used Proportional-Integral-Derivative (PID) controller designed by Immune Genetic Algorithm with Elitism (IGEA) called as IGAEPID controller for the improved functioning of the intelligent leg prosthesis. Villalpando et al. [2008] observed that the main reason for the implementation of active knee joint was to minimize the metabolic energy consumption. Delis et al. [2009] used a myoelectric knee angle estimation algorithm to control the trans-femoral prosthesis, where the maintenance of the prosthetic leg was observed to be difficult. Varol et al. [2010] developed a control architecture and intent recognition approach for the supervisory control of the powered lower limb prosthesis.

Joshi et al. [2011] utilized an Adaptive Neuro-Fuzzy Inference System (ANFIS) to control the lateral knee angle for different walking speed, where the knee angle trajectory was also derived from the ANFIS control system. Duvinage et al. [2011] proposed a Programmable Central Pattern Generator (PCPG) algorithm, which generated an output signal to control the actuation of prosthesis to move in a smooth way. Zhang et al. [2012] used a Cyper-Physical Systems to control the artificial leg based on neuron signals, which gave intended movement for the amputee. Peng et al. [2012] used fuzzy control for the automatic movement of the prosthesis with respect to gait cycle, where the four-bar link was actuated by means of a pneumatic cylinder. Dabiri et al. [2013] developed a powered prosthetic knee joint inspired from the musculoskeletal system. It was observed from the gait trials that the developed artificial muscles were similar to the electromyography (EMG) of biological knee muscles. Pfeifer et al. [2015] developed an angle dependent biomimetic trans-femoral prosthesis, where the torque and stiffness varied with the knee angle and the concept is still under pilot stage.

2.1.3.2 Semi-active knee joint

Kim et al. [2001] made a magneto-rheological (MR) damper based prosthetic knee joint, which showed good performance only in the swing phase. Yokogushi et al. [2004] developed a prototype of semi-active knee joint. The biomechanical parameters such as stance duration, knee flexion angle and hip flexion angle were studied at different cadence (rhythm of person's walk) of 88, 96 and 104 step/min. It was observed that there was no significant difference in biomechanical parameters for the different cadences. Zhang et al. [2010] developed a semi-active knee joint using a closed-loop position servo control system for the powered prosthesis in a human leg. However, the device was found to be heavy.

2.1.3.3 Passive knee joint

Radcliffe [1977] suggested to manufacture an inexpensive and light-weight prosthesis to reduce the metabolic cost of an amputee. Cummings [1996] described that the high end prosthetic components were found to be more complex, less durable, bulky and heavy, which are unsuitable for pediatric amputees. It was also suggested that the

prosthetic components were required to have the following features in order to increase their acceptability: inexpensive, light weight, aesthetically acceptable, good durability, easy maintenance, locally producible at large scale, psychologically acceptable and reduced environmental degradation. Andrysek [2010] reported that the high end prosthetic knee joints made of hydraulic and pneumatic dampers were more expensive and it was inaccessible for the people residing in under-resourced part of the world compared to passive knee joints. It was also reported that the high end prosthetic components were costly to repair and maintain. Furse et al. [2011] reported that maintenance of the knee joint in addition to its cost and the distance travelled to the prosthetic repair centers forced the amputees to think about having the prosthetic knee joint. Failure of the high end prosthetic knee joints and leakage in the hydraulic and the pneumatic knee joints led to critical situation of the amputees and proceeded to lose their confidence level on the devices.

During the last few decades, there were many developments in passive prosthetic knee joint. Campbell et al. [1977] used the braking control and shock absorbing device in the prosthesis to achieve the normal gait cycle and avoid the terminal impact, respectively. Thompson et al. [1978] introduced a pivot pawl arrangement for the locking system by the weight bearing configuration. However, the arrangement lost its function with time. Thompson et al. [1984] designed an automatic lock in the knee joint based on the weight of an amputee. Nevertheless, the durability of the automatic lock system is still a concern. Martel et al. [1985] used a spring damper system, which acted as an extension bias during the swing phase to take care of the terminal impact and minimize the impact on the residual stump. Still, the normal walking gait cycle was not achieved. Gramnas et al. [2004] used a holder for locking the knee joint during the full extension and got released during the swing phase. But, the groove in the holder failed after continuous usage. Andrysek et al. [2006] achieved the stance phase control by means of a latch for holding the knee joint during the full extension. It was observed that the lock was activated during load transmission through the knee joint and got relieved when the load was released. However, the controlled activation for holding the knee was not obtained. Wild et al. [2006] achieved the extension bias using an elastic cable, though the durability of the cable was a great concern. Grafinger et al. [2009] developed a knee

joint with four links to achieve the natural gait cycle. Nonetheless, the extension bias was not added in the design feature. Velez et al. [2010] used a brake disc to activate the knee stabilization in the passive polycentric knee joint. Still, the system was difficult to reach the stabilization. Oddsson et al. [2010] used the spring system in the knee joint, which helped in giving the cushioning effect and bias during the swing phase. Lang et al. [2013] developed a load activated stabilizing knee joint, including an activated lock for restricting the flexion motion while standing.

The above literature discussed various features in the passive polycentric knee joint including stance phase control, controlled bending of the knee joint, extension bias, polymer knee joint and the spring damper system to take care the terminal impact. However, the technology for the stance phase control failed due to its continuous usage. Many trials with resilience devices, compression springs and two-spring system have been proposed in a passive polycentric knee joint to achieve the extension bias. However, obtaining the near sound leg gait pattern in a prosthetic knee joint is still a great concern.

2.1.4. Important parameters in the knee joint

The important parameters of the knee joint for its satisfactory function are the gait analysis of it and the metabolic cost of an amputee.

2.1.4.1 Gait analysis of the knee joint

Kapti et al. [2006] used the gait cycle of the prosthesis to describe the complex activity of walking. The knee extension in stance phase and free knee motion in swing phase were calculated by Yakimovich et al. [2006] using the knee flexion resistance and it was reported that the peak value of knee joint moment was observed to be 65 Nm at the knee flexion angle of 40°. Lambrecht et al. [2009] studied the hip hike, a phenomenon where the patient's pelvis abducts the thigh, in order to keep the artificial foot off the ground. The torque generated by the hip during the swing phase was reduced by adding power to the knee, which helped in climbing the stairs and ramps. Masouros et al. [2010] reported that the stance phase occurred for the first 60% of the gait cycle and the remaining 40% contributed to the swing phase of the normal knee joint.

Dumas et at. [2015] determined the effect of rehabilitation program and prosthetic fitting in trans-femoral amputees using the gait parameters, which was used to generate a stabilizing strategy. Guirao et al. [2015] evaluated the walking abilities of the trans-femoral amputees with a distal weight bearing implant through gait parameters. Shirota et al. [2015] developed recovering strategies using the gait parameters to avoid trips in trans-femoral amputees. Raggi et al. [2006] developed an inertial sensor based gait analysis technique, which is portable and less expensive. It was confirmed that the developed gait analysis was comparable with the patient-specific gold standard gait. Tura et al. [2010] assessed the gait symmetry and regularity in trans-femoral amputees by single accelerometer method. It is confirmed from the above discussion that the inertial sensor method for gait evaluation will provide added advantage because of its portable and affordable nature.

2.1.4.2 Metabolic cost of an amputee

Au et al. [2009] used powered prosthesis for analyzing the metabolic cost of an amputee, where a 14 % reduction was observed in comparison to that of conventional prosthesis. Waters et al. [2010] calculated the energy cost by two ways: the amount of oxygen consumed per minute and the amount of oxygen consumed per meter walk, where no significant difference between them was observed. Unal et al. [2010] reported that the knee absorbed certain amount of energy during flexion and gave back the same for its extension during the stance phase. Behrens et al. [2011] observed that an amputee consumed 60% additional metabolic energy to compensate the lack of lost muscles. It was observed that the knee joint acted as an energy absorber and an ankle joint performed as an energy generator. It was also found that the energy generated by an ankle joint during the push-off was roughly equal to the total energy absorbed by the knee at all intervals.

2.1.5 Dynamic analysis of the knee joint

The gait pattern of a human walking cycle is one of the most important parameters for the lower extremity amputee. Mark et al. [1992] used Euler-Lagrangian equation along with energy approach for the dynamic analysis of the links used in robotics system. Tang [2006] discussed the minimal coordinate for obtaining the dynamic equation of

the four-bar mechanism. Faramand et al. [2006] reported that the mathematical modeling can be effectively used to study the dynamic characteristics of the lower limb. Several theoretical models were proposed to derive the equation of motion of the knee joint during the swing phase and stance phase, Shandiz et al. [2009].

2.1.6 Simulation analysis of the knee joint

Guo et al. [2009] simulated the knee joint using FEM, where the flexion boundary conditions for the heel strike, mid stance and toe-off of the human knee were set at 5.5, 15.5 and 3.5°, respectively, and they reported the maximum stress of 21 MPa at the medial part of the knee during the toe-off condition. Omasta et al. [2012] noted that the experimental strain in pylon during bending and tension condition was observed to be 270 and 60 μm/m, respectively, which were about 25% deviation in comparison to that of theoretical strain. The peak stress of 216 MPa was observed in the toe-off condition on the posterior adjusting screw.

2.2. Materials used for the knee joint

The main factor deciding the appropriate functioning of the knee joint is the strength of the material used for the same. Currently used metals and their alloys are heavy and more expensive limiting their applications. Because of the light weight along with attractive characteristics, polymers and their composites are the best candidates to replace the existing materials. Polypropylene (PP), Polyethylene terephthalate (PET), Poly(methyl methacrylate) (PMMA) are the most commonly used low cost polymers having the excellent mechanical properties.

2.2.1. Polymer based composites

Ash et al. [2002] reinforced PP and PMMA with carbon nano fibers (CNF). The PP showed a significant enhancement of mechanical properties up to 15 wt. % of CNF reinforcement beyond which the properties were found to be decreased. It was also observed that the PMMA composites showed the highest enhancement of mechanical properties compared to other polymer composites for the same concentration of reinforcement. Zeng et al. [2004] reported that the tensile modulus of 5 wt. % PMMA/CNF composite was found to be increased by 50 % in comparison to that of virgin polymer. Serbetci et al. [2004] studied the mechanical, thermal and biological

properties of PMMA having various concentration of Hydroxyapatite (HA). The optimum value of HA was found to be 14.3 wt. %, where the fatigue life of the composite was found to be increased significantly. Kotha et al. [2006] evaluated the mechanical properties of PMMA reinforced with short Titanium fiber. The fracture toughness of composites was found to be increased by 30 % by the addition of 3 vol. % of fiber. Lopes et al. [2009] evaluated the mechanical properties of bioactive glass ($3CaO\text{-}P_2O_5\text{–}MgO\text{–}SiO_2$) reinforced PMMA. The composites having 0, 30, 40 and 50 wt. % of bio-active glass were prepared by melt mixing technique. The maximum flexural strength and the elastic modulus of composite were obtained at 30 wt. % of bio-active glass in PMMA. Kane et al. [2010] compared the fatigue life of PMMA reinforced with straight and variable diameter Zirconia fibers (VDF). The composites were prepared with 5, 10, 15, and 20 vol. % of the filler material using vacuum mixing technique. The optimum concentration of reinforcement for maximum fatigue life was found to be 10 vol. % of filler. Moreover, the VDF reinforced composites had higher fatigue life in comparison to straight fiber reinforced composites.

Since the fiber reinforced plastics (FRP) and micron particle reinforced polymers failed to achieve the required properties, the polymers reinforced by nanofillers were evolved. Variety of nanofillers including Ti nanotubes, silica clay, organoclay, Zirconium nanotubes and multi walled carbon nanotubes (MWCNT) are available to enhance the properties of the polymer. Zeng et al. [2004] used various filler materials including chopped carbon fiber (CCF), MWCNT and CNF in PMMA by melt compounding technique. It was found that the MWCNT had significant effect in PMMA with an increase of creep resistance. Wang et al. [2006] reinforced PMMA using layered double hydroxides (LDH). The Young's modulus of PMMA composite was found to be increased by 38 and 80 % for the reinforcement of 3 and 5 wt. % of LDH, respectively, compared to that of pure polymer. Fu et al. [2006] reported that the mechanical properties of PMMA/nanoclay composites such as elastic modulus, tensile strength and strain at fracture were found to be increased by 25, 54 and 97 %, respectively at 0.5 wt. % of nanoclay. Tanoğlu et al. [2007] prepared the PMMA nanocomposites with organo-montmorillonite (OMMT). The results confirmed that the reinforcement of 1 wt. % of OMMT led to increase both tensile stress and Young's

modulus by 90 %. Etienne et al. [2007] studied the thermal and mechanical properties of PMMA/silica nanocomposites. It was observed that the maximum enhancement of storage modulus for 3 wt. % of silica reinforced nanocomposites was found to be 40 % compared to pure PMMA. Unnikrishnan et al. [2011] reported that the tensile strength and stiffness of 0.1 wt. % of PMMA/MWCNT composites prepared by an injection moulding process were found to be increased by 15 and 17.5 %, respectively. Logakis et al. [2011] prepared the composites using melt mixing technique and confirmed the homogeneous dispersion of MWCNT in PMMA using the electrical percolation technique, where the threshold limit was found to be 0.5 wt. % of MWCNT. Pat et al. [2012] observed that the MWCNT functionalized using acid treatment gave the better enhancement of mechanical properties of PET, where the tensile strength and Young's modulus of 0.5 wt. % PET/MWCNT composites were found to be increased by 47.5 and 2.5 %, respectively compared to pure PET. Jindal et al. [2015] evaluated the mechanical properties of PMMA/MWCNT composites and it was observed that the 5 wt. % of MWCNT reinforcement increased the hardness and modulus of PMMA by 44 and 27 %, respectively compared to virgin polymer.

2.2.2 Degradation of a polymer

Degradation of a polymer is an important issue as it leads to the loss of its properties and reduced longevity of polymer based products. The polymer degradation is classified into photo-oxidative degradation, thermal degradation, ozone-induced degradation, mechano-chemical degradation, catalytic degradation and biodegradation. The effect of photo-oxidative degradation is the most influencing degradation of the polymers subjected to environmental conditions compared to other types of degradation. The lifetime of the polymeric products used in an environmental condition is reduced by the radiation of Ultraviolet (UV) and visible light rays. The damaging effects were influenced from the cleavage of C-C, C-O and C-H bonds and the change in molecular weight of the polymer after the UV exposure, Singh et al. [2008a].

2.2.3 UV rays induced degradation of a polymer

Ceaykara et al. [1999] performed the UV radiation on PMMA by keeping the samples 10 cm away from the mercury light source at room temperature. The chain scission of an ester side group of PMMA was confirmed by Fourier transform infrared spectroscopy (FTIR). It was observed that the tensile strength of PMMA was found to be reduced by 51 % after the radiation. Eve et al. [2009] analyzed the effect of UV radiation dose up to 10 J/cm^2 on the degradation behavior of PMMA. The tensile strength of PMMA was found to be reduced by 46 % at 10 J/cm^2 of radiation compared to pristine polymers. Littlejohn et al. [2009] studied the degradation of an acrylic material by ASTM G173 standard. The samples were exposed to 343 nm UV radiation for 4 hours and 24 hours, where a significant reduction of transmittance loss of the radiated sample was observed in both short and long exposure. Darowicki et al. [2010] studied the effect of UV radiation of 200-280 nm wavelength for 500 hrs on PMMA thin film, which induced the polymer degradation along with initiation of micro cracks. The roughness of PMMA film was found to be increased by 62.4 % for the UV radiated sample compared to unradiated specimen. Al-mashhadan et al. [2011] evaluated the degradation of PMMA doped with 6.7 % of methyl orange. The influence of UV rays of 300 nm wavelength for 10-40 hr on PMMA was studied and found that the doping acted as a chain scission inhibitor for preventing the degradation of a polymer.

2.2.4 Nanofiller and MWCNT as a chain scission inhibitor

Rosa et al. [2005] confirmed the defects generated on the test specimen due to UV radiation by the morphological analysis confirming the presence of micro-cracks. Zhao et al. [2006] studied the usage of ZnO and UV stabilizers in PP to study the effect of UV radiation on the properties of polymer composites. It was found that the nanosized ZnO exhibited better screening of the UV light in PP composites compared to pure polymer and UV stabilizer blended PP. The reduction of tensile strength of pure PP after 600 hrs of UV radiation was found to be 33.3 %, whereas the 3 wt. % reinforced ZnO showed the reduction by 15.8 % only. Li et al. [2008] evaluated the natural photo-degradation of PP reinforced with SiO_2 and $CaCO_3$, 3 wt. % each, up to 88 days based on the crystallinity of the composites. Though the crystallinity of PP was found to be reduced by 5.3 % with UV radiation, SiO_2 and $CaCO_3$ reinforced PP showed the

improvement of crystallinity by 10.8 and 9.1 %, respectively, compared to virgin sample after aging. Grigoriadou et al. [2010] studied the effect of 2.5 wt. % of MWCNT pristine, modified montmorillonite, and SiO_2 nanoparticles as a reinforcement in high density polyethylene (HDPE) to reduce the effect of UV radiation, where the sample was exposed to 280 nm wavelength UV rays for 100 hrs. It was observed that the MWCNT reinforcement restricted the degradation of Young's modulus, tensile strength and elongation by 42, 50 and 93 %, respectively, compared to pure HDPE, where the MWCNT acted as a best nanofiller to restrict the UV rays induced degradation compared to other tested nanofillers. Asmatulu et al. [2011] observed that the coating thickness of pure epoxy was reduced by 24 % after 16 days of UV radiation, whereas it was reduced by 7 % in case of 2 wt. % of MWCNT reinforced composites and it was concluded that MWCNT reinforcement restricted the UV rays induced degradation of the polymer. Petersen et al. [2014] observed that the reinforcement of 3.5 wt. % of MWCNT retarded the photo-degradation of epoxy matrix and it is expected to increase the longevity of the polymer composites.

2.3 Socket

The socket is the interfacing component between the residual stump and prosthetic knee joint. A famous French military surgeon Ambroise Pare invented many devices to fit the missing limbs, but, most of the devices were found to be not satisfactory by the amputees. Burgess et al. [1960] proposed a cushioning socket system, which was wider in order to distribute the weight bearing of the human. After 1960, various socket design with different materials evolved to achieve the problems faced in this field. However, an inadequate length of the stump and tissue ulcerations led to the limited usage of conventional prosthesis, and an amputee was forced to depend on the crutches and wheel chairs, Hynd et al. [2000].

Fig. 2.2 shows the layout of the socket discussion starting from the manufacturing of the mould to the recent developments in socket materials including nanocomposites, which are discussed below in detail. In addition, the performance of the socket was analyzed based on the material related factors and personality factors.

2.3.1 Manufacturing of a socket

2.3.1.1 Types of manufacturing technique

The socket was manufactured by two methods: traditional method and CAD/CAM method. The traditional method starts from the manual measurement of the residual stump along with preparation of negative plaster cast, positive plaster model and the lamination of a socket by the reinforcement techniques. In case of CAD/CAM method, the measurements were captured and modified to have the positive model. The CAD/CAM model uses reverse engineering, virtual prototyping, simulation and rapid prototyping for the better development of the design process of a socket, Vannier et al. [1997].

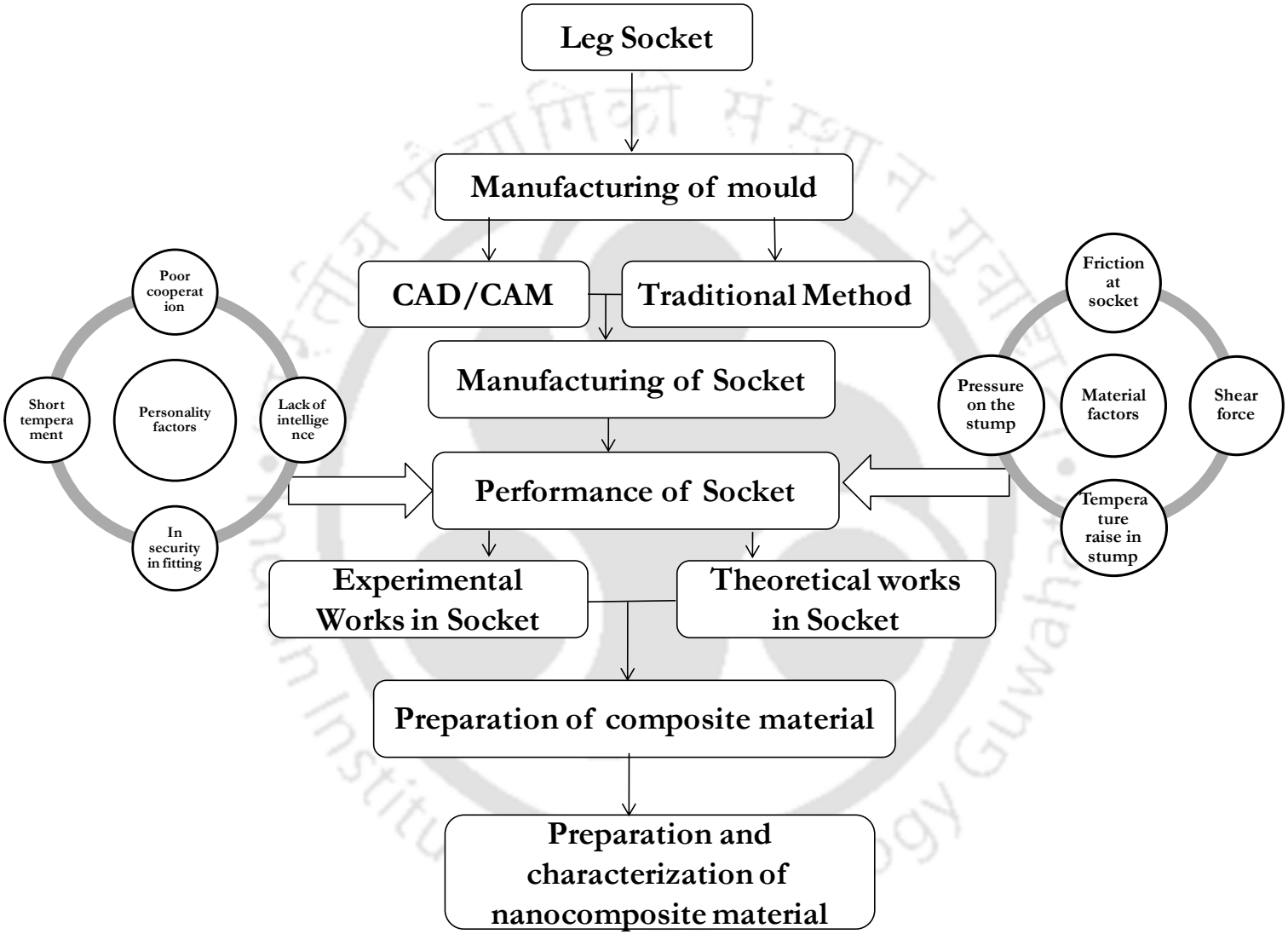

Fig. 2.2 Layout of the socket discussion

Sanders et al. [2007] proposed a way for quantifying the manufacturing of a socket by measuring the specific errors in socket shape quality. In the existing traditional methods, quantifying the specific errors and further modification of the measured values are difficult, rather, it would be easy and convenient in CAD/CAM method. Computer-Aided Socket Design (CASD) software was used for further modification of the data and the positive mould was made using the computer-controlled milling machine. It was observed that the time required for making the socket using CAD/CAM method was comparatively lower than that of the traditional method. The shape obtained from CAD/CAM model and the traditional method was compared and it was revealed that the socket manufactured by CAD/CAM method showed consistent error. Sanders et al. [2012] concluded that the surface normal angle error and radial error confirmed the poor quality of the socket manufactured by CAD/CAM method. In addition, some of the sockets with undersize and oversize led to the unacceptable manufacturing method of a socket by CAD/CAM. Gerschutz et al. [2012a] used CAD/CAM method to manufacture a positive mould of the particular shank and confirmed that the quality of the socket produced was lower than the socket produced by the traditional method. Based on the above discussion, it was decided to follow the traditional method to manufacture a patient specific socket.

Gerschutz et al. [2011] reported that the socket made of thermoplastic polymer and thermoset polymer was called as moulded socket and laminated socket, respectively. In a moulded socket, there are different fabrication methods: blister forming, machine-pulled, and drape. The blister forming includes the manually pulling of oven-heated thermoplastic sheet over the plaster positive model oriented from distal to proximal. Once the pulling was completed, vacuum was created over the model leading to uneven thickness of the socket. The machine-pulled method uses automatic machines to pull the thermoplastic materials over the preformed bell-shaped mould, where the socket having the uniform thickness is obtained. In the drape method, the oven-heated thermoplastic sheet is manually draped over the positive model. In case of laminated socket, the shape of the positive mould is replicated by the thermoset resin. The laminated sockets have the advantages of uniform thickness, and good mechanical strength compared to the moulded socket. Gerschutz et al. [2012b] observed that the

laminated socket provided uniform compressive strength, Young's modulus and easy fabrication compared to the moulded socket. Hence, the laminated socket method has been used as an effective method for making the socket.

2.3.1.2 Fitting

In addition to the fabrication techniques as discussed above, the fitting of the socket is also one of the major factors. Two fitting techniques are used: conventional belt method and suction socket. The conventional belt method includes the fitting of a socket with the help of a belt around the hip. The suction socket is generally used because of its inherent accurate fixing capability compared to belt fitting technique. Thus, it is used for more than 75% of trans-femoral amputees, Haddan et al. [1954].

It is observed from the above discussion that the fabrication technique under traditional method and suction fitting were found to be the best way for the manufacturing and fitting of a socket, respectively.

2.3.2 Factors influencing the function of a socket

The following factors are expected to influence the efficiency of the socket, Arthur et al. [2001].

1. Personality factors
2. General physical factors
3. Stump characteristics
4. Social and economic consideration
5. Friction between the socket interfaces
6. Pressure acting on the stump
7. Temperature raise in the socket interface

The personality factors, which include short temperament, lack of intelligence, insecurity in fitting and poor cooperation of the patient, caused the failure of a socket. Other causes for the socket failure include general physical factors such as skin trouble, overweight, circulatory difficulties, general weakness and allergy to the socket materials. Though the above said factors cannot be fully decided by the researchers, the common factors such as friction at the socket-skin-socks interface, pressure acting on

the stump, shear force and temperature raise in the socket-skin-socks interface can be controlled up to certain extent based on the materials used for the socket.

2.3.2.1 Slippage of the socket system

Vannier et al. [1997] confirmed the quality of fit and the slippage of a socket using a marker made on the residual limb. Cochrane et al. [2001] analyzed the slippage of the socket using the skin markers with respect to the socket. It was found that the maximum slippage of 151 and 19 mm was found in case of fast-stop and step-down condition, respectively. The slippage can be reduced by increasing the coefficient of friction (COF) between the stump-liner and the liner-socket interface, which minimized the movement of two interfaces. Arthur et al. [2001] observed that the friction increased the shear stress at the socket-sock interface leading to tissue distortion and the skin abrasion. On contrary, the friction at the skin surface supported the ambulatory load and gave appropriate suspension to the prosthesis. Sanders et al. [2007] studied the compressive stiffness of the material used for the socket system and the COF at different interfaces. It was observed that the COF at sock-socket interface was found to be higher than that of skin-sock interface leading to slippage of the socket system.

2.3.2.2 Heat transfer in a socket system

An increase of temperature and moisture within the socket create skin maceration leading to bacterial invasion. The natural heat dissipation mechanism of the socket reduces the skin diseases. Pain created by pulling-off the liner and the wrinkling of liner and socks during the function of the knee are the important factors for the inappropriate functioning of the socket, Cochrane et al. [2001]. It was found that the conductive heat transfer through the layers of a socket was limited due to its low thermal conductivity. The accumulation of heat inside the socket led to raise the temperature and it was found that the temperature raise of 1°C led to increase the metabolic cost of the cells by 10 %, Arthur et al. [2001]. Klute et al. [2007] studied the quality of life and the side effect of the prosthesis due to raise in stump-skin interface temperature, which led to thermal discomfort in hot and humid conditions. It was also observed that the thermal conductivity of the liner and socket material varied from 0.085 to 0.266 W/mK and 0.148-0.150 W/mK, respectively. The existing socket system

acts as a physical barrier by blocking the heat transfer between the stump and the surroundings.

2.3.2.3 Pressure distribution in a socket system

Zhang et al. [1998] developed a setup to measure the pressure and bi-axial shear stresses at the body-support interface. The maximum peak pressure was measured to be 320 kPa in the popliteal area (hollow at the back of the knee) and the maximum shear stress was found to be 61 kPa over the medial tibia area (middle of the knee). Arthur et al. [2001] reviewed the biomechanics of the socket with pressure and friction related phenomenon at the socket-sock interface. It was observed from the studies that the slippage was induced by loose fit of the socket, whereas very tight fit led to increase the interfacial pressure. Jia et al. [2005] predicted the socket-sock interfacial pressure during walking, which was observed to be high on the residual limb during the stance phase. Ogawa et al. [2008] developed a magneto-rheological (MR) filled socket, which can vary its hardness and the volume based on the user's requirement. The different size and viscosity of MR fluid filled bags were fixed on the inner side of the socket to vary the socket properties. Wolf et al. [2009] found that the pressure at the stump was influenced by the knee movements during walking condition and the highest peak pressure was found at incline ascent position compared to level walking. Colombo et al. [2010] studied the pressure distribution in the socket, biomechanical behavior of the socket-sock interface and the optimization of the socket shape using FEM. It was observed that the peak pressure of 12.5 kPa was observed in the mid-surface of socket-sock interface. Papaioannou et al. [2010] observed that the socket was found to cause internal limb pain, discomfort and skin ulcers due to excessive pressure and shear force developed within the socket.

2.3.3 Materials used for the socket system

Currently, thermoplastics and thermoset plastics were used to make the sockets. In case of thermoset polymers, epoxy, polyester and polyurethane resin were used. Thermoplastics such as polymethyl methacrylate (PMMA), polyethelene teraphthalate (PET), poly propylene (PP) and Derlin $(CH_2O)_n$ were used for the same. Current et al. [1999] prepared a socket from the acrylic, epoxy and polyester based composites. The

reinforcement materials used in their study were stockinet fabric, E-glass, aramid, nylon and carbon fiber and it was reported that the epoxy resin was preferred because of its low cost combined with required mechanical properties and availability.

2.3.3.1 Fiber reinforced composites for the socket system

Hitchen et al. [1995] studied the mechanical properties of various length of carbon fiber reinforced epoxy composites. It was observed that the fatigue life of the composites was independent of fiber length for 20 vol. % of fiber reinforcement. However, the tensile strength and Young's modulus of 15 mm length fibre reinforced polymer (FRP) composites were found to be increased by 44.1 and 18.9 %, respectively compared to that of FRP composites having 1mm fiber length. Deng et al. [1999] studied the tensile and flexural properties of round, peanut and oval shaped fiber reinforced epoxy composites. It was observed that the round shaped fibers showed the enhancement of flexural strength and Young's modulus by 6.8 and 22 %, respectively, compared to oval shaped fibers. Zhao et al. [2000] studied the mechanical properties of water-sized (2500 filaments/bundle), Epoxy-saline and methacryl-silane treated glass fiber-epoxy composites. It was observed that the tensile strength and ultimate strain of 32.5 vol. % methacryl-silane treated fibre reinforced composites were found to be enhanced by 57.8 and 60 %, respectively compared to water-sized FRP composites. Taylor [2005] evaluated the reinforced plastics with textile pre-form material and woven fabrics to provide required strength and durability. Irawan et al. [2011] developed the socket made of ramie fiber reinforced epoxy composites. The tensile strength of 66 wt. % fibre reinforced composites was found to be increased by 28.4 and 38.7 % compared to ramie and glass fiber reinforced polyester composites, respectively. Dong et al. [2013] reported the flexural strength of hybrid composites made of glass and carbon fiber laminates. The overall hybrid effect of fiber was achieved, when both glass and carbon fiber combined volume fraction was 70 %. It was observed that the flexural strength of hybrid composites was found to be increased by 16.6 and 42.6 % compared to that of individual carbon and glass fibre configuration, respectively. The maximum strength of hybrid composites was observed, when the combination of 30 vol. % of carbon and 50 vol. % of glass fiber were used to prepare the same.

2.3.3.2 Epoxy nanocomposites

The usage of nanoparticles as a reinforcement in the polymer matrix is increased enormously to achieve the desired properties. Among all the available fillers, multi walled carbon nanotubes (MWCNT) were paid a lot of attention because of their attractive mechanical, thermal and electrical properties, Florian et al. [2005]. High aspect ratio of MWCNT along with its specific surface area of 1300 m^2/g helped to have the effective stress transfer from the matrix, Peigney et al. [2001]. To increase the desired properties of epoxy/MWCNT nanocomposites, the homogenous dispersion of the MWCNT must be ensured, which gives good interaction between the matrix and the reinforcement, Kim et al. [2009]. Wichmann et al. [2006] observed that the laminates prepared with the reinforcement of carbon nanotubes exhibited a relatively high electrical conductivity, mechanical and thermal properties at very low filler content than the fumed silica and carbon black.

2.3.3.3 Influence of different types of functionalization of CNT on epoxy

Abdalla et al. [2008] studied the effect of carboxyl and fluorine modified MWCNT on the curing behavior of epoxy. It was confirmed that the carboxyl functionalization of MWCNT increased the compatibility with epoxy by forming the stronger interface. Gojny et al. [2004] reported that the functionalization of MWCNT increased the interfacial interaction between the polymer and MWCNT. From the above studies, it was confirmed that the functionalization of MWCNT was one of the important factors to improve the properties of composites. Theodore et al. [2011] investigated the effect of functionalization on the enhancement of mechanical properties with the reinforcement of 1 wt. % MWCNT. It was found that the flexural strength and flexural modulus of MWCNT-COOH nanocomposites were increased by 25.5 and 54.8 %, respectively, compared to that of nanocomposites prepared using the unmodified MWCNT. The epoxy/MWCNT nanocomposites were found to carry the maximum stress compared to that of neat epoxy. The order of enhancement of mechanical properties of epoxy nanocomposites was as follows: neat epoxy, unmodified MWCNT, fluorine attached MWCNT and carboxyl attached MWCNT. The enhancement of mechanical properties of carboxyl group attached MWCNT reinforced composites was due to strong

interfacial bonding strength between the epoxy and MWCNT compared to epoxy reinforced with fluorine or unmodified MWCNT.

Lee et al. [2010a] examined the tensile strength and fracture toughness of epoxy/MWCNT nanocomposites after sea water absorption. Two different types of functionalization technique such as oxidized MWCNT and silanized MWCNT were followed and it was observed that the composites prepared with silanized MWCNT showed the enhanced mechanical properties compared to unmodified and oxidized MWCNT. It was also observed that the nanocomposites prepared with 0.1 wt. % silanized MWCNT showed the enhancement of tensile strength, Young's modulus, and fracture toughness by 21.1, 16.3, and 7.5 %, respectively, compared to nanocomposites prepared with unmodified MWCNT after sea water absorption.

2.3.3.4 Dispersion of CNT

Suárez et al. [2013] used batch mode and time controlled mode for evaluating the dispersion of MWCNT in epoxy resin. Though the time controlled mode of dispersion showed a 4.5 % enhancement of Young's modulus, the tensile strength of the composites was observed to be decreased by 2.5 % compared to that of batch mode based composites at 0.25 wt. % MWCNT. Villoria et al. [2006] studied the purification and dispersion of single walled carbon nanotubes (SWNT) in epoxy by two different curing cycles. The nanocomposites having 0.1 wt. % SWNT cured for 48 hr at room temperature followed by 24 hr at 60°C showed the enhancement of tensile strength by 31.7 % compared to that of the sample cured at room temperature for 24 hr followed by 4 hr at 60°C. Moniruzzaman et al. [2006a] developed a method to achieve the homogeneous dispersion of SWNT in the epoxy. It was observed that the improvement of flexural strength and flexural modulus of 0.05 wt. % epoxy/SWNT composites was observed to be 10 and 17 %, respectively, compared to that of pure epoxy. Park et al. [2008] investigated the influence of different dispersion solvents for mixing MWCNT with epoxy resin using electrical resistivity technique. It was observed that the turbidity was observed to be high for all types of solvent up to 60 min. and the dispersion stability was found to be decreased with time. It is confirmed that the acetone was found to be the best solvent to prepare the homogeneous dispersion of MWCNT compared to other solvents such as ethanol, 2-propanal and water.

Park et al. [2012a] studied the change in electrical resistance of MWCNT dispersed resin in acetone against the dispersion time, where the settling of MWCNT was observed during the initial stage and then the formation of its agglomeration was noted. Further dispersion of MWCNT decreased the electrical resistance of the solution and it became stable after 6 hr. The low resistance at later stage is related to high electrical conductivity of the MWCNT dispersed resin solution and confirmed the high contact points among the MWCNT networks.

2.3.3.5 Mechanical properties of Epoxy/CNT

Li et al. [2004] studied the epoxy/MWCNT nanocomposites along with co-polymer of 0.03 wt. % epoxy as a dispersant for strengthening. The Young's modulus and fracture stress of 0.3 wt. % nanocomposites were found to be increased by 50 and 20 %, respectively in comparison to that of pure epoxy. Zhao et al. [2006] observed that the modulus and flexural strength of epoxy were increased by 110.7 % at 0.4 wt. % MWCNT and 28.3 % at 0.3 wt. % MWCNT reinforcement, respectively. Wang et al. [2008] observed that the tensile strength and Young's modulus of 7 wt. % of SWNT reinforcement in epoxy were found to be increased by 55.7 and 45.5 %, respectively compared to pure epoxy. Yu et al. [2008] reported that the fracture toughness of 1 and 3 wt. % MWCNT reinforced epoxy was increased by 1.29 and 1.62 times, respectively, and the corresponding fatigue life was enhanced by 9.3 and 10.5 times for the same MWCNT concentration. Montazeri et al. [2011] observed that the rigidity and tensile modulus of the epoxy nanocomposites were increased but the cross linking density was decreased with an increase of MWCNT concentration. The tensile strength and Young's modulus of 2 wt. % nanocomposites were increased by 17 and 23 %, respectively compared to pure epoxy. Starkova et al. [2012] prepared epoxy/MWCNT nanocomposites and it was observed that the tensile strength of 0.3 wt. % MWCNT in epoxy was increased by 10.5 %. Srikanth et al. [2012] studied the tensile and flexural strength of the nanocomposites prepared with 0.5 wt. % MWCNT and the respective improvement was observed to be 10.4 and 15.3 % compared to pure epoxy.

The enhancement of mechanical properties of the epoxy/CNT nanocomposites obtained from different sources is shown in Table 1 and it is observed that the mechanical properties of epoxy were found to be increased significantly for less than 1

wt. % of MWCNT reinforcement. In case of SWNT reinforced composites, the same effect was observed for less than 0.1 wt. %. In general, the reinforcement of carbon nanotubes in epoxy enhanced its mechanical properties.

Table 2.1 Enhancement of mechanical properties of Epoxy/CNT composites

Author	MWCNT wt. %	SWNT wt. %	Properties	% Enhancement
Theodore et al. [2011]	1		Flexural strength	25.5
			Flexural modulus	54.8
Moniruzzaman et al. [2006a]		0.05	Flexural strength	10
			Flexural modulus	17
Srikanth et al. [2012]	0.5		Flexural strength	15.3
Zhao et al. [2006]	0.3		Flexural strength	28.3
	0.4		Young's modulus	110.7
Wang et al. [2008]		7	Tensile strength	55.7
			Young's modulus	45.5
Lee et al. [2010a]	0.1		Tensile strength	21.1
			Young's modulus	16.3
			Fracture toughness	7.5
Suárez et al. [2013]	0.25		Young's modulus	4.5
Villoria et al. [2006]		0.1	Tensile strength	31.7
			Young's modulus	1.32
Starkova et al. [2012]	0.3		Tensile strength	10.5
			Young's modulus	1.1
Srikanth et al. [2012]	0.5		Tensile strength	10.4
Montazeri et al. [2011]	2		Tensile strength	17
			Young's modulus	23
Li et al. [2004]	0.3		Young's modulus	50
			Fracture stress	20
Yu et al. [2008]	3		Fracture toughness	62
			Fatigue life	105

2.3.3.6 Thermal properties of Epoxy/CNT

Puglia et al. [2003] studied the curing reaction of epoxy/SWNT nanocomposites by thermal analysis, where a shift in crystallization peak was observed for the nanocomposites compared to that of pure epoxy. Guadagno et al. [2009] found that the presence of MWCNT accelerated the curing process and the increase in glass transition temperature confirmed the homogeneous dispersion of MWCNT with epoxy. Chapartegui et al. [2010] observed the physical network between the epoxy and MWCNT beyond 0.13 wt. % of reinforcement. Cui et al. [2011] observed that the enhancement of thermal conductivity of epoxy/MWCNT was found to be 51 and 67% for 0.5 and 1 wt. % of MWCNT, respectively. Chapartegui et al. [2011] found that the MWCNT concentration of 0.3 wt. % and more confirmed the physical network between the epoxy and MWCNT, which reduced its the curing time by 30 min. Pillai et al. [2011] studied the interfacial bonding and uniform dispersion of MWCNT in epoxy. The shifting of glass transition temperature (Tg) with the reinforcement of MWCNT confirmed the good interfacial bonding between epoxy and MWCNT. Theodore et al. [2011] reported that the glass transition temperature of 1 wt.% epoxy/fluorinated MWCNT composites was found to be increased by 13°C compared to that of the composites prepared with unmodified MWCNT. Omrani et al. [2012] reinforced epoxy with MWCNT and it was observed that the cured nanocomposites showed 7°C raise in glass transition temperature compared to pure epoxy, which confirmed the interaction of MWCNT with epoxy resin. Srikanth et al. [2012] studied the cross linking density of the nanocomposites using DSC and observed that the nanocomposites prepared with 1 wt. % of MWCNT showed the enhancement of 32 % compared to that of pure epoxy. Park et al. [2012b] prepared epoxy/MWCNT-sheet nanocomposites for the analysis of thermal conductivity. It was observed that the 40 % stretched long-MWCNT sheet reinforced epoxy nanocomposites showed the thermal conductivity of 103 W/mK, whereas the same for random short-MWCNT nanocomposites showed the value of 6 W/mK.

The characteristics of epoxy/CNT nanocomposites are shown in Table 2 and it is observed that the thermal conductivity, glass transition temperature and cross linking density of epoxy were found to be increased significantly with the MWCNT

reinforcement. It is confirmed that the reinforcement of CNT in the epoxy matrix increased its mechanical and thermal properties.

Table 2.2 Characteristics of Epoxy/CNT composites

Author	MWCNT wt. %	Parameters	Enhancement/Observation
Omrani et al. [2012]	5	Tg	7 °C
Theodore et al. [2011]	1	Tg	22 %
Srikanth et al. [2012]	1	Cross linking density	32 %
Chapartegui et al. [2011]	0.3	Physical network	Formation of physical network among epoxy and MWCNT
Cui et al. [2011]	0.5	Thermal Conductivity	51 %
	1		67 %
Park et al. [2012b]	10	Thermal Conductivity	103 W/mK

2.3.3.7 FRP/CNT nanocomposites

Siddiqui et al. [2009] coated 0.3 wt. % MWCNT on the fiber and prepared FRP nanocomposites and they studied their bonding mechanism. The MWCNT coated fibre acted as a bridge on the fibre surface, which in turn delayed the crack opening in the composites. The interfacial adhesion of FRP composites was sensitive towards the wettability of the fibre, which was increased by the coating of functionalized MWCNT and reduced the interply failure of FRP composites. It was observed that the increase in interply adhesion led to changes in the failure mode from longitudinal to transverse direction of FRP composites and MWCNT coated FRP composites, respectively. Lee et al. [2010b] prepared salinized-MWCNT/basalt/epoxy composites and it was reported that the tensile strength and Young's modulus of the composites were observed to be increased by 34 and 60 % compared to that of FRP composites. Böger et al. [2010] reinforced 0.3 wt. % of MWCNT in FRP composites. It was observed that the addition of MWCNT led to the enhancement of inter fiber fracture strength up to 16 % compared to FRP composites. Kim et al. [2011] studied the flexural properties of carbon fiber/salinized-MWCNT/epoxy nanocomposites. It was observed that the flexural strength and flexural modulus of 2 wt. % nanocomposites were found to be increased by 58.1 and 22.2 %, respectively, compared to FRP composites. Davis et al. [2011] evaluated the mechanical properties of SWNT and fibre reinforced epoxy composites. It

was observed that the tensile strength and Young's modulus of 0.5 wt. % SWNT reinforced FRP were found to be increased by 11.1 and 19 %, respectively, compared to that of pure FRP. Lee et al. [2011] prepared 1 wt. % of saline-modified MWCNT/carbon/epoxy composites and studied their mechanical properties. It was observed that the Young's modulus and tensile strength of the composites were found to be increased by 18 and 15.8 %, respectively, compared to FRP composites. The MWCNT-epoxy resin mixture was poured over the carbon fabric arrangement and the composites were fabricated using the hand lay-up technique. Later, the laminate was cured at 130°C under 2.9 Pa for 2 hr. Rahman et al. [2012] observed that the strength, Young's modulus and strain at fracture of epoxy/E-glass/amino functionalized 0.3 wt. % MWCNT nanocomposites were found to be enhanced by 37, 21 and 21 %, respectively.

Siddiqui et al. [2013] prepared epoxy-based CFRP composites with MWCNT. It was observed that the 0.5 wt. % MWCNT reinforcement was found to be optimum and the inter-laminar shear strength, torsional modulus and torsional strength were found to be increased by 12, 17 and 19.5 %, respectively, compared to FRP composites. Li et al. [2013] coated 0.3 wt. % of carboxylic acid-functionalized MWCNT over the carbon fiber and prepared FRP composites, and their interfacial shear strength and tensile strength were found to be increased by 43 and 11.2 %, respectively, compared to pure FRP composites. Zainuddin et al. [2014] developed the E-glass/epoxy/MWCNT composites and studied their flexural properties. The flexural strength and flexural modulus of 0.3 wt. % of MWCNT reinforced composites were found to be increased by 42 and 20 %, respectively, compared to pure composites.

The enhancement of mechanical properties of FRP composites with the reinforcement of CNT is listed in Table 2.3. It is observed that the mechanical properties of MWCNT reinforced FRP composites were found to be increased with the reinforcement concentration. It is also observed that the MWCNT reinforcement of less than 1 wt. % showed good enhancement of mechanical properties of the composites in all cases.

Table 2.3 Enhancement of the mechanical properties of CNT-FRP composites

Author	MWCNT wt. %	SWNT wt. %	Properties	% Enhancement
Lee et al. [2011]	1		Tensile strength	15.8
			Young's modulus	18
Rahman et al. [2012]	0.3		Tensile strength	37
			Young's modulus	21
			Fracture Strain	21
Li et al. [2013]	0.3		Shear strength	43
			Tensile strength	11.2
Davis et al. [2011]		0.5	Tensile strength	11.1
			Young's modulus	19
Lee et al. [2010b]	1		Tensile strength	34
			Young's modulus	60
Kim et al. [2011]	2		Flexural strength	58.13
			Flexural modulus	22.2
Siddiqui et al. [2013]	0.5		Interlaminar shear strength	12
			Torsional modulus	17
			Torsional strength	19.5
Böger et al. [2010]	0.3		Inter fiber fracture strength	16

2.3.3.8 Aligned CNT nanocomposites

Abdalla et al. [2010] studied the mechanical properties of epoxy/fluorinated MWCNT nanocomposites under the magnetic field. It was observed that the Young's modulus of the nanocomposites under random direction, parallel and perpendicular to the magnetic field was found to be increased by 32, 72 and 24 %, respectively, compared to pure epoxy. Cheng et al. [2010] fabricated the controlled alignment of CNT in epoxy composite by resin transfer moulding. The Young's modulus and tensile strength of 16.5 wt. % MWCNT in epoxy were found to be 20.4 GPa and 231.5 MPa, respectively, corresponding to 716 and 160 % of enhancement compared to pure epoxy. Dassios et al. [2012] prepared MWCNT mats and the mechanical properties of the composites made of those mats with epoxy resin were studied. It was found that the Young's modulus of the composite was increased by 25 % compared to pure epoxy. Camponeschi et al. [2007] reported that the 3 wt. % fluorinated SWNT and MWCNT in epoxy resin under

the magnetic field led to the enhancement of Young's modulus by 111.5 and 25 %, respectively, compared to pure epoxy. Mecklenburg et al. [2015] aligned the MWCNT in epoxy and it was reported that the 68 wt. % of unidirectional aligned MWCNT increased the Young's modulus to 36 GPa, whereas the modulus of pure epoxy was noted to be 3 GPa.

2.4 Rehabilitation studies on above knee amputees

The status of health after prosthesis fixation was evaluated using a short form questionnaire report (SF-36), which consists of a physical and mental component score. It was also noted that the survey was applicable for the persons above 14 years old, Ware et al. [1992]. Ware et al. [1995] carried out the validation of SF-36 survey and relative validity was obtained for each measure by comparing with the best score in the same tests. It was confirmed that the SF-36 was a reliable measure for the health outcome. Burger et al. [1997a] examined the changes in social life and free time activities of the lower limb amputees. It was observed that the participation in social activities was decreased drastically especially for older amputees. The free time activities were also changed from cycling, outdoor games and farm work to reading, watching television and housekeeping. Pezzin et al. [2000] examined the health related quality of life (HRQL) for trauma related amputation using SF-36, where a huge difference was observed in physical health compared to HRQL before amputation. It is also reported that one fourth of total amputees have problems related to body pain, sores and phantom pain. Hagberg et al. [2001] reported the HRQL for unilateral trans-femoral amputation, which was caused by non-vascular problem. The reduction in HRQL parameters was observed due to heat or sweating in the socket, irritation, difficulty in rough surfaces, speed walk, stump pain, phantom pain, back pain and pain in other leg. Hays et al. [2002] suggested that the limitation for evaluating the person with disabilities was required to be included in HRQL measurement.

Holden et al. [1987] reported the prosthetic use of unilateral trans-tibial amputation based on the age group of below and above 65 years old. It was observed that the younger amputees progressed the gait training more quickly compared to older amputees. Walker et al. [1994] reported the satisfaction of the prosthesis fixation in lower limb amputee. It was observed that the delayed amputation after setting the

stump muscle was more satisfied with end results. Burger et al. [1997b] estimated the mobility of people having trauma induced lower limb amputation. It was reported that a 74.2 % of amputees used the prosthesis for 7 hr/day, 57.8 % of amputees climbed more than 20 stairs/day and 52.5 % of amputees walked outdoors without using crutches. Gagnon et al. [1999] evaluated the frequency of the prosthetic usage for lower limb amputation using prosthetic profile of an amputee. It was found that a 53 and 64 % of amputees used the prosthesis for indoor and outdoor locomotion, respectively. Dillingham et al. [2001] examined the satisfaction and problems with prosthetic devices for the trauma related lower limb amputation. It was noticed that a 43 % of the amputees satisfied with the prosthesis and one quarter of all users reported with problems like wound, skin irritation and pain. Hagberg et al. [2004] evaluated the prosthetic performance using Questionnaire for Persons with a Transfemoral Amputation (Q-TFA). It was noticed that the scores obtained from Q-TFA report showed better reliability for the amputees having the trans-femoral socket prosthesis. Puhalski et al. [2008] determined the usage of prosthesis in trans-femoral amputee by means of prosthetic profile of an amputee and locomotor capabilities index (LCI). It was found that the LCI score was positively influenced by wearing time and negatively influenced by age. Desmond et al. [2010] accounted the phantom limb pain and residual limb pain after upper limb amputation based on the questionnaire report. It was reported that one third of the amputees had pain in most of the days.

2.5 Gait analysis of the leg prosthesis

Yokogushi et al. [2004] developed a new prosthetic knee joint and compared with the hydraulic knee joint. The performance of a knee joint based on the gait cycle of 10 healthy volunteers was compared. It was found that the gait pattern of newly developed knee joint was comparable with that of the existing knee joint. Gard [2006] reported that the walking performance of an amputee was evaluated using gait analysis; however the data was highly influenced by the prosthetic socket, suspension system and components used. Segal et al. [2006] compared the performance of a C-Leg and Mauch SNS model at the controlled walking speed in terms of gait. It was observed that the amputees walked faster using the C-Leg with decrease of vertical ground reaction force compared to Mauch SNS model. Thorn et al. [2009] compared the gait

pattern of five trans-femoral amputees fitted with total knee 2000 model and 3R80 model. It was reported that the amputees felt more stable and confident on the total knee 2000 than that of 3R80 model. Taheri et al. [2012] reported that the knee joint has a great influence on the function of total prosthesis. Moreover, the comparison of gait was made between 3R15 and 3R20 model knee joints for 7 amputees. It was found that the 3R20 model knee joint performed better in high walking speed compared to 3R15 model. Lura et al. [2015] compared the gait of Genium prosthetic knee and C-Leg. It was found that the Genium prosthetic knee decreased the level of impairment compared to C-Leg because of its increased flexion in swing.

2.6 Closure on literature

Even with substantial development, obtaining the near sound leg gait pattern in prosthetic polycentric knee joint is still a great concern. The necessity of a user friendly and inexpensive passive polycentric knee joint to be used by the above-knee amputees is important. Also, it was observed from the literature that a very little attempt was focused on the development of a passive polycentric knee joint, examining the HRQL and performance of the knee joint. The work on the selection of a polymeric material for the passive polycentric knee joint was also very limited. As the degradation of polymer due to UV radiation cannot be avoided, the limitation on the effect of the same is not received full attention to increase the longevity of the polymeric products. Though a very few attempts were made to limit the degradation of polymeric properties by reinforcing different types of particles, the influence of MWCNT for the same is yet to be explored in detail. Based on the few reported studies, it is observed that the MWCNT acted as an effective nanofiller in limiting the UV rays induced degradation. However, the detailed studies on the degradation of the mechanical properties of a polymer and the mechanism involved in restricting the same are yet to be reported. As the rate of heat transfer and weight of the socket influenced the metabolic cost of an amputee, which could be reduced by selecting a suitable material for the same. It is noticed that the selected concentration of reinforcement used for improving the heat transfer characteristics and mechanical properties of sandwich composites is also not reported.

The following technical gaps were observed from the detailed literature review:

- The polycentric knee joint along with required functionality is very expensive.
- The constraints such as instantaneous centre of rotation, optimum link parameters, flexion angle, and voluntary control zone are not included successfully in the existing knee joint.
- The existing active knee joints are found to be heavy, bulky and expensive due to the presence of actuators.
- The maintenance free extension unit was not incorporated in the existing passive polycentric knee joint.
- A testing device for evaluating the gait of the knee joint was not reported.
- The near sound leg gait pattern was not attained successfully with the existing passive polycentric knee joint
- The knee joint material having the reduced environmental degradation was not developed successfully.
- The friction among the skin, socks and socket develops the shear stress, which initiates skin lesions such as calluses, corns, thickening, abrasions, and blisters.
- Due to lack of heat transfer via socket, the temperature of the residual stump is raised leading to increased metabolic cost to activate the joint and causing the skin incursions.
- Socket-socks slippage within the socket can cause discomfort, internal limb pain, and eventually skin ulcers.
- The increased number of stockinet layer in the socket gains its weight leading to raise the metabolic cost of an amputee.

2.7 Objectives of present work

The major objective of the proposed work is to design, develop and test the user-friendly, light weight and inexpensive artificial limb to achieve the near sound leg gait pattern of a trans-femoral amputee

The sub-objectives of the proposed work are as follows:

- Design of a polymeric based passive polycentric prosthetic (4Ps) knee joint and the static and dynamic analysis of the same.
- Rehabilitation feedback from the patient trials to improve the design features of a knee joint.
- Development of a light weight, highly durable and easy-maintenance material for the knee joint.
- Selection of suitable concentration of MWCNT reinforcement in PMMA and epoxy based sandwich composites proposed to be used to make the knee joint and socket, respectively, based on their characteristics.
- Influence of aging on the mechanical properties of proposed materials used for the knee joint.

Chapter 3

Materials and Methods

The characterization of composites involves several analytical tools and experimental techniques in order to confirm whether the desired properties are achieved or not. The chapter 3 is focused on discussing the various techniques used and methods employed for the preparation of composites beginning with the materials used, design of an aging setup and methods used to reinforce the filler in the polymer matrix. A series of different analytical instruments/techniques is used at various stages of developing and testing the composites, which are discussed below.

3.1 Multi walled carbon nanotubes (MWCNT)

The MWCNT was purchased from M/s Shenzhen Nanotech Port Co., Ltd., China. The PMMA/MWCNT composites were prepared using the MWCNT having the following specifications: outer diameter 40-60 nm; ash content < 1.5 wt. %; and specific surface area > 40 m^2/g. The epoxy/MWCNT composites were prepared using the MWCNT having the following specifications: outer diameter 10-20 nm; ash content < 3 wt. %; and specific surface area > 250 m^2/g. Both the types of as received MWCNT have the length of 5- 15 µm, purity of 95 wt. % and the density of 2.16 g/cc.

3.2 Polymethyl methacrylate (PMMA)

The industrial grade LG chemical, IG-840, PMMA pellets were purchased from M/s Kamdar plastics, Gujarat having the following specifications: specific gravity - 1.18 g/cm^3, melt flow index - 5.0g/10 min., softening temperature - 109 °C and melting temperature 200 - 250°C.

3.3 Epoxy and hardener

Epoxy resin having the density of 2.25 g/cm^3 and the viscosity of 900 mPa-s at room temperature and the hardener having the density of 0.94 g/cm^3 were purchased from M/s Endolite, India, Inc.

3.4 E-glass woven fabric and stockinet layer

The stockinet and E-glass woven fabric were purchased from M/s Endolite, India, Inc., The specifications of the stockinet are as follows: cotton 100 %, Type C of IS: 11273, plain weave pattern. The specifications of E-glass woven fabric are as follows: plain weave and 13μm diameter.

3.5 Chemical treatment of MWCNT

MWCNT is known to have very high specific surface area and tends to agglomerate, which acts as defects and stress raisers in the composites leading to the reduction of overall properties of them. Thus, as-received MWCNT is required to undergo a suitable surface modification by which the required functional groups are attached on the surface of MWCNT. The presence of functional groups facilitates the chemical bonding with polymer and also allows uniform dispersion in the polymer matrix and the same was also reported by Datsyuk et al. [2008]. In order to effectively use the characteristics of MWCNT, it is required to be incorporated in the polymer as a reinforcement and ensure confirmed interfacial bonding between them. As a result, the unique mechanical properties of the MWCNT can be transferred to the composites. Thus, it is required to perform chemical treatment on as-received MWCNT to ensure its homogeneous dispersion in the polymer and improve interfacial stress transfer from the polymer matrix, which determine the overall properties of the composites. The chemical treatment of MWCNT was performed as described by Esumi et al. [1996], which is briefly described here.

The MWCNT was heated with nitric acid and sulphuric acid mixture having the volume ratio of 1:3 at 140 °C in an oil bath with continuous stirring for 45 min. Then, the MWCNT was washed with deionized water till the supernatant showed a pH value of around 7. The same was dried in a hot air oven at 100 °C to remove the moisture content and then ground to get the fine powder of MWCNT. Fig. 3.1 shows the Thermo Fisher IS10 Fourier transform infrared spectroscope (FTIR), which was used to confirm the presence of different functional groups attached on the surface of MWCNT. In FTIR, the infrared rays were passed through the KBr and MWCNT mixed pellet, where a part of the rays was absorbed by the sample and thereafter the transmitted rays were

analysed to obtain the molecular bonding present in the sample based on their vibrations/rotations. The FTIR was also used to obtain the oxidation index of the specimen after environmental aging.

Fig. 3.1 FTIR spectrometer

3.6 Preparation of PMMA/MWCNT composites

PMMA/MWCNT composites were prepared as per the following procedure: the functionalized MWCNT was dispersed in distilled water, nanofluid, by sonicating the mixture for 45 min. with various concentrations such as 0.10, 0.20, 0.25, 0.30 and 0.4 wt. % using a tip sonicator of a model VCX 750 from M/s Sonics, USA and it is shown in Fig. 3.2. In the tip sonicator, the vibration of the tip causes cavitation, which generates and disintegrates the million number of micron sized bubbles. The collapse of thousands of bubbles releases tremendous energy, which disperses the MWCNT in the fluid. The well dispersed nanofluid was mixed with PMMA pellets and heated using a magnetic hot plate stirrer up to 100 °C for 6 hr in order to ensure the uniform coating of MWCNT over the PMMA pellets and the same was dried in a hot air oven to remove the moisture present on the surface of PMMA. Then the dried pellets were blended using a co-rotating twin-screw extruder, which is shown in Fig. 3.3, make: Specific Engineering and Automats, model: ZV-20, at 150 rpm, where the temperature of the heating zone was maintained between 180 to 250°C for the homogeneous mixing of MWCNT in PMMA. The co-rotating twin-screw blends the polymer-MWCNT mixture rigorously to obtain the uniformly dispersed mixture. Later, an injection moulding machine, as shown in Fig. 3.4, make: Texair, JTS-40 model was used to prepare the

tensile and three-point bending specimen as per the ASTM standards, where the temperature of heating zone and nozzle was maintained in the range of 180 - 250°C and 70°C, respectively. A single screw extruder inside the injection moulding machine moved the PMMA/MWCNT mixture into the mould and thereafter the specimen was obtained. The sample made of pure PMMA was also obtained after following through all the procedure cited above without MWCNT.

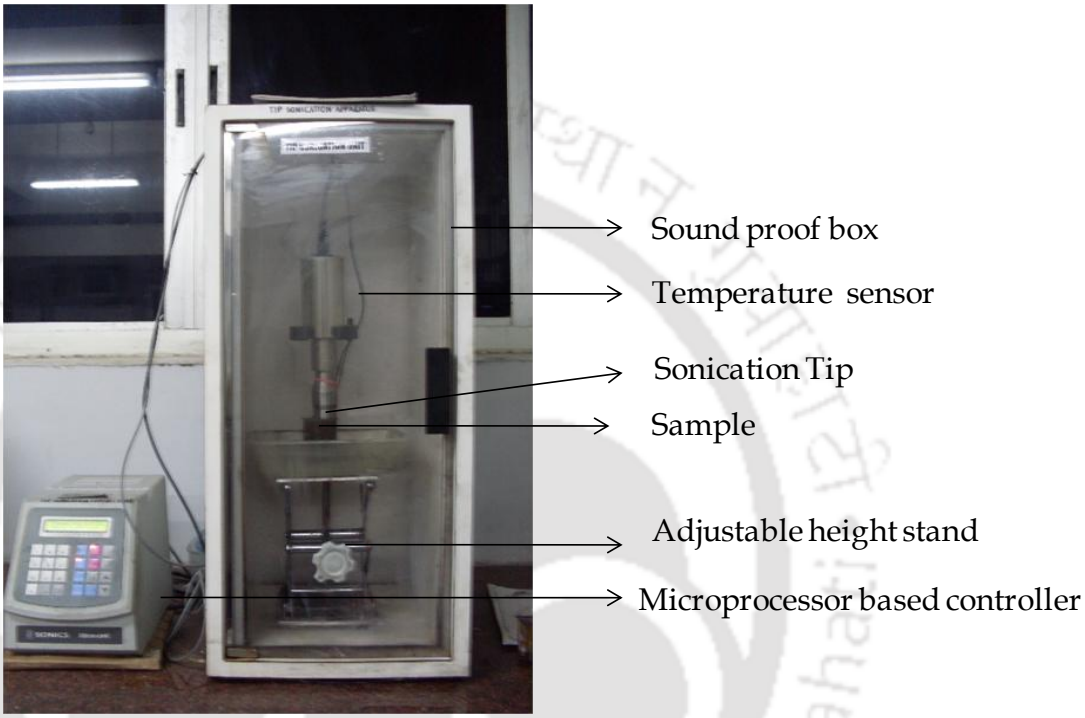

Fig. 3.2 Tip sonicator

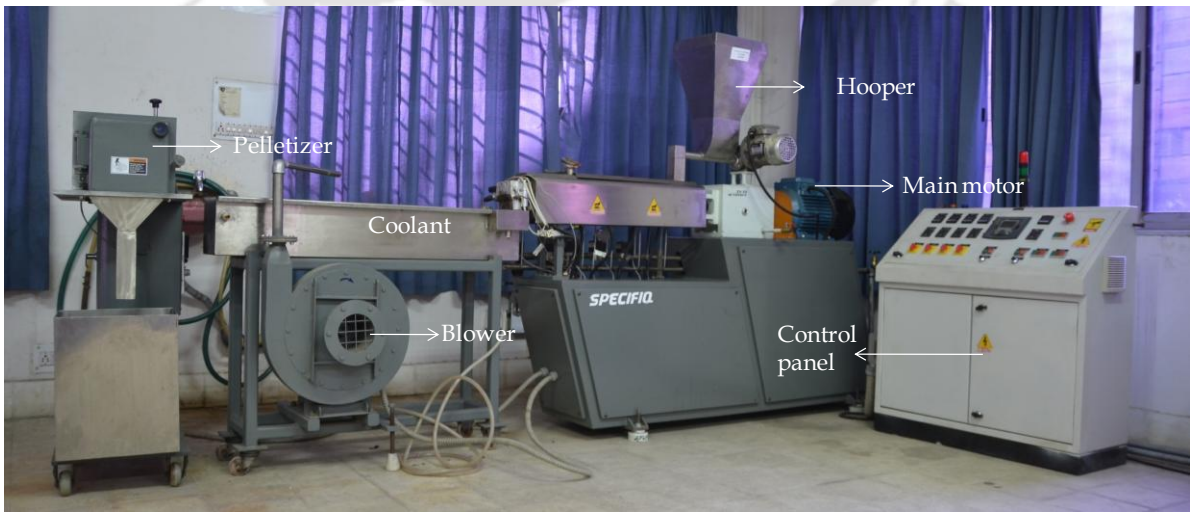

Fig. 3.3 Twin screw extruder

Fig. 3.4 Injection moulding machine

3.7 Preparation of Epoxy/MWCNT composites

The resin and hardener having the weight ratio of 1:0.4 were hand-mixed using a stirrer rod for 15 min. and poured into a die having the dimension of 50 mm length and 8 mm diameter. Then, the mold was allowed to cure at 26 ± 2°C for 3 hrs to obtain the pure epoxy specimen. In case of epoxy composites, the epoxy resin was dissolved in acetone using a bath sonicator for 30 min., and the MWCNT was dispersed in acetone using the tip sonicator for 30 min. Thereafter, both were mixed together and bath-sonicated for another 45 min. to obtain the homogeneous mixture of epoxy resin-MWCNT-acetone mixture. The acetone was evaporated using three methods, namely, hot air oven at 55 °C (evaporating temperature of acetone is 55 °C), magnetic stirrer at 55 °C, and under vacuum at room temperature to obtain the acetone free epoxy resin-MWCNT mixture. Then, the epoxy-MWCNT mixture was mixed with required quantity of hardener by the hand mixing process for 15 min. and poured into the die. Thus, the composites were prepared using three methods and the processing method was optimized based on their mechanical properties. Later, the MWCNT was dispersed with epoxy matrix-hardener under vacuum at room temperature (optimized processing method) and the respective composites were prepared.

3.8 Preparation of Epoxy/MWCNT/E-glass fabric/stockinet sandwich composites

The sandwich composites with the cross sectional area of 200 × 200 mm were prepared using stockinet layers, E-glass woven fabric and epoxy resin with and without MWCNT reinforcement by a hand lay-up technique after 3 hrs of curing at room temperature, where the number of stockinet layers was varied from 2 to 10 with an increment of 2 layers. The following methodology were adopted to prepare the composites: (i) A release gel was sprayed over the mold surface to avoid the sticking of a polymer on the surface; (ii) a thin plastic sheet was used at the top and bottom of the mold to get the required surface finish of the sandwich composites; (iii) the stockinet layer was placed over the thin plastic sheet and the thermosetting polymer with required resin-hardener mixture was poured as one layer; (iv) the E-glass woven fabric was placed and filled with resin and (v) finally, the stockinet layer was used and the required quantity of resin was poured. Similarly, the process was repeated for the required number of stockinet layers (4, 6, 8 and 10) for obtaining the sandwich composites having the desired thickness. In case of MWCNT reinforced sandwich composites preparation, the resin-hardener mixture was replaced by resin-hardener-MWCNT mixture. The density of the composites was measured by using the Archimedes principle.

3.9 Melt flow index studies on MWCNT coated PMMA pellets

The melt flow index (MFI) of MWCNT coated PMMA pellets was studied as per ASTM D1238 [2012] in order to understand the influence of the concentration of MWCNT on the viscous behavior of PMMA. The melt flow index setup used in the present study is shown in Fig. 3.5. The following steps were adhered to determine the melt flow index of the test samples. Initially, the barrel was pre-heated for 5.5 min. at the melting temperature of PMMA and the polymer pellets were poured into the barrel and piston was inserted. Thereafter, the weight as per ASTM standard was placed over the piston and the material starts extruded from the bottom of the barrel. After the specified period of time (10 min.), extrudate material was collected and weighed to obtain the melt flow index in g/10 min.

Fig. 3.5 Melt flow index setup

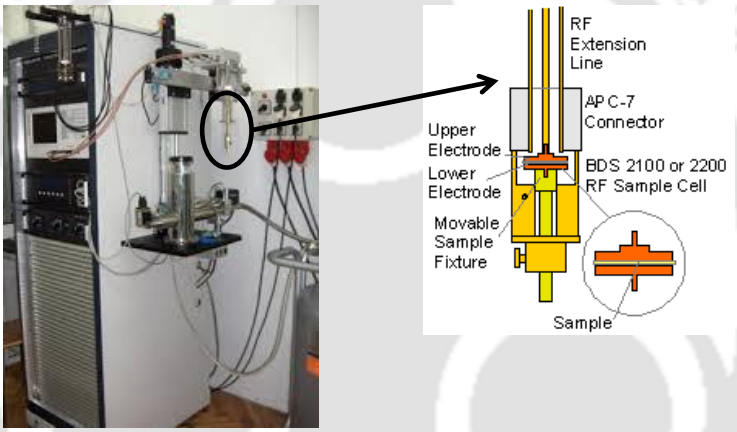

Fig. 3.6 Novocontrol RF impedance analyser

3.10 Electrical conductivity in the composites

The electrical conductivity of PMMA/MWCNT and Epoxy/MWCNT composites was measured using the RF impedance analyzer, Novocontrol, Model: BDS 2300, which is shown in Fig. 3.6, to confirm the homogeneous dispersion of MWCNT in the matrix. The impedance analyser applies a constant voltage and measures the current, which will be used to obtain the ac electrical conductivity of the sample. The test was performed in the frequency range of 10^{-2} to 10^{6} Hz at room temperature. The composite test sample was coated with silver paste and placed between two gold-plated brass electrodes, where a micrometer screw was used to clamp the two parallel plates. The dc conductivity of the composites was determined from the frequency dependency of the ac conductivity in the region of low-frequency plateau.

3.11 Thermal characteristics of the composites

The differential scanning calorimeter/thermo gravimetric analyser (DSC/TGA) was used to study the glass transition temperature (Tg) and thermal stability of the PMMA/MWCNT and Epoxy/MWCNT composites. A derivative of thermogravimetric curve (DTG) was obtained from TGA, which is used to find the degradation temperature of the test material. A NETZSCH simultaneous thermal analyser; model STA 449F3 having the DSC resolution of < 1µW and the microbalance resolution of < 1µg along with a heating rate accuracy of 1 mK/min. was used for calorimetric analysis of the test samples according to ASTM F2625-10 standard. The test was performed from room temperature to 600 °C at a heating rate of 10 K/min. The sample holder, Alumina, was heated in a muffle furnace upto 1200 °C to remove any volatile contaminants from the pan, later it was sonicated in an ultrasonic bath and dried in an oven to ensure the contaminant and moisture free sample holder. Alumina pan with a perforated lid was used with a sample weighing 5-6 mg. The height of the sample was maintained to be within 1mm, and the base of the sample was ensured to have a complete contact with base of the pan in order to maintain uniform heat flow and avoid any thermal gradient in the sample. Argon was used to purge the sample chamber and the furnace at 20 and 60 ml/min., respectively. The test set up was calibrated with Indium standard at a heating rate of 10 K/min. prior to testing the sample. The DSC/TGA set up used in the present study is shown in Fig. 3.7, which measures the mass change and energy absorbed with an increase of temperature.

Fig. 3.7 Differential Scanning Calorimeter/Thermo Gravimetric Analyser

3.12 Morphological studies on composites and MWCNT

A 200 kV Transmission Electron Microscope, JEOL JEM 2100, was used to study the surface of MWCNT after the chemical treatment and to identify its defects. Fig. 3.8 shows the Transmission electron microscopy (TEM) used in the present study. The TEM provides the quality, shape and size information of MWCNT by assessing the electron beam transmitted through the specimen.

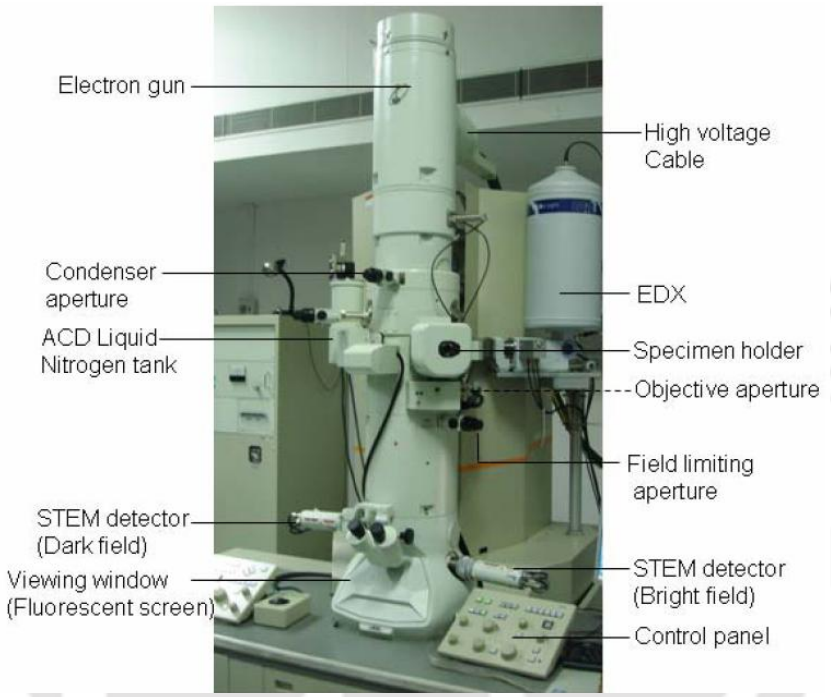

Fig. 3.8 Transmission electron microscopy

The surface morphology of the polymer and its composites was observed using Leo 1430 VP Scanning electron microscope (SEM) with a magnification and spatial resolution of 250 kX and ~10 nm, respectively. The test specimen was sputtered with Au in order to make a conductive surface on the sample. Fig. 3.9 shows the Scanning electron microscope, where a beam of highly concentrated electrons impinge over the sample and generated primary backscattered electrons, secondary electrons and Auger electrons. The SEM uses primary backscattered electrons and secondary electrons for obtaining the information about the sample.

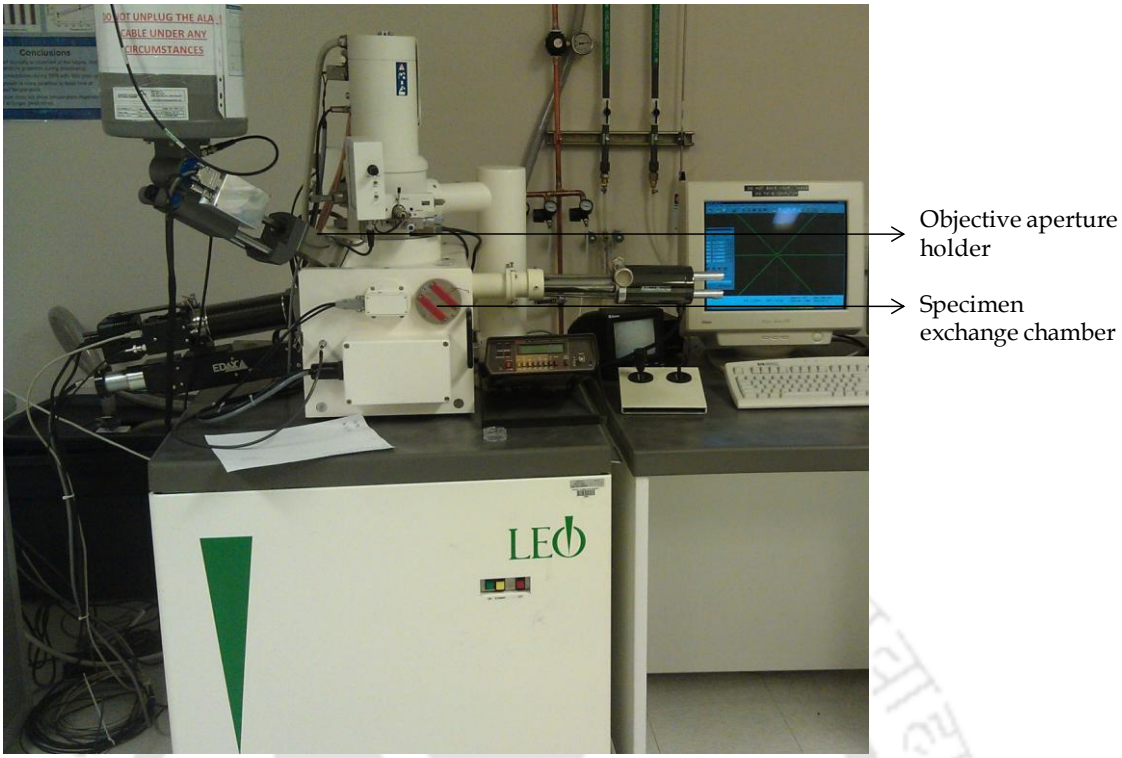

Fig. 3.9 Scanning electron microscope

The voids present in the test sample were confirmed using the upright optical microscope (ZEISS Model: Axiotech with halogen lamp, 200X), which is shown in Fig. 3.10. The reflective rays from the specimens were used to obtain their morphology.

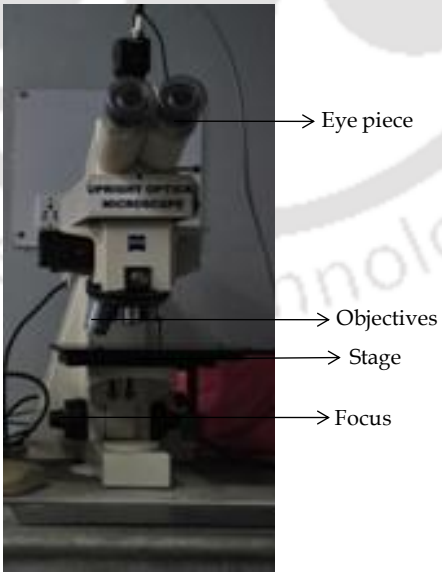

Fig. 3.10 Optical microscope

3.13 Viscosity studies on composites

The viscosity of epoxy/MWCNT mixture was tested in a Rheometer, Make: M/s Anton Parr, Model: Physica MCR 101 to study the influence of MWCNT on the viscosity of epoxy. The tests were conducted using a parallel plate 25mm (PP25) under oscillatory mode with constant shear strain amplitude of 5 % at an angular frequency of 10 rad/s. The test sample is placed in a circular disc of 25 mm diameter. The PP25 plate is set for zero-gap and the heating plate is maintained at room temperature. The rheometer used in the present study is shown in Fig. 3.11.

Fig. 3.11 Rheometer

3.14 Mechanical characterization of PMMA/MWCNT and Epoxy/MWCNT composites

The tensile and flexural properties of the PMMA/MWCNT composites were studied as per ASTM D-638 [2010] and ASTM D-790 [2012], respectively, using Instron-8801, which is shown in Fig. 3.12, where the crosshead speed of 1mm/min. at the operating temperature of 25 ± 1°C was maintained. An extensometer was used to measure the elongation of the test samples during the tensile test. The compression test of the epoxy/MWCNT composites was carried out as per ASTM D695-10 [2010], where the crosshead speed of 0.5 mm/min. at 25 ± 1°C was maintained throughout the test. A double-acting servo-hydraulic actuator was used to enter the crosshead speed in positive and negative direction to carry out the tensile and three point bending test. In

order to ensure the repeatability of the results, three samples were tested per material type and the average of the results is reported.

Fig. 3.12 INSTRON universal testing machine with closed loop servo hydraulic system.

3.15 Thermophysical properties of Epoxy/MWCNT sandwich composites

The thermophysical properties of the epoxy/MWCNT and sandwich composites were measured as per ISO 22007-2 using a Hot Disk, Model: TPS 2500 and it is shown in Fig. 3.13. It works on the principle of transient plane source technique, where thermal diffusivity and thermal conductivity were measured and thereafter volumetric specific heat was calculated.

Fig. 3.13 Thermal property analyser

3.16 Relative crystallinity of composites

The relative crystallinity of the composite sample was measured using the ratio of the summation of scattering of the crystalline phases to the total scattering. The X-ray diffractometer (XRD), Make: PANalytical Model: X'Pert used in this study is shown in Fig. 3.14 and it works as per the principle of Bragg's Law.

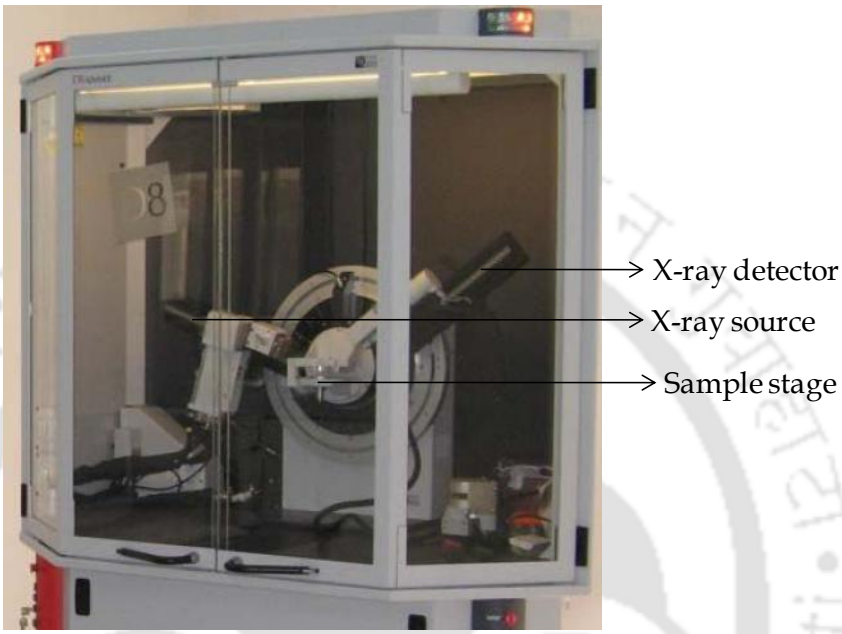

Fig. 3.14 X-Ray diffractometer

3.17 Stress transfer confirmation studies in composites

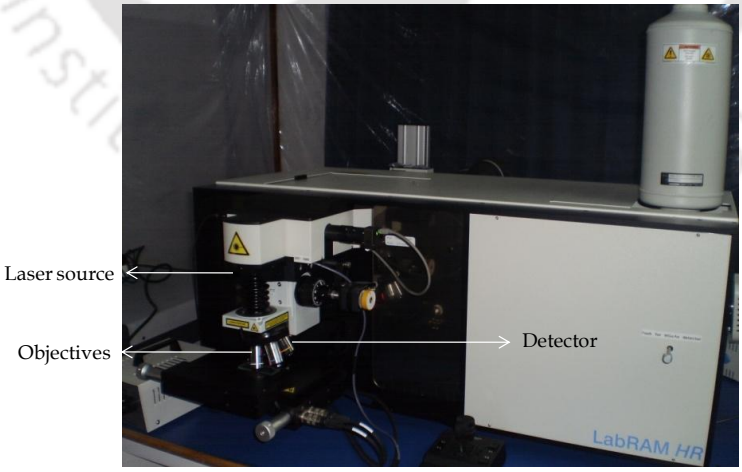

Fig. 3.15 Laser Raman spectroscopy

A laser Raman spectroscopy (Jovin Yvon, Triax 550) in the backscattering mode equipped with 488 nm blue laser (Argon) and a CCD detector coupled with a

monochromator having the XY step resolution of 0.1 µm and the wave number accuracy of ±1 cm^{-1} was used in this study to confirm the effective stress transfer from the matrix to the reinforcement and also to study the defects produced on the surface of MWCNT. Fig. 3.15 shows the photographic view of the Raman spectroscopy, which works on the principle of Raman effect.

3.18 Accelerated aging studies on composites

The accelerated aging studies on PMMA/MWCNT composites as per ASTM G154 were carried out upto 0.25 wt. % of MWCNT in order to understand the influence of reinforcement on aging of PMMA. An UV exposure dosage for the period of 8 hrs at 70 ± 4 °C and then condensation at 50 ± 3 °C for 4 hrs were considered as one exposure cycle. The total radiation dosage was calculated by multiplying the number of cycles with the radiation dosage per cycle, where 20W UV lamb was used to conduct the accelerated aging studies. The energy intensity per unit area was calculated by considering the cross sectional area of the aging unit, where the samples were placed throughout the test section. The radiation dosage per unit area per exposure cycle was calculated to be 0.28 kJ/cm^2 (8 hrs of accelerated exposure). The aging studies on PMMA/MWCNT composite samples having the MWCNT concentration of 0, 0.1, 0.2 and 0.25 wt. % were carried out for different dosages such as 1.99, 3.98, 5.97, 11.94, 17.91 and 23.89 kJ/cm^2 of UV radiation, where the equivalent number of cycles was calculated to be 7, 14, 21, 42, 63 and 84, respectively. As per Martin et al. [2005], one thousand hours of accelerated exposure was equivalent to one year of natural weathering. Based on it, a relation between accelerated exposure cycles and the natural weathering in terms of hours was derived and expressed in equation 3.1 and the equivalent aging period for the 7, 14, 21, 42, 63 and 84 cycles of exposure was found to be 1, 2, 3, 6, 9 and 12 months of natural weathering. Later, the accelerated aged samples were considered for the characterization and the mechanical properties of PMMA/MWCNT composites were studied for the each set of specimens after the required period of aging.

$$T_N = 8.76T_A \quad \ldots (3.1)$$

The aging setup used in this study is shown in Fig. 3.16, where the hot air oven was utilized as a heating chamber to carry out the accelerated studies along with the UV lamb.

Owing to the repeated changes in the residual stump dimension of an amputee after the fixation of prosthesis, it is necessary to change the socket for every two years at maximum. Hence, the influence of environmental aging on the socket material (epoxy based sandwich composites) was not carried out.

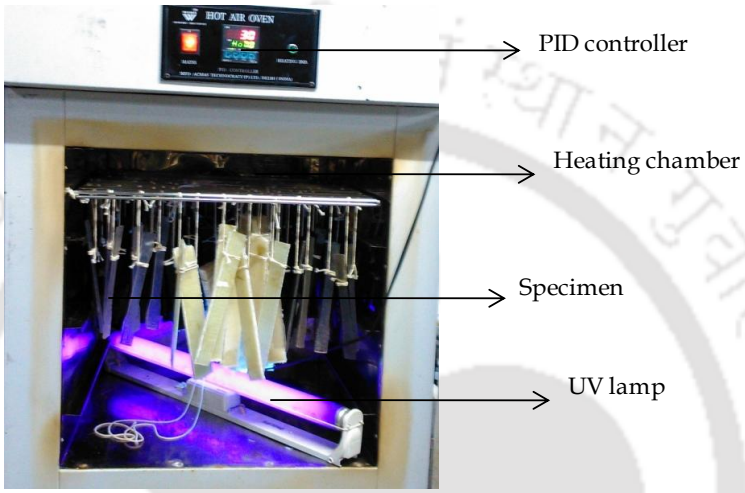

Fig. 3.16 Accelerated aging setup

3.19 Studies on free radical measurements in the accelerated test samples

Electron spin resonance (ESR) is a technique that can directly detect and quantify unpaired or odd electrons in atomic or molecular systems. ESR is the technique for detection and quantitative analysis of free radicals in a solid or fluid, Kurtz [2009]. The identification of a particular species of radical is dependent on the spectral splitting factor or the g- value, which is given by equation 3.2.

$$g = \frac{hf}{\omega H_r} \qquad \ldots (3.2)$$

The g-value for organic or polymeric radicals varies slightly from the free electron value range between 2.001 to 2.005. Figure 3.17 shows the ESR set up used in this study. The various parameters that are selected during the test were given below:

Magnetic field parameters: Center field 350 mT, Sweep width 25×, Time 30s; Current parameters: Modulation width 0.35×1, Time constant 0.3, Microwave power 1mW; Acquisition parameters: Total sweep 1. The experimental spectrum obtained from the

instrument is a first derivative curve and the intensity is directly proportional to the radical concentration. The area under the integral curve (also called absorption curve) of the experimentally obtained first derivative spectrum is proportional to the radical concentration present in the sample. PMMA/MWCNT composites, which were measured after the accelerated aging period of 1, 2, 3, 6, 9 and 12 months. As the radical concentration depends on the mass of the sample, the sample weight used in all studies was maintained at 4 ± 0.1 mg.

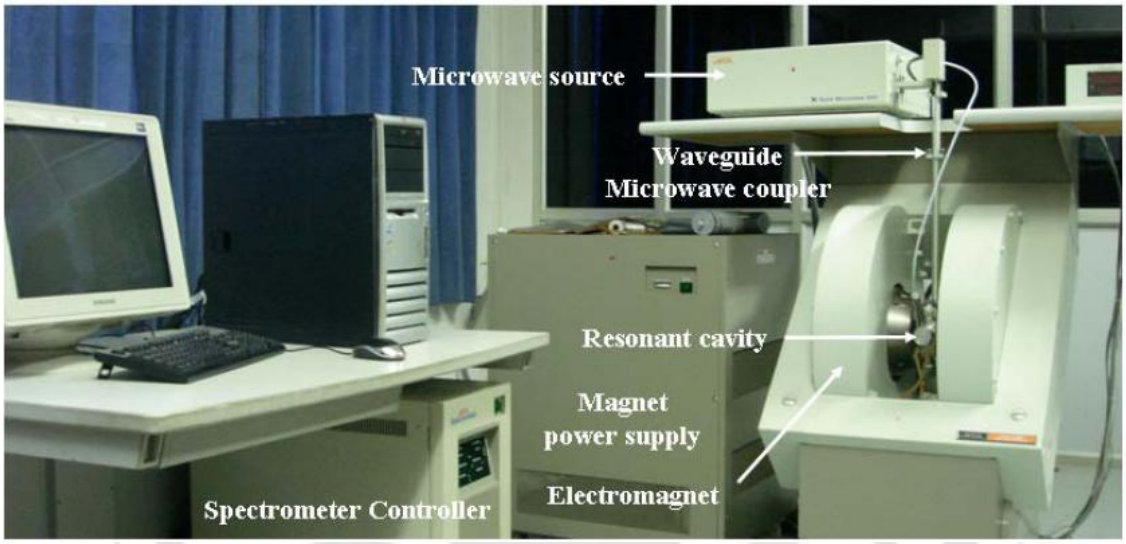

Fig. 3.17 ESR spectrometer

3.20 Miscellaneous

The weight of the link 0, link1, link 2, link 3, pylon and foot was obtained using a weighing balance, Make: Sartorius Mechatronics India pvt. ltd., Max: 30 kg with an accuracy of 1g. Angle φ, θ_a, θ_b and θ_d of the developed knee joint were obtained using a profile projector.

Chapter 4

Results and Discussion

The results and discussion section gives a detailed technical insight into the various experimental and theoretical outcomes in a sequential order mentioned below:

1. Design, development and analysis of the prosthetic knee joint
2. Patient trial and rehabilitation feedback after the fixation of the developed knee joint
3. Evaluation of the material proposed to be used for the knee joint
4. Evaluation of the sandwich composites proposed to be used for the socket

4.1 Design, development and analysis of the prosthetic knee joint

The prosthetic knee joint is classified into single axis and multi-axes knee joint. In case of a single axis knee joint, it has a fixed ICR, whereas the multi-axes knee joint has variable ICR, which stabilizes the prosthetic knee throughout the walking gait. Thus, the stance and swing phase stability of the multi-axes knee joint is superior compared to that of single axis knee joint. In addition to that the flexion-extension is unable to achieve in a single axis knee joint, whereas the polycentric knee joint allows the same. Hence, the polycentric knee joint was chosen for the present work.

4.1.1 Design approach for a polycentric knee joint

The polycentric knee joint consists of a four-bar mechanism to achieve its flexion-extension. In order to confirm the working mechanism of the four-bar link, it is required to follow the Grashof or non- Grashof criterion. The Grashof criterion defines that sum of the shortest and longest link of a planar quadrilateral linkage is less than or equal to sum of the remaining two links, whereas the non- Grashof criterion does not follow the above constraints. Moreover, the rocker in the Grashof criterion doesn't cross the line of frame of the mechanism, whereas it crosses the same in case of Non-Grashof criterion. Hence, adopting the Non-Grashof criterion led to the instability of polycentric

knee joint, which headed to select the Grashof criterion for the design of a polycentric knee joint. In case of Grashof criterion, the mechanism such as crank-rocker and double-rocker can be obtained, where the crank undergoes full rotation in crank-rocker mechanism, whereas the coupler link undergoes full rotation in case of double-rocker mechanism. A full rotation of the coupler link can be utilized to achieve the maximum flexion for walking as well as in sitting position. Hence, the double-rocker mechanism achieved by the Grashof criterion was chosen to obtain the flexion-extension of the knee joint.

4.1.2 Design of the four-bar mechanism of a polycentric knee joint

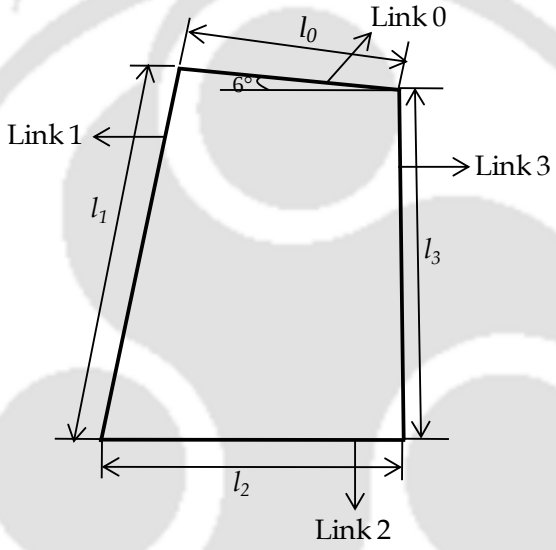

Fig. 4.1 Schematic diagram of the four-bar mechanism

The schematic diagram of the four-bar mechanism is shown in Figure 4.1, where the four links were named as link 0, link 1, link 2 and link 3. The link 0 and link 2 correspond to the top and bottom part of the four-bar mechanism, respectively. The major constraints used to achieve the knee joint design were as follows: link 3 was made perpendicular to the link 2 in order to limit the extension of a knee joint; link 0 was made at 6° inclined to horizontal plane for the initiation of the swing phase and to avoid buckling of the knee joint; width of the knee joint was fixed at 70 mm in order to avoid the bulkiness of the knee joint and following the standard implant size with due allowances [http://www.orthobullets.com/trauma/1044/tibial-plateau-fractures]. As part of the preliminary design, a stopper was placed at 115° flexion angle to limit the

required flexion of the knee joint. The link parameters of the proposed polycentric knee joint were chosen using the graphical method. There are three important factors involved in the selection of kinematic parameters of the knee joint, which are discussed below in detail:

(a) Beta stability of the knee joint

The beta value is the vertical distance between the knee centre and ICR of the polycentric knee joint. The buckling of polycentric knee joint can be restricted by providing the sufficient beta stability. Fig. 4.2 depicts the free body diagram of the shin and thigh of the prosthetic leg fitted with the polycentric knee joint, where "f" is a point of contact of the prosthetic foot on the floor during heel strike; "I" is an instantaneous centre of rotation of the polycentric knee joint. The effect of beta stability in restricting the buckling of the knee joint can be obtained from Fig. 4.2a and it is given in equation 4.1.

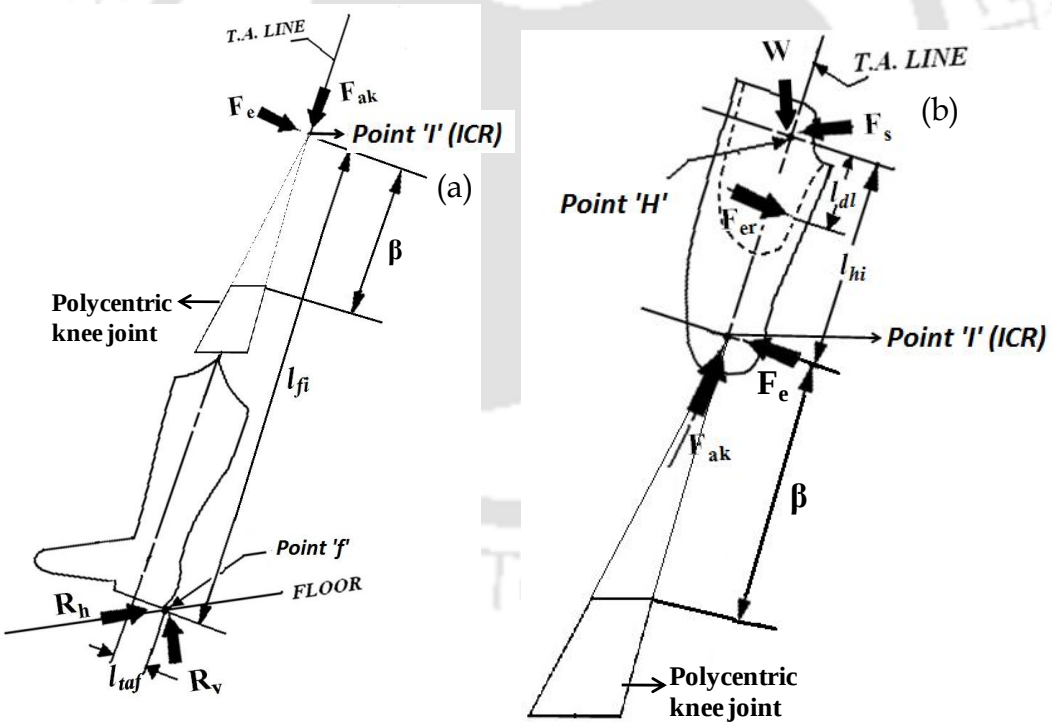

Fig. 4.2 Free body diagram of the (a) shin and (b) thigh of the prosthetic leg

Considering the moment equilibrium at point 'f' in Figure 4.2a, $\Sigma M_f = 0$

$$F_{ak} \times l_{taf} = F_e \times l_{fi}$$

$$\beta \propto l_{fi}$$

$$F_e = \frac{F_{ak} \times l_{taf}}{l_{fi}} \propto \frac{C_4}{l_{fi}} \quad \ldots (4.1)$$

It is observed from the equation 4.1 and Fig. 4.2a that the increase in beta stability caused to increase the distance between the heel strike and ICR (l_{fi}), which led to decrease the buckling of knee joint (F_e) causing to reduce the force exerted by the residual limb to prevent the buckling (F_{er}), and it is shown in equation 4.2.

$$F_{er} \propto F_e \quad \ldots (4.2)$$

The effect of beta stability in limiting the leverage of the residual limb can be confirmed from equation 4.3 by taking the moment at point H, which is shown in Fig. 4.2b.

$$\Sigma M_H = 0 \ , \ F_{er} \times l_{dl} = F_e \times l_{hi} \quad \ldots (4.3)$$

It is observed from Fig. 4.2b that l_{dl} is constant and thus Eqn. (4.3) can be modified as

$$F_{er} \propto F_e \times l_{hi} \quad \ldots (4.4)$$

F_{er} is proportional to l_{hi} with reference to eqn. (4.4), hence, it is noted from Fig. 4.2b that the increase in beta stability led to decrease the distance between ICR and centre of the hip joint (l_{hi}), which reduced the extension force applied by the residual limb (F_{er}) and its corresponding leverage.

(b) Width of the top part

As per the design constraints and the tibial plateau diameter of adults, the width of the top part was fixed to be 70 mm. Figure 4.3 shows the right hand view of the top-part of the knee joint along with its dimension and clearance. A blind hole allowance was considered to be more than the radius of the hole throughout the design. Equation 4.5 relates the width of the top part along with different parameters. The dimension of r_p, l_{pa}, l_a, l_{spa} and d_{sp} was fixed to be 4, 5, 14, 2 and 2 mm, respectively based on the standard parts available in the market in order to accommodate the bolt for knee adopter, large link and small link within the available space. After substituting the corresponding values, the length of the link 0 was obtained to be 32 mm.

$$l_0 + l_a + d_{sp} + 2\left(l_{pa} + l_{spa} + r_p\right) = 70\ mm \quad \text{... (4.5)}$$

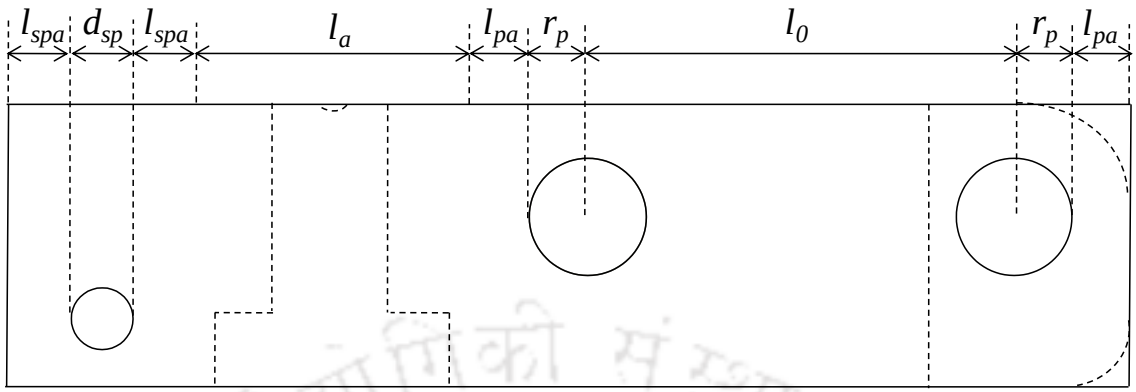

Fig. 4.3 Different dimension and clearance of right hand view of the top part of the knee joint

(c) Width of the bottom part

The width of the bottom part was also taken as 70 mm. The right hand view of the bottom part along with different parameters is shown Fig. 4.4 and the following relation was obtained.

$$l_2 + l_{sa} + d_{sp} + 2\left(l_{pa} + l_{spa} + r_p\right) = 70\ mm \quad \text{... (4.6)}$$

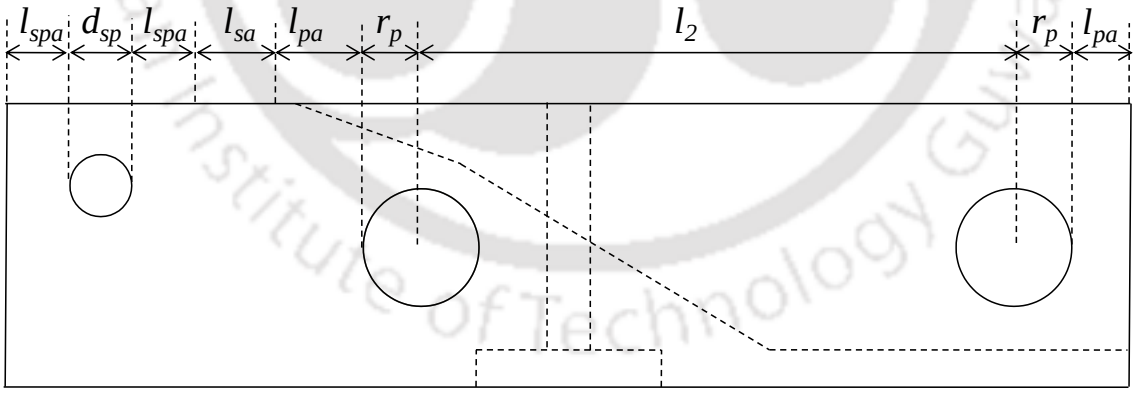

Fig. 4.4 Different dimension and clearance of right hand view of the bottom part of the knee joint

The dimension of l_{sa}, r_p, l_{pa}, l_{spa} and d_{sp} was fixed to be 4, 4, 5, 2 and 2 mm, respectively based on the standard parts available in the market and thus the length of link 2 was obtained as 42 mm from equation 4.6.

4.1.2.1 Selection of the kinematic parameters of the knee joint

From the above discussion, the length of link 0 and link 2 was obtained as 32 and 42 mm, respectively. Initially, the link 2 (l_2) was assumed to be fixed horizontally and the link 3 (l_3) was fixed perpendicular to it at one end, B, as shown in Figure 4.5.

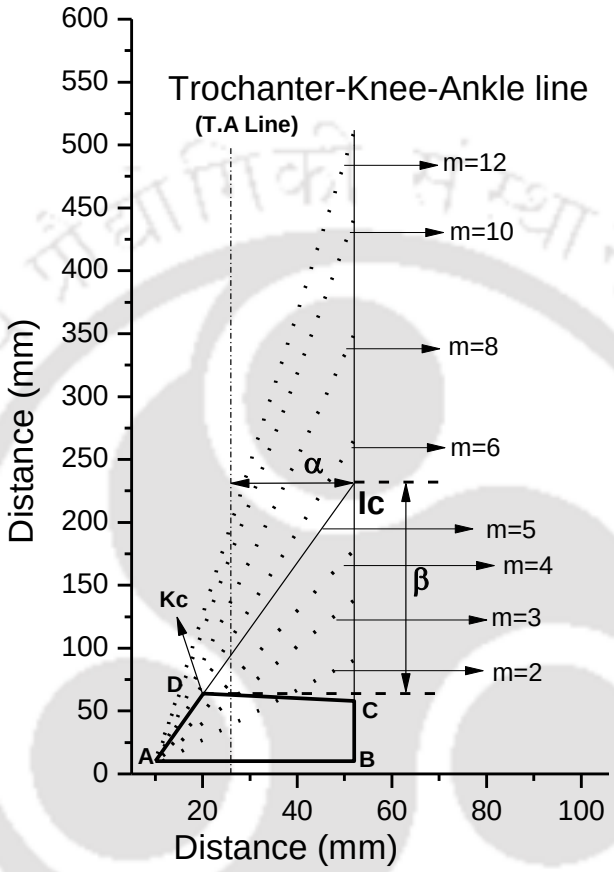

Fig. 4.5 Selection of the link parameters

Further, the link 3 (l_3) was extended from point B in order to obtain the ICR. Later, the link 1 (l_1) was drawn from other end 'A' of the link 2 with different slope (m) varying from 2 to 12 in order to obtain the kinematic parameters and suitable ICR to have the improved beta stability of the knee joint. The beta stability was measured as a vertical distance between the knee centre (Kc) and ICR. Thereafter, length of the link 0 (32mm) was fixed between link 1 and link 3 in the different slope line, as discussed above and the corresponding length of the link 1 and 3 was obtained, which satisfies the Grashof criterion. The fixation of link 0 is shown in Figure 4.5, which was termed as CD, where the point D falls on the slope 5 line and the length of the link 1 and 3 was obtained as AD and BC, respectively.

The provision for the fixation of pylon was made at the centre of the bottom part and thus the T-A line was fixed at half of the width (35 mm). Since the link 2 was noted to be 42 mm, the allowance and radius of the pin were kept as 15 and 4 mm, respectively. The distance between the point A and T-A line was obtained to be 16 mm and thus the T-A line was drawn as shown in Fig. 4.5. The alpha value is the distance between the T-A line and the ICR in horizontal direction, which was observed to be a fixed positive value of 2.6 cm and it is posterior to the T-A line.

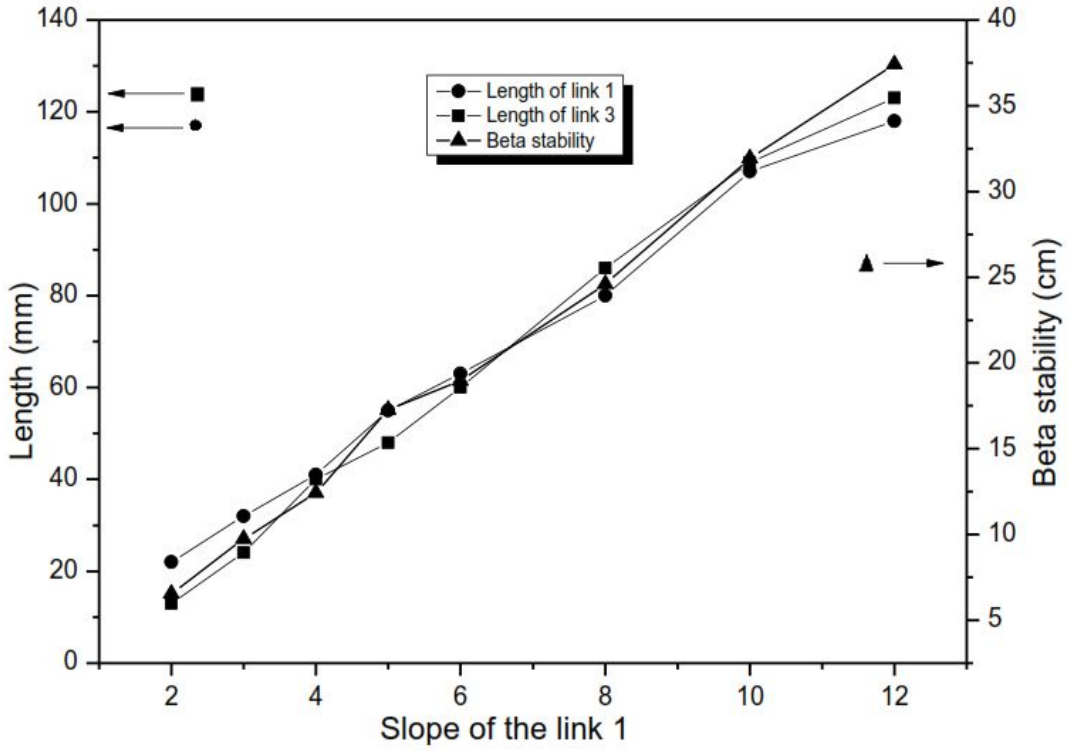

Fig. 4.6 Length of the link 1 and 3 and the beta stability against slope of the link 1

Figure 4.6 shows the length of the link 1 and 3 against the slope of link 1. It was observed that the length of link 1 and 3 was found to be increased with slope of the link 1. The l_1 for the slope line of 12, 10, 8, 6, 5, 4, 3 and 2 was found to be 118, 107, 80, 63, 55, 41, 32 and 22 mm, respectively, whereas the corresponding l_3 was observed to be 123, 109, 86, 60, 48, 40, 24 and 13 mm. Figure 4.6 also shows the beta stability of the knee joint against slope of the link 1, where it was observed that the beta stability was found to be increased with the slope. The beta stability for the slope of 2, 3, 4, 5, 6, 8, 10 and 12 was found to be 6.6, 9.8, 12.4, 17.3, 18.9, 24.6, 32 and 37.4 cm, respectively. Based on the Grashof criterion, the l_1 and l_3 obtained from the slope 5 were observed to be 55 and 48

mm, respectively. By considering the pin allowance of 5 mm on both directions of the links, the length of l_{1a} and l_{3a} was calculated to be 65 and 58 mm, respectively, where the beta stability of the knee joint was 17.3 cm. Though the slope of line 6 has the l_1 and l_3 of 63 and 60 mm, respectively along with the beta stability of 20 cm, the length of the corresponding link including the pin allowance was found to be 73 and 70 mm, where the former was found to violate the design constraints and thus it was not chosen. In case of slope 4, all the constraints were met by the parameters obtained from it and the beta stability was found to be 12.4 cm, which is nearly 40 % lower than that of the value obtained from the slope 5. Hence, the length of the link 1 and link 3 was observed to be 55 and 48 mm, respectively, along with the beta stability of 17.3 cm based on the slope 5.

All the link length obtained from the different slope of l_1 are given in Table 4.1. It was noticed that the Grashof criterion was satisfied by the all range of slope except the slope 2 and 3. As discussed, the link length of l_0, l_1, l_2 and l_3 was found to be 32, 55, 42 and 48 mm, respectively as per the slope 5.

Table 4.1 Kinematic link parameters for the different slope of the link 1

Slope	Link 0 (mm)	Link 1 (mm)	Link 2 (mm)	Link 3 (mm)	Summation of shortest and longest link length (mm)	Summation of the length of remaining two links (mm)	Grashof Criterion
12	32	118	42	123	155	160	Satisfied
10	32	107	42	109	141	149	Satisfied
8	32	80	42	86	118	122	Satisfied
6	32	63	42	60	95	102	Satisfied
5	32	55	42	48	87	90	Satisfied
4	32	41	42	40	74	81	Satisfied
3	32	32	42	24	74	56	Not Satisfied
2	32	22	42	13	55	54	Not Satisfied

4.1.2.2 Comparison of the alpha stability of newly developed knee joint with different commercially available devices

Fig. 4.7 shows the comparison of alpha (α) stability of the proposed knee joint and that of other commercially available knee joints such as Ottobock- Haderman-3R20, Ottobock 3R21 for knee disarticulation, 5H100 by US Manuf. Co., US Manuf. Co. Small polycentric knee disarticulation, Hosmer 4-Bar polycentric knee (70507), Tehlin TK-4000 and Polymatic knee joint. The corresponding data were referred from Greene [1983]. It was observed that the proposed knee joint has the positive value of 2.6 cm for the alpha stability, which was posterior to the T.A. line. Ottobock 3R21 for knee distraculation and US Manuf. Co. small polycentric knee distraculation showed the negative α value of -0.3 and -0.2 cm, respectively, which were 111.5 and 107.7 % lower than the α-stability of proposed knee joint. However, the Hosmer 4-Bar polycentric knee (70507), US Manuf. Co. (5H100), Polymatic knee joint, Ottobock- Haderman-3R20 and Tehlin TK-4000 model were found to be more stable with respective α value of 2.6, 3, 5.5, 6.7, and 10.4 cm, corresponding to the enhancement of 0, 15.4, 111.5, 157.7 and 300 % in comparison to that of proposed knee joint.

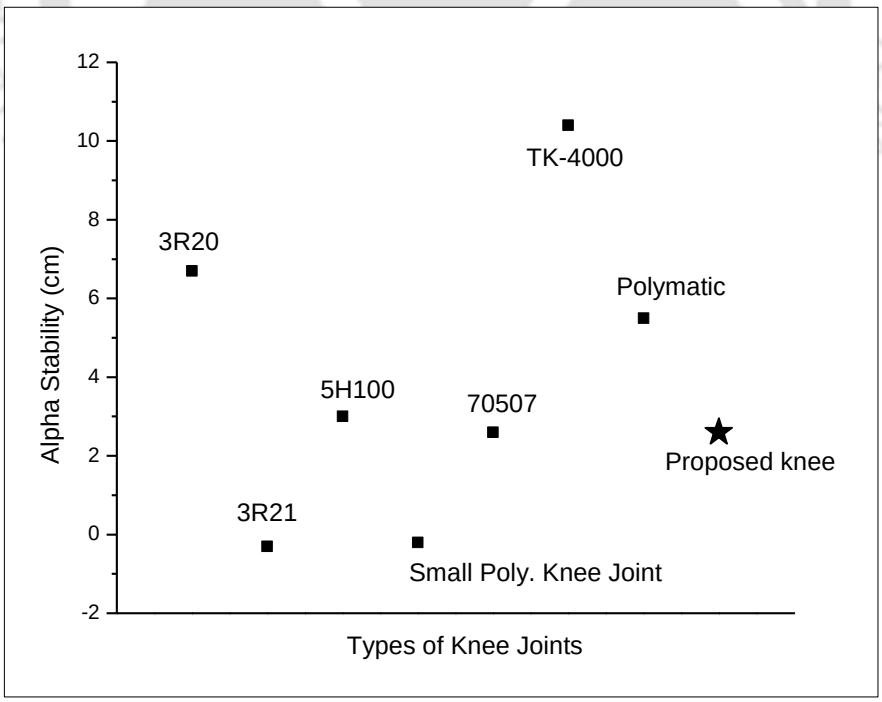

Fig. 4.7 Comparison of the alpha stability of different commercially available knee joints and that of newly developed knee joint

4.1.2.3 Comparison of the beta stability of newly developed knee joint with different commercially available devices

Fig. 4.8 shows the comparison of beta stability of different knee joints with that of the proposed knee joint. The beta stability of the proposed knee joint was found to be 17.3 cm, which was quite comparable to that of other commercially available knee joints, and it was improved by 39.3, 46.2, 73.9 and 101.1 % compared to that of the US Manuf. Co. Small polycentric knee disarticulation, US Manuf. Co. (5H100), Ottobock 3R21 for knee disarticulation and Hosmer 4-Bar polycentric knee (70507), respectively. In addition to that Ottobock- Haderman-3R20, Tehlin TK-4000 and Polymatic knee joint showed the increased β stability by 6, 72, and 73 %, respectively compared to that of proposed knee joint.

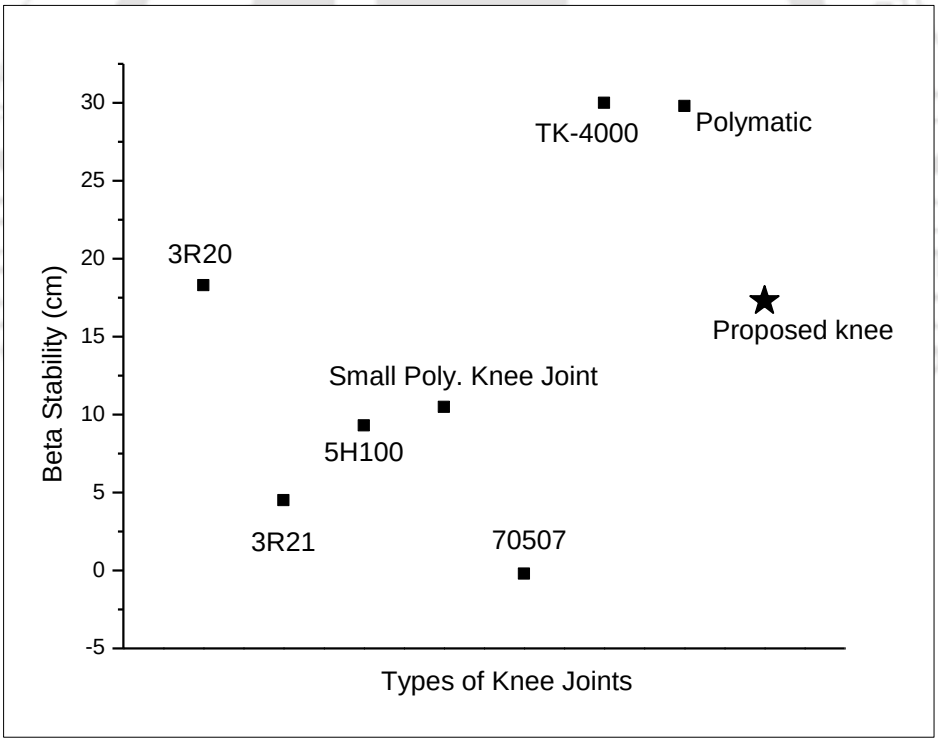

Fig. 4.8 Comparison of the beta stability of different commercially available knee joints and that of newly developed knee joint

It was observed that the alpha and beta stability of proposed knee joint were found to be the positive value, which confirmed the good stability of the proposed knee joint and also comparable with that of the commercially available knee joints.

4.1.2.4 Floor clearance of the knee joint

When the leg position is changed from full extension to flexion during the swing phase of the polycentric knee joint, the shank length gets shortened and it led to sudden fall of an amputee. In order to overcome the same, a floor clearance was made available in the polycentric knee joint. The floor clearance was calculated by measuring the length of the thigh and shank at full extension, mid swing position (65°) and sitting position. In addition, excessive floor clearance should be given to the amputees having long shank in order to sit them comfortably in a chair. In case of a small chair, a tall amputee faces uncomfortable situation due to the excessive hip flexion. Hence, the floor clearance at sitting position, the length of thigh and shank were measured at 90° flexion of the knee joint. Fig. 4.9a, b and c shows the position of thigh and shank at full extension, mid swing condition and sitting position, respectively.

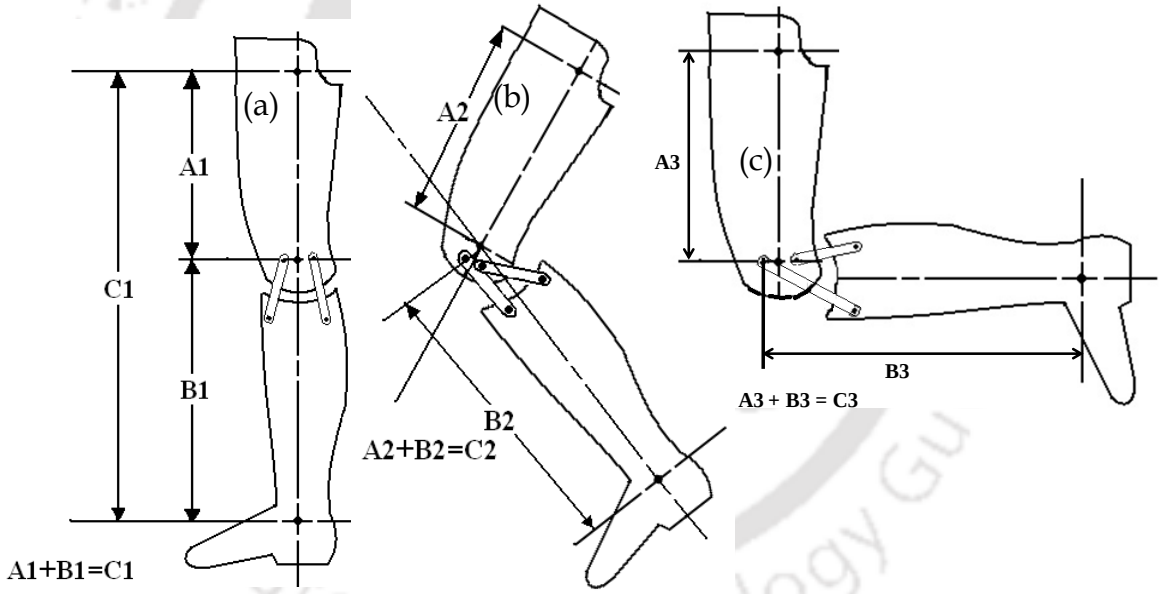

Fig. 4.9 Position of thigh and shank at (a) full extension, (b) mid swing condition and (c) sitting position

The following relations can be observed from Fig. 4.9.

$$A_1 + B_1 = C_1 \quad \ldots (4.7)$$

$$A_2 + B_2 = C_2 \quad \ldots (4.8)$$

$$A_3 + B_3 = C_3 \quad \ldots (4.9)$$

$$C_m = C_1 - C_2 \quad \ldots (4.10)$$

$$C_n = C_1 - C_3 \quad \ldots (4.11)$$

Equation 4.7, 4.8 and 4.9 describes the sum of length of thigh and shank at full extension, mid swing position and 90° flexion of the knee joint, respectively. Equation 4.10 and 4.11 denotes the floor clearance at mid swing position (C_m) and 90° flexion position (C_n), respectively and the corresponding values are found to be 1.6 and 2.3 cm. The clearance denotes the overall shortening of the prosthetic leg. Since, the floor clearance during the mid stance position was found to be less compared to that of 90° flexion, the floor clearance was adopted as 2.3 cm. It was also required that the difference in height of 2.3 cm should be maintained in the prosthetic leg compared to that of sound leg in order to avoid the uneasiness during the sitting position and fall of an amputee.

Fig. 4.10a and b shows the comparison of the floor clearance of proposed knee joint with commercially available different types of knee joints at mid swing position and 90° flexion, respectively. The floor clearance at mid swing position of proposed knee joint was found to be 1.6 cm, which was found to be 43.7, 50 and 56.3 % higher than the Tehlin TK-4000, Ottobock- Haderman-3R20 and US Manuf. Co. Small polycentric knee distraculation, respectively. In case of 90° flexion, the proposed knee joint has the floor clearance of 2.3 cm and it showed the enhancement of 4.3, 4.3, 17.4 and 95.6 % compared to that of Tehlin TK-4000, Hosmer 4-Bar polycentric knee (70507), US Manuf. Co. Small polycentric knee distraculation and Ottobock- Haderman-3R20, respectively. Other knee designs such as Polymatic knee joint, Ottobock 3R21 for knee distraculation and US Manuf. Co. (5H100) showed the respective enhancement of 43.7, 50 and 56.2 % at mid-stance and 78.3, 73.9 and 104.3 % at 90° flexion compared to that of proposed knee joint. It was observed that the floor clearance of proposed knee joint at 65° mid stance and 90° flexion was well within the range of existing commercially available knee joints.

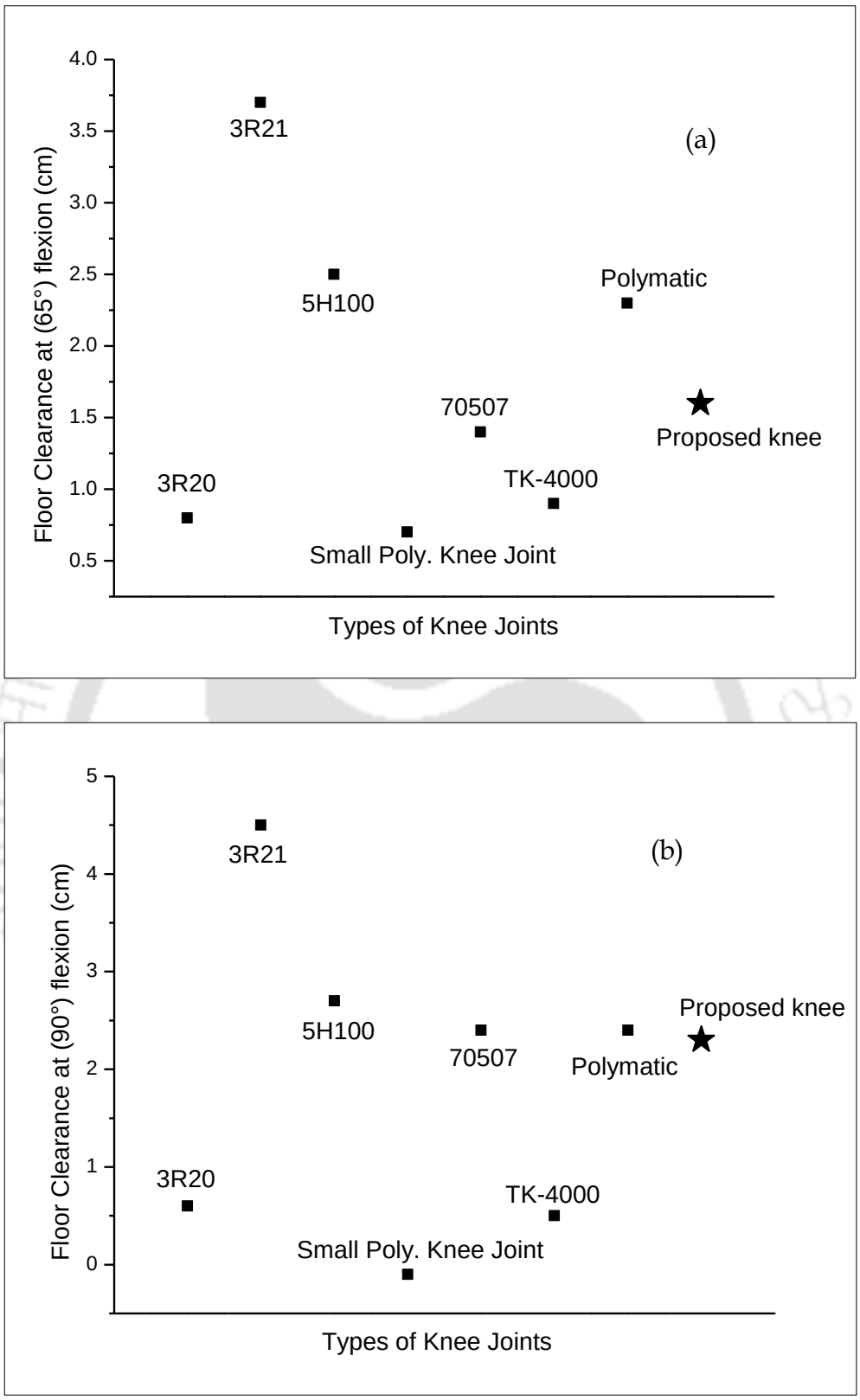

Fig. 4.10 Comparison of the floor clearance at (a) mid swing (65°) and (b) 90° flexion of the newly developed knee joint and commercially available different types of knee joints.

4.1.2.5 Design of a compression spring to integrate the polycentric and single axis knee joint

A compression spring was used to assist a pin in order to restrict the flexion-extension motion of the polycentric knee joint i.e. conversion of polycentric knee joint to single axis knee joint or vice versa.

The compression spring was assumed to be made of stainless steel and having the spring index of (C_c) 10, which is the ratio of mean coil diameter to the wire diameter of the spring. The allowable shear strength and shear modulus of stainless steel used for the spring are 358 MPa and 80 GPa, respectively, PSG data book [2015]. The design methodology of the spring was made as per the procedure cited in the design data book.

Wahl's correction factor is calculated to be

$$K_w = \frac{4C_c - 1}{4C_c - 4} + \frac{0.615}{C_c} = 1.145$$

The maximum shear stress acting on the spring is given by

$$\tau_s = \frac{8F_c K_w C_c}{\pi d_c^{\,2}} \quad \text{... (4.12)}$$

$$358 = \frac{8F_c 1.145 \times 10}{\pi d_c^{\,2}}$$

It is assumed that the allowable shear stress of the spring is equal to the maximum shear stress acting on the compression spring. By substituting the known parameters in equation (4.12), it is reduced to

$$\frac{F_c}{d_c^{\,2}} = 12.278 \quad \text{... (4.13)}$$

In order to convert the single axis knee joint to polycentric knee joint, the force required to brought down the pin using a handle is assumed to be equivalent to that the force required to open the slide barrel bolt fixed at the interior of the door and it is taken as (F_c) 3.5 N, Eastman [1986]. Using the equation (4.13), the wire diameter of the spring was calculated to be 0.55 mm and the mean coil diameter was found to be 5.5 mm.

The working deflection of the spring is given by

$$\partial = \frac{8F_c nD^3}{Gd^4} \quad \text{... (4.14)}$$

As per the proposed knee joint design, the working deflection is required to be 25 mm in order to convert the polycentric knee joint to single axis knee joint. By substituting the known values in equation 4.14, the number of active coils was calculated.

$$25 = \frac{8 \times 3.5 \times n \times 5.5^3}{80 \times 10^3 \times 0.55^4}$$

$$n = 55$$

The designed parameters of a compression spring are as follows:

Wire diameter = 0.55 mm

Mean coil diameter = 5.5 mm

Number of active coils = 55

End condition: Plain end

Material: Stainless steel

4.1.2.6 Extension assist in a prosthetic knee joint

An extension assist is the elastic or spring like material, which is used to simulate the muscular action of the quadriceps muscles. The main function of the extension assist is to restrict the knee flexion and restore the extension. It helps to increase the walking velocity of an amputee and paves a way to decrease the heel raise after toe-off or before starting the swing-phase. Once, the maximum flexion is achieved, the extension assist tends to move the leg towards the full extension and it intends to increase the cadence upto certain extent based on its stiffness. If it is not used, the amplitude of the flexion is increased and cause excessive knee flexion at mid-swing position leading to buckling of the knee joint. before heel contact and it is expected to cause damage/pain to an amputee. The extension assist also helps to control the movement of the prosthetic leg during the swing phase.

Increasing the stiffness of the extension assist creates the following difficulties to the amputees.

(a) It may lead to unstable knee flexion and uncomfortable shock to the residual stump.
(b) The increase in walking velocity of amputees leads to move the toe forward rapidly, which may raise to toe stubbing leading to accidental fall.
(c) The extension bias also creates more uncomfortable condition due to increased stiffness while sitting due to full extension of the knee.

4.1.2.7 Selecting the stiffness of an extension assist

The dynamic analysis of the proposed passive polycentric knee joint was carried out in ADAMS and the stiffness of an extension spring was choosed using the following constraints.

- Only swing phase was simulated during the dynamic analysis.
- The weight of the foot adapter cum Solid Ankle Cushion Heel (SACH) foot and pylon was taken as 650 and 330 g, respectively, (http://www.protechortho.com/index.php)
- The length of the pylon was taken as 500 mm, (http://www.protechortho.com/index.php)
- Initial torque was given to the pylon to lift the leg

The stiffness of an extension assist was selected in the range of 0.25, 0.5, 0.75, 1, 2, 4, 8, 16 and 32 N/mm with the applied torque of 2000 N-mm, Ishai et al. [1983], in order to avoid the fall of an amputee and to achieve the smooth flexion-extension using the prosthetic leg.

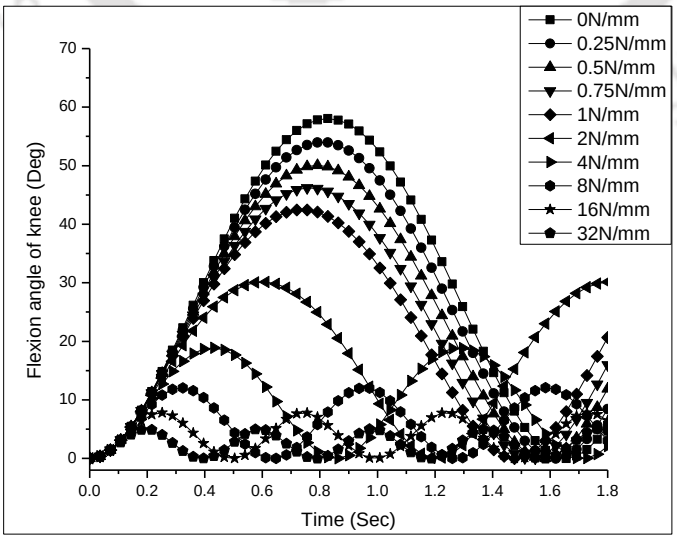

Fig. 4.11 Flexion angle of knee against different stiffness of an extension assist

Fig. 4.11 shows the influence of stiffness of an extension assist on the flexion angle of the knee joint against time and it was observed that the maximum flexion angle and the time required to reach the maximum flexion angle were found to be decreased with an increase of stiffness.

Table 4.2 Gait parameters with different stiffness of an extension assist

Stiffness (N/mm)	Extension Assist	Maximum Flexion		Flexion Duration		Walking Speed	
		(deg)	% Reduction	(sec)	% Reduction	(m/s)	% Increase
0	No Spring	58.18	-	0.82	-	0.83	-
0.25	Single	54	7.2	0.78	4.9	0.85	1.9
0.5	Single	50.63	13.0	0.74	9.8	0.90	7.8
0.75	Single	46.58	20.0	0.71	13.4	0.92	10.0
1	Single	42.94	26.2	0.67	18.3	0.94	12.2
2	Single	30.35	47.8	0.57	30.5	1.15	37.5
4	Single	19.18	67.0	0.4	51.2	1.62	94.1
8	Single	12.5	78.5	0.3	63.4	2.19	161.9
16	Single	8.03	86.2	0.25	69.5	2.70	223.5
32	Single	5.18	91.0	0.18	78.0	3.45	312.5

Table 4.2 shows the effect of stiffness on different gait parameters of the knee joint, and it is noted that the maximum flexion angle and flexion duration of the knee joint were found to be decreased by 7.2, 13, 20, 26.2, 47.8, 67, 78.5, 86.2 and 91 % and 4.8, 9.8, 13.4, 18.3, 30.5, 51.2, 63.4, 69.5 and 78 % for 0.25, 0.5, 0.75, 1, 2, 4, 8, 16 and 32 N/mm of stiffness of an extension assist, respectively compared to no spring condition, whereas the corresponding walking velocity of the knee joint was increased by 1.9, 7.9, 10, 12.2, 37.5, 94.1, 161.9, 223.5 and 312.5 %. As the daily activities such as shopping, gardening and household tasks are categorized as low activity, which can afford low stiffness extension bias in order to avoid the heel raise. Hence, the stiffness of an extension assist for low activity user was selected to be 0.5 N/mm based on the reduction of maximum

flexion and flexion duration by 13 and 9.8 %, respectively and 7.8 % increase of walking speed and the same is expected to provide smooth movement of the stump with required heel raise and negligible fall of an amputee. A similar method was also used by Furse et al. [2011] to select the extension assist, where 10.5 % increase of walking speed, 11.7 and 16.7 % reduction of maximum flexion angle and flexion duration, respectively were reported.

The parallel arrangement of an extension assist was incorporated by means of a simply supported beam in order to share the load equally by the two springs, where the equivalent spring stiffness of 0.5 N/mm and individual spring stiffness of 0.25 N/mm were maintained.

4.1.2.8 Design of an extension spring

During the flexion condition, the extension spring stores the energy in addition to restricting the maximum flexion in order to avoid the buckling. It also helps to bring back the leg from the maximum flexion condition to full extension without increasing the metabolic cost of an amputee.

The tension spring was assumed to be made of stainless steel and having the spring index of (C_t) 10. The design methodology of the spring was made as per the procedure cited in the PSG data book [2015].

Wahl's correction factor is calculated to be

$$K_w = \frac{4C_t - 1}{4C_t - 4} + \frac{0.615}{C_t} = 1.145$$

The maximum shear stress acting on the spring is given by

$$\tau_s = \frac{8F_t K_s C_t}{\pi d_t^{\,2}} \qquad \text{... (4.15)}$$

It is assumed that the allowable shear stress of the spring is equal to the maximum shear stress acting on the tension spring. The allowable shear strength and shear modulus of stainless steel used for the spring are 358 MPa and 80 GPa, respectively, PSG data book [2015]. By substituting the known parameters in equation (4.15), it is reduced to

$$358 = \frac{8F_t \times 1.145 \times 10}{\pi d_t^{\,2}},$$

$$\frac{F_t}{d_t^{\,2}} = 12.278 \qquad \text{... (4.16)}$$

Based on the hand's strength required to extend the tension spring, F_t was assumed to be 6 N, Eastman [1986]. Using the equation (4.16), the wire diameter of the spring was calculated to be 0.7 mm and the mean coil diameter was found to be 7 mm.

The stiffness of the spring is

$$K_t = \frac{Gd_t^{\,4}}{8n_t D_t^{\,3}} \qquad \text{... (4.17)}$$

As per the dynamic simulation discussed in section 4.1.2.7, the stiffness of the extension spring was chosen to be 0.25 N/mm.

Substitute the known parameters in equation (4.17), the number of active coils was calculated to be

$$\frac{80 \times 10^3 \times (0.7)^4}{8 \times n_t \times 7^3} = 0.25$$

$$n_t = 27.98 \approx 28$$

Initial tension

For C_t = 10, the initial shear stress (τ_i) varies from 60-100 N/mm², PSG data book, [2015]

The initial tension of the spring is given by

$$T_i = \frac{\pi \tau_i d_t^{\,3}}{8D_t} \qquad \text{... (4.18)}$$

Substituting the known values in equation (4.18)

$$T_i = \frac{\pi \times 80 \times 0.7^3}{8 \times 7} = 1.54N$$

Single full loop over centre hook was chosen for the extension spring based on the holding beam, which also helps in distributing the stress gradually throughout the hook.

The design parameters of tension spring are as follows:

Wire diameter = 0.7 mm

Mean coil diameter = 7 mm

Number of active coils = 28

Hook type: full loop over centre hook

Material: Stainless steel

4.1.2.9 Important features of the proposed knee joint

As the knee joint is proposed to be made of a polymeric material, the weight and the terminal impact of the knee joint are expected to be decreased significantly. The polymer also acts as a damper to absorb the shock during the full extension condition. The walking speed of the knee joint is increased with the addition of a spring as an extension assist, whereas the heel raise and the duration of swing phase are noted to be decreased. By adding a washer wherever the metal and metal interface come, it is expected to decrease the heel raise and flexion amplitude by increasing the friction between them, Furse et al. [2011].

Fig. 4.12 shows the different parts of the proposed polycentric knee joint. It consists of a top part, bottom part, small link and large link pivoted as a multi body system to achieve the flexion-extension of the prosthetic leg. The link assembly of the knee joint is made of a rigid polymer, which provides the required relative motion, compact and cost effective. The knee joint is provided with non-rotatable adapter coupled firmly to transfer the load from the stump of an amputee via socket. A compression spring along with a cylindrical rod is positioned in the interior of the bottom part, which provides the engaging and disengaging of the top and bottom part corresponding to switch over between the single axis knee joint and the polycentric knee joint or vice versa. The extension bias is also achieved with the spring assisted system using a simply supported beam and it was made using two parallel extension springs in a symmetric manner in top and bottom part of the knee joint, where the stability of the joint during

the flexion-extension motion, swing phase and stance phase is maintained. The extension springs aid to bring the knee joint back to original position after flexion. Because of the inherent self lubricating characteristics of the Nylon, which is selected to check the design feasibility, wear occurred between the top and bottom part of the knee joint is reduced. Hence, a light weight-passive- prosthetic knee joint made of a polymer was designed and developed along with spring assisted extension bias to have the required stability. It has the significant advantages such as light weight, inexpensive, high stability, compatible knee adapter, extension bias, integrated form of polycentric and single axis knee joint, durability and compression spring for single axis access.

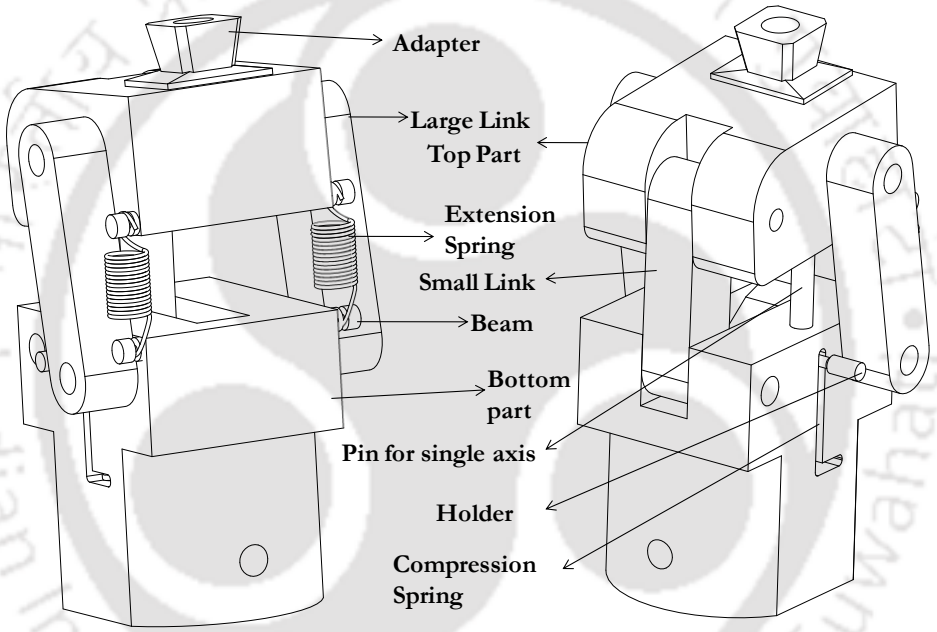

Fig. 4.12 Different parts of a polycentric knee joint

4.1.2.10 Stress analysis and fabrication of a knee joint

The stress analysis of the knee joint was made as per Von Mises stress theory to confirm the ductile failure. Fig. 4.13 shows the Von Mises stress pattern of the knee joint. The boundary condition was considered by fixing the bottom part and the loading was given on top of the knee joint. The boundary condition of P6 (4860N) as per ISO 10328 loading was selected from the top of the knee joint, whereas the bottom section of the knee joint has displacement constraint in all the directions. Rigid body contact element was used in all the contact points throughout the analysis. The maximum Von Mises stress was observed to be 30 MPa. Since, the yield strength of the Nylon-66 was 58 MPa,

Endura Plastic [2015] and it is inexpensive compared to other engineering polymers, the nylon was chosen as a material for the knee joint. It is also noted that the stress developed was less than that of the yield stress of the material selected and the knee joint was manufactured using the conventional machining process. The fabricated knee joint in different views are shown in Fig. 4.14.

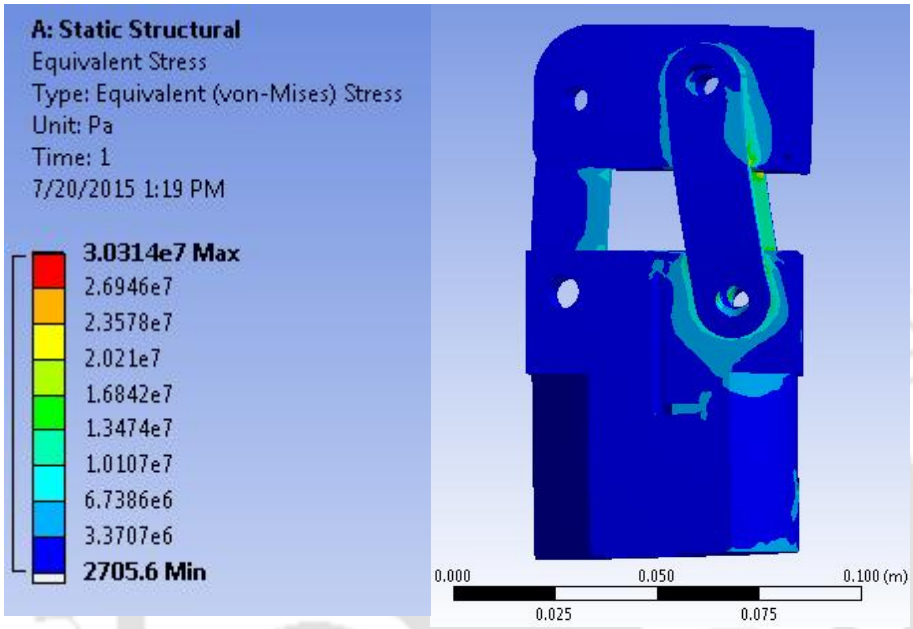

Fig. 4.13 Von Mises stress developed in the polycentric knee joint

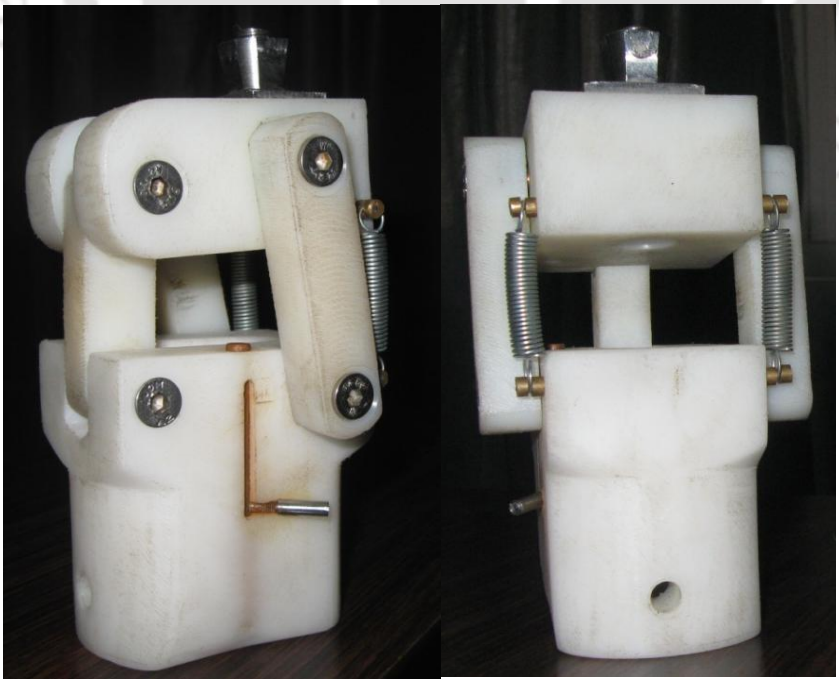

Fig. 4.14 Fabricated polycentric knee joint

4.1.3 Dynamic analysis of the knee joint

The gait pattern of a human walking cycle is one of the most important parameters for the lower extremity amputee. Faramand et al. [2006] reported that the mathematical modelling can be effectively used to study the dynamic characteristics of the lower limb. Several theoretical models were proposed to derive the equation of motion including swing and stance phase of the knee joint, Shandiz et al. [2009]. However, the equation of motion of the passive polycentric knee joint with extension assist is yet to be reported, as per author's knowledge, which can predict the effective functioning of the extension unit to improve the performance of a knee joint.

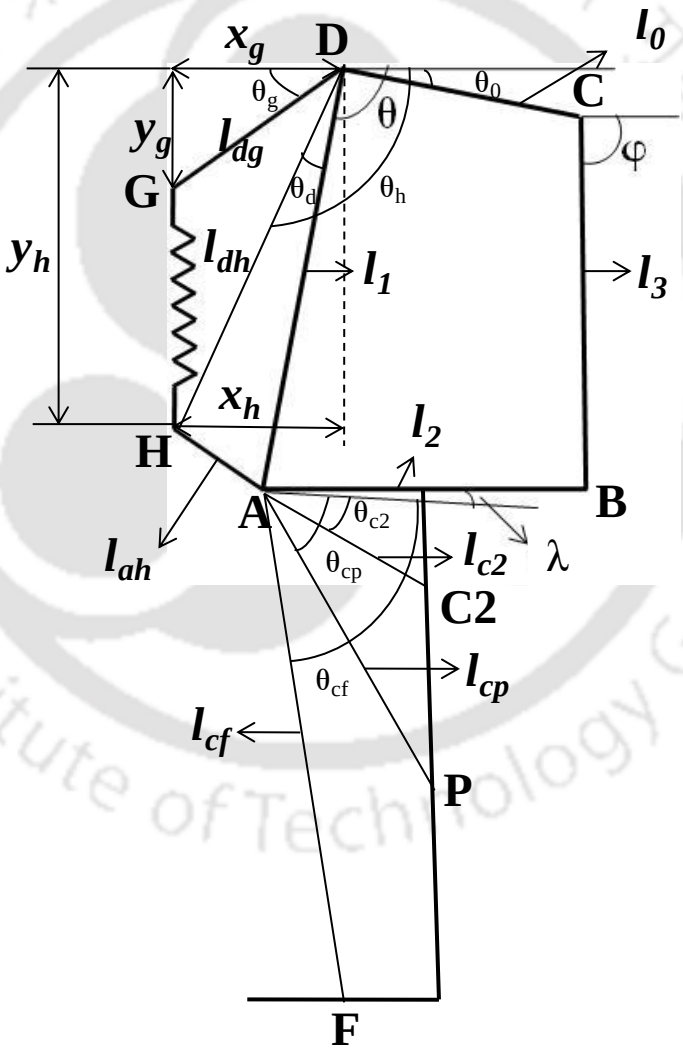

Fig. 4.15 Rigid body model of the passive polycentric knee joint

A two-dimensional prosthetic leg from knee joint to foot along with an extension unit was considered for the dynamic analysis. The system consists of a knee joint having four links, an extension spring, a pylon and foot, where pylon and foot were fixed with bottom part of the knee joint. The equation of motion of the above system was derived using Euler-Lagrangian equation along with energy approach. Mark et al. [1992] also used the same kind of approach for the dynamic analysis of the robotic links. The dynamic equation was obtained by taking three generalized coordinates such as φ, θ and λ. Later, θ and λ were replaced in terms of φ. Hence, the dynamic equation was obtained with a generalized coordinate. Tang [2006] also discussed the minimal coordinate for obtaining the dynamic equation of the four-bar mechanism. All the angles were incorporated using positive direction approach, as discussed by Ackermann et al. [2009]. Fig. 4.15 depicts the rigid body model of the passive polycentric knee joint along with an extension unit.

4.1.3.1 Position analysis

The position analysis starts with the loop closure equation of the four-bar mechanism.

$$l_2 \cos\lambda = l_0 \cos\theta_0 + l_3 \cos\varphi - l_1 \cos\theta \quad \ldots (4.19)$$

$$l_2 \sin\lambda = l_0 \sin\theta_0 + l_3 \sin\varphi - l_1 \sin\theta \quad \ldots (4.20)$$

The loop closure equations 4.19 and 4.20 were adopted from Freudenstein equation, which is generally used in four-bar linkages, Freudenstein [1954]. The above loop closure equation gives the relation between the link length and angle of all the links in the knee joint. In the present work, the θ and λ were replaced in terms of φ. Thus, the equation 4.19 and 4.20 were rearranged to obtain θ in terms of φ.

Sum of the square of equation 4.19 and 4.20 gives

$$(2l_1l_3\sin\phi + 2l_1l_0\sin\theta_0)\sin\theta + (2l_1l_3\cos\phi + 2l_1l_0\cos\theta_0)\cos\theta + l_2^2 - l_0^2 - l_1^2 - l_3^2 - 2l_0l_3\cos\phi\cos\theta_0 - 2l_0l_3\sin\phi\sin\theta_0 = 0 \quad \ldots (4.21)$$

The equation 4.21 can be written as

$$k_1(\phi)\sin\theta + k_2(\phi)\cos\theta + k_3(\phi) = 0$$

where,

$$k_1 = 2l_1l_3\sin\phi + 2l_1l_0\sin\theta_0$$

$$k_2 = 2l_1l_3\cos\phi + 2l_1l_0\cos\theta_0$$

$$k_3 = l_2^{\,2} - l_0^{\,2} - l_1^{\,2} - l_3^{\,2} - 2l_0l_3\cos\phi\cos\theta_0 - 2l_0l_3\sin\phi\sin\theta_0$$

Let,

$$t = \tan\frac{\phi}{2}\ ,\ \sin\phi = \frac{2t}{1+t^2}\ ,\ \cos\phi = \frac{1-t^2}{1+t^2}$$

Substituting the above values in equation 4.21, it is simplified as:

$$(k_3 - k_2)t^2 + 2k_1t + (k_3 + k_2) = 0 \qquad \ldots (4.22)$$

Solving the quadratic equation (4.22), the value of 't' becomes

$$t = \frac{-k_1 \pm \sqrt{k_1^{\,2} + k_2^{\,2} - k_3^{\,2}}}{k_3 - k_2} \qquad \ldots (4.23)$$

$$\theta(\phi) = 2\tan^{-1}\left[\frac{-k_1 \pm \sqrt{k_1^{\,2} + k_2^{\,2} - k_3^{\,2}}}{k_3 - k_2}\right] \qquad \ldots (4.24)$$

Now, in order to get λ, divide the equation (4.20) and (4.19)

$$\lambda(\phi,\theta) = \tan{-1}\left[\frac{l_0\sin\theta_0 + l_3\sin\varphi - l_1\sin\theta}{l_0\cos\theta_0 + l_3\cos\varphi - l_1\cos\theta}\right] \qquad \ldots (4.25)$$

Substituting 'θ' in equation 4.25, it becomes

$$\lambda(\phi) = \tan{-1}\left[\frac{l_0\sin\theta_0 + l_3\sin\varphi - l_1\sin\left[2\tan^{-1}\left[\frac{-k_1 \pm \sqrt{k_1^{\,2} + k_2^{\,2} - k_3^{\,2}}}{k_3 - k_2}\right]\right]}{l_0\cos\theta_0 + l_3\cos\varphi - l_1\cos\left[2\tan^{-1}\left[\frac{-k_1 \pm \sqrt{k_1^{\,2} + k_2^{\,2} - k_3^{\,2}}}{k_3 - k_2}\right]\right]}\right] \qquad \ldots (4.26)$$

The above equations 4.24 and 4.26 relate the θ and λ in term of φ.

4.1.3.2 Velocity Analysis

The velocity analysis was carried out by differentiating the loop closure equation 4.19 and 4.20, and it was written in a matrix form.

$$\begin{pmatrix} l_1\sin\theta & l_2\sin\lambda & -l_3\sin\varphi \\ -l_1\cos\theta & -l_2\cos\lambda & l_3\cos\varphi \\ 0 & 0 & 0 \end{pmatrix}\begin{pmatrix} \dot{\theta} \\ \dot{\lambda} \\ \dot{\varphi} \end{pmatrix}=\begin{pmatrix} 0 \\ 0 \\ 0 \end{pmatrix}$$

$$\begin{pmatrix} \dot{\theta} \\ \dot{\lambda} \end{pmatrix}=\begin{pmatrix} \dfrac{l_3\sin(\lambda-\varphi)}{l_1\sin(\lambda-\theta)} \\ \dfrac{l_3\sin(\varphi-\theta)}{l_2\sin(\lambda-\theta)} \end{pmatrix}\dot{\varphi} \qquad \ldots (4.27)$$

Substituting equation (4.25) and (4.26) in equation (4.27), it can be written as

$$\dot{\theta}=\left[\frac{l_3\sin(\lambda-\varphi)}{l_1\sin(\lambda-\theta)}\right]\dot{\varphi}$$

$$=\left[\frac{l_3\sin\left(\left[\tan{-1}\left[\dfrac{l_0\sin\theta_0+l_3\sin\varphi-l_1\sin\left[2\tan^{-1}\left[\dfrac{-k_1\pm\sqrt{k_1^{\,2}+k_2^{\,2}-k_3^{\,2}}}{k_3-k_2}\right]\right]}{l_0\cos\theta_0+l_3\cos\varphi-l_1\cos\left[2\tan^{-1}\left[\dfrac{-k_1\pm\sqrt{k_1^{\,2}+k_2^{\,2}-k_3^{\,2}}}{k_3-k_2}\right]\right]}\right]\right]-\varphi\right)}{l_1\sin\left(\left[\tan{-1}\left[\dfrac{l_0\sin\theta_0+l_3\sin\varphi-l_1\sin\left[2\tan^{-1}\left[\dfrac{-k_1\pm\sqrt{k_1^{\,2}+k_2^{\,2}-k_3^{\,2}}}{k_3-k_2}\right]\right]}{l_0\cos\theta_0+l_3\cos\varphi-l_1\cos\left[2\tan^{-1}\left[\dfrac{-k_1\pm\sqrt{k_1^{\,2}+k_2^{\,2}-k_3^{\,2}}}{k_3-k_2}\right]\right]}\right]\right]-2\tan^{-1}\left[\dfrac{-k_1\pm\sqrt{k_1^{\,2}+k_2^{\,2}-k_3^{\,2}}}{k_3-k_2}\right]\right)}\right]\dot{\varphi}=S_1\dot{\varphi}$$

… (4.28)

$$\dot{\lambda}=\left[\frac{l_3\sin(\varphi-\theta)}{l_2\sin(\lambda-\theta)}\right]\dot{\varphi}$$

$$=\left[\frac{l_3\sin\left(\varphi-2\tan^{-1}\left[\dfrac{-k_1\pm\sqrt{k_1^{\,2}+k_2^{\,2}-k_3^{\,2}}}{k_3-k_2}\right]\right)}{l_2\sin\left(\left(\tan{-1}\left[\dfrac{l_0\sin\theta_0+l_3\sin\varphi-l_1\sin\left(2\tan^{-1}\left[\dfrac{-k_1\pm\sqrt{k_1^{\,2}+k_2^{\,2}-k_3^{\,2}}}{k_3-k_2}\right]\right)}{l_0\cos\theta_0+l_3\cos\varphi-l_1\cos\left(2\tan^{-1}\left[\dfrac{-k_1\pm\sqrt{k_1^{\,2}+k_2^{\,2}-k_3^{\,2}}}{k_3-k_2}\right]\right)}\right]\right)-2\tan^{-1}\left[\dfrac{-k_1\pm\sqrt{k_1^{\,2}+k_2^{\,2}-k_3^{\,2}}}{k_3-k_2}\right]\right)}\right]\dot{\varphi}=S_2\dot{\varphi}$$

… (4.29)

Where,

$$S_1 = \left[\frac{l_3 \sin\left(\left[\tan{-1} \left[\frac{l_0 \sin\theta_0 + l_3 \sin\varphi - l_1 \sin\left[2\tan^{-1}\left[\frac{-k_1 \pm \sqrt{k_1^{\,2} + k_2^{\,2} - k_3^{\,2}}}{k_3 - k_2} \right] \right]}{l_0 \cos\theta_0 + l_3 \cos\varphi - l_1 \cos\left[2\tan^{-1}\left[\frac{-k_1 \pm \sqrt{k_1^{\,2} + k_2^{\,2} - k_3^{\,2}}}{k_3 - k_2} \right] \right]} \right] \right] - \varphi \right)}{l_1 \sin\left(\left[\tan{-1} \left[\frac{l_0 \sin\theta_0 + l_3 \sin\varphi - l_1 \sin\left[2\tan^{-1}\left[\frac{-k_1 \pm \sqrt{k_1^{\,2} + k_2^{\,2} - k_3^{\,2}}}{k_3 - k_2} \right] \right]}{l_0 \cos\theta_0 + l_3 \cos\varphi - l_1 \cos\left[2\tan^{-1}\left[\frac{-k_1 \pm \sqrt{k_1^{\,2} + k_2^{\,2} - k_3^{\,2}}}{k_3 - k_2} \right] \right]} \right] \right] - 2\tan^{-1}\left[\frac{-k_1 \pm \sqrt{k_1^{\,2} + k_2^{\,2} - k_3^{\,2}}}{k_3 - k_2} \right] \right)} \right]$$

$$S_2 = \left[\frac{l_3 \sin\left(\varphi - 2\tan^{-1}\left[\frac{-k_1 \pm \sqrt{k_1^{\,2} + k_2^{\,2} - k_3^{\,2}}}{k_3 - k_2} \right] \right)}{l_2 \sin\left(\left[\tan{-1} \left[\frac{l_0 \sin\theta_0 + l_3 \sin\varphi - l_1 \sin\left(2\tan^{-1}\left[\frac{-k_1 \pm \sqrt{k_1^{\,2} + k_2^{\,2} - k_3^{\,2}}}{k_3 - k_2} \right] \right)}{l_0 \cos\theta_0 + l_3 \cos\varphi - l_1 \cos\left(2\tan^{-1}\left[\frac{-k_1 \pm \sqrt{k_1^{\,2} + k_2^{\,2} - k_3^{\,2}}}{k_3 - k_2} \right] \right)} \right] \right] - 2\tan^{-1}\left[\frac{-k_1 \pm \sqrt{k_1^{\,2} + k_2^{\,2} - k_3^{\,2}}}{k_3 - k_2} \right] \right)} \right]$$

Equation 4.28 and 4.29 can be used to determine the velocity of $\dot{\theta}$ and $\dot{\lambda}$ in terms of $\dot{\varphi}$.

4.1.3.3 Length of an extension assist

It is noted from Fig. 4.16 that the point G (a point connecting the extension assist on top part of the knee joint) was fixed in the top part. Since the top part was fixed, G was not having any relative motion with respect to the bottom part. As the bottom part was moving with respect to the top part, the point H (a point connecting the extension assist on bottom part of the knee joint) was found to have the relative motion. The reference was chosen as D, which is a pin joint connecting the link 0 and link 1. The distance between G and H is the length of the extension assist, which was derived analytically and it is given below:

Applying cosine rule in the triangle HDA in Fig. 4.16.

$$\cos\theta_d = \frac{l_{dh}^{\,2} + l_1^{\,2} - l_{ah}^{\,2}}{2 l_{dh} l_1}$$

$$\theta_d = \cos^{-1}\left[\frac{l_{dh}^{\ 2} + l_1^{\ 2} - l_{ah}^{\ 2}}{2 l_{dh} l_1}\right]$$

$\theta_h = \theta + \theta_d$; $x_{dg} = l_{dg}\cos\theta_g$; $y_{dg} = l_{dg}\sin\theta_g$; $x_{dh} = l_{dh}\cos\theta_h$ and $y_{dh} = l_{dh}\sin\theta_h$

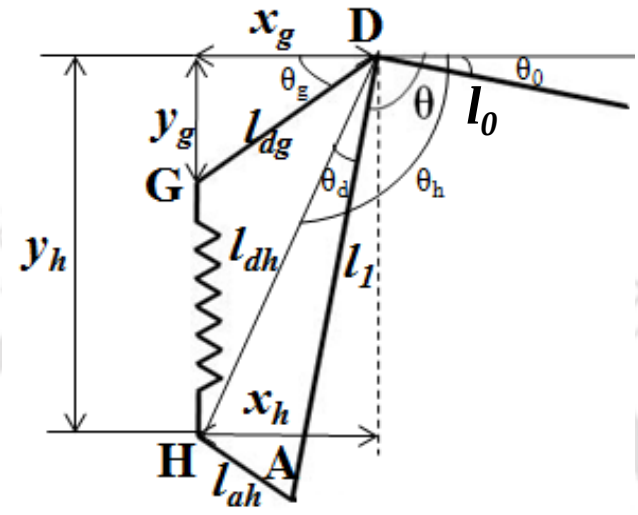

Fig. 4.16 Rigid body model of an extension assist

The length of the extension assist (GH) at any instant was derived using the distance formula between G and H as shown below and it is denoted by *e*.

$$e = \sqrt{(x_{dh} - x_{dg})^2 + (y_{dh} - y_{dg})^2}$$

$$e = \sqrt{l_{dh}^{\ 2}\cos^2\theta_h + l_{dg}^{\ 2}\cos^2\theta_g - 2 l_{dg} l_{dh}\cos\theta_g\cos\theta_h + l_{dh}^{\ 2}\sin^2\theta_h + l_{dg}^{\ 2}\sin^2\theta_g - 2 l_{dg} l_{dh}\sin\theta_g\sin\theta_h} \quad \ldots (4.30)$$

Using the equation 4.30, the length of the extension assist during the dynamic condition of the knee joint can be obtained.

4.1.3.4 Lagrangian Formulation

The Lagrangian of the total system is used to derive the equation of motion of the system, which is defined as the difference between total kinetic energy and the total potential energy.

Kinetic Energy

The total kinetic energy of the system is the summation of kinematic energy of link 1, link 2, link 3, pylon and foot, which is given below:

$$T = \underbrace{\frac{1}{2}m_1 V_{c1}^{\ 2} + \frac{1}{2}I_1\dot{\theta}^{2}}_{\text{KE of link 1}} + \underbrace{\frac{1}{2}m_2 V_{c2}^{\ 2} + \frac{1}{2}I_2\dot{\lambda}^{2}}_{\text{KE of link 2}} + \underbrace{\frac{1}{2}m_3 V_{c3}^{\ 2} + \frac{1}{2}I_3\dot{\varphi}^{2}}_{\text{KE of link 3}} + \underbrace{\frac{1}{2}m_p V_{cp}^{\ 2} + \frac{1}{2}I_p\dot{\lambda}^{2}}_{\text{KE of pylon}} + \underbrace{\frac{1}{2}m_f V_{cf}^{\ 2} + \frac{1}{2}I_f\dot{\lambda}^{2}}_{\text{KE of foot}}$$

… (4.31)

Where the velocity of each link was derived by taking top part as a reference and it is given below

$$|V_{c1}|^2 = l_{c1}^{\ 2}\dot{\theta}^{2}$$

$$|V_{c2}|^2 = \left[l_1\dot{\theta} + l_{c2}\left(\theta_{c2} + \dot{\lambda}\right)\right]^2$$

$$|V_{cp}|^2 = \left[l_1\dot{\theta} + l_{cp}\left(\theta_{cp} + \dot{\lambda}\right)\right]^2$$

$$|V_{cf}|^2 = \left[l_1\dot{\theta} + l_{cf}\left(\theta_{cf} + \dot{\lambda}\right)\right]^2$$

$$|V_{c3}|^2 = l_{c3}^{\ 2}\dot{\varphi}^{2}$$

Potential Energy

$$V = m_1 g y_1 + m_2 g y_2 + m_3 g y_3 + m_p g y_p + m_f g y_f + \frac{1}{2}ke^2 \qquad \text{… (4.32)}$$

V= PE of link 1+ PE of link 2+ PE of link 3+ PE of pylon + PE of foot+ elastic potential energy of extension assist

Where, the vertical distance between the centre of mass of each link and its respective reference point is shown below,

$y_1 = l_{c1}\sin\theta$, $lc_1 = \frac{l_1}{2}$, $y_2 = l_1\sin\theta + l\,c_2\sin(\theta_{c2} + \lambda)$, $y_3 = l_{c3}\sin\varphi$, $l_{c3} = \frac{l_3}{2}$,

$y_p = l_1\sin\theta + l_{cp}\sin(\theta_{cp} + \lambda)$ and $y_f = l_1\sin\theta + l_{cf}\sin(\theta_{cf} + \lambda)$

The Lagrangian of the total system is calculated as

$$L = T - V$$

$$L = \left[\frac{1}{2}m_1 l_{c1}^{\ 2} + \frac{1}{2}I_1 + \frac{1}{2}m_2 l_1^{\ 2} + \frac{1}{2}m_p l_1^{\ 2} + \frac{1}{2}m_f l_1^{\ 2}\right]\dot{\theta}^2$$
$$+\left[\frac{1}{2}m_2 l_{c2}^{\ 2} + \frac{1}{2}I_2 + \frac{1}{2}m_p l_{cp}^{\ 2} + \frac{1}{2}I_p + \frac{1}{2}m_f l_{cf}^{\ 2} + \frac{1}{2}I_f\right]\dot{\lambda}^2 + \left[\frac{1}{2}m_3 l_{c3}^{\ 2} + \frac{1}{2}I_3\right]\dot{\varphi}^2$$
$$+\left[m_2 l_{c2}^{\ 2}\theta_{c2} + m_p l_{cp}^{\ 2}\theta_{cp} + m_f l_{cf}^{\ 2}\theta_{cf}\right]\dot{\lambda}$$
$$+\left[m_2 l_1 l_{c2}\theta_{c2}\cos\left[\theta-(\theta_{c2}+\lambda)\right] + m_p l_1 l_{cp}\theta_{cp}\cos\left[\theta-(\theta_{cp}+\lambda)\right] + m_f l_1 l_{cf}\theta_{cf}\cos\left[\theta-(\theta_{cf}+\lambda)\right]\right]\dot{\theta}+$$
$$\left[m_2 l_1 l_{c2}\cos\left[\theta-(\theta_{c2}+\lambda)\right] + m_p l_1 l_{cp}\cos\left[\theta-(\theta_{cp}+\lambda)\right] + m_f l_1 l_{cf}\cos\left[\theta-(\theta_{cf}+\lambda)\right]\right]\dot{\theta}\dot{\lambda}+$$
$$\left[\begin{array}{l}\frac{1}{2}m_2 l_{c2}^{\ 2}\theta_{c2}^{\ 2} + \frac{1}{2}m_p l_{cp}^{\ 2}\theta_{cp}^{\ 2} + \frac{1}{2}m_f l_{cf}^{\ 2}\theta_{cf}^{\ 2} - m_1 g l_{c1}\sin\theta - m_2 g l_1\sin\theta - m_2 g l_{c2}\sin(\theta_{c2}+\lambda)\\ -m_3 g l_{c3}\sin\varphi - m_p g l_1\sin\theta - m_p g l_{cp}\sin(\theta_{cp}+\lambda) - m_f g l_1\sin\theta - m_f g l_{cf}\sin(\theta_{cf}+\lambda)\end{array}\right]$$
$$-\frac{1}{2}k\left(\begin{array}{l}l_{dh}^{\ 2}\cos^2(\theta+\theta_d) + l_{dg}^{\ 2}\cos^2\theta_g - 2l_{dg}l_{dh}\cos\theta_g\cos(\theta+\theta_d)\\ +l_{dh}^{\ 2}\sin^2(\theta+\theta_d) + l_{dg}^{\ 2}\sin^2\theta_g - 2l_{dg}l_{dh}\sin\theta_g\sin(\theta+\theta_d)\end{array}\right)$$

and it is simplified as

$$L\left(\theta,\lambda,\varphi,\dot{\theta},\dot{\lambda},\dot{\varphi}\right) = J_1\dot{\theta}^2 + J_2\dot{\lambda}^2 + J_3\dot{\varphi}^2 + J_4(\theta,\lambda)\dot{\theta} + J_5\dot{\lambda} + J_6(\theta,\lambda)\dot{\theta}\dot{\lambda} + J_7(\theta,\lambda,\varphi) \quad \ldots (4.33)$$

The equation (4.33) is in terms of $\dot{\theta}$, $\dot{\lambda}$ and $\dot{\varphi}$, and it can be written in terms of $\dot{\varphi}$ by utilizing the equation (4.28) and (4.29) and the final equation can be written as.

$$L\left(\theta,\lambda,\varphi,\dot{\theta},\dot{\lambda},\dot{\varphi}\right) = \left[J_1 S_1(\theta,\lambda,\varphi)^2 + J_2 S_2(\theta,\lambda,\varphi)^2 + J_3 + J_6(\theta,\lambda)S_1(\theta,\lambda,\varphi)S_2(\theta,\lambda,\varphi)\right]\dot{\varphi}^2 +$$
$$\left[J_4(\theta,\lambda)S_1(\theta,\lambda,\varphi) + J_5 S_2(\theta,\lambda,\varphi)\right]\dot{\varphi} + J_7(\theta,\lambda,\varphi)$$

$\ldots$ (4.34)

The Lagrangian equation was derived in terms of $\dot{\varphi}$, however, the equation (4.34) still contains θ and λ, which can be replaced in terms of φ by substituting the equation (4.24) and (4.26).

4.1.3.5 Equation of motion

From the above Lagrangian equation (4.34), the equation of motion of the complete system can be developed using the Euler-Lagrangian formulation and it is given below.

$$\frac{d}{dt}\left(\frac{\partial L}{\partial \dot{\varphi}}\right)-\frac{\partial L}{\partial \varphi}=T_{ext} \qquad \ldots (4.35)$$

$$\frac{\partial L}{\partial \dot{\varphi}}=2\left[J_1S_1(\theta,\lambda,\varphi)^2+J_2S_2(\theta,\lambda,\varphi)^2+J_3+J_6(\theta,\lambda)S_1(\theta,\lambda,\varphi)S_2(\theta,\lambda,\varphi)\right]\dot{\varphi}+ \left[J_4(\theta,\lambda)S_1(\theta,\lambda,\varphi)+J_5S_2(\theta,\lambda,\varphi)\right] \qquad \ldots (4.36)$$

$$\frac{d}{dt}\left(\frac{\partial L}{\partial \dot{\varphi}}\right)=2\left[J_1{S_1}^2+J_2{S_2}^2+J_3+J_6S_1S_2\right]\ddot{\varphi}+ 2\left[\begin{array}{l}2J_1S_1\left(\frac{\partial S_1}{\partial\theta}\frac{\partial\theta}{\partial\varphi}+\frac{\partial S_1}{\partial\lambda}\frac{\partial\lambda}{\partial\varphi}+\frac{\partial S_1}{\partial\varphi}\right)+2J_2S_2\left(\frac{\partial S_2}{\partial\theta}\frac{\partial\theta}{\partial\varphi}+\frac{\partial S_2}{\partial\lambda}\frac{\partial\lambda}{\partial\varphi}+\frac{\partial S_2}{\partial\varphi}\right)+S_1S_2\left(\frac{\partial J_6}{\partial\theta}\frac{\partial\theta}{\partial\varphi}+\frac{\partial J_6}{\partial\lambda}\frac{\partial\lambda}{\partial\varphi}\right)+\\ J_6S_2\left(\frac{\partial S_1}{\partial\theta}\frac{\partial\theta}{\partial\varphi}+\frac{\partial S_1}{\partial\lambda}\frac{\partial\lambda}{\partial\varphi}+\frac{\partial S_1}{\partial\varphi}\right)+J_6S_1\left(\frac{\partial S_2}{\partial\theta}\frac{\partial\theta}{\partial\varphi}+\frac{\partial S_2}{\partial\lambda}\frac{\partial\lambda}{\partial\varphi}+\frac{\partial S_2}{\partial\varphi}\right)\end{array}\right]\dot{\varphi}^2+ \left[S_1\left(\frac{\partial J_4}{\partial\theta}\frac{\partial\theta}{\partial\varphi}+\frac{\partial J_4}{\partial\lambda}\frac{\partial\lambda}{\partial\varphi}\right)+J_4\left(\frac{\partial S_1}{\partial\theta}\frac{\partial\theta}{\partial\varphi}+\frac{\partial S_1}{\partial\lambda}\frac{\partial\lambda}{\partial\varphi}+\frac{\partial S_1}{\partial\varphi}\right)+J_5\left(\frac{\partial S_2}{\partial\theta}\frac{\partial\theta}{\partial\varphi}+\frac{\partial S_2}{\partial\lambda}\frac{\partial\lambda}{\partial\varphi}+\frac{\partial S_2}{\partial\varphi}\right)\right]\dot{\varphi} \qquad \ldots (4.37)$$

$$\left(\frac{\partial L}{\partial\varphi}\right)=\left[\begin{array}{l}2J_1S_1\left(\frac{\partial S_1}{\partial\theta}\frac{\partial\theta}{\partial\varphi}+\frac{\partial S_1}{\partial\lambda}\frac{\partial\lambda}{\partial\varphi}+\frac{\partial S_1}{\partial\varphi}\right)+2J_2S_2\left(\frac{\partial S_2}{\partial\theta}\frac{\partial\theta}{\partial\varphi}+\frac{\partial S_2}{\partial\lambda}\frac{\partial\lambda}{\partial\varphi}+\frac{\partial S_2}{\partial\varphi}\right)+S_1S_2\left(\frac{\partial J_6}{\partial\theta}\frac{\partial\theta}{\partial\varphi}+\frac{\partial J_6}{\partial\lambda}\frac{\partial\lambda}{\partial\varphi}\right)+\\ J_6S_2\left(\frac{\partial S_1}{\partial\theta}\frac{\partial\theta}{\partial\varphi}+\frac{\partial S_1}{\partial\lambda}\frac{\partial\lambda}{\partial\varphi}+\frac{\partial S_1}{\partial\varphi}\right)+J_6S_1\left(\frac{\partial S_2}{\partial\theta}\frac{\partial\theta}{\partial\varphi}+\frac{\partial S_2}{\partial\lambda}\frac{\partial\lambda}{\partial\varphi}+\frac{\partial S_2}{\partial\varphi}\right)\end{array}\right]\dot{\varphi}^2+ \left[S_1\left(\frac{\partial J_4}{\partial\theta}\frac{\partial\theta}{\partial\varphi}+\frac{\partial J_4}{\partial\lambda}\frac{\partial\lambda}{\partial\varphi}\right)+J_4\left(\frac{\partial S_1}{\partial\theta}\frac{\partial\theta}{\partial\varphi}+\frac{\partial S_1}{\partial\lambda}\frac{\partial\lambda}{\partial\varphi}+\frac{\partial S_1}{\partial\varphi}\right)\right]\dot{\varphi}+\frac{\partial J_7}{\partial\theta}\frac{\partial\theta}{\partial\varphi}+\frac{\partial J_7}{\partial\lambda}\frac{\partial\lambda}{\partial\varphi}+\frac{\partial J_7}{\partial\varphi} \qquad \ldots (4.38)$$

Substituting the equation 4.36, 4.37 and 4.38 in the equation 4.35, the complete dynamic equation of the knee joint with extension assist can be obtained and it is written as:

$$2\left[J_1{S_1}^2+J_2{S_2}^2+J_3+J_6S_1S_2\right]\ddot{\varphi}+ \left[\begin{array}{l}2J_1S_1\left(S_1\frac{\partial S_1}{\partial\theta}+S_2\frac{\partial S_1}{\partial\lambda}+\frac{\partial S_1}{\partial\varphi}\right)+2J_2S_2\left(S_1\frac{\partial S_2}{\partial\theta}+S_2\frac{\partial S_2}{\partial\lambda}+\frac{\partial S_2}{\partial\varphi}\right)+S_1S_2\left(S_1\frac{\partial J_6}{\partial\theta}+S_2\frac{\partial J_6}{\partial\lambda}\right)+\\ J_6S_2\left(S_1\frac{\partial S_1}{\partial\theta}+S_2\frac{\partial S_1}{\partial\lambda}+\frac{\partial S_1}{\partial\varphi}\right)+J_6S_1\left(S_1\frac{\partial S_2}{\partial\theta}+S_2\frac{\partial S_2}{\partial\lambda}+\frac{\partial S_2}{\partial\varphi}\right)\end{array}\right]\dot{\varphi}^2+ \left[J_5\left(S_1\frac{\partial S_2}{\partial\theta}+S_2\frac{\partial S_2}{\partial\lambda}+\frac{\partial S_2}{\partial\varphi}\right)\right]\dot{\varphi}-S_1\frac{\partial J_7}{\partial\theta}-S_2\frac{\partial J_7}{\partial\lambda}-\frac{\partial J_7}{\partial\varphi}=T_{ext} \qquad \ldots (4.39)$$

and it is modified as follows:

$$2\left[J_1{S_1}^2+J_2{S_2}^2+J_3+J_6S_1S_2\right]\ddot{\varphi}+KS_1\begin{bmatrix}\frac{1}{2}{l_{dh}}^2\sin 2(\theta+\theta_d)-l_{dg}l_{dh}\cos\theta_g\sin(\theta+\theta_d)\\-\frac{1}{2}{l_{dh}}^2\sin 2(\theta+\theta_h)+l_{dg}l_{dh}\sin\theta_h\cos(\theta+\theta_d)\end{bmatrix}+$$

$$\left[J_5\left(S_1\frac{\partial S_2}{\partial\theta}+S_2\frac{\partial S_2}{\partial\lambda}+\frac{\partial S_2}{\partial\varphi}\right)\right]\dot{\varphi}+$$

$$\begin{bmatrix}2J_1S_1\left(S_1\frac{\partial S_1}{\partial\theta}+S_2\frac{\partial S_1}{\partial\lambda}+\frac{\partial S_1}{\partial\varphi}\right)+2J_2S_2\left(S_1\frac{\partial S_2}{\partial\theta}+S_2\frac{\partial S_2}{\partial\lambda}+\frac{\partial S_2}{\partial\varphi}\right)+S_1S_2\left(S_1\frac{\partial J_6}{\partial\theta}+S_2\frac{\partial J_6}{\partial\lambda}\right)+\\J_6S_2\left(S_1\frac{\partial S_1}{\partial\theta}+S_2\frac{\partial S_1}{\partial\lambda}+\frac{\partial S_1}{\partial\varphi}\right)+J_6S_1\left(S_1\frac{\partial S_2}{\partial\theta}+S_2\frac{\partial S_2}{\partial\lambda}+\frac{\partial S_2}{\partial\varphi}\right)\end{bmatrix}\dot{\varphi}^2$$

$$-S_1\frac{\partial J_8}{\partial\theta}-S_2\frac{\partial J_7}{\partial\lambda}-\frac{\partial J_7}{\partial\varphi}=T_{ext}$$

… (4.40)

Where,

$$\frac{\partial S_1}{\partial\theta}=\frac{l_3\sin(\lambda-\varphi)\cos(\lambda-\theta)}{l_1\sin^2(\lambda-\theta)}$$

$$\frac{\partial S_1}{\partial\lambda}=\frac{2l_3\sin(\varphi-\theta)}{l_1-l_1\cos 2(\lambda-\theta)}$$

$$\frac{\partial S_1}{\partial\varphi}=-\frac{l_3\cos(\lambda-\theta)}{l_1\sin(\lambda-\theta)}$$

$$\frac{\partial S_2}{\partial\theta}=\frac{2l_3\sin(\varphi-\lambda)}{l_2-l_2\cos 2(\lambda-\theta)}$$

$$\frac{\partial S_2}{\partial\lambda}=\frac{-l_3\sin(\varphi-\theta)\cos(\lambda-\theta)}{l_2\sin^2(\lambda-\theta)}$$

$$\frac{\partial S_2}{\partial\varphi}=\frac{l_3\cos(\varphi-\theta)}{l_2\sin(\lambda-\theta)}$$

$$\frac{\partial J_6}{\partial\theta}=-m_2l_1l_{c2}\sin\left(\theta-\theta_{c2}-\lambda\right)-m_pl_1l_{cp}\sin\left(\theta-\theta_{cp}-\lambda\right)-m_fl_1l_{cf}\sin\left(\theta-\theta_{cf}-\lambda\right)$$

$$\frac{\partial J_6}{\partial\lambda}=m_2l_1l_{c2}\sin\left(\theta-\theta_{c2}-\lambda\right)+m_pl_1l_{cp}\sin\left(\theta-\theta_{cp}-\lambda\right)+m_fl_1l_{cf}\sin\left(\theta-\theta_{cf}-\lambda\right)$$

$$\frac{\partial J_7}{\partial \theta} = m_1 g l_{c1} \cos\theta - m_2 g l_1 \cos\theta - m_p g l_1 \cos\theta - m_f g l_1 \cos\theta + \frac{1}{2} k {l_{dh}}^2 \sin 2(\theta + \theta_d) -$$

$$k l_{dg} l_{dh} \cos\theta_g \sin(\theta + \theta_d) - \frac{1}{2} k {l_{dh}}^2 \sin 2(\theta + \theta_h) + k l_{dg} l_{dh} \sin\theta_h \cos(\theta + \theta_d)$$

$$\frac{\partial J_7}{\partial \lambda} = -m_2 g l_{c2} \cos\left(\theta_{c2} + \lambda\right) - m_p g l_{cp} \cos\left(\theta_{cp} + \lambda\right) - m_f g l_{cf} \cos\left(\theta_{cf} + \lambda\right)$$

$$\frac{\partial J_7}{\partial \phi} = -m_3 g l_{c3} \cos\varphi$$

$$\frac{\partial J_8}{\partial \theta} = m_1 g l_{c1} \cos\theta - m_2 g l_1 \cos\theta - m_p g l_1 \cos\theta - m_f g l_1 \cos\theta$$

In a compact form, the dynamic equation can be written as:

$$M \ddot{\varphi} + Kf(\varphi) + C\dot{\varphi} + A\dot{\varphi}^2 = T \qquad \ldots (4.41)$$

$$M = 2\left[J_1 {S_1}^2 + J_2 {S_2}^2 + J_3 + J_6 S_1 S_2 \right]$$

$$f(\varphi) = S_1 \begin{bmatrix} \frac{1}{2} {l_{dh}}^2 \sin 2(\theta + \theta_d) - l_{dg} l_{dh} \cos\theta_g \sin(\theta + \theta_d) \\ -\frac{1}{2} {l_{dh}}^2 \sin 2(\theta + \theta_h) + l_{dg} l_{dh} \sin\theta_h \cos(\theta + \theta_d) \end{bmatrix}$$

$$C = \left[J_5 \left(S_1 \frac{\partial S_2}{\partial \theta} + S_2 \frac{\partial S_2}{\partial \lambda} + \frac{\partial S_2}{\partial \varphi} \right) \right]$$

$$A = \begin{bmatrix} 2J_1 S_1 \left(S_1 \frac{\partial S_1}{\partial \theta} + S_2 \frac{\partial S_1}{\partial \lambda} + \frac{\partial S_1}{\partial \varphi} \right) + 2J_2 S_2 \left(S_1 \frac{\partial S_2}{\partial \theta} + S_2 \frac{\partial S_2}{\partial \lambda} + \frac{\partial S_2}{\partial \varphi} \right) + S_1 S_2 \left(S_1 \frac{\partial J_6}{\partial \theta} + S_2 \frac{\partial J_6}{\partial \lambda} \right) + \\ J_6 S_2 \left(S_1 \frac{\partial S_1}{\partial \theta} + S_2 \frac{\partial S_1}{\partial \lambda} + \frac{\partial S_1}{\partial \varphi} \right) + J_6 S_1 \left(S_1 \frac{\partial S_2}{\partial \theta} + S_2 \frac{\partial S_2}{\partial \lambda} + \frac{\partial S_2}{\partial \varphi} \right) \end{bmatrix}$$

$$T = T_{ext} + S_1 \frac{\partial J_8}{\partial \theta} + S_2 \frac{\partial J_7}{\partial \lambda} + \frac{\partial J_7}{\partial \varphi}$$

Equation 4.41 describes the equation of motion for the four-bar passive polycentric knee joint with an extension assist fitted between top (link 0) and bottom part (link 2).

4.1.3.6 Simulation of the dynamic equation

The dynamic model was simulated using MATLAB Simulink, where the Dormand-Prince, ODE45 scheme was utilized to integrate the equation of motion by the fixed time-step solver.

Simulation parameters

The simulation parameters of the dynamic model are given in Table 4.3. All the parameters were obtained from the newly developed knee joint.

Table 4.3 Simulation parameters of the passive polycentric knee joint

Parameters	Value	Parameters	Value
l_0	3.2 cm	k	5 N/cm
l_1	5.5 cm	θ_0	0.1047 radian (6°)
l_2	4.2 cm	φ (initial condition)	1.5708 radian (90°)
l_3	4.8 cm	θ_a	2.6437 radian (151°)
l_a	2.63 cm	θ_b	2.0242 radian (116°)
l_b	6 cm	θ_d	0.2568 radian (14.7°)
l_{c1}	2.75 cm	θ_{c2}	1.0472 radian (60°)
l_{c2}	2.1 cm	θ_{cp}	1.3090 radian (75°)
l_{c3}	2.4 cm	θ_{cf}	1.4835 radian (85°)
l_{cf}	65 cm	I_1	0.0091 kgcm^2
l_{cp}	30 cm	I_2	1.553 kgcm^2
m_1	0.1 kg	I_3	0.01 kgcm^2
m_2	0.3 kg	I_p	0.399 kgcm^2
m_3	0.12 kg	I_f	3.482 kgcm^2
m_p	0.65 kg	T	-20 N-cm, Ishai et al. [1983]
m_f	0.16 kg	g	981 cm/s^2

The kinematic link length of l_1, l_2, l_3 and l_0 was given as simulation parameters. The initial position of the link was given using φ, and the other angles were derived based on the position analysis. The length between centre of the mass and respective reference point and the included angle between the respective length against horizontal plane were obtained using ADAMS by importing the 3D model of the knee joint with pylon and foot. It is to be noted that all the data sets for analysis purpose were given from the developed knee joint to predict its dynamic behavior.

After the MATLAB simulink simulation, the dynamic behavior of the proposed passive polycentric knee joint was obtained and it is shown in Fig. 4.17. It was observed that the angle φ, θ, and λ were found to be decreased with an increase of time till 4.7 sec.

It is observed from Fig 4.17 that the angle φ started with 90° from the initial position and reached its maximum of -118° at 4.7 sec. Angle θ and λ started with an initial angle of 101 and -3.39°, respectively and reversed back at an angle of 11 and -91° and the corresponding trends are shown in Fig. 4. 17. Fig. 4.18 shows the photographic image of the polycentric knee joint at various dynamic condition. The positioning of different links against time was also compared with that of actual state of developed knee joint. The angle of φ, θ, and λ obtained from the dynamic equation was found to be closely matched with the angle obtained from the fabricated knee joint under dynamic condition, which validates the proposed dynamic equation.

The change in extension length of the spring against time was obtained and it is shown in Fig. 4.19. It was observed that the extension length of the spring was found to be increased with time till 4.7 sec. It was also observed that the extension length was found to be increased with flexion and it is reached its maximum at 106.3° of flexion, which was also confirmed using the fabricated knee joint. Hence, it was found that the obtained equation of motion of the polycentric knee joint with extension assist can be used to predict the dynamic behavior of the passive polycentric knee joint.

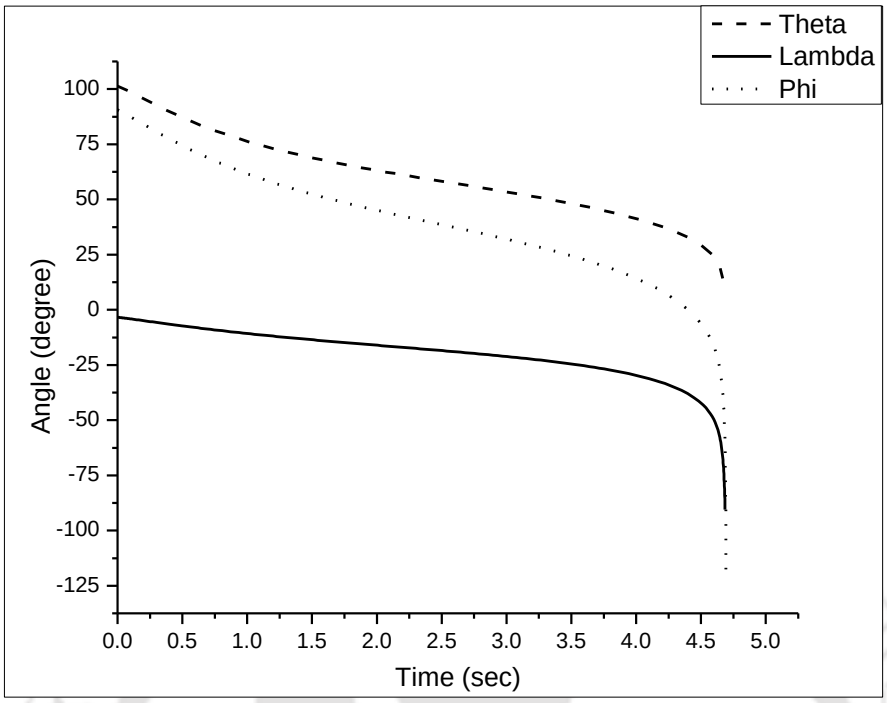

Fig. 4.17 Time evolution of φ, θ, and λ from the dynamics model

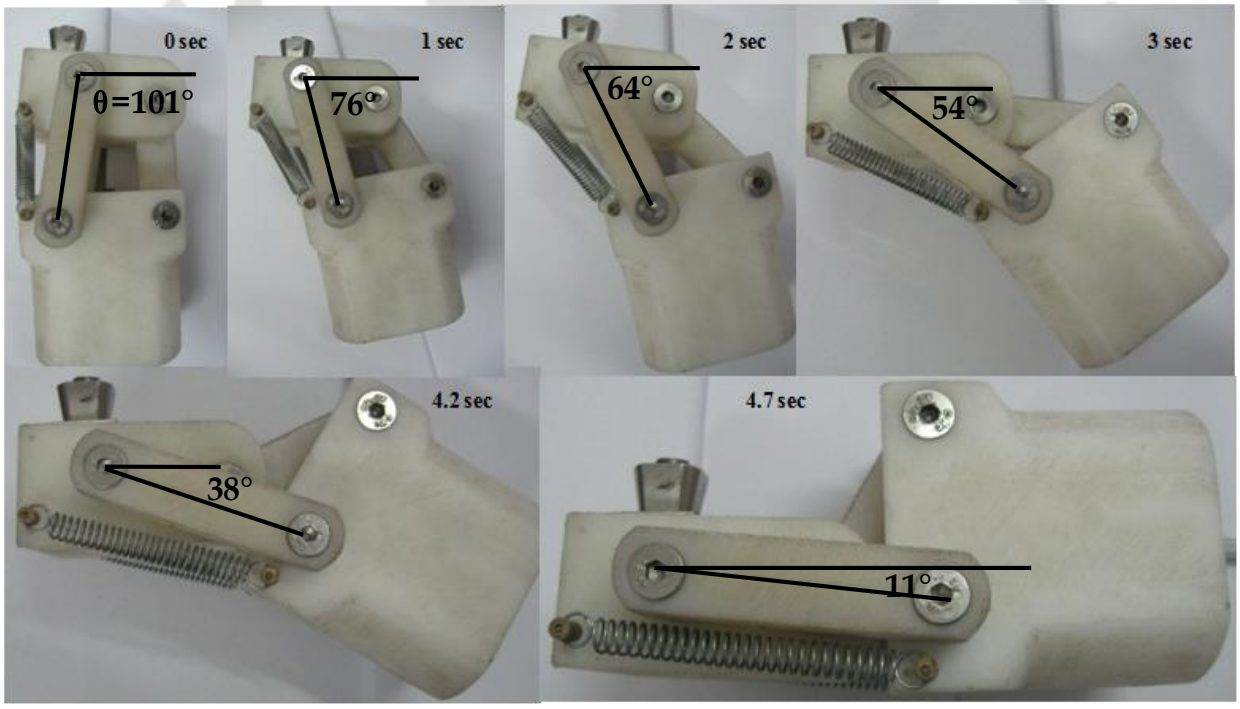

Fig. 4.18 Time evolution of the developed passive polycentric knee joint

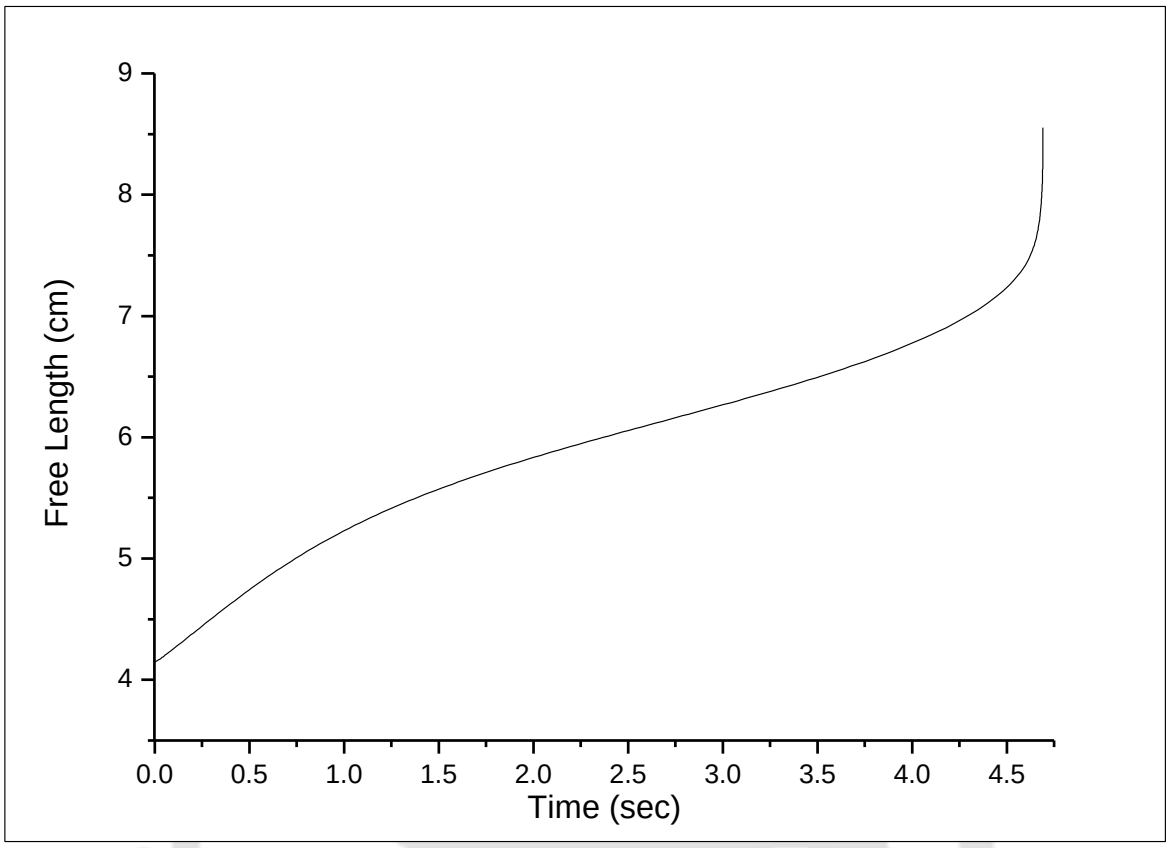

Fig. 4.19 Time evolution of free length of an extension spring

4.1.4 Comparison of the proposed knee joint with commercially available different types of knee joints

Table 4.4 shows the comparison of different features in the proposed knee joint with that of the commercially available existing knee joints. All the reported knee joints were constructed with various extension assists such as compression spring, rubber band and leaf springs, whereas the proposed knee joint has the extension spring. It was found that the knee joints reported by Karlsson et al. [2013], Chen et al. [2011] and Cheng [2007] were made of metals and the stopper was made of polymer composites. The metal knee has the provision of inner housing, external housing and spring guide for the proper functioning of the extension bias. However, the knee joint reported by Narayan et al. [2012] and Gonzalez et al. [2011] were made of polymer and it was not having the housing arrangement and spring guide due to the complexity in manufacturing the knee joint. The bumper used by Gonzalez et al. [2011] was made of composites.

Though a compression spring was used for the extension bias by Karlsson et al. [2013], Chen et al. [2011] and Cheng [2007], a leaf spring and a rubber band were used by Narayan et al. [2012] and Gonzalez et al. [2011], respectively, due to the complexity involved in adopting a compression spring as an extension bias in the polymer knee joint. It was also observed that the attachment of an extension bias in a knee joint proposed by Narayan et al. [2012] and Gonzalez et al. [2011] was in between the top and bottom part and in the middle linkage, respectively. It was suggested that the construction of an extension bias could be made by different ways such as adhesive bond, bolt, button screw and wrapping the rubber band between the knee adapter and the pylon due to inherent limitation of its manufacturing technique. The construction of an extension assist by Narayan et al. [2012] is expected to fail due to the fatigue failure of the adhesive bond. The durability of the rubber band used in a knee joint by Gonzalez et al. [2011] is expected to lose with usage. Hence, a new design was proposed to use the extension assist in polymer and its composites, where the extension bias fixation was made rigidly to achieve the flexion-extension using an extension spring. Though Narayan et al. [2012] and Gonzalez et al. [2011] suggested to fabricate the knee joint using polymer materials, which are expected to degrade in the environment due to Ultraviolet radiation leading to loss of their mechanical properties. However, the same is restricted using polymer composites in the proposed knee joint.

Table 4.4 Comparison of the proposed knee joint with different knee joints

Features	Karlsson et al. [2013]	Chen et al. [2011]	Cheng [2007]	Narayan et al. [2012]	Gonzalez et al. [2011]	Proposed Knee Joint
Extension Assist	Yes	Yes	Yes	Yes	Yes	Yes
Type of Extension assist	Compression Spring	Compression Spring	Compression Spring	Leaf Spring (Thin sheets of steel)	Rubber band	Extension Spring
Housing or Guide for Extension Assist	Yes	Yes	Yes	Nil	Nil	Nil
Durability of Extension assist	Comparatively high	Comparatively high	Comparatively high	Comparatively low	Comparatively low	Comparatively high
Position of Extension Bias	Compression spring was placed in the bottom part using a hole.	Compression spring was placed in the bottom part using a hole.	Compression spring was placed in the bottom part using a hole.	(a) Leaf spring is disposed internally between top and bottom parts (b) Leaf spring is coupled to the middle linkage	Between top and bottom part of the prosthetic knee joint	Between top and bottom part of the prosthetic knee joint

Connection of Extension assist	Compression spring was placed between a small link and a bottom part. The adjustable external housing, coaxial inner housing, and the spring guide were also used to assist the compression spring during flexion-extension.	Compression spring was placed between the bottom part and small link to achieve the flexion-extension of the knee joint.	Compression spring was connected between the small link and the bottom part, where the top part provides the space for placing and guiding the compression spring.	(a) Leaf spring is fixed using adhesive placed between top and bottom part. (b) Leaf spring is connected to the back of the middle linkage using the button screw.	(a) The rubber band was used between the top and bottom part, which was connected using the screw, bolt or adhesives (b) Knee joint used a hole in top and bottom part to fix the extension assist (c) Knee joint used the rubber band as extension assist, which was connected between the knee adapter and pylon	Extension spring was connected using a beam, which rigidly holds during the flexion and extension. It also guides for the smooth function of the prosthetic knee joint.

Material Used	The flexion stopper was made of carbon fiber spring, polymers or composites. The knee joint was made of metal	Metals	Metals	Polymer material for knee joint and composites for bumper	Polymer	Polymer composites for knee joint parts such as top part, bottom part, small link and large link
Degradation of knee joint material	N/A	N/A	N/A	Comparatively more	Comparatively more	Comparatively less
Rotation stopper in knee joint and knee adapter	Integrated knee adapter	Integrated knee adapter	Integrated knee adapter	No rotation stopper	No rotation stopper	Rotation stopper in knee joint and knee adapter.

4.1.5 Cost analysis of the knee joint

A detailed analysis on manufacturing cost of the knee joint was carried out and presented in the Table 4.5 (http://www.spsteelandinternational.com/product%20 range.html.). The cost includes the sum of all direct cost of the actual manufacturing of the product and the indirect cost, which includes the cost of labor, electricity, maintenance and depreciation of the equipment. The material cost was estimated based on the consumption of raw material used to manufacture the product. By considering the direct and indirect cost of the product, each knee joint is estimated to be within Rs. 5000 only.

The commercially available different types of knee joint and its cost along with different parameters are shown in Table 4.6 (http://pdf.medicalexpo.com/pdf/ossur/ ossur-prosthetic-s-c-atalog/74948-94723. html#open). Among them, the power knee manufactured by Ossur was found to be the highest and the proposed knee joint was found to be easily affordable. The commercially available existing knee joint such as power knee, rheo knee and total knee (passive) was found to be 500, 238 and 50% more weight, respectively, in comparison to that of proposed knee joint. Hence, the decrease in weight of the proposed knee joint is expected to reduce the metabolic cost of an amputee.

Table 4. 5 Cost analysis of knee joint

Component	Raw material used (gram)	Material utilized cost (INR)	Direct manufacturing cost (INR)	Grant total (INR)
Knee joint parts	300	100	3000	3100
Stainless steel 304 pins and springs	75	30	1000	1030
Stainless steel 304 adapter	75	30	800	830
			Total	4960 ≈ 5000

Table 4. 6 Comparison of the proposed knee with the commercially available knee joint

Sl. No.	Make	Cost ($)	Model	Maximum patient weight (kg)	Weight of knee (kg)	Knee flexion (°)	Material used
1.	OSSUR	20,000	Power knee (Active)	125	2.7	120	Aluminum alloy
2.	OSSUR	18,000	RKN 120007 (Active)	125	1.52	120	Aluminum alloy
3.	OSSUR	800	Total knee (Passive)	100	0.675	160	Aluminum alloy
4.	D Rev	80	ReMotion Knee (Passive without extension assist)	100	0.45	165	Oil filled nylon-66
5.	IIT Guwahati	50	Proposed model with extension assist	125	0.45	115	Nylon

4.1.6 Summary of the design of a knee joint

A passive polycentric knee joint was designed and fabricated with an extension assist having the stiffness of 0.5 N/mm. The dynamic analysis was carried out for the proposed knee joint to obtain the equation of motion, which predicted the behaviour of the knee joint against time and it was also confirmed using the fabricated knee joint. The equation of motion obtained for the passive polycentric knee joint with extension assist could be used to predict the dynamic behaviour of the same. The developed knee joint has significant advantages such as light-weight, less bulky, ease maintenance, and novel passive extension unit compared to that of conventional knee joints. Hence, the developed knee joint is expected to increase the affordability and stability of an amputee with required flexion without compromising the safety aspects.

4.2 Patient trial and rehabilitation feedback after the fixation of the developed knee joint

4.2.1 Rehabilitation studies on the knee joint

4.2.1.1 Amputees

The fit and healthy amputee having amputation since last two years was the main selection criteria for the volunteer. Nine healthy unilateral trans-femoral amputees volunteered for testing the developed prosthetic knee joint. During the usage of prosthesis, one of the amputees was not willing to participate in the rehabilitation feedback program and another amputee has not completed six month usage period to take his feedback. The details of amputees are given in Table 4.7.

The pylon and foot were not varied with amputees. In case of a socket, the moulded and laminated sockets were used based on the amputee's convenience. The SACH foot and an aluminium alloy pylon were obtained from M/s Proactive Technical Orthopaedics, Pune, Maharashtra, India for all the amputees and given to them at free of cost. Based on the clinical importance, the gait analysis was carried out in the presence of two prosthetists, an orthopaedic surgeon and experts for their individual feedback at North Eastern Indira Gandhi Regional Institute of Health and Medical Sciences (NEIGRIHMS), Shillong and L.G.D Hi-tech Orthotic and Prosthetic Centre, Kanyakumari. The consent form was filled by the amputees before the fixation of prosthetic devices. The gait data was obtained using the Phantom v711 digital high speed camera, which was then converted into individual frame to sort out the gait parameters of hip, knee and ankle using the MB ruler and compared with sound leg gait pattern. Initially, the sound leg gait pattern of healthy volunteer was obtained and compared with published literature in order to validate the data obtained from the high speed camera.

The use of patient data for research purpose was approved by the committee on research ethics at North Eastern Indira Gandhi Regional Institute of Health and Medical Sciences, Shillong, where the research was conducted in accordance with the Declaration of the World Medical Association. The patient trial registry number is NEIGRIHMS/Micro/IEC-II/191/2012-13.

Table 4. 7Amputee details

Amputee	Gender	Amputation type	Cause	Age (yrs)	Weight (kg)	Height (cm)
1	Male	Trans-femoral Left	Accident	15	44	148
2	Female	Trans-femoral Left	Accident	15	41	138
3	Male	Trans-femoral Left	Accident	23	52	158
4	Male	Trans-femoral Left	Accident	39	63	173
5	Male	Trans-femoral Right	Accident	42	68	166
6	Male	Trans-femoral Left	Accident	46	71	160
7	Male	Trans-femoral Left	Accident	54	76	164
8	Male	Trans-femoral Right	Accident	60	73	166
9	Female	Trans-femoral Left	Accident	60	75	162

4.2.1.2 Inclusion/exclusion criteria

Amputee

Inclusion Criteria	Exclusion criteria
Unilateral trans-femoral amputee with at least 15 years of age	Amputation in contralateral limb
Accept the developed prosthesis	Not willing to accept the developed prosthesis (severe debilitating medical illness)
Able to follow the instructions	Unable to follow the instructions
Able to walk a distance of minimum 4 meters	Unable to walk prior to amputation due to medical condition eg, spinal injury, stroke
Willing to attend hospital-based rehabilitation program	Unable to provide consent to take part in the study

Healthy volunteer

The volunteers aged between 18 to 35 years of age were selected for obtaining the hip, knee and ankle gait to compare with that of amputees gait pattern. If the volunteers

had musculoskeletal disorders and other medical illness, they were excluded from the list of volunteers. The gait pattern of five non-disabled healthy volunteers was obtained and the average was made as a baseline for the comparison of gait pattern of an amputee.

4.2.2 Amputees fitted with developed prosthetic knee joint

Nine amputees were fitted with the developed polymer based passive prosthetic knee joint and the photographic views of all the amputees are shown in Fig. 4.20. All the amputees were instructed to walk at their own comfortable speed. The feedback from the amputees was collected if the prosthetic leg was used by them atleast for the period of 6 months.

4.2.3 Rehabilitation feedback using the developed knee joint

Short form 36 Health survey (SF-36)

The short form 36 Health survey (SF-36) is a self-report measure, and it is a document validity to measure the Health related quality of life (HRQL) within certain population, Andresen et al. [2000]. The SF-36 is commonly used in orthopedic research, Pezzin et al. [2000]. The survey was categorized into eight different dimensions such as Physical Functioning (PF), Role Functioning from a physical perspective (RP), Bodily Pain (BP), General Health (GH), Vitality (VT), Social Functioning (SF), Role Functioning from an emotional perspective (RE) and Mental Health (MH). The eight parameters were divided into physical and mental components. The average of PF, RP, BP and GH were considered under physical component, whereas the average of VT, SF, RE and MH were represented as the mental component. The score was given from 0 to 100 starting from poor to better health for the each question. The average mental and physical component score were used to evaluate the average HRQL before and after the fixation of newly developed prosthetic knee joint.

Fig. 4.20 Photographic view of all nine amputees fitted with the developed prosthetic knee joint

Questionnaire for persons with a trans-femoral amputation (Q-TFA)

To study the rehabilitation feedback about the prosthesis function, Q-TFA as suggested by Hagberg et al. [2004] was taken. Q-TFA consists of 70 questions, where 54 questions were taken for the analysis and the remaining 16 questions were used to understand the usage of prosthesis. Among the 54 questions, the Prosthetic Use score (PU) (2 questions), the Prosthetic Mobility score (PM) (19 questions), the Problem score (P) (30 questions) and the Global score (G) (3 questions) were calculated to study the amount of normal prosthetic wear per week, the capability and performance of moving by themselves, specific problems related to the prosthesis, their impact on quality of life, and the perception of the current overall amputation situation. The score was given from 0 to 100 starting from worse to better function of the prosthesis.

4.2.3.1 Health related quality of life (HRQL) and questionnaire for persons with a trans-femoral amputation (Q-TFA) assessment

The feedback data collection after six months of the prosthesis fixation in two of the amputees's home is shown in Fig. 4.21.

Fig. 4.21 Feedback collection from the amputees

The answer to question in the consent form was collected based on the availability of the amputees with prior appointment. The SF-36 answers were divided into PF, RP, BP, GH, MH, RE, SF and VT as discussed earlier. The 36 questions were scored on a scale from 0 to 100, where the score of 100 represents the highest level of its respective positive function. The detailed questions are appended in Annexure-I, where an answer to question number 1, 2, 20, 21, 22, 23, 26, 27, 30, 34 and 36 started the scoring

from 100 to 0, whereas the answer for the question number 3 - 19, 24, 25, 28, 29, 31, 32, 33 and 35 was scored from 0 to 100. The PF (3 - 12), RP (13 - 16) BP (21 - 22) and GH (1, 33 - 36) correspond to the physical component. Improvement in moderate activities such as moving a table and carrying groceries was observed in all the amputees after the fixation, but the score was moderate for the two amputees, who are aged at 60. The reason for the moderate score was due to the lack of practice after the fixation compared to the amputees below 54 years old. Vigorous activities such as running, lifting heavy objects, bending, kneeling and stooping were not attempted by the amputees fitted with the developed prosthetic knee joint. It was found that all the amputees walked several blocks and two amputees walked even several miles. Development of body pain during the usage of prosthetic knee joint was not reported by 5 amputees, however, 2 amputees, who are aged at 60, confirmed the mild pain. Five amputees changed their mind to lead a happy life after the fixation, whereas remaining two of them were not.

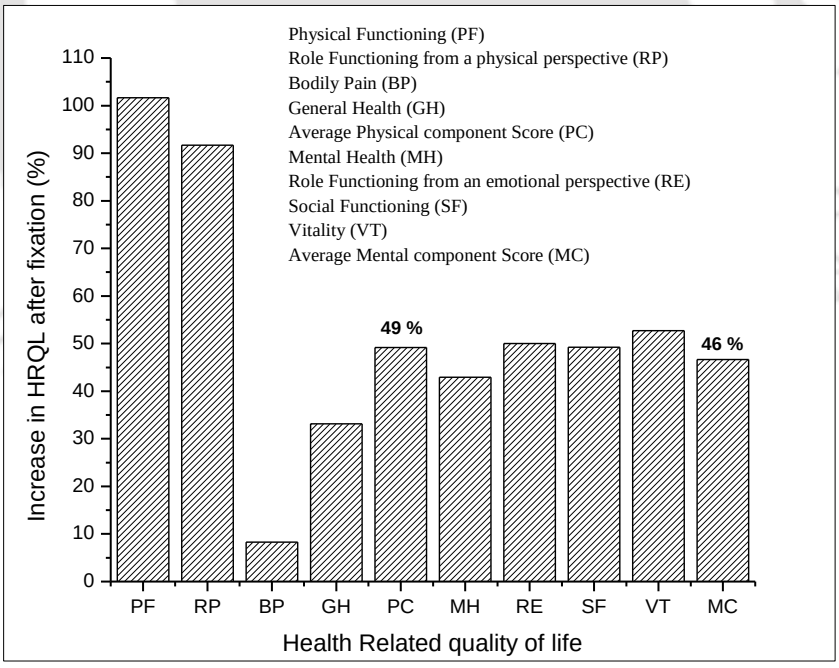

Fig. 4.22 Increase in HRQL after fixation using SF-36 in comparison with pre-fixation stage

The increase in physical component score after the fixation of prosthetic leg was observed in comparison to that of before fixation stage and it is shown in Fig. 4.22. The

increase in Physical Functioning, Role Functioning from a physical perspective, General Health and Body Pain after the fixation was found to be 101, 91, 33 and 8 %, respectively in comparison to that of before fixation stage. The average physical component score was found to be increased by 49 %, which confirmed the increase in HRQL. The increase in physical component score confirmed that the amputees felt to be physically fit in order to involve the regular activities. The physical fitness also initiated them to participate in different household activities and assistance for their beloved ones. The increase in physical component was attributed due to the performance of the developed prosthetic knee joint, which increased the possibilities of getting work opportunities and productivity.

The Mental Health (question no. 24 - 26, 28, 30), Role Functioning from an emotional perspective (question no. 17, 18, 19), Social Functioning (question no. 20, 32) and Vitality (question no. 23, 27, 29, 31) represented the mental component. It was noticed that only two amputees out of 7 could be able to take bath and dress themselves and rest of them depended on their family members for assistance after the fixation. It was due to the increase in confidence level of an amputee after the fixation. The emotional interference influenced much in participating the social activities by all the amputees. It was noticed that no significant differences were observed in the general sickness, anger and tiredness of an amputee before and after the fixation. The reasons for the improvement of HRQL were also confirmed using the Q-TFA answers and the gait pattern of an amputee after fixation. The increase in score for mental health, social functioning, role functioning from an emotional perspective and vitality after the fixation was found to be 42, 49, 50, and 52 %, respectively in comparison with pre-fixation stage. The average mental score was increased by 46 %. The increase in HRQL after the fixation was achieved by the combined average of physical and mental component. Thus, the psycho-social acceptance of the developed prosthesis was well anticipated from the above results. The increase in mental health involved the amputees to participate in the decision making of their personnel life. Also, the thought of worn out is expected to be decreased after the fixation. In due course of time, the amputees are expected to feel that the prosthetic device has become an integral part of their body.

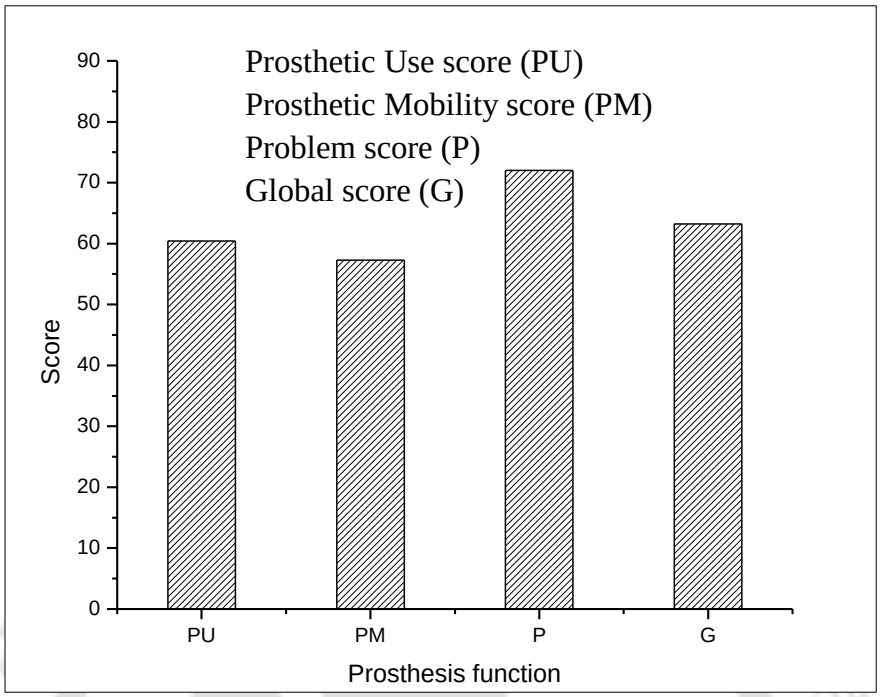

Fig. 4.23 Prosthetic score based on Q-TFA

Fig. 4.23 depicts the score related to the fixation of prosthesis based on Q-TFA. All questions are scored on a scale from 0 to 100, where 100 represents the highest level of respective positive functioning. The average of PU, PM and problem score gives the global score for the prosthetic function. Based on the Q-TFA feedback, it was observed that five amputees were able to move considerably, whereas two amputees aged at 60 were able to move slowly. Five amputees wore the prosthesis daily for 7-9 hr/day, however two amputees aged at 60 wore 4-6 hr/day, with an average of 4 days/week due to socket fitting and skin related problems and they removed the prosthesis when they were at home. It was noticed that all the amputees used their prosthesis on daily basis in most of the cases and 75 % of usage time was spent for their study and work. The amputees preferred to wear the prosthesis during cooking, gardening and driving; however it was not preferred during rest and sleep. Five amputees have been walking with no support and remaining two amputees aged at 60 have been walking with an aid of walking frame and crutch in outdoor as well as indoor. The amputees managed to walk in stairs, uphill, downhill and terrain using the single axis provision. Five amputees stood-up without any support, and walked with a tray in two hands, however remaining two amputees aged at 60 managed to walk only with support.

Sitting on the floor and tying the shoe-laces were not attempted by any amputee. After the prosthesis fixation, all the amputees walked more than 200 m several times. It was reported that no amputees fell, while using the prosthesis. Though the quality of life due to back pain, shoulder pain and pain in residual limb using the said prosthesis was observed to be not affected, one of the amputees, who was 60 years old, had phantom limb pain, pain in other leg and back pain, which resulted in moderate score in HRQL and Q-TFA for a particular amputee. The same reason for the reduction of HRQL was also reported by Pezzin et al. [2000].

Though the quality of life of all the amputees having the prosthesis was significantly influenced by emotional feelings, some of the limitations such as participating in social function, use of public transport and use of outdoor sports were observed by all amputees before and after the fixation of the prosthesis. As the usage of public transport by the lower limb amputees is a major concern, most of the amputees preferred Taxi/car/auto for their travel. Walker et al. [1994] reported that the increase in emotional feelings and the difficulty in transport led to the reduction of HRQL. Almost all the amputees reported that there was no difficulty in standing, donning, reliability and noise generation in the prosthesis, and thus it is expected to increase the quality of life of an amputee. One of the amputees reported the problem in maintaining the hygiene of the residual stump, increased tear of the clothes and skin irritation, which decreased the quality of life after the fixation. All the amputees felt that the prosthesis was light weight, easy to maintain, good appearance and good control of the swing and stance phase stability in the prosthesis. It was also reported that none of the amputees refrain to use the prosthesis due to its poor performance. It was confirmed from the above discussion that the positive global score increased the HRQL of an amputee after the fixation. The Prosthetic Use score, the Prosthetic Mobility score, the Problem score and Global score were found to be 60, 57, 72 and 63 out of 100, which confirmed that the amputees satisfied with the function of the prosthesis. It was also reported from Hagberg et al. [2004] that the global score of less than 50 showed the poor performance of the prosthetic device and the device should be rejected. As the developed prosthetic knee joint obtained the global score of 63, it confirmed the acceptance of the prosthetic knee joint based on its performance.

The above study was a non-random study as the selection of an amputee was done by the selected prosthetic and orthotic clinic. In general, the HRQL and Q-TFA of a young amputee were found to be higher compared to an older amputee. The same trend was also reported by Burger et al. [1997a], where the HRQL was evaluated for the lower limb amputees. It was reported that the overall general health of an amputee was observed to be good after fixation of the prosthesis compared to before fixation stage. It was anticipated that refrain to use the prosthesis was not observed in any of the amputees due to the usage of developed prosthetic knee joint, which was also reflected in the better HRQL. It was noticed that the amputees reduced their outdoor activities such as roaming with friends, shopping and house hold works before the fixation. However, these activities were significantly increased after the fixation. Reading and watching television remains the same before and after the fixation. The same observation was also noticed by Burger et al. [1997a]. The major problem observed for the moderate score in one of the amputees was the sores in the stump and tearing of clothes, which was originated from the proximal edge of the socket. Moreover, the prosthetic use by all the amputees was restricted heavily for sitting on the floor. The above mentioned problem was also observed by Legro et al. [1999]. It was also reported that the bone anchored prosthesis can reduce the tear, Branemark et al. [1996]. Waddling and limping were observed in most of the amputees, who preferred to use the single axis, which increased the metabolic cost and reduced the walking speed. The waddling was the result of the previous walking habits, because four amputees used single axis knee joint previously. Jaegers et al. [1995] also discussed the same reason for the waddling and limping of the prosthetic leg.

It was observed that the quality of life of most of the amputees was found to be increased significantly after fixing the polycentric knee joint. Furthermore, the flexion-extension movement of the prosthetic leg was confirmed by an amputee without any difficulties. The above studies confirmed the good functional efficiency of the newly developed polycentric knee joint; further validation was also carried out by comparing the gait pattern of prosthetic and normal leg.

4.2.4 Gait analysis of a trans-femoral amputee

Fig. 4.24 shows the gait cycle of a amputee. The amputees fitted with polycentric knee joint were allowed to walk with comfortable walking speed. The regular recurrence with consistent cycle was observed in all the amputees. The leg muscle worked in an orchestrated manner to achieve the gait, where the stance phase and swing phase were found to be 59 and 41 % of the total gait cycle. Each gait cycle starts and ends with heel strike including a toe off and mid-stance intermediately. The gait pattern of an amputee was found to be comparable with that of healthy volunteer and no significant difference between them was observed. Yokogushi et al. [2004] also developed a new prosthetic knee joint, where the gait pattern was observed to be 62 and 38 % for stance and swing phase, respectively.

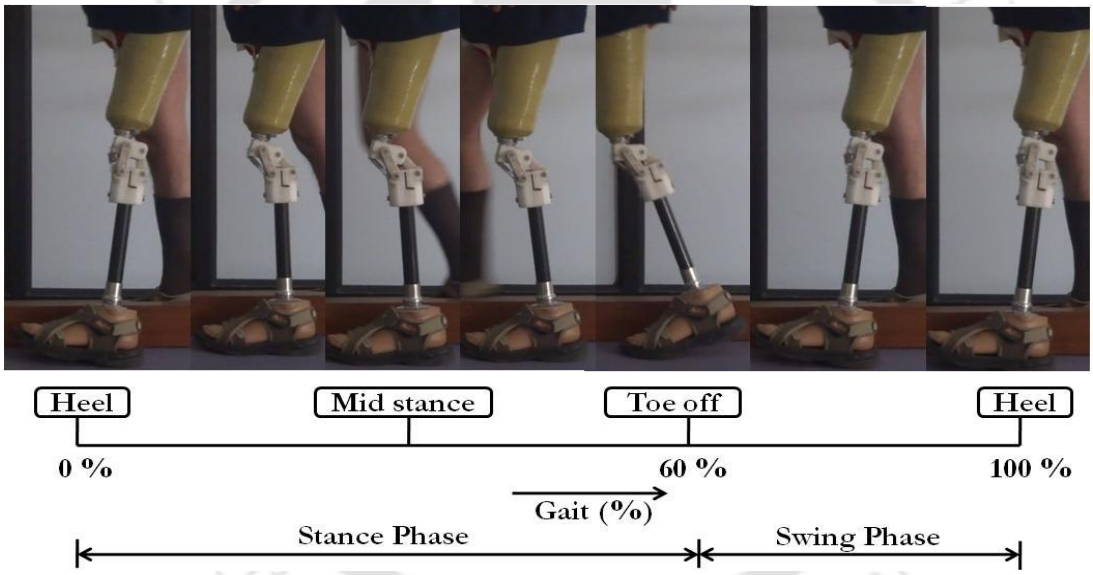

Fig. 4.24 Gait pattern of an amputee

Fig. 4.25a shows the knee angle with gait cycle. It was found that the knee angle of prosthetic leg followed the trend of a sound leg. The flexion angle was found to be more for sound leg compared to prosthetic leg at 16 % of gait cycle. The difference of 9° was noticed between prosthetic and sound leg at this instant. However, the toe-off condition was found to be the same for the sound and prosthetic leg. In case of swing-phase, the sound leg showed the maximum flexion angle of 59° compared to 45° for prosthetic leg at 80 % gait cycle. Fig. 4.25b describes the hip angle with gait cycle. It was confirmed that the hip angle of sound and prosthetic leg was found to be similar

condition up to midstance of 40 % gait cycle. In case of toe-off, the hip angle of prosthetic and sound leg was found to be 4 and 14°, respectively. Fig. 4.25c shows the ankle angle with gait cycle. It was observed that the sound and prosthetic ankle angle followed the same trend.

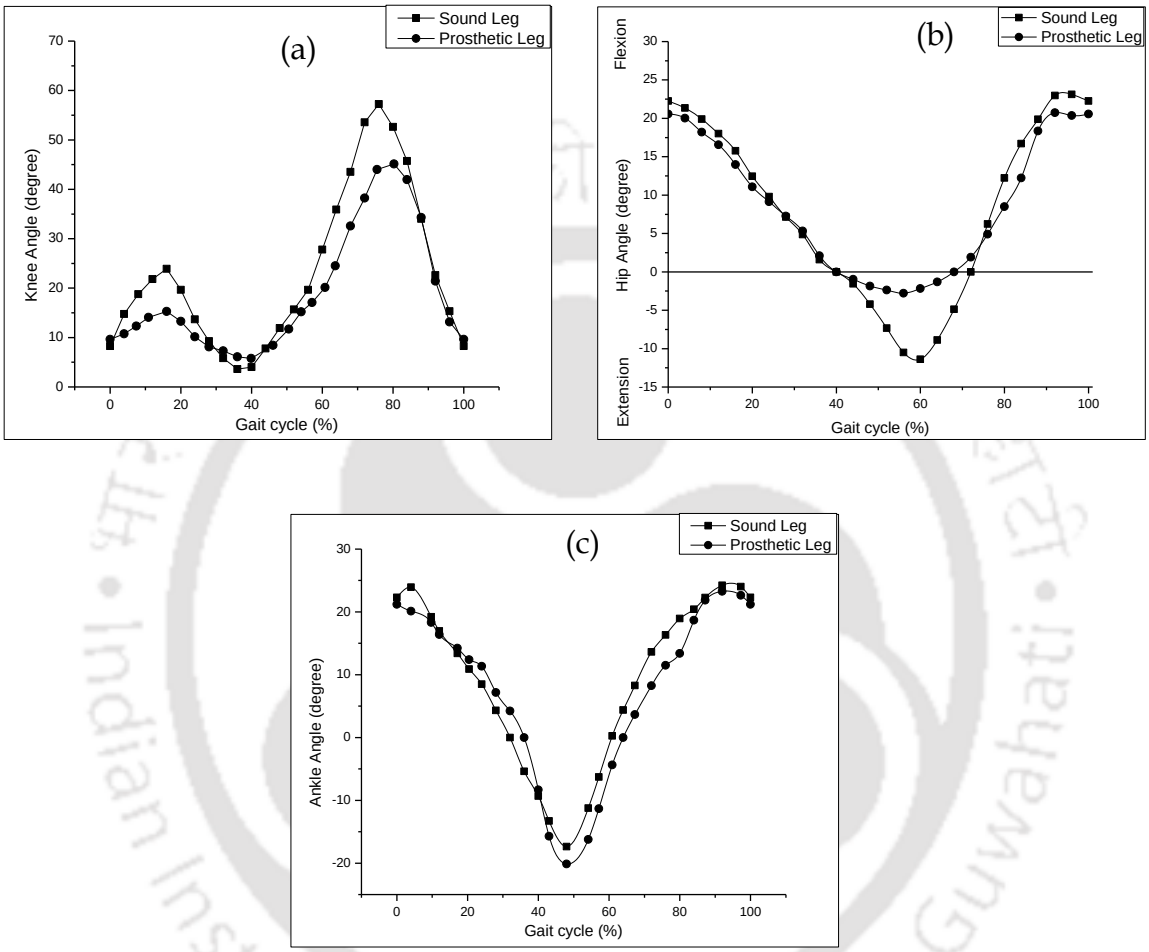

Fig. 4.25 (a) Knee angle (b) Hip angle (c) Ankle angle vs gait cycle

The variation between prosthetic and sound leg gait pattern was to preserve the pendulum action, which was achieved using the physical effort or by varying the step rate by an amputee, Radcliffe [1994b]. The reason for the difference was also due to the lack of muscle function in case of an amputee compared with healthy volunteers. Another reason for the difference in the gait cycle of an amputee and healthy volunteer was the variation in the flexor and extensor muscle strength and power of the muscle near the hip joint. The above discussion was also supported by Taheri et al. [2012]. One of the major points to be noted in this study was that the amputee volunteer was found

to be fit and active; hence the results reported for the active amputees are not expected to be matched with other partially active or in-active amputees.

The number of amputees completed in the present study was seven and the statistical analysis of the results within the amputees was done and compared with that of healthy volunteers. Though the power of the statistical analysis depends on the number of samples, it also depends on the number of trials experienced. The amputees were attempted with more than five trials with prior appointment and the average was reported. Increasing the number of amputees is most welcome to obtain the reliability in addition to reduction of number of ambulation by the amputees, where the number of trials can be reduced. In the existing literature, the number of amputees used for obtaining the gait pattern after the fixation of existing knee joint was three, five, seven and eight by Yokogushi et al. [2004], Thorn et al. [2009], Taheri et al. [2012] and Segal et al. [2006], respectively. It was observed from the literature that the better performance of the prosthesis could be identified with increased values of the HRQL, which was also confirmed using the gait analysis.

4.2.5 Summary of the amputee trial and rehabilitation feedback after the fixation of the developed knee joint

The newly designed polymeric based passive polycentric knee joint was developed and fitted with nine unilateral trans-femoral amputees and the feedback was taken from seven amputees. The HRQL was found to be increased significantly after the fixation of the prosthetic knee joint. The increase in HRQL due to fixation of the prosthesis confirmed the active involvement of the amputees in their daily activities. The average physical and mental score of the amputees after the fixation of prosthesis were found to be increased by 49 and 46 %, respectively, which confirmed the increase in HRQL. The global score for the prosthetic function was found to be 63, confirming the acceptance of the prosthetic devices. Moreover, the biomechanical gait pattern of an amputee was compared with that of the non-disabled healthy volunteer and there was no significant difference between them. It also validates the improved performance of the developed prosthetic knee joint. It is concluded that the developed knee joint can be used by the trans-femoral amputees to improve their quality of life. It is anticipated that the

developed knee joint is expected to make huge impact due to its function, performance, affordability and near sound leg gait pattern.

4.3 Evaluation of the material proposed to be used for the knee joint

As the conventionally used metallic polycentric knee joint is heavy, it consumes significant metabolic cost of the amputees leading to reduced productivity of them. Thus, an attempt was made to select a polymer and its composites without limiting the function of the knee joint after confirming the required failure analysis. As reported by Smith et al. [2013], the metabolic cost of an amputee was increased by 12 %, if there was 100 % mass difference between the intact and the prosthetic leg. As there is a huge density difference between the metal and polymer, the replacement of metal prosthetic knee joint by polymer based device is expected to reduce the metabolic cost significantly. Since, the von Mises stress concentration for the proposed knee joint was noted to be 30 MPa, the factor of safety was observed to be 0.5, 1, 1.17, 2, 1.67, 2.17 and 2.17, respectively, when HDPE, PP, ABS, Nylon-6, PET, PMMA and PC were used, (http://www.matweb.com). The cost of PET, HDPE, PP, Nylon-6, PMMA, ABS and PEEK was found to be INR 80, 85, 165, 165, 200, 330 and 400/kg respectively, and thus the PMMA was selected to fabricate the polycentric knee joint based on its factor of safety and cost, (http://www.alibaba.com/showroom/plastic-pellets-for-injection-molding.html). The detailed comparison of the different polymeric materials proposed to be used for the knee joint is shown in Table 4.8. The literature studies also confirmed the improved mechanical properties of PMMA compared to that of PP, HDPE and Nylon-66, Ash et al. [2002], Zeng et al. [2004] and Serbetci et al. [2004]. As the degradation of polymeric products due to ultraviolet (UV) radiation cannot be avoided, the limitation on the effect of same on PMMA was attempted using the MWCNT reinforcement based on the literature. Thus, studies on polymer based composites are reported in the present study.

Table 4. 8 Comparison of polymer materials

Sl. No.	Material	Yield strength (MPa)	Factor of safety based on the design	Cost (INR)
1	PC	65	2.17	400
2	ABS	35	1.17	330
3	PMMA	65	2.17	200
4	Nylon-6	60	2.00	165
5	PP	30	1.00	165
6	HDPE	15	0.50	85
7	PET	50	1.67	80

4.3.1 PMMA/MWCNT composites

4.3.1.1 Characterization of MWCNT

After the chemical treatment of MWCNT, different functional groups were attached on its surface. The same was confirmed using FTIR and the results are shown in Fig. 4.26a. The peaks identified at 1376, 1577, 1695, and 3691 cm^{-1} were attributed to the presence of C-O, C=C, C=O and O-H bonds, respectively in the chemically treated MWCNT. The TEM image of the untreated MWCNT is shown in Fig 4.26b, where its agglomerated form and the presence of amorphous carbon were observed. Fig 4.26c shows the TEM image of treated MWCNT, where the amorphous carbon content was drastically reduced.

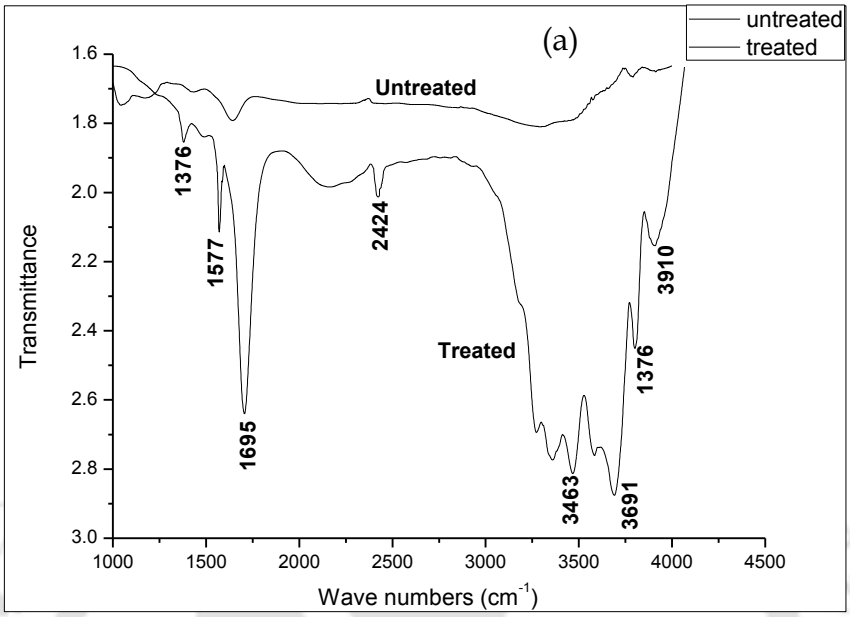

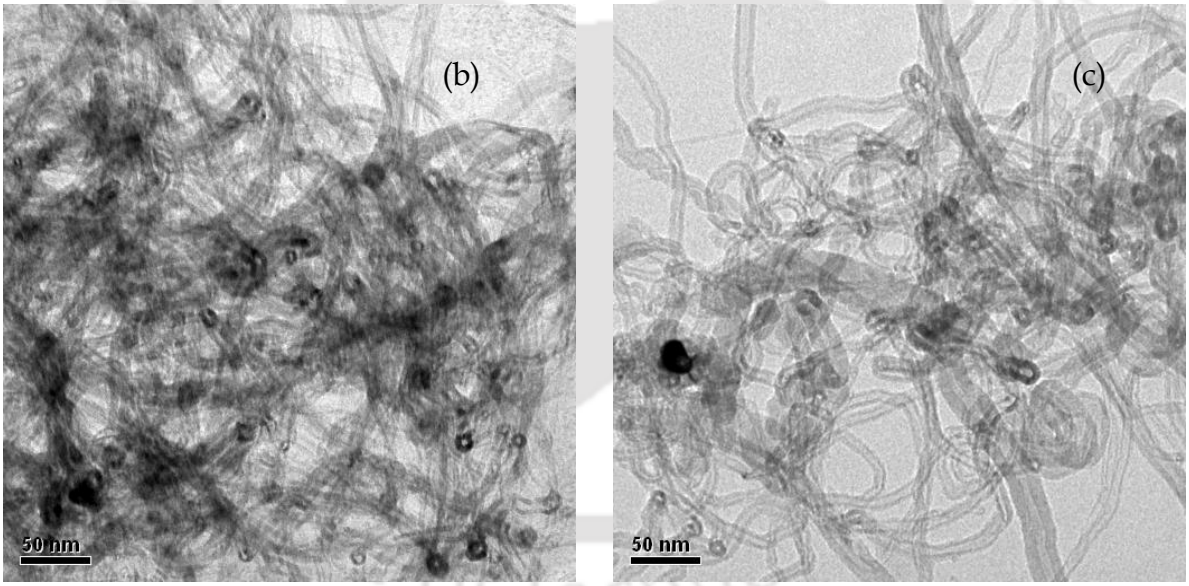

Fig. 4.26 (a) FTIR spectrum confirming the functionalization of chemically treated MWCNT, TEM image of (b) untreated MWCNT (c) treated MWCNT

4.3.1.2 Mechanical properties of PMMA/MWCNT composites

The mechanical characteristics of PMMA composites having different MWCNT concentrations were studied as per ASTM-D638 and D790 and the results are reported. Fig. 4.27, 4.28, 4.29 and 4.30 shows the strength, modulus, strain and percentage enhancement, respectively, of tensile and flexural properties of the PMMA composites,

which were found to be increased upto 0.25 wt. % of MWCNT reinforcement in PMMA beyond which the properties were decreased.

Fig. 4.27 shows the tensile and flexural strength of PMMA/MWCNT composites, where it is observed that the tensile strength of PMMA was found to be increased by 5.5, 20, 32.9, 27 and 10.6 % for the reinforcement of 0.1, 0.2, 0.25, 0.3 and 0.4 wt. % MWCNT, respectively, compared to that of unfilled polymer. In case of flexural strength, the respective enhancement was observed to be 3.8, 7.5, 26.3, 11.2 and 10.8 % in comparison with pure PMMA.

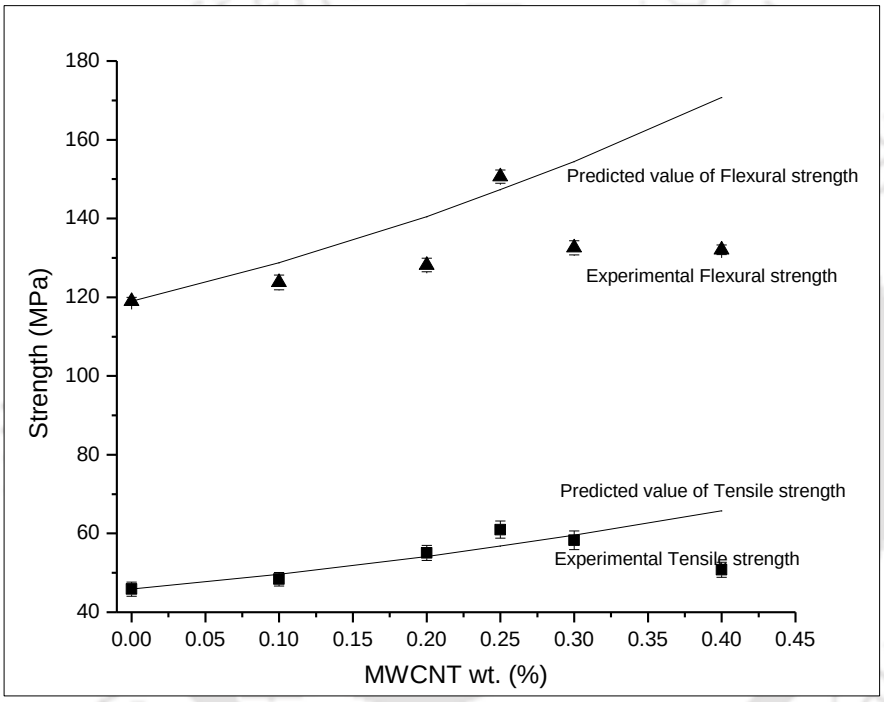

Fig. 4.27 Comparison of experimental and theoretical value of tensile and flexural strength of PMMA/MWCNT composites

The theoretical values of tensile strength were predicted using a model proposed by Pukanszky et al. [1988], and it is shown in equation 4.42. The comparison between experimental and theoretical results of tensile strength was done and the results are shown in Fig. 4.27.

$$\sigma_C = \left(\frac{1 - V_{NT}}{1 + 2.5V_{NT}} \sigma_m \right) \exp\left(BV_{NT}\right) \quad \ldots (4.42)$$

Since, the flexural strength of the composites was not reported using a theoretical model in the literature, an attempt was made to predict the same using the Pukanszky's model, as the tensile strength model was derived on the basis of interfacial bonding between the filler and matrix, the same was also adopted for flexural strength model. The tensile strength and flexural strength of PMMA were observed to be 45 and 119 MPa, respectively, which were obtained from the experiments. It is observed from Fig. 4.27 that the tensile and flexural strength of composites were observed to be increased with MWCNT concentration, where the Pukanszky model showed a good correlation between experimental and theoretical values upto 0.3 wt. % of MWCNT for tensile strength and 0.25 wt. % of MWCNT in case of flexural strength with the deviation of 2.2 % for both, which was found to be increased with MWCNT concentration and reached around 29 % deviation at 0.4 wt. % MWCNT reinforcement in PMMA. As the deviation between experimental and theoretical results was observed to be within the limit of experimental variation, the Pukanszky's model can be used to predict both the tensile and flexural strength of the PMMA composites up to 0.25 wt. % reinforcement of MWCNT.

Fig. 4.28 shows the Young's modulus and flexural modulus of PMMA/MWCNT composites, where the Young's modulus of PMMA was observed to be improved by 11.1, 25.3, 41.9, 25.2 and 19.1 % for the reinforcement of 0.1, 0.2, 0.25, 0.3 and 0.4 wt. % of MWCNT, respectively, compared to that of unfilled polymer and the respective enhancement of flexural modulus was noted to be 6.7, 13.8, 24.1, 17.2 and 12 % in comparison with unfilled PMMA.

In order to predict the Young's modulus of PMMA/MWCNT composites, the modified form of Halpin-Tsai equation was used with an orientation factor, which was suggested by Srivastava et al. [2012] and Yeh et al. [2006].

$$E_C = \left[\frac{3}{8} \frac{1 + 2\left\{ \frac{l_{NT}}{d_{NTo}} \right\} \eta_L V_{NT}}{1 - \eta_L V_{NT}} + \frac{5}{8} \frac{1 + 2\eta_T V_{NT}}{1 - \eta_T V_{NT}} \right] E_m \quad \ldots (4.43)$$

Where, η_L and η_T are as follows:

$$\eta_L = \frac{\left(\frac{\gamma E_{NT}}{E_m}\right) - 1}{\left(\frac{\gamma E_{NT}}{E_m}\right) + 2\left\{\frac{l_{NT}}{d_{NTo}}\right\}} \qquad \text{and} \qquad \eta_T = \frac{\left(\frac{\gamma E_{NT}}{E_m}\right) - 1}{\left(\frac{\gamma E_{NT}}{E_m}\right) + 2}$$

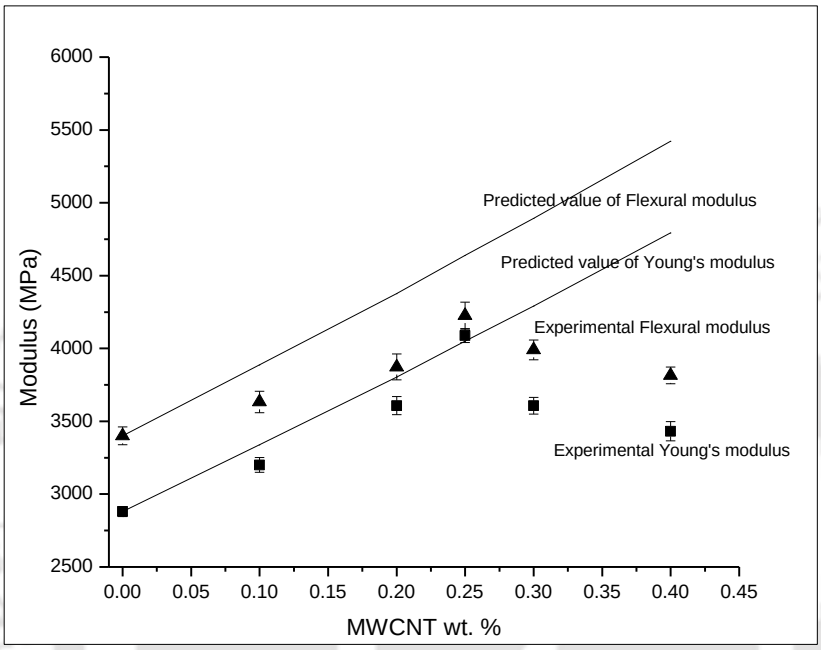

Fig. 4.28 Comparison of experimental and theoretical value of Young's modulus and flexural modulus of PMMA/MWCNT composites

As per the dimension of MWCNT, the maximum and minimum aspect ratio was calculated to be 375 and 84, respectively and thus the average value of the same, ie. 230, was used as an aspect ratio in the above equation. It is also noted that the modulus of composites as per the equation 4.43 was observed to be not influenced by the range of aspect ratio. The Young's modulus, and density of PMMA were observed to be 2.88 GPa and 1.14 g/cc, respectively, which were obtained from the experimental study. The Young's modulus of MWCNT was observed to be 900 GPa, Demczyk et al. [2002]. The modification of Halpin-Tsai equation is the inclusion of the orientation factor, which describes the randomness of the MWCNT distribution. As the length of MWCNT used in the present study was 5-15 μm, which was comparatively less than that of the

specimen thickness (2.9 ± 0.1 mm), the randomness of the filler seems to be very high, which was confirmed from Fig. 4.26c, where a high intensity entanglement of MWCNT was observed and thus the orientation factor was chosen as 0.02 for the calculation, Yeh et al. [2006].

Fig. 4.28 also shows the comparison of experimental and predicted values of Young's modulus of PMMA/MWCNT composites. It is observed that the Young's modulus of PMMA was found to be increased with the MWCNT concentration. The results obtained from the modified Halpin-Tsai equation for Young's modulus showed a close correlation between experimental and theoretical results upto 0.25 wt. % of MWCNT reinforcement with the deviation of 9.3 %, which was found to be increased with MWCNT concentration, where the maximum deviation was found to be 39.7 % at 0.4 wt. % of MWCNT.

Since, no literature was reported for predicting the flexural modulus and the modified Halpin-Tsai model was derived from the rule of mixture principle, an attempt was made to use the same model to predict the flexural modulus of the composites. The flexural modulus of PMMA was 3.3 GPa, which was obtained from the experimental study, whereas the same for MWCNT was noted to be 910 GPa, Demczyk et al. [2002]. The comparison of experimental and theoretical values of flexural modulus of PMMA/MWCNT composites is shown in Figure 4.28, where it was observed to be increased with concentration of reinforcement. It is also observed that a close correlation between the experimental and theoretical values of flexural modulus was maintained below 0.25 wt. % of reinforcement. The deviation between theoretical and experimental results of flexural modulus at 0.25 wt. % of MWCNT reinforcement was found to be 9.7 %, which was increased with MWCNT concentration and it was noted to be 42.2 % at 0.4 wt. % MWCNT reinforcement. Since, the difference between theoretical and experimental results of flexural modulus of composites up to 0.25 wt. % MWCNT reinforcement was found to be within the experimental deviation, the modified Halpin-Tsai model is suggested to be used to predict the flexural modulus of the composites. Based on the above observation, it may be inferred that the modified Halpin-Tsai model could be used to predict the Young's modulus and flexural modulus

of PMMA/MWCNT composites within the acceptable level of deviation up to 0.25 wt. % MWCNT reinforcement.

A close correlation between the experimental and theoretical results of modulus and strength of the PMMA composites upto 0.25 wt. % of MWCNT reinforcement was due to good interfacial bonding between the matrix and reinforcement and the homogeneous dispersion of MWCNT in the matrix, which were confirmed from the experimental studies. The reasons for the increased deviation between experimental and theoretical values beyond 0.25 wt. % of MWCNT could be due to significant presence of voids and agglomerated form of reinforcement, which were also confirmed experimentally but those factors were not considered while deriving the models. Thus, the modified Halpin-Tsai model and Pukanszky's model can be used to predict the mechanical properties of PMMA/MWCNT composites upto 0.25 wt. % of reinforcement, where a close correlation between experimental and theoretical results was observed.

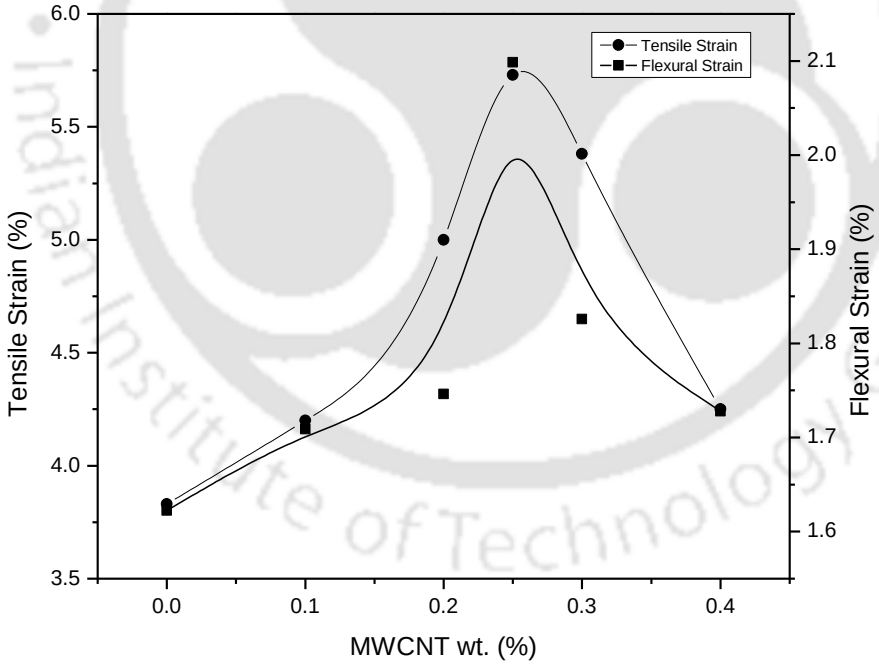

Fig. 4.29 Tensile and flexural strain of PMMA/MWCNT composite

Fig. 4.29 shows the tensile and flexural strain of the PMMA against MWCNT concentration. It is observed that the tensile strain of the composites was increased by 9.7, 30.5, 49.6, 40.5 and 10.9 % for the reinforcement of 0.1, 0.2, 0.25, 0.3 and 0.4 wt. % of MWCNT in PMMA, respectively, in comparison to that of unfilled PMMA and the

corresponding enhancement of flexural strain was calculated to be 5.3, 7.6, 29.3, 12.5 and 6.5 %. Fig. 4.30 shows the enhancement of mechanical properties of PMMA/MWCNT composites. It is observed that the maximum enhancement of tensile strength, Young's modulus, tensile strain, flexural strength, flexural modulus and flexural strain was observed to be 32.9, 41.9, 49.5, 26.3, 24.1 and 29.3 %, respectively at 0.25 wt. % of PMMA/MWCNT composite compared to unfilled PMMA.

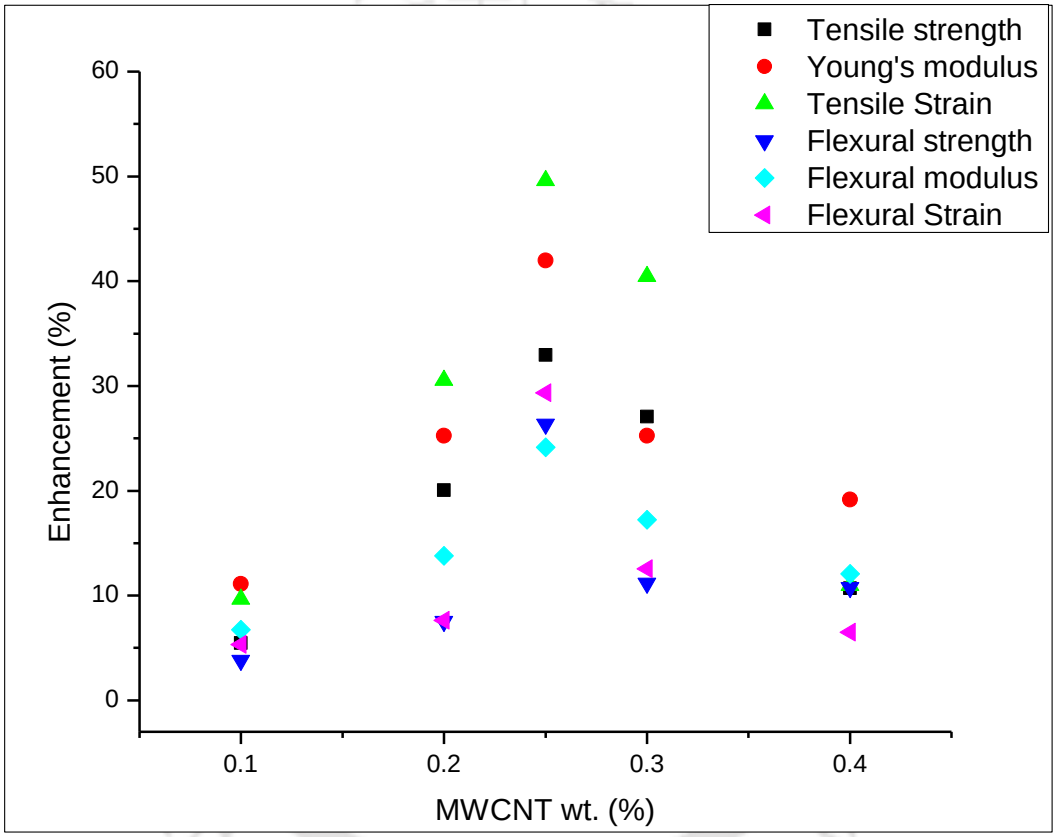

Fig. 4.30 Percentage enhancement of tensile and flexural properties of PMMA/MWCNT composite properties against MWCNT concentration

The mechanism for the enhancement and the reduction of tensile and flexural properties of PMMA/MWCNT composites is discussed below in detail.

4.3.1.3 Reasons for the enhancement of mechanical properties of PMMA upto 0.25 wt. % MWCNT reinforcement

The mechanical properties of composites compared to PMMA were increased due to the following reasons: (a) Due to attractive mechanical properties of MWCNT, its

reinforcement helped to improve the mechanical and flexural properties of PMMA. (b) The functionalization of MWCNT helped to have a perfect bonding with PMMA in addition to increase of its specific surface area, which aids in the effective stress transfer from the polymer to MWCNT. Her et al. [2013] and Yu et al. [2000] reported that the attachment of carboxylic acid functional group over the side walls of MWCNT and the increase of specific surface area of MWCNT led to effective stress transfer from the matrix to reinforcement.

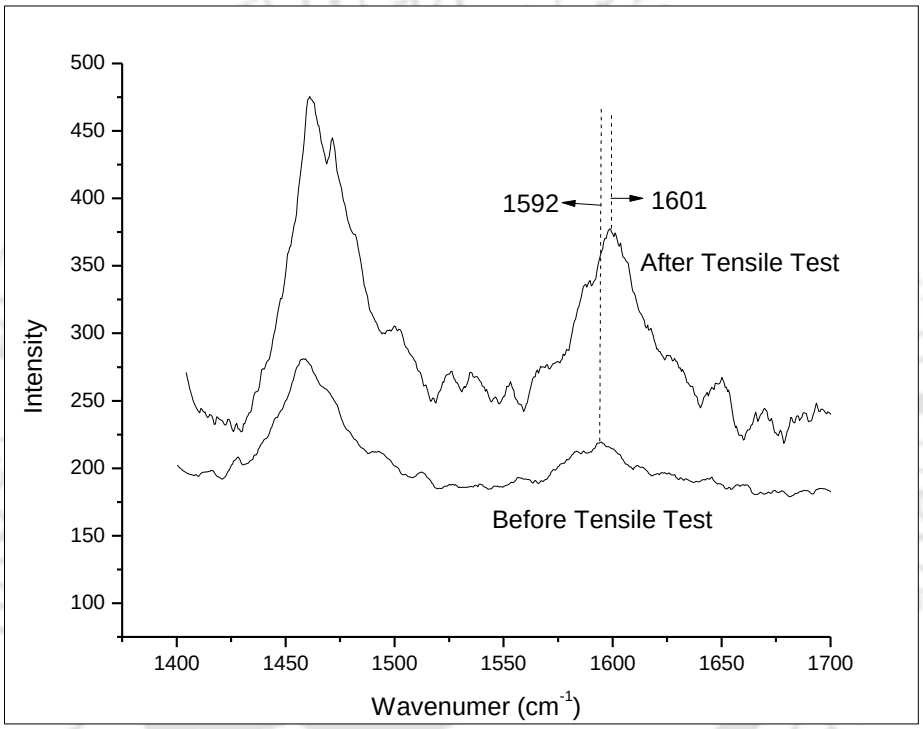

Fig. 4.31 Raman spectra before and after the tensile test of PMMA composites

The Raman spectra of the PMMA composite having 0.25 wt. % MWCNT before and after the tensile test is shown in Fig. 4.31. The peak shift in the range of 1500 to 1600 cm^{-1} belongs to the G-band, which is caused either by tensile or compressive strain on the MWCNT. The G-band peak before and after the tensile test was observed to be 1592 and 1601 cm^{-1}, respectively, corresponding to the shift of 9 cm^{-1}, which confirms the effective stress transfer from PMMA to MWCNT. Bounos et al. [2014] also observed that the vibration in sp^2 C-C bond was generated by the induced strain, which was reflected in the Raman spectra.

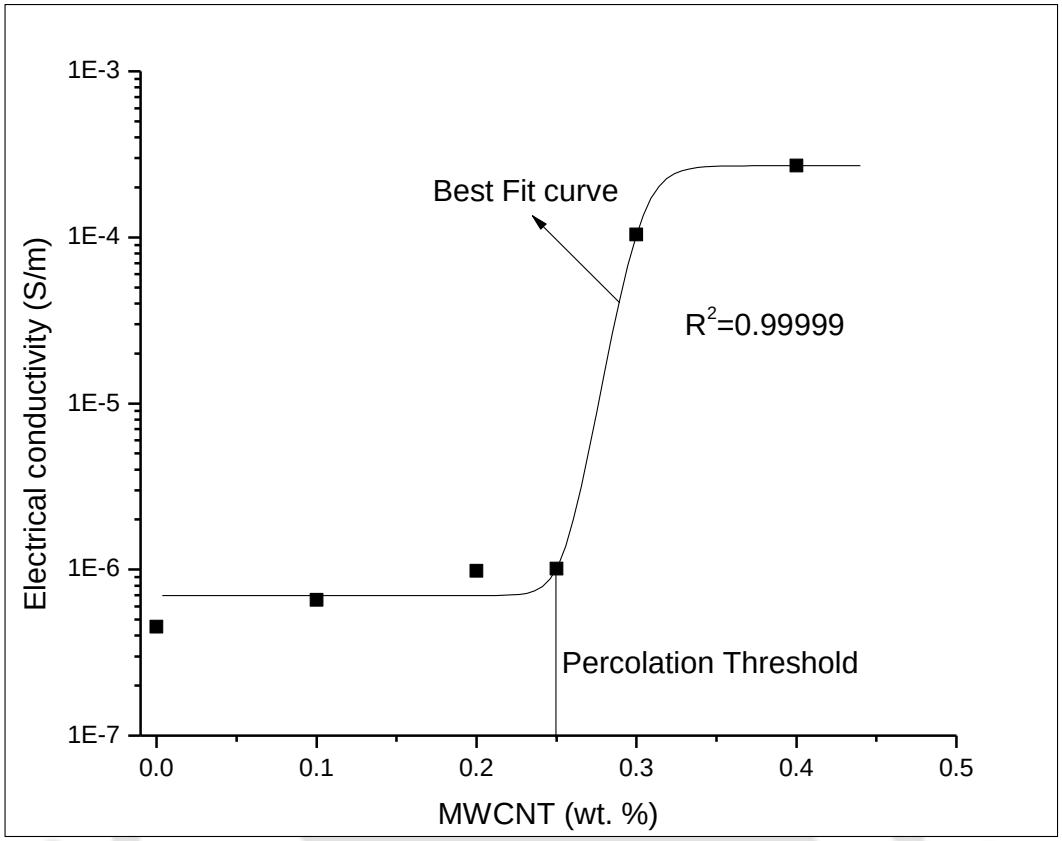

Fig. 4.32 Electrical conductivity of PMMA/MWCNT composites

(c) Homogeneous dispersion of MWCNT assists to increase the mechanical properties of the composites. The electrical percolation analysis was done to confirm the homogeneous dispersion of MWCNT in PMMA matrix. The DC electrical conductivity of PMMA/MWCNT composites was measured from the critical frequency of AC conductivity and the results are shown in Fig. 4.32. The electrical conductivity was observed to be very marginally increased upto 0.25 wt. % of MWCNT concentration, which confirms the homogeneous dispersion of MWCNT in PMMA and no interconnectivity between MWCNT along thickness direction of the sample. The electrical conductivity of 0.3 wt. % of PMMA/MWCNT composite was observed to be 2-order more than that of the 0.25 wt. % composite. A drastic increase in electrical conductivity of the composite was due to the formation of MWCNT network, which showed the interconnectivity among MWCNT by electron tunneling. As the lower percolation threshold suggests a better de-bundling of the reinforcement, Moisala et al. [2006], the above observation confirms the homogeneous dispersion of MWCNT in

PMMA. As per Shang et al. [2009], the electrical percolation threshold was found to be 1.8 wt. % for the PMMA/MWCNT composite, whereas it was observed to be 0.25 wt. % in our case. It is to be noted that the threshold values are expected to differ due to different parameters such as processing conditions, type of functional groups attached on MWCNT, method of attachment of functional group and the dispersion techniques followed.

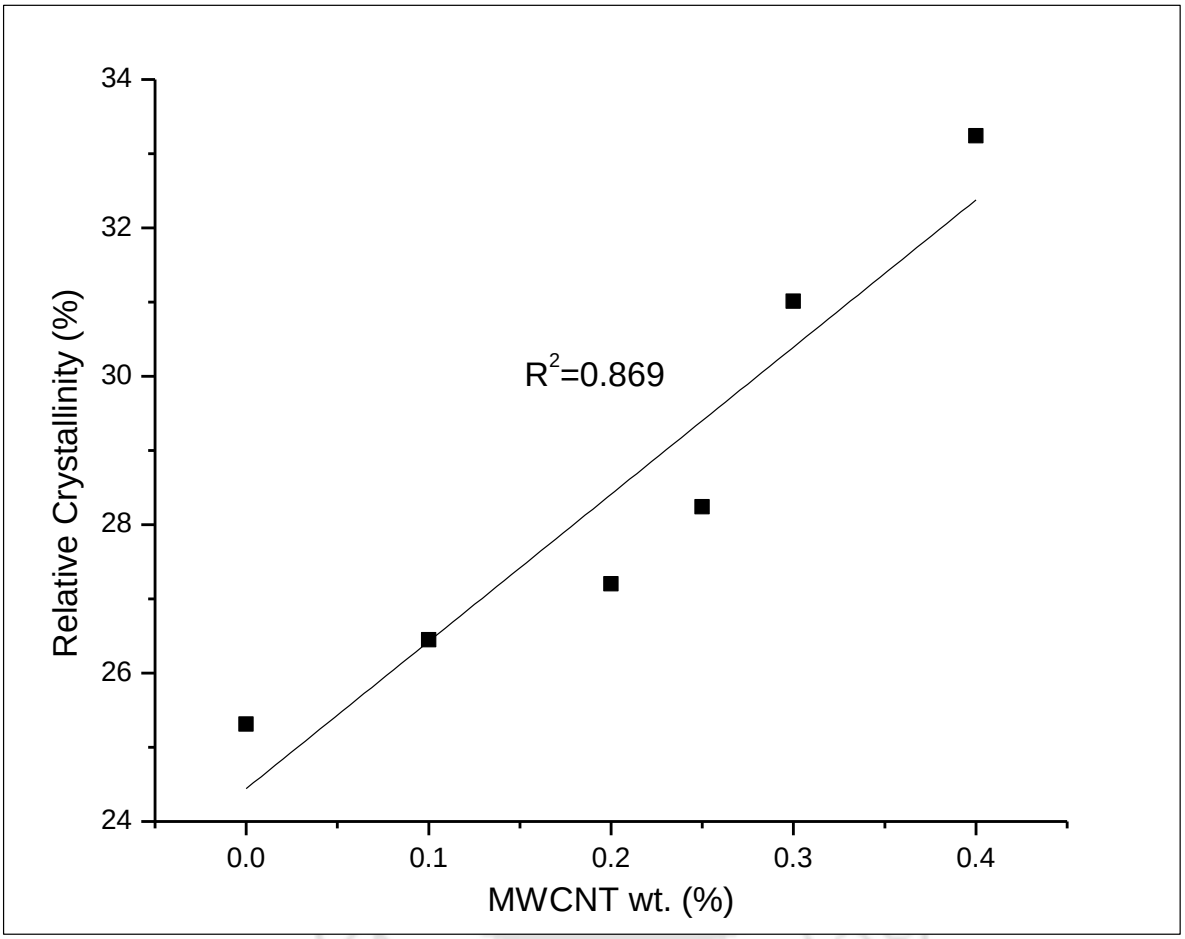

Fig. 4.33 Relative crystallinity of PMMA/MWCNT composites

(d) Another factor which influences the mechanical properties was the crystallinity of the composites. The relative crystallinity of the composites was measured using XRD technique and the results are shown in Fig. 4.33. It was calculated by dividing the sum of the individual area under each peak by the total area with reference to base line of the diffracted pattern, as suggested by Gowariker et al. [1986]. It was observed that the relative crystallinity of PMMA was found to be linearly increased with MWCNT

concentration. The relative crystallinity of 0.4 wt. % of PMMA/MWCNT composite was found to be 33.2 %, whereas it was 25.3 % for pure PMMA. The increased relative crystallinity of the composites is due to the fact that the MWCNT acted as a nucleating agent to initiate the formation of new crystallites. The above discussion was also supported by Zhang et al. [2008] for the increase in crystallinity of the composites with MWCNT reinforcement.

(e) The enhancement of mechanical properties was supported by the confirmation of the interfacial bonding between MWCNT and PMMA matrix. It was observed from the literature that the increase in Tg and thermal stability was used to confirm the interaction between the matrix and reinforcement, Jin et al. [2002]. Fig. 4.34a shows the thermal stability of pure PMMA and its composites. The TGA plots showed the delayed decomposition of composites compared to pure PMMA, which is clearly noticed from the inset. It was observed that the thermal stability of PMMA was increased with MWCNT concentration. The presence of MWCNT in PMMA restrains the heat and acts as a hindrance for the thermal degradation of PMMA. Furthermore, the improvement of thermal stability of pure PMMA by the reinforcement of MWCNT could be easily observed using the derivative of TGA curves, which are depicted from Fig. 4.34b. The peak in the derivative curve represents the temperature at which the maximum rate of degradation occurs. The degradation temperature of pure PMMA and PMMA/0.4 wt. % of MWCNT was found to be 378.6 and 387.7°C, respectively, which showed the influence of MWCNT on the degradation temperature of PMMA.

Fig. 4.35 shows the Tg of PMMA/MWCNT composites, which was obtained from the DSC studies. The interaction between PMMA and MWCNT was confirmed by the increasing trend of Tg of composites against the MWCNT reinforcement. The Tg was found to be increased by 9°C for 0.25 wt. % of composite, whereas it was observed to be 11°C for 0.4 wt. % of composite compared to that of PMMA.

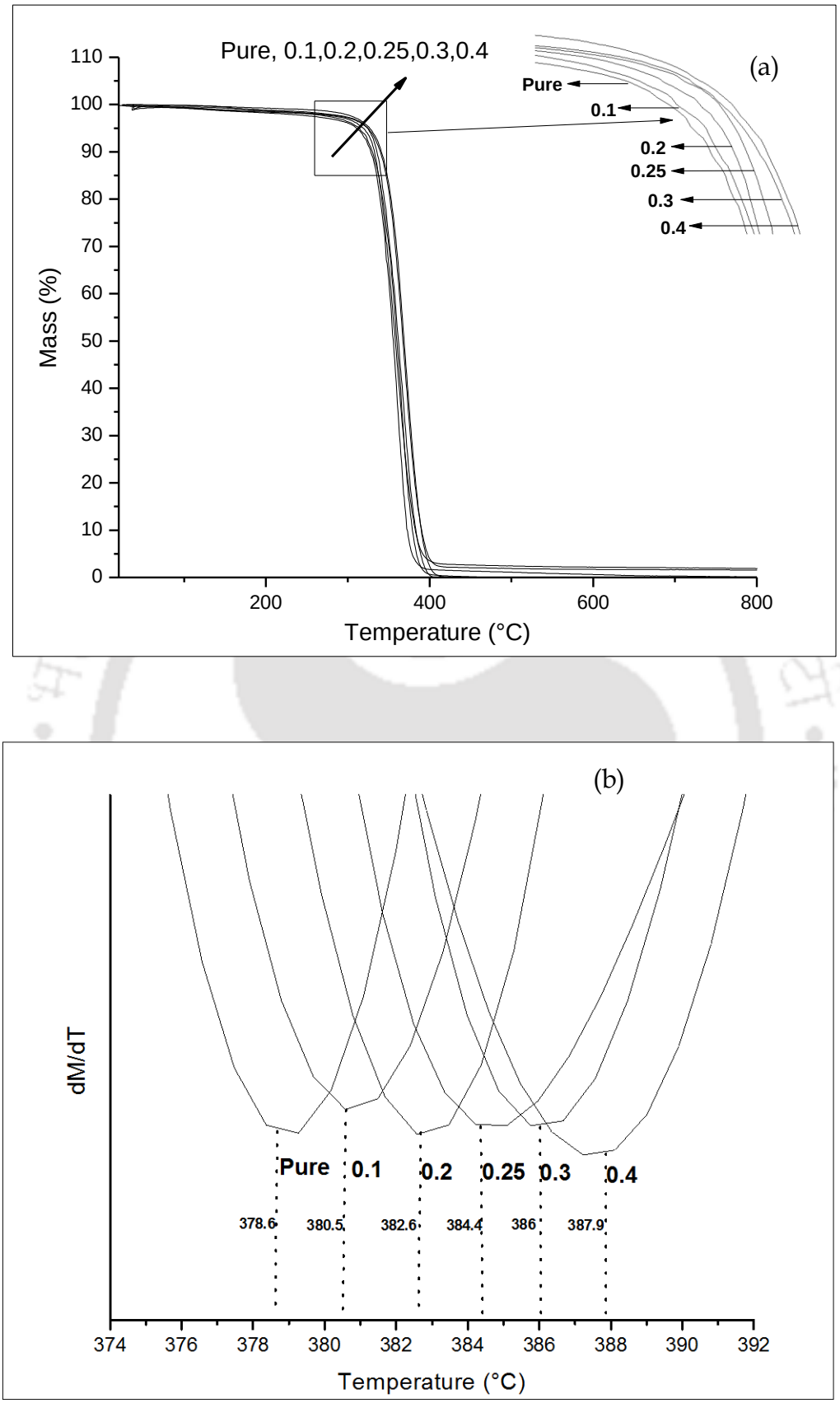

Fig. 4.34 (a) Thermal stability (b) Derivation of a part of TGA curve of PMMA/MWCNT composites

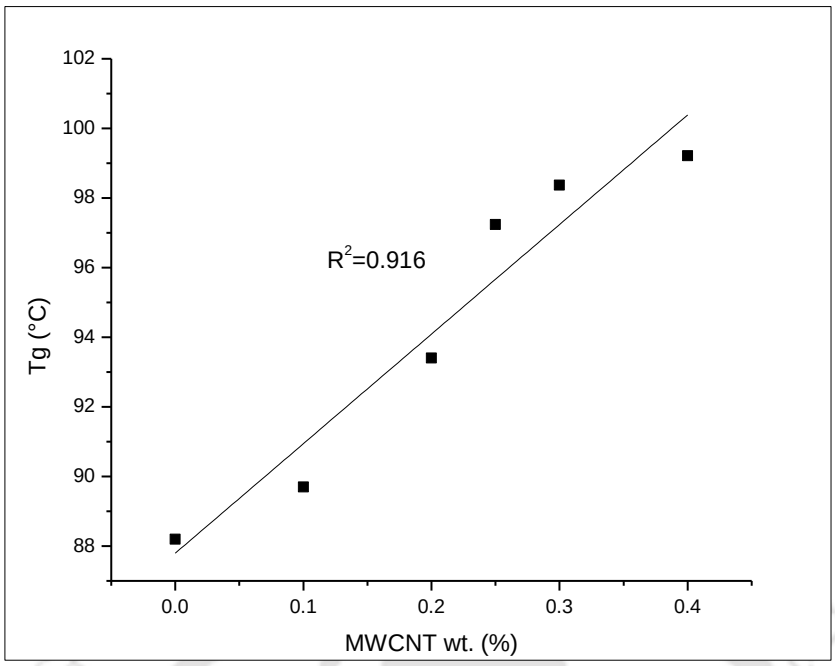

Fig. 4.35 Glass transition temperature (T_g) of PMMA/MWCNT composites

It is clearly understood from the above discussion that the electrical percolation threshold, shift in G-band peak and increase in Tg and thermal stability were used to confirm the interaction between MWCNT and PMMA and they resulted the enhancement of mechanical properties of PMMA/MWCNT composites.

4.3.1.4 Reasons for the reduction of mechanical properties of PMMA composites beyond 0.25 wt. % MWCNT reinforcement

The following are the causes for the reduction of mechanical properties of PMMA/MWCNT composites beyond 0.25 wt. % of reinforcement:

(a) The shedding of side walls after the chemical treatment process led to increase the specific surface area of MWCNT, which is expected to interact with polymer. The specific surface area of MWCNT before and after the chemical treatment process was observed to be 43.6 and 77.3 m^2/g, respectively, corresponding to the enhancement of 77.3 %. The PMMA may not able to wet the MWCNT fully due to its increased specific surface area leading to the formation of micro-voids during the preparation of composites. The voids in the composites at higher concentration of MWCNT were also reported by Singh et al. [2008b] and Sreekanth et al. [2013].

(b) The variation of thermal properties such as thermal conductivity and specific heat capacity of PMMA and MWCNT might lead to the formation of voids in the composites. MWCNT has good thermal properties such as thermal conductivity of 3000 W/m-K and specific heat capacity of 710 J/kg-K, Yang et al. [2009] and Pradhan et al. [2009]. The thermal conductivity and specific heat capacity of PMMA, obtained from the experimental study, were observed to be 0.215 W/mK and 1618 J/kg-K, respectively, which showed that the specific heat capacity of PMMA was more than twice that of MWCNT. PMMA is expected to take approximately 2 times more amount of heat compared to MWCNT in order to have 1°C temperature raise. The thermal conductivity of MWCNT was found to be about 4-order more than that of PMMA. When equal amount of heat is supplied to the PMMA and MWCNT mixture in the heating chamber of an injection molding machine, the heat is expected to transfer easily to MWCNT than PMMA. Though the polymer requires large amount of heat due to its high specific heat capacity for melting, the heat is not transferred effectively to the polymer during the processing condition. It led to the incomplete consolidation of a polymer and the formation of micro-voids in the composites prepared with higher concentration of MWCNT, and thus it led to the reduction of mechanical properties beyond 0.25 wt. % of MWCNT. The above hypothesis was also supported by Sreekanth et al. [2013]

(c) The voids present in the composites were also resulted from the increase of complex viscosity of the melt-mix at higher concentration of MWCNT leading to decrease the mechanical properties, which was confirmed by the melt flow index (MFI) of the MWCNT coated PMMA pellets. The MFI of PMMA was found to be decreased with an increase of MWCNT concentration and the results are shown in Fig. 4.36. In order to confirm the trend, the MFI of the composites was studied, which was found to be reduced by 32.5 % at 0.4 wt. % of MWCNT reinforcement compared to that of pure PMMA confirming the significant increase of viscosity. Annala et al. [2012] and Sreekanth et al. [2013] also confirmed that the higher concentration of MWCNT in polymers was found to decrease their mechanical properties by developing the micro-voids. The increase in viscosity of polymer melt during the processing condition led to

the reduction of mechanical properties of PMMA composites beyond an optimum concentration of reinforcement.

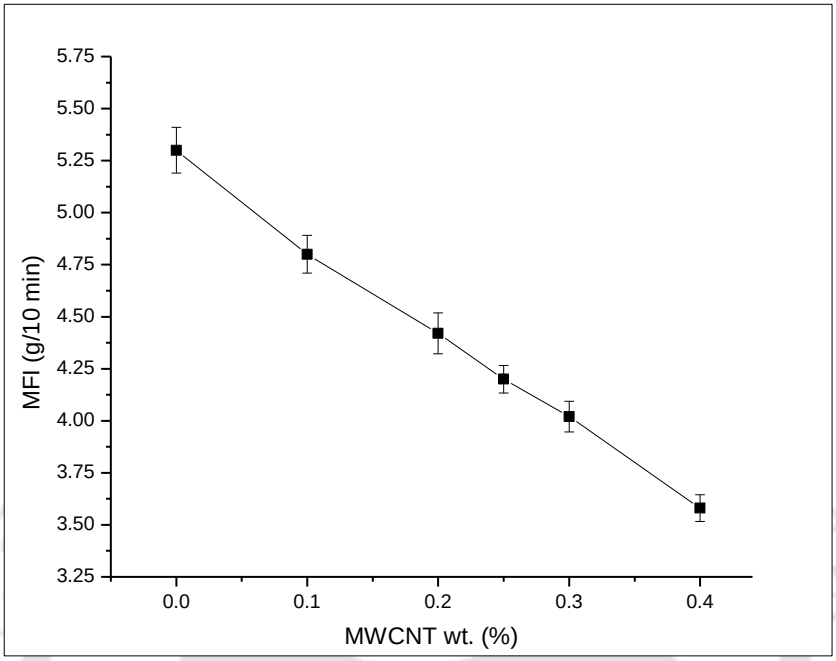

Fig. 4.36 Melt Flow Index of PMMA/MWCNT composites

To confirm the presence of voids in the PMMA composites, the specimens of 0.3 and 0.4 wt. % MWCNT reinforced PMMA were studied for their topography. Fig. 4.37a and b shows the micro-voids present in the specimens at 0.3 and 0.4 wt. % of MWCNT reinforcement, respectively, where the increased number of micro-voids was observed with MWCNT concentration

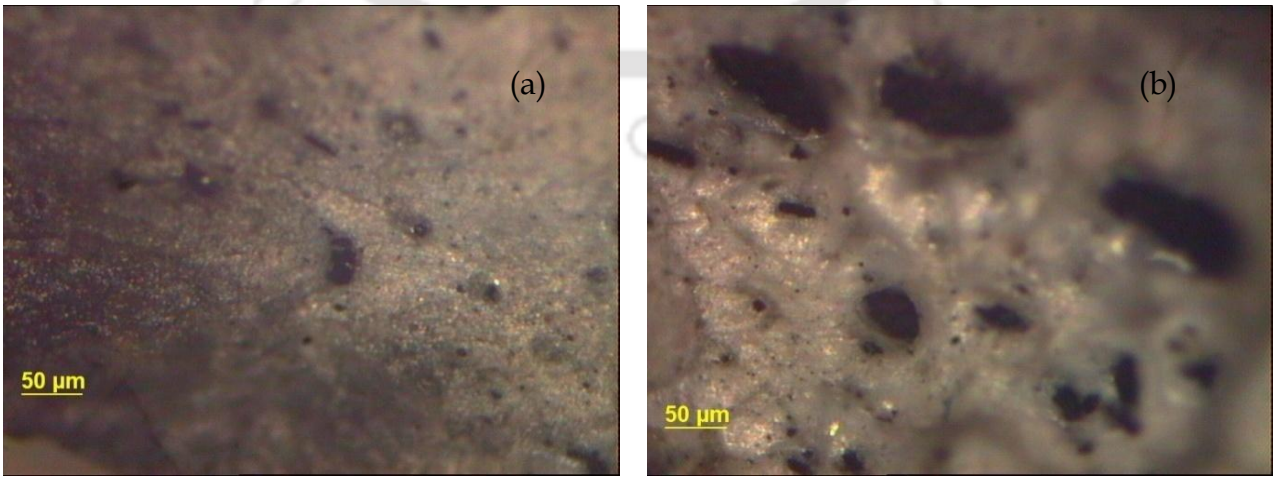

Fig. 4.37 Optical microscope image of (a) 0.3 wt. % and (b) 0.4 wt. % PMMA composite

Thus, the combined effects of increased viscosity of composites and poor thermal conductivity of PMMA played a major role for the generation of micro-voids leading to decrease the mechanical properties of PMMA composites beyond 0.25 wt. % reinforcement of MWCNT.

4.3.2 Aging studies on PMMA/MWCNT composites

4.3.2.1 Mechanical properties of PMMA/MWCNT composites after aging

Fig. 4.38, 4.39 and 4.40 shows the tensile strength, Young's modulus and tensile strain, respectively, of PMMA/MWCNT composites aged for the period of up to 12 months. The aging duration was limited to 84 cycles, about 75 days, due to practical constraints.

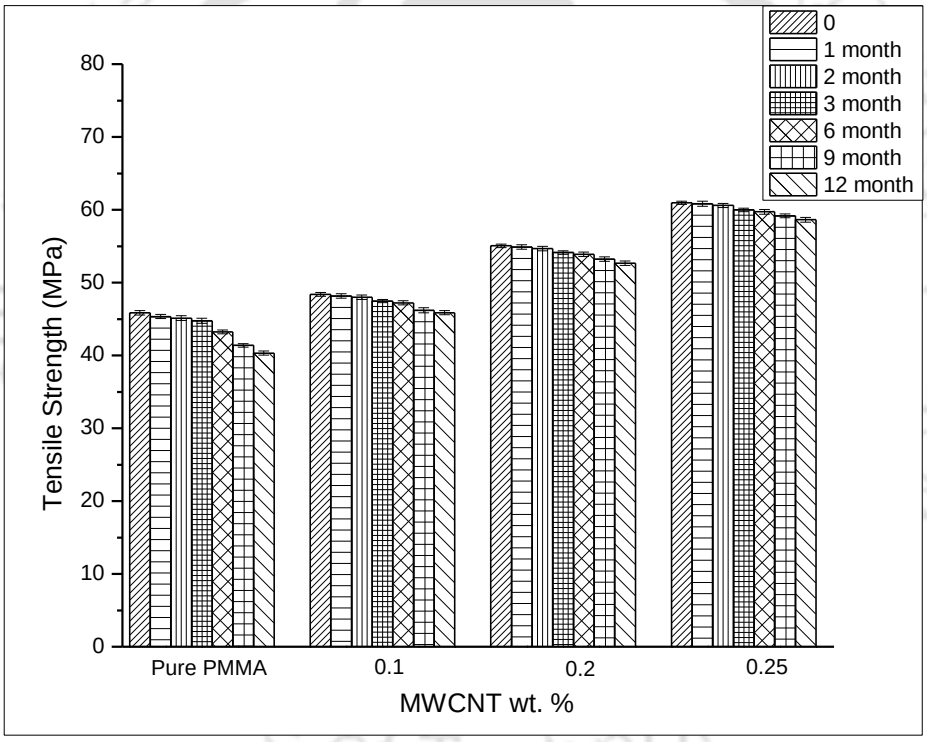

Fig. 4.38 Tensile strength of PMMA/MWCNT composites against aging period

It was observed from Fig. 4.38 that the tensile strength of pure PMMA and PMMA/MWCNT composites was found to be linearly decreased with aging period. However, the reduction of tensile strength was found to be high in case of pure PMMA compared to PMMA/MWCNT composites. The tensile strength of PMMA was found to be reduced from 45.8 to 40.3 MPa after 12 months of aging. For the same condition, the tensile strength of PMMA with 0.25 wt. % of MWCNT reinforcement was reduced

from 60.9 to 58.6 MPa. The tensile strength of PMMA/MWCNT composites irrespective of the concentration of reinforcement up to 3 months of aging was observed to be within the deviation of - 2.4 % in comparison to that of unaged respective samples.

It is observed from Figure 4.39 that the Young's modulus of PMMA was found to be reduced from 2.8 to 2.2 GPa after 12 months of aging, whereas 0.25 wt. % of MWCNT reinforced PMMA showed the reduction from 4 to 3.8 GPa.

The tensile strain of pure PMMA and 0.25 wt. % composites after 12 months of aging was found to be 2.3 and 4.8 %, respectively as shown in Fig. 4.40, and the respective unaged samples showed the strain of 3.8 and 5.7 %. The tensile strength, Young's modulus, and tensile strain of 12 months aged PMMA/0.25 wt. % of MWCNT composite were observed to be 45.5, 76.5 and 113.9 %, respectively, higher than that of PMMA after the same period of aging. It is also noted that the tensile strength of PMMA/0.25 wt. % MWCNT composites after 12 months of aging was observed to be 26.2 % more than that of fresh PMMA samples.

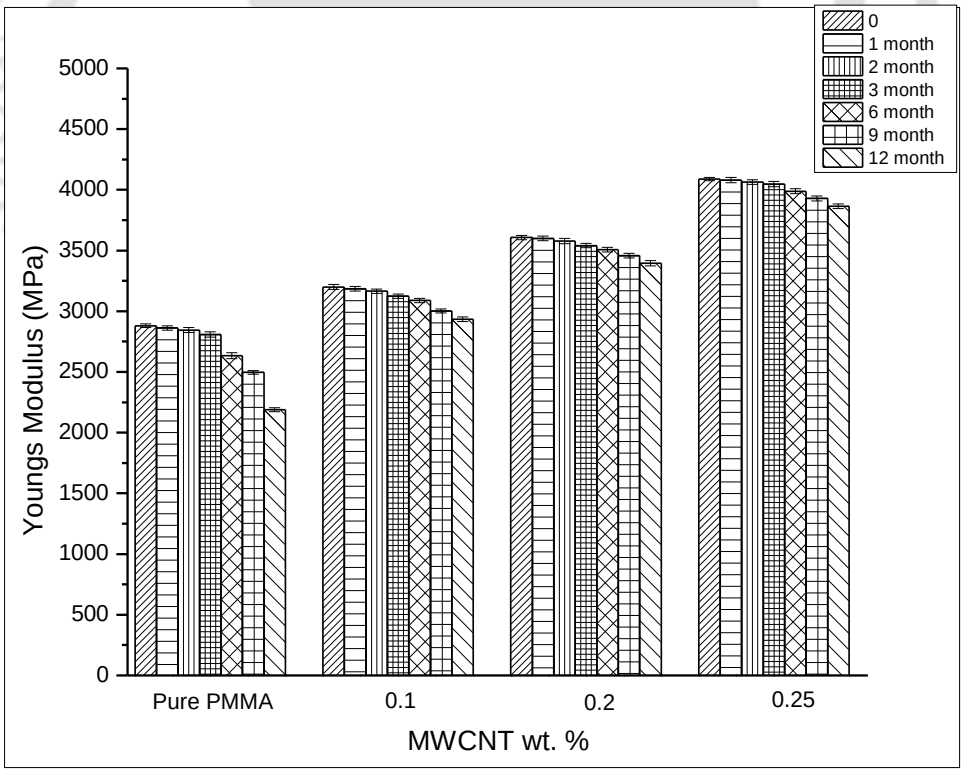

Fig. 4.39 Young's modulus of PMMA/MWCNT composites against aging period

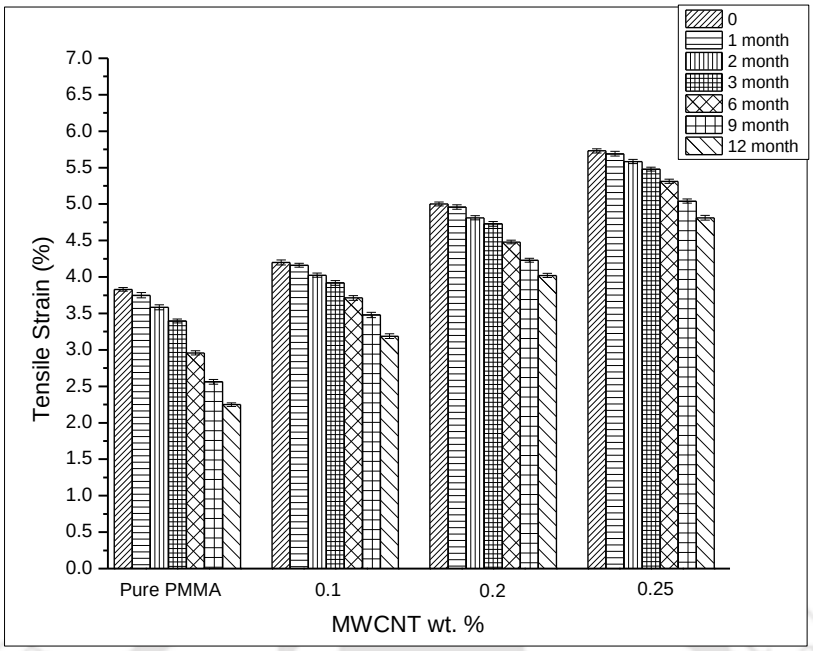

Fig. 4.40 Tensile strain of PMMA/MWCNT composites against aging period

Fig. 4.41 shows the extrapolated aging trend of the tensile strength of PMMA/0.25 wt. % MWCNT composite and pure PMMA with an assumption of the same rate of degradation beyond 12 months of aging and it was noted that the tensile strength of the said composite was expected to reach the unaged PMMA sample strength after 78 months aging, which confirmed the increased longevity of the composites.

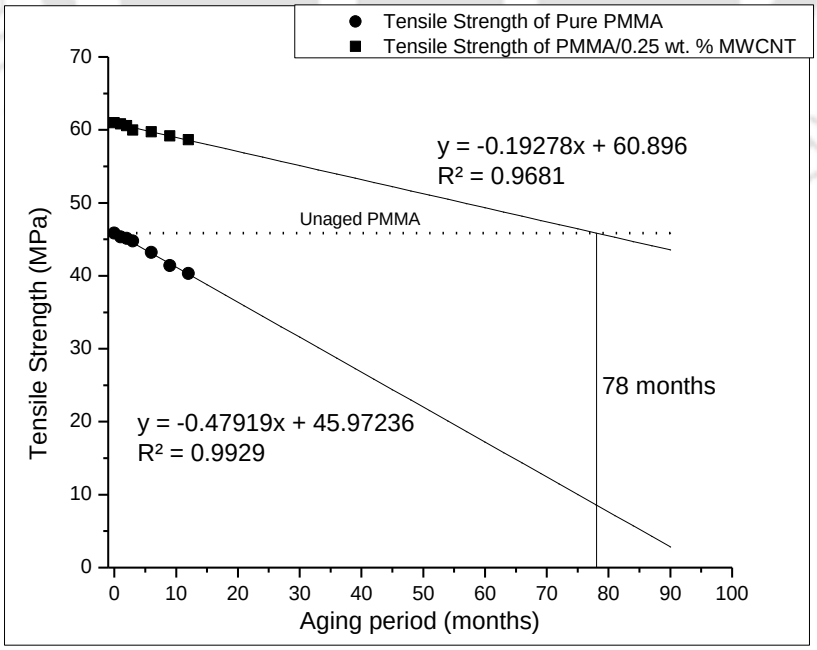

Fig. 4.41 Extrapolated aging trend of tensile strength of PMMA/0.25 wt % MWCNT composites and pure PMMA

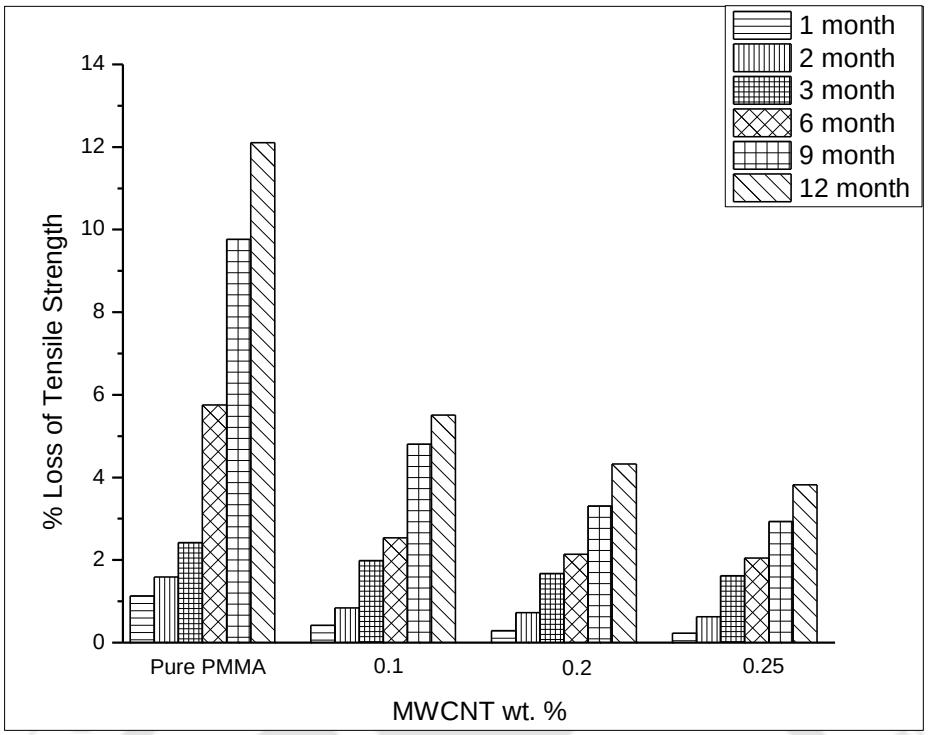

Fig. 4.42 Loss of tensile strength of PMMA and its composites in comparison with respective unaged sample

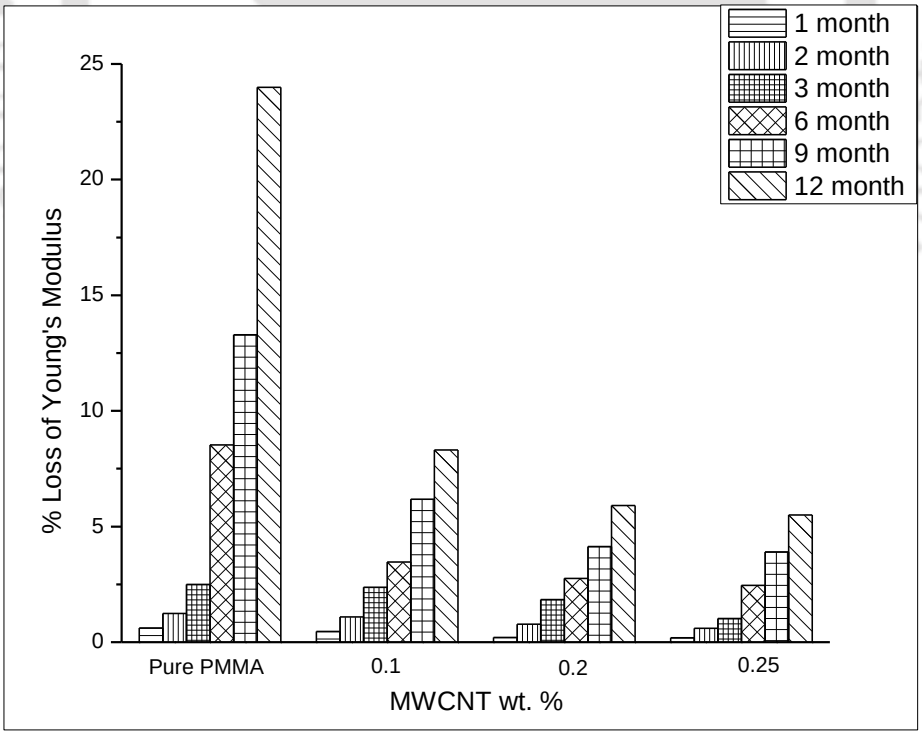

Fig. 4.43 Loss of Young's modulus of PMMA and its composites in comparison with respective unaged sample

The Young's modulus of pure PMMA was reduced by 0.6, 1.2, 2.5, 8.5, 13.3 and 23.9 % after 1, 2, 3, 6, 9 and 12 months of aging, respectively, whereas the reduction was confined to 0.2, 0.6, 1, 2.5, 3.9 and 5.5 % for 0.25 wt. % MWCNT reinforced PMMA and the results are shown in Fig. 4.43.

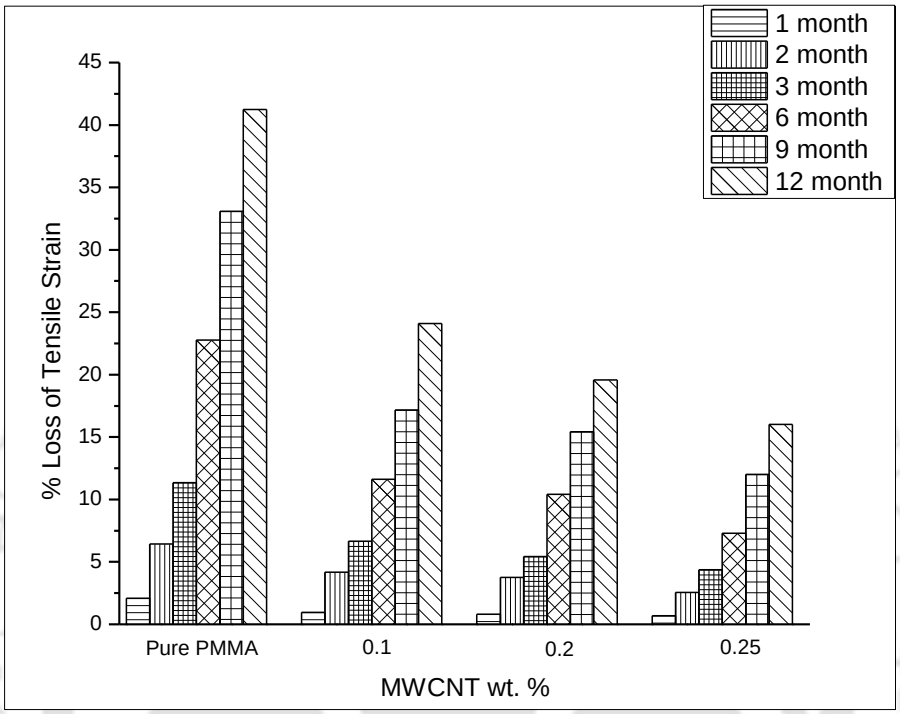

Fig. 4.44 Loss of tensile strain of PMMA and its composites in comparison with respective unaged sample

The reduction of tensile strain of pure PMMA, as shown in Fig. 4.44, was noted to be 2, 6.4, 11.3, 22.8, 33 and 41.3 %, whereas the same was limited to 0.7, 2.6, 4.4, 7.3, 12 and 16 %, using 0.25 wt. % MWCNT reinforcement in PMMA after the aging period of 1, 2, 3, 6, 9 and 12 months, respectively. The loss of ductile characteristics of PMMA or the ductile to brittle transition of PMMA after 12 months of aging was limited by more than 61.3 % by the reinforcement of 0.25 wt. % MWCNT and thus, the ductile characteristics of the PMMA were significantly retained by the reinforcement of MWCNT even after 12 months of aging.

In all cases, the reduction of tensile properties of PMMA within 3 months of aging was noted to be within the variation of - 2.5 % in comparison to that of unaged PMMA and thus the effective utilization of MWCNT for restricting the degradation of PMMA was

not significant. However, the MWCNT reinforcement was very much helpful and sensitive to limit the degradation of PMMA after 6 months of aging.

Fig. 4.45 shows the flexural strength of PMMA/MWCNT composites having different concentration of reinforcement against the aging period. It was observed that the flexural strength of pure PMMA was found to be reduced from 119.2 to 98.5 MPa, whereas the same for 0.25 wt. % MWCNT reinforced PMMA showed the reduction from 150.6 to 139.1 MPa after 12 months of aging.

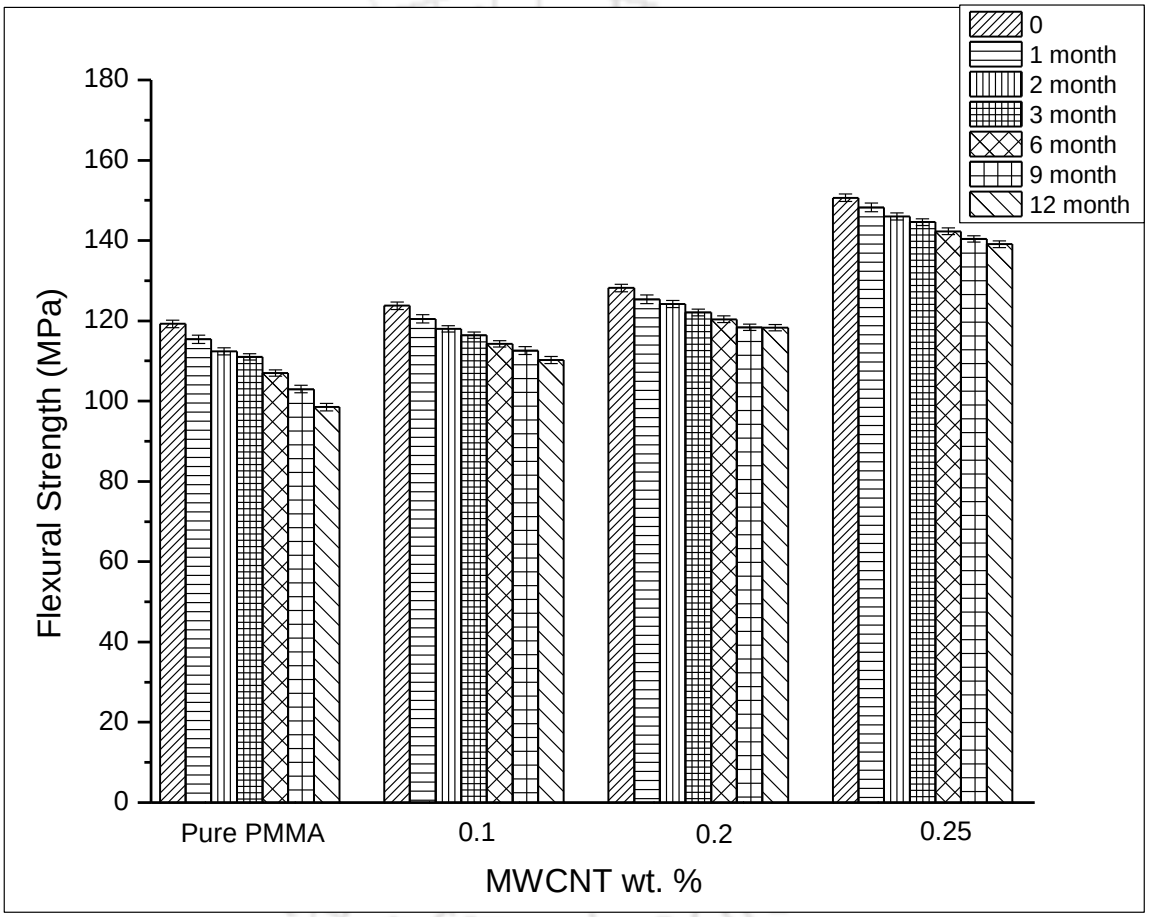

Fig. 4.45 Flexural Strength of PMMA and its composites in comparison with respective unaged sample

Fig. 4.46 shows the flexural modulus of the test samples after 12 months of aging. It was observed that the flexural modulus of PMMA was brought down from 3404 to 3128 MPa, whereas the same was reduced from 4226 to 4131 MPa in case of 0.25 wt. % MWCNT reinforced PMMA.

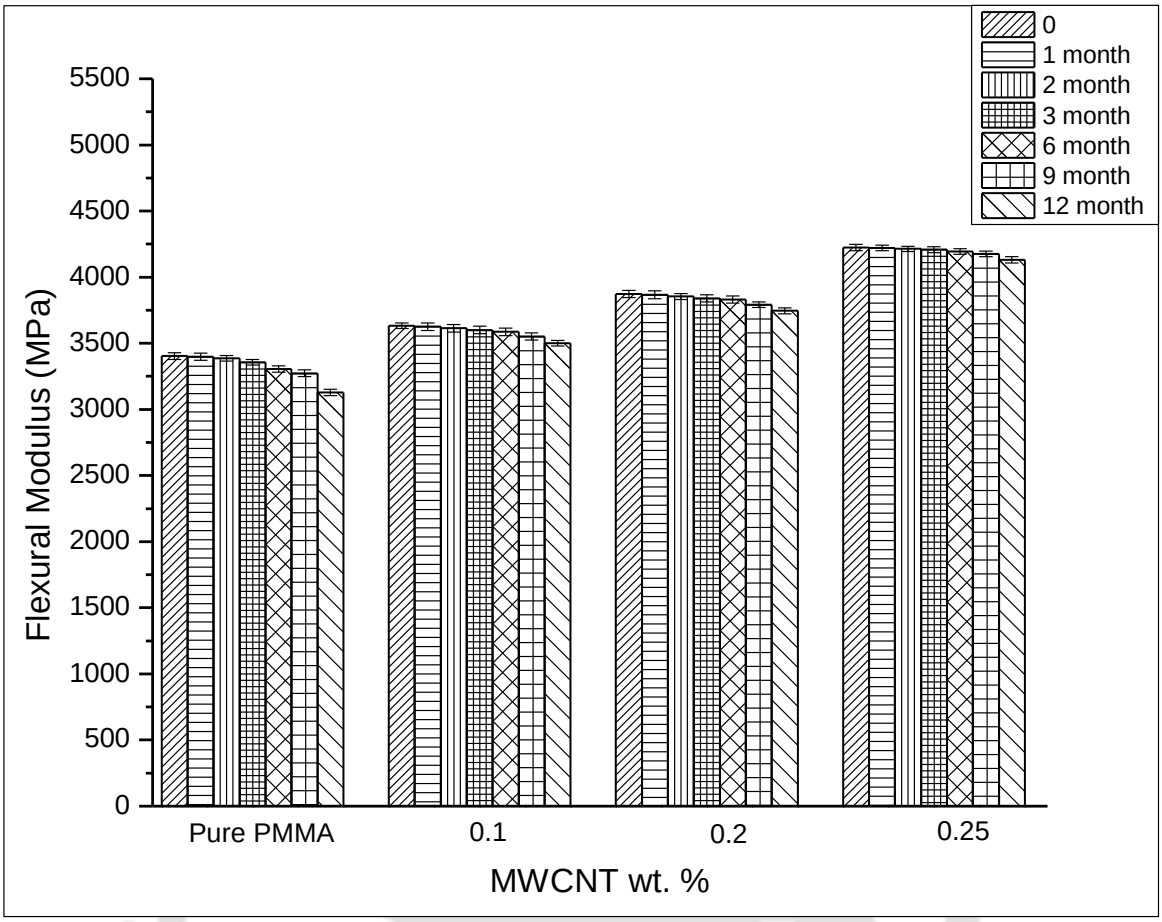

Fig. 4.46 Flexural modulus of PMMA and its composites in comparison with respective unaged sample

Fig. 4.47 shows the bending strain of PMMA/MWCNT composites against the reinforcement concentration till 12 months of aging. The bending strain of pure PMMA was reduced from 1.6 to 1.35 % at the end of aging period, whereas the PMMA reinforced with 0.25 wt. % of reinforcement exhibited the reduction from 2.1 to 1.96 %. It is observed that the bending strain of PMMA and its composites was not significantly influenced upto 12 months of aging. Overall, it is observed that the reduction of flexural properties of PMMA and its composites up to 3 months of aging was noticed to be within the deviation of - 6.9 % in comparison to that of respective unaged sample. After 12 months of aging, the flexural strength, flexural modulus and the bending strain of PMMA/0.25 wt. % MWCNT composite were noted to be 41.2, 32, and 44.2 % higher than that of PMMA. The flexural strength of said composite was 16.7 % more than that of unaged PMMA after 12 months of aging.

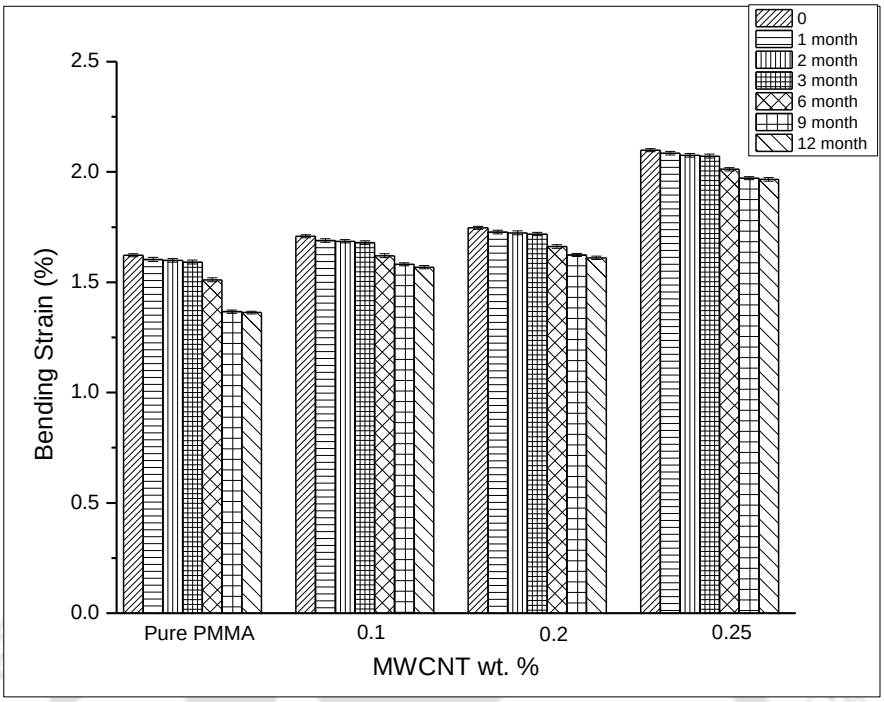

Fig. 4.47 Bending strain of PMMA and its composites in comparison with respective unaged sample

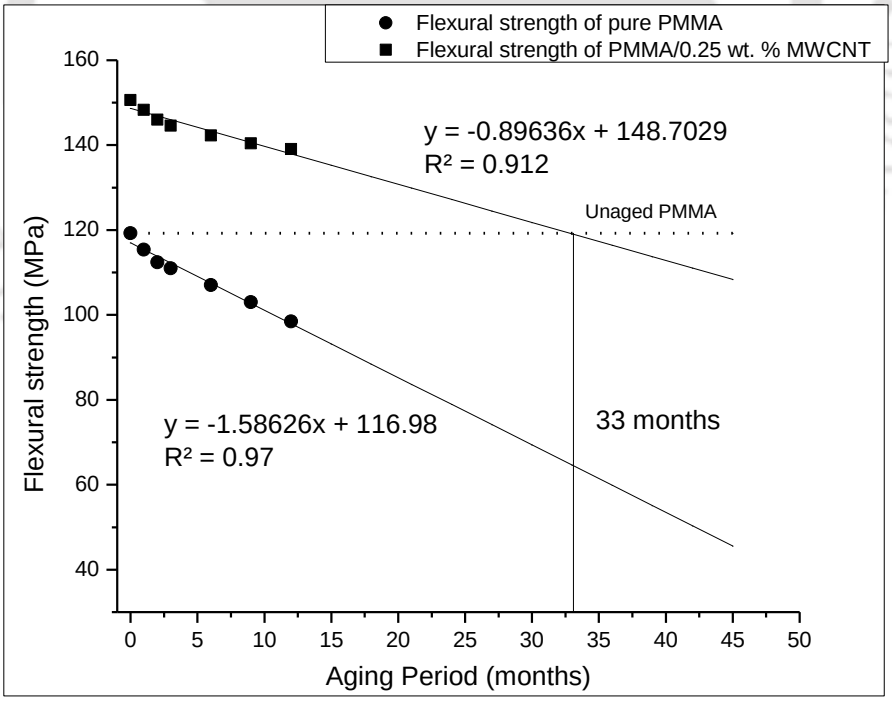

Fig. 4.48 Extrapolated aging trend of flexural strength of PMMA/0.25 wt % MWCNT composites and pure PMMA

Fig. 4.48 shows the extended degradation behavior of the flexural strength of PMMA and PMMA/0.25 wt. % MWCNT composites with aging. It was observed that the

flexural strength of 0.25 wt. % of MWCNT reinforced PMMA after 33 months of aging was noted to be equivalent to that of pure PMMA without aging. Hence, the reinforcement of MWCNT with PMMA limited the degradation behavior of its flexural strength. The flexural properties of the tested composites after 12 months of aging is more than that of fresh PMMA samples and thus the durability of proposed composites are expected to be increased significantly.

Fig. 4.49, 4.50 and 4.51 shows the loss of flexural strength, flexural modulus and bending strain of the aged samples, respectively, compared to respective unaged sample. It was noted that the reduction of flexural properties was found to be more in case of pure PMMA compared to that of PMMA/0.25 wt. % of MWCNT composite. It was observed from Fig. 4.49 that the loss of flexural strength of pure PMMA after 1, 2, 3, 6, 9 and 12 months of aging was found to be 3.2, 5.7, 6.9, 10.3, 13.6 and 17.4 %, respectively, while the same was restricted to 1.5, 3.0, 4.0, 5.5, 6.8 and 7.6 % by reinforcing 0.25 wt. % of MWCNT.

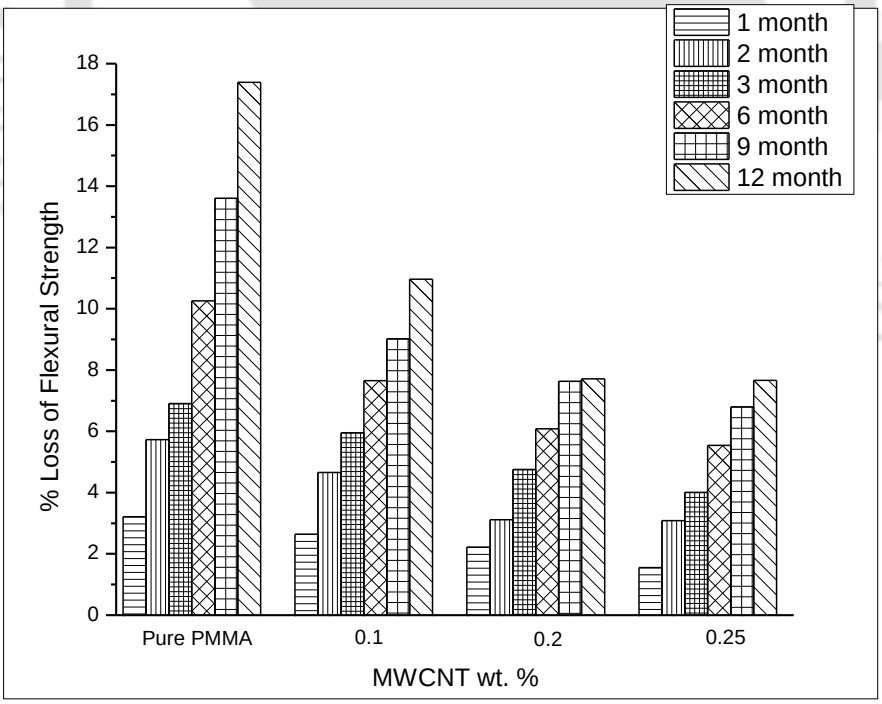

Fig. 4.49 Loss of flexural strength of PMMA and its composites in comparison with respective unaged sample

Fig. 4.50 shows the loss of flexural modulus of PMMA/MWCNT composites with aging. The reduction of flexural modulus of pure PMMA after 1, 2, 3, 6, 9 and 12 months of aging was found to be 0.2, 0.5, 1.4, 2.9, 3.8 and 8.1 %, respectively, which were limited to 0.1, 0.3, 0.4, 0.8, 1.2 and 2.2 %, for the 0.25 wt. % of MWCNT reinforced PMMA composite. In case of flexural modulus of PMMA, the maximum loss was noted to be 8.1 % after 12 months of aging, which was limited to 2.2 % in case of composites. The loss of flexural modulus of PMMA/0.25 wt. %MWCNT composites after one year of aging was found to be insignificant and the results are found to be within the deviation of -3.6 % compared to respective unaged composites.

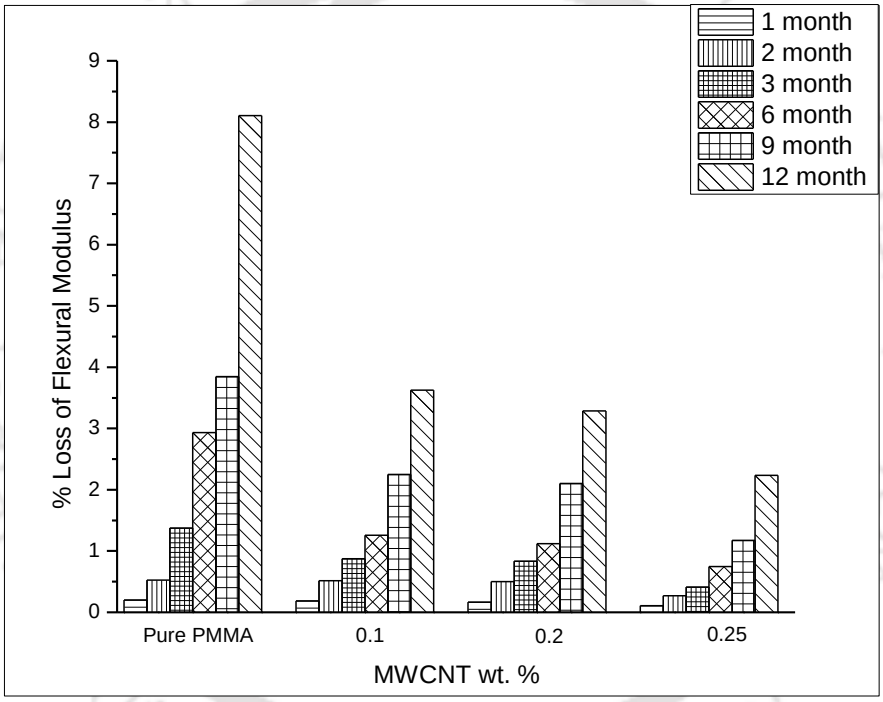

Fig. 4.50 Loss of flexural modulus of PMMA and its composites in comparison with respective unaged sample

The loss of bending strain of pure PMMA was observed to be 1.2, 1.4, 1.9, 6.8, 15.7 and 15.9 %, which was limited to 0.6, 1, 1.3, 4.1, 6 and 6.3 % for 0.25 wt. % of composite, respectively, for the corresponding aging period of 1, 2, 3, 6, 9 and 12 months, and it is shown in Fig. 4.51. The loss of bending strain of PMMA up to 3 months of aging was found to be insignificant and it was noted to be within the deviation of - 1.9 % in comparison to that of unaged PMMA.

The tensile and flexural properties of PMMA were found to be decreased after 1, 2, 3, 6, 9 and 12 months of aging. However, the loss of mechanical properties was restricted significantly with the MWCNT reinforcement. Hence, it was expected that the MWCNT in PMMA acted as a hindrance for the UV rays induced degradation of the polymer. The reasons for the same are discussed below in detail.

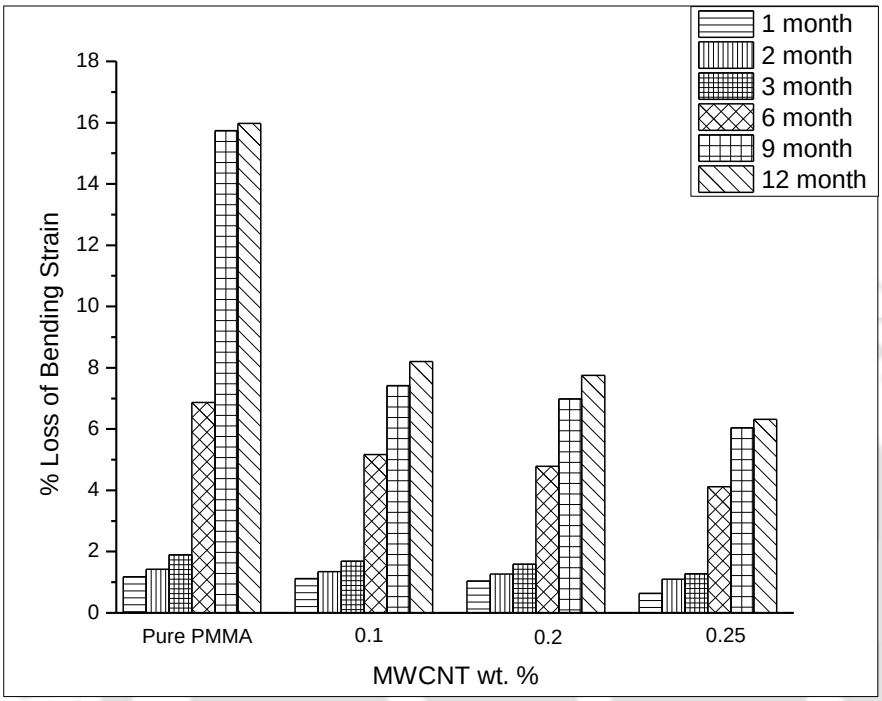

Fig. 4.51 Loss of bending strain of PMMA and its composites in comparison with respective unaged sample

4.3.2.2 MWCNT as a radical scavenger

The energy present during the exposure of UV rays led to break the chemical bonds present in the polymer such as C-C, C-H and C-O bond, and it is shown in Fig. 4.52. The radicals generated during the cleavage acted as an initiator for the degradation of a polymer. The bond dissociation energy of 358, 375 and 420 kJ/mol. headed to the cleavage of C-O, C-C and C-H bond, respectively, Singh et al [2008a]. It was observed that the reduction of mechanical properties of PMMA up to 3 months of aging was observed to be within the deviation of - 6.9 % in comparison to that of unaged PMMA. The possible reason for the above observation was that the energy intensity per unit area might be lower than the bond dissociation energy. However, a significant reduction of mechanical properties of pure PMMA was observed after 6, 9 and 12

months of aging and it was due to the increase in exposure intensity beyond the bond dissociation energy of C-O, C-C and C-H bond. It led to their cleavage and the formation of free radicals, which caused the propagation of the degradation of a polymer. During aging, the oxygen present in the environment reacted with these free radicals and the oxygen atoms were attached with the polymer chain. Later, the propagation of UV rays induced degradation was increased with time. It is also called as oxidative chain scission, which controls the time bound degradation of the polymer. Hence, an increase of the free radicals plays a vital role in propagating the degradation of the polymer, causing the reduction of mechanical properties due to chain scission reaction. This was also supported by Singh et al. [2008a], where the possible mechanism for the UV rays induced degradation of the polymer was discussed.

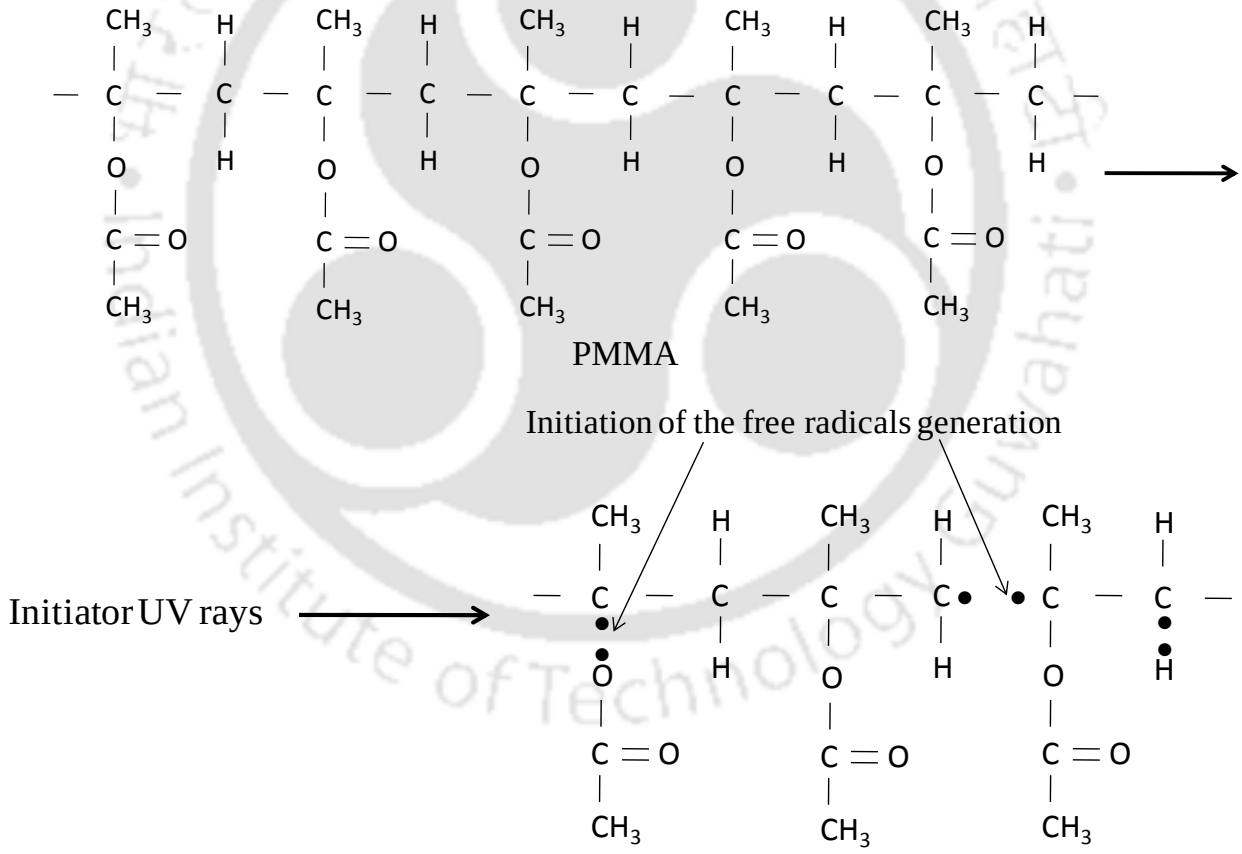

Fig. 4.52 Initiation of UV rays induced degradation of PMMA

The termination mechanism of the generated free radicals in order to reduce the degradation of the polymer can be achieved in two ways:

(i) An addition of two polymer chains with free radicals in each chain led to the termination of degradation cycle by themselves. Similarly, the oxidative chain scission also terminates by itself with the addition of another oxidative chain or free radical chain. As the termination of this kind was found to be very less, it is not expected to limit the polymer degradation significantly.

(ii) Another means of termination of free radicals was due to the reinforcement of MWCNT in two different ways in the polymer, which are explained below in detail.

(a) Increase in defects after MWCNT functionalization

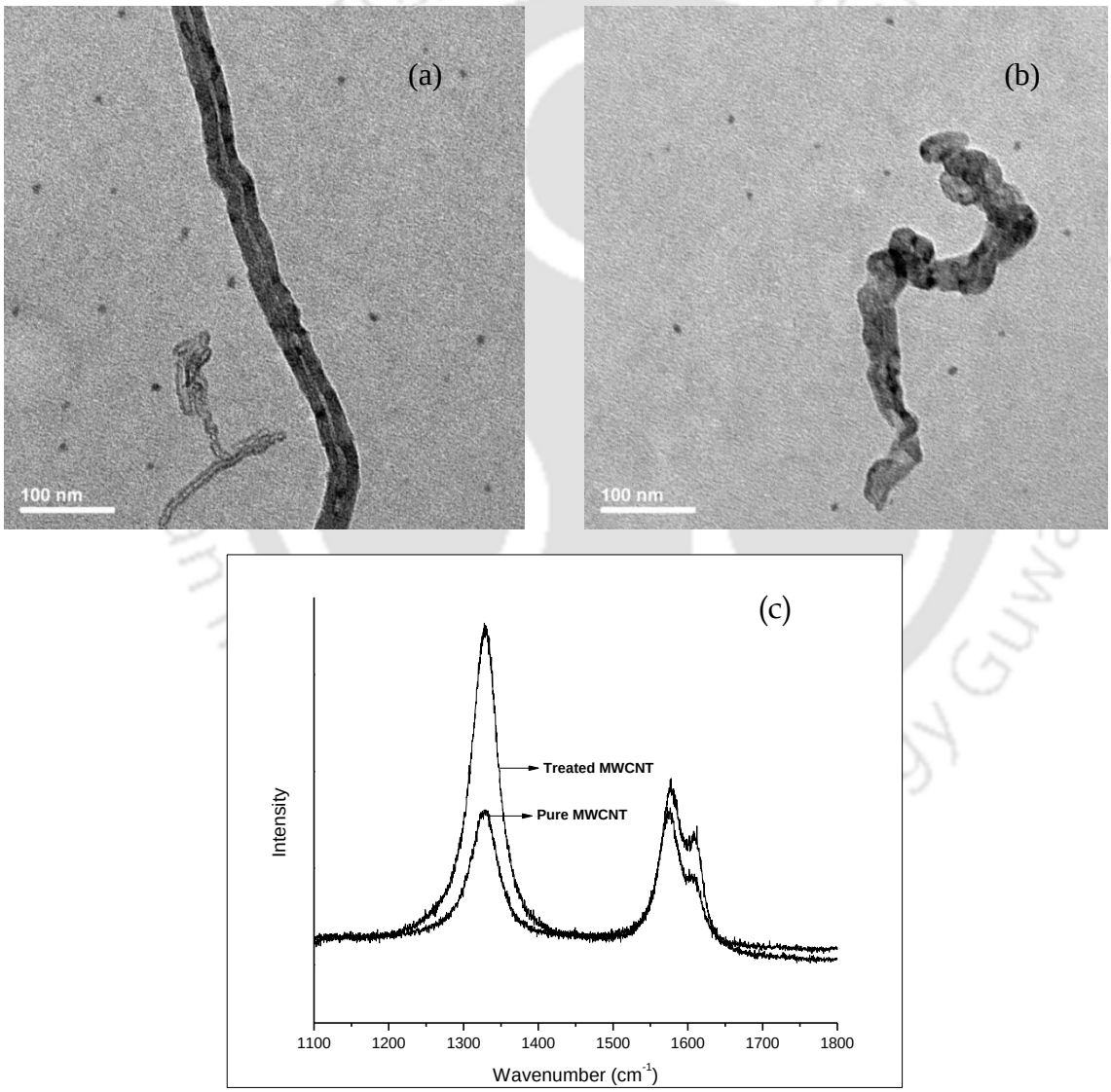

Fig. 4.53 Defects observed in MWCNT after functionalization (a) surface defects (b) bending of MWCNT and (c) Raman spectra before and after the chemical treatment of MWCNT

Though the chemical treatment of MWCNT was used for its purification and attachment of required functional groups on its surface, it also induced few defects on the surface of MWCNT. It was observed from Fig. 4.53a and b that the functionalized MWCNT has a good number of surface defects, wall damage, amorphous formation and bending, which acted as trapping regions of free radicals because of their high electron affinities, Sreekanth et al. [2013]. The defects in the MWCNT were also qualitatively confirmed using the Raman spectroscopy, which is shown in Fig. 4.53c, The I_D:I_G ratio obtained from the Raman's spectra was observed to be 1.1 and 1.49 for the as-received and treated MWCNT, respectively, corresponding to the increased defect by 35.5 % due to the chemical treatment process. Hence, the reinforcement of PMMA by chemically treated MWCNT is expected to trap the free radicals evolved during the aging process. Sreekanth et al. [2013] also discussed the trapping of free radicals in UHMWPE generated by γ-irradiation using MWCNT.

(b) Defects observed in MWCNT after UV radiation

Due to UV radiation, there were simple and complex defects such as surface defects, wall damage, formation of amorphous carbon, pentagon defects and stone wales defects on the surface of MWCNT, which was also reported by Royan et al. [2013]. With an increase of aging period from 1 to 12 months, the defects on the surface of MWCNT are expected to increase significantly and it was also reported by Grigoriadou et al. [2011] and Sreekanth et al. [2013]. These surface defects were reported to have high electron affinities, Zeynalov et al. [2010], and expected to trap a good number of free radicals. Hence, the number of free radicals and the oxidative chain scission process in PMMA were significantly reduced in the presence of MWCNT and the degradation of the mechanical properties of PMMA was restricted considerably. Fig. 4.54 explains the absorption of free radicals by the MWCNT reinforcement in PMMA. The chain scission process was also observed to be in randomized order and the homogeneously dispersed MWCNT acted as a radical scavenger leading to the reduction of the degradation of PMMA. According to Krasheninnikov et al. [2004], the defects in the MWCNT resulted in constituting bonds with the free radicals and polymer matrix. Thus, the formation of defects in MWCNT after UV radiation and the chemical

treatment led to the scavenging of free radicals and played a major role in restricting the degradation of mechanical properties of PMMA. Sreekanth et al. [2013] also discussed that a strong network between MWCNT and polyethylene was observed due to the bonding between the free radicals and MWCNT. The above results were also confirmed by the quantification of free radicals and oxidation index studies using ESR and FTIR, respectively.

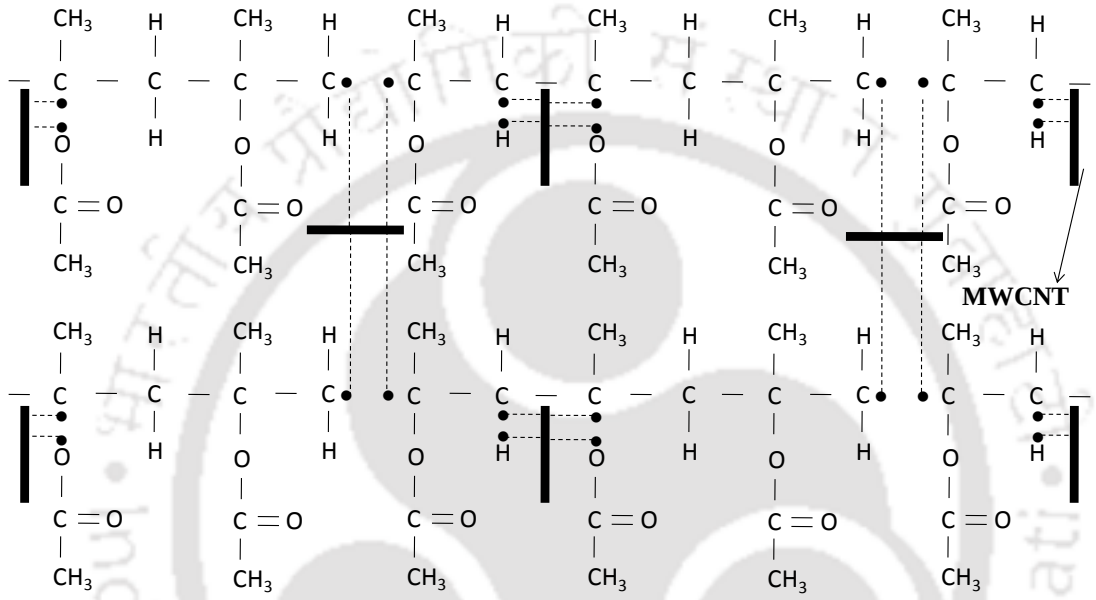

Fig. 4.54 Mechanism of restricting the degradation of PMMA/MWCNT composite

ESR technique was used to identify and quantify the free radicals present in the molecular structure of a polymer and composites. Though the termination of some of the free radicals was observed in PMMA due to the presence of MWCNT, a good number of unpaired free electrons was still present in the composites, which propagate the degradation of PMMA and generate new free radicals leading to the reduction of its mechanical properties with aging. The ESR spectra of PMMA/MWCNT composites after 12 months of aging are shown in Fig. 4.55. It was observed that the peak intensity was found to be high in case of pure PMMA after aging, but it was decreased with the concentration of MWCNT reinforcement, where the minimum peak intensity was noticed at PMMA/0.25 wt. % MWCNT composite. It was observed from Silva et al. [2009] that the range of g-value or spectral splitting factor to confirm the presence of

free radicals was between 2.001 to 2.005, and the same was found to be 2.002 to 2.004 in case of PMMA/MWCNT composites.

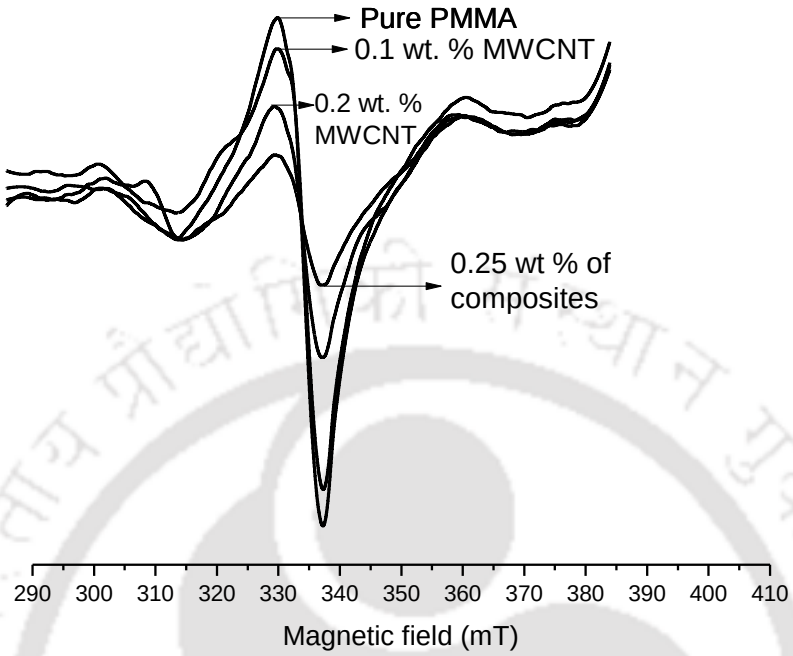

Fig. 4.55 ESR spectra of PMMA/MWCNT composites after 12 months of aging

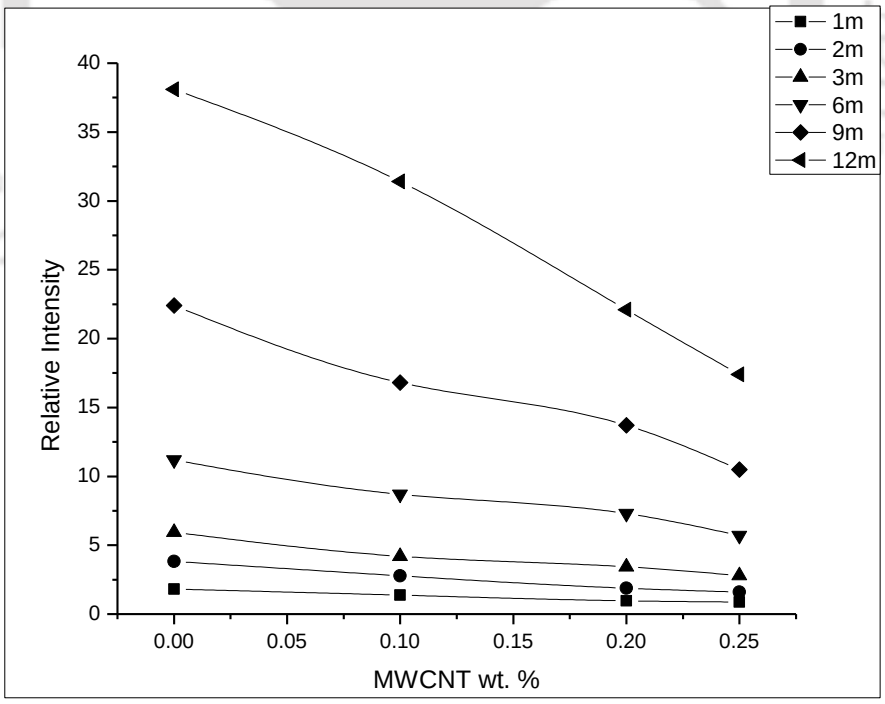

Fig. 4.56 Relative intensity of PMMA/MWCNT composites with respect to aging

The ESR spectrum was integrated to obtain the absorption curve, where the area under the absorption curve is directly proportional to the concentration of free radicals. Fig. 4.56 shows the relative intensity of PMMA against MWCNT concentration and aging duration. The relative intensity of composites at different aging periods was obtained by normalizing the area under the absorption curve of each composite with that of fresh unaged sample. It was observed that the relative intensity was found to be decreased with an increase of MWCNT concentration.

It was noticed that there was no significant change in relative intensity of free radicals in PMMA during first 3 months of aging irrespective of MWCNT concentration. It is also reflected in the form of mechanical properties of PMMA, where the reduction of mechanical properties was varied within -6.9 % in comparison to that of unaged PMMA. However, the relative intensity of PMMA was found to be significantly increased beyond 3 months of aging. It was also observed that the reinforcement of MWCNT in PMMA reduced the relative intensity, which confirmed the reduction of number of free radicals present in the composites. The relative intensity of pure PMMA was increased from 1.8 to 38.1 in case of 1 and 12 months of aging, respectively, which was restricted to 0.87 and 17.4 in case of 0.25 wt. % MWCNT reinforcement, where a 38 % reduction of relative intensity was reported. It was summarized that the MWCNT played a major role in restricting the concentration of free radicals compared to pure PMMA and it was confirmed that the MWCNT acted as a radical scavenger in trapping the free radicals leading to confine the reduction of mechanical properties of PMMA. Sreekanth et al. [2013] also supported the radical scavenging capability of the reinforcement in γ-radiated MWCNT reinforced HDPE against shelf aging.

The oxygen present in the atmosphere was absorbed during the processing of PMMA/MWCNT composites in a twin-screw extruder and an injection moulding machine leading to the formation of different types of oxides in the material. The environmental oxygen continued to diffuse and the oxidative chain scission process propagated for a long period of time, Sreekanth et al. [2013]. The oxidation index of the polymer reveals the quantity of oxidative chain scission, which is the ratio of area under the peak at 1260-1415 to 1775-1820 cm^{-1} corresponding to the carbonyl to CH_2/CH_3 peak. The FTIR spectrum of pure PMMA and 0.25 wt. % of MWCNT

reinforced composite after 9 and 12 months of UV aging are shown in Fig. 4.57. The area under 1775-1820 cm^{-1} peak was found to be increased with aging and the same was noticed to be decreased with the reinforcement of MWCNT in PMMA. Hence, the oxidation index of pure PMMA after 12 months of aging was found to be more compared to that of PMMA/MWCNT composites.

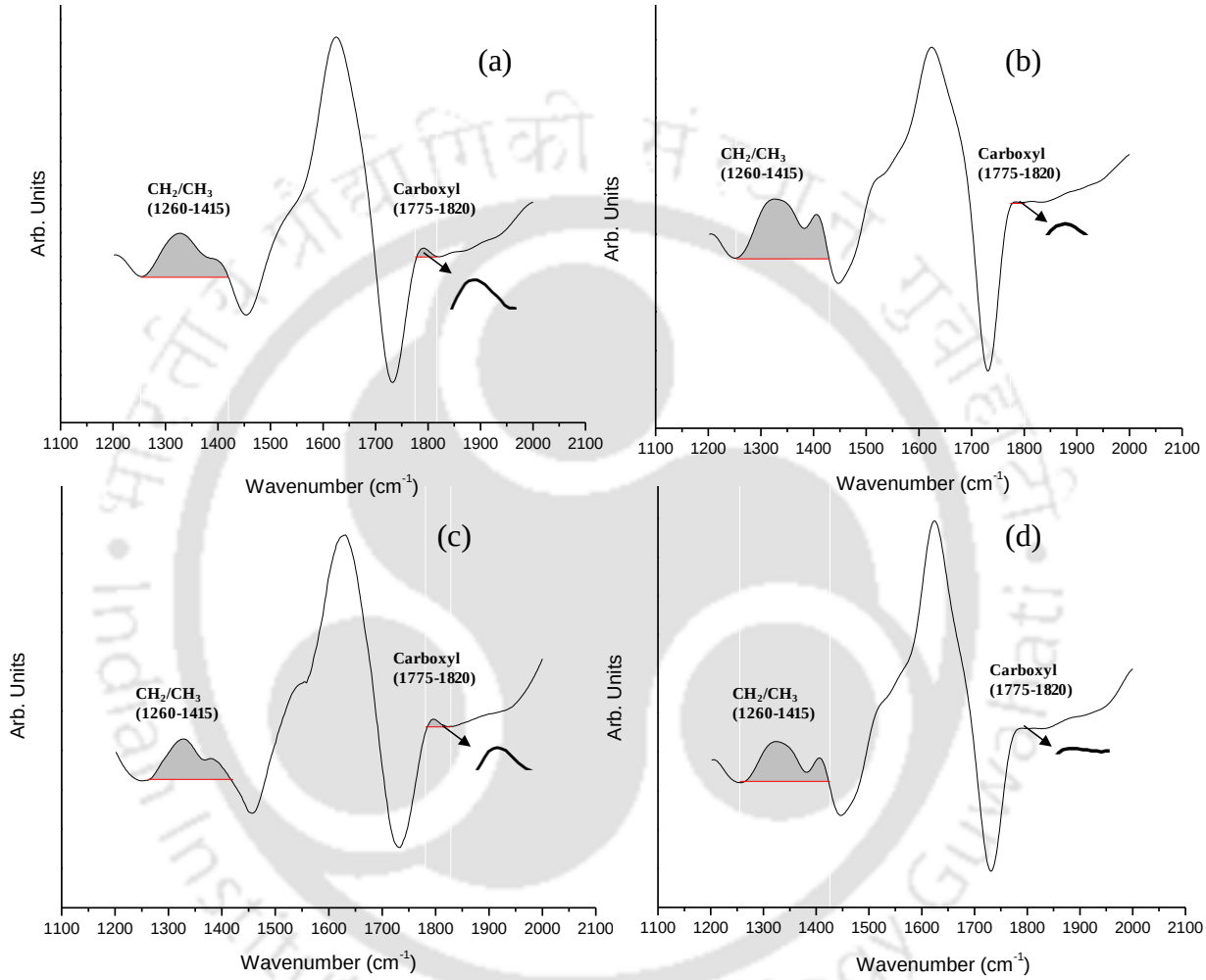

Fig. 4.57 FTIR spectrum of (a) Pure PMMA after 12 months of aging (b) PMMA/0.25 wt. % MWCNT composite after 12 months of aging (c) Pure PMMA after 9 months of aging (d) PMMA/0.25 wt. % MWCNT composite after 9 months of aging

The oxidation index of PMMA/MWCNT composites against aging period is shown in Fig. 4.58, where it was observed to be decreased with an increase of MWCNT concentration and increased with aging period. The oxidation index of PMMA/MWCNT composites after 1 and 2 months of aging was found to be nearly equal to zero and the same was observed to be 0.019 after 3 months of aging. The

oxidation index of PMMA after 12 months of aging was reduced from 0.198 to 0.044, when it was reinforced with 0.25 wt. % MWCNT, corresponding to the reduction of 77.7 %. The reason for the reduction of oxidation index with the reinforcement was due to high electron affinities of MWCNT, which acted as a strong radical trap, Watts et al. [2003]. It was inferred that the MWCNT acted as a hindrance for the degradation of mechanical properties of PMMA. It was also noticed that the defects in the MWCNT trapped the free radicals upto certain extent and led to restrict the oxidative degradation of PMMA/MWCNT composites.

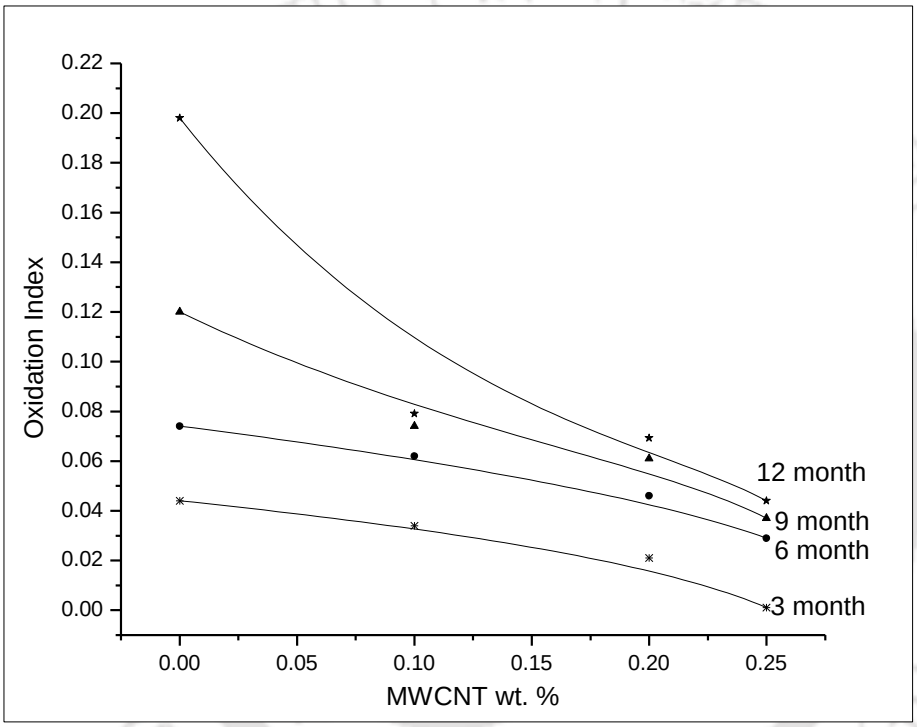

Fig. 4.58 Oxidation index of PMMA/MWCNT composites against aging

4.3.3 Summary of the material proposed for a knee joint

The PMMA/MWCNT composites were fabricated through the melt mixing process by the twin-screw extruder followed by an injection moulding machine, whereas the film casting process and thermosetting process were reported in most of the literature. The tensile and flexural properties of composites were studied as per ASTM standards by varying the concentration of reinforcement. The optimum mechanical properties were observed at 0.25 wt. % of MWCNT reinforcement in PMMA, where the flexural modulus, flexural strength, flexural strain, tensile strength, Young's modulus and

tensile strain were observed to be increased by 24.1, 26.3, 29.3, 32.9, 41.9 and 49.5 %, respectively compared to that of pure PMMA. The reasons for the enhancement and reduction of mechanical properties were also discussed in detail. The enhancement of mechanical properties was also validated using suitable theoretical models. The accelerated UV exposure studies were carried out for the equivalent aging period of 1, 2, 3, 6, 9 and 12 months for the composites having up to 0.25 wt. % of MWCNT reinforcement. The degradation of MWCNT reinforced composites after 12 months of aging was found to be restricted significantly compared to that of pure PMMA. The initiation, propagation and termination mechanism of free radicals in PMMA and its composites were also explained in detail. Thus, the 0.25 wt. % of MWCNT reinforcement in PMMA is suggested to be explored for the fabrication of polycentric knee joint.

4.4 Evaluation of the characteristics of sandwich composites proposed to be used for the socket

4.4.1 Selection of the processing method of epoxy based composites

The epoxy/MWCNT composites were prepared by solvent dispersion technique. In order to select the processing conditions, three methods of solvent evaporation technique such as hot air oven at 55 °C (A-H), magnetic stirrer at 55 °C (B-M) and vacuum drying at room temperature (C-V) were followed in the preparation of 0.1 and 0.2 wt. % of MWCNT reinforced epoxy composites.

The compressive strength and Young's modulus of epoxy/MWCNT composites against the processing conditions are shown in Figure 4.59a and b, respectively. It was observed that the properties of epoxy were increased with the reinforcement of MWCNT. However, the sample prepared through a hot air oven technique showed the reduction of compressive strength and Young's modulus by 11.4 and 11.8%, respectively for A-H 0.1 composites in comparison to that of pure epoxy. It is due to the fact that the method of removal of acetone by hot air oven led to destroy the chemical bonding existing between the MWCNT and epoxy leading to decrease the properties of the composites. However, it was restricted when the MWCNT concentration was increased. As the heat supplied to evaporate the acetone was not sufficient enough to

destroy the chemical bonding between them at 0.2 wt.% MWCNT, it led to the reduction of compressive strength and Young's modulus of epoxy by only 0.8 and 3.3%, respectively.

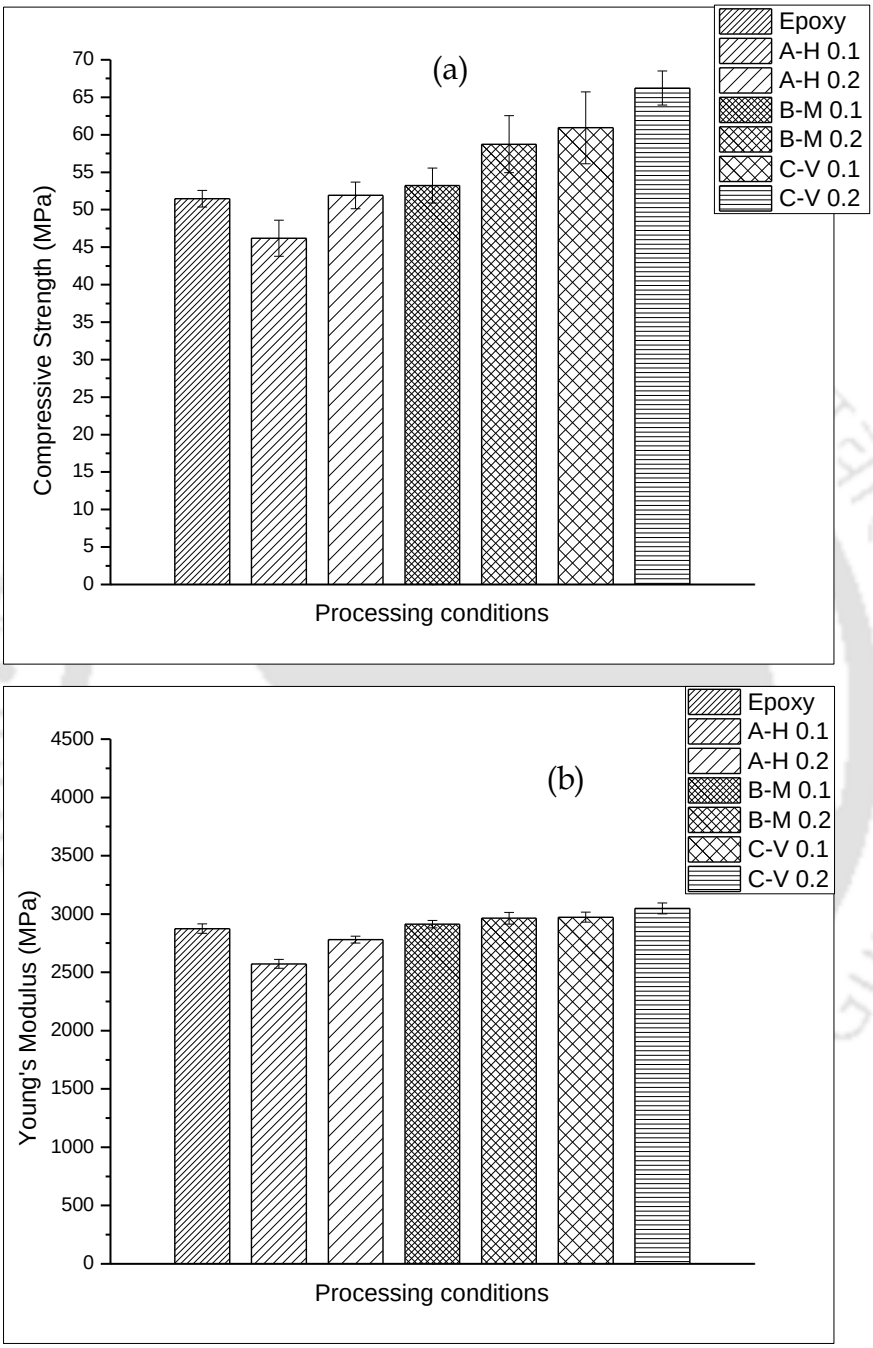

Fig. 4.59 (a) Compressive strength and (b) Young's modulus of the test samples prepared by different processing method

It was observed that the compressive strength and Young's modulus of B-M 0.1 sample were increased by 3.4 and 1.4 %, respectively, compared to that of pure epoxy and the

corresponding enhancement for B-M 0.2 sample were found to be 14.2 and 3 %. The enhancement of mechanical properties is due to the fact that the continuous stirring of an epoxy and MWCNT in acetone reduced the debonding between them at the evaporation temperature of acetone, and it is expected to ensure the homogeneous dispersion of MWCNT in epoxy. The sample C-V, where the vacuum oven was used for evaporating the acetone at room temperature, showed the significant enhancement of the mechanical properties compared to that of the samples A-H and B-M. During the vacuum condition at room temperature, the solvent was fully removed compared to rest of the process. The enhancement of compressive strength and Young's modulus of C-V 0.1 sample were observed to be 18.4 and 3.4 %, respectively, compared to pure epoxy and the corresponding values for C-V 0.2 sample was found to be 39.4 and 10.7 %. Hence, the vacuum oven was used at room temperature to evaporate the acetone while preparing the polymer composites.

4.4.2 Mechanical characterization of Epoxy/MWCNT composites

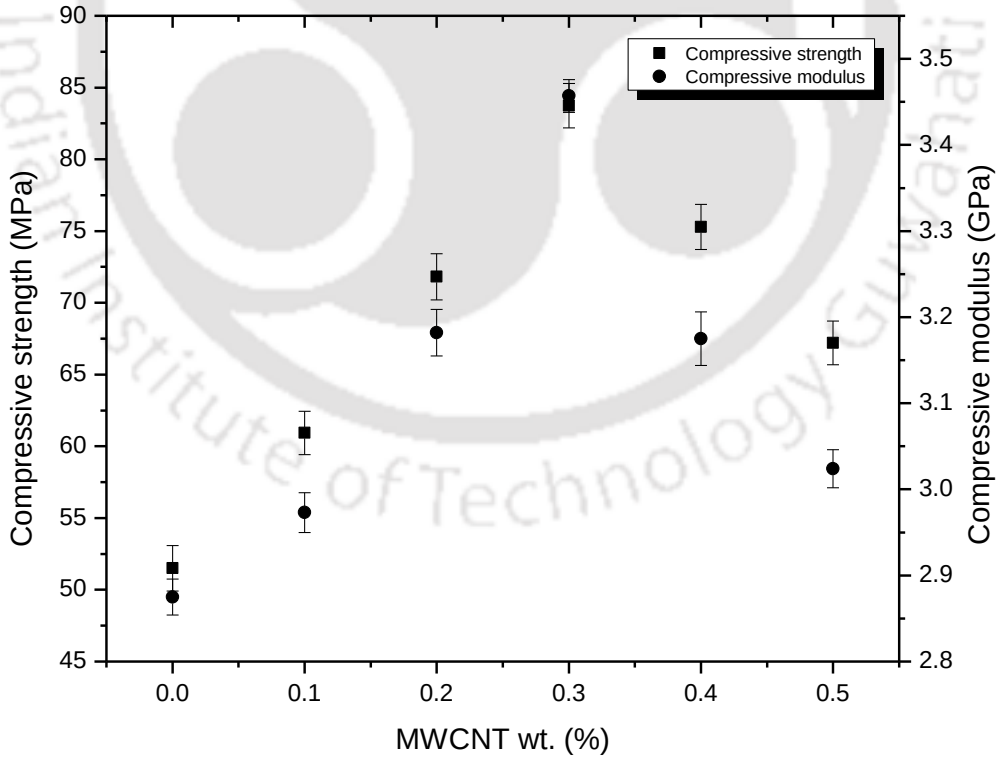

Fig. 4.60 Compressive strength and modulus of epoxy/MWCNT composites

Fig. 4.60 shows the compressive strength and compressive modulus of various concentration of MWCNT such as 0.1, 0.2, 0.3, 0.4 and 0.5 wt. % with epoxy. It was observed that the properties of epoxy/MWCNT composites were enhanced upto 0.3 wt. % of MWCNT beyond which the enhancement was found to be decreased. The compressive strength and modulus of epoxy with 0.1, 0.2, 0.3, 0.4 and 0.5 wt. % of MWCNT reinforcement were increased by 18.3, 39.4, 62.6, 46.2 and 30.5 %, and 3.4, 10.7, 20.2, 10.4 and 5.2 %, respectively. It is noted that the maximum enhancement of the compressive strength and modulus was found to be 62.6 and 20.2 %, respectively compared to that of pure epoxy at 0.3 wt % of MWCNT reinforcement. The reasoning for the enhancement and reduction of the mechanical properties of epoxy/MWCNT composites due to the reinforcement concentration are discussed below in detail.

4.4.2.1 Reasons for the enhancement of mechanical properties

The different possible reasons for the enhancement of mechanical properties of epoxy upto 0.3 wt. % of MWCNT reinforcement are given below:

a) Inherent mechanical properties of MWCNT

b) Effective stress transfer from epoxy to MWCNT

c) Homogeneous dispersion of MWCNT in epoxy

d) Increased crystallinity of the composites and interfacial bonding between the epoxy and MWCNT.

(a) Inherent mechanical properties of MWCNT:

Due to inherent characteristics of MWCNT, the mechanical properties of epoxy/MWCNT composites were found to be increased. The modulus and strength of MWCNT and epoxy were observed to be 950 GPa and 1 TPa, Ruoff et al. [2003], and 2.8 GPa and 55 MPa, obtained from the experiments, respectively. As the mechanical properties of MWCNT were found to be high compared to that of epoxy, it is expected to increase the mechanical properties of the composites significantly.

b) Effective stress transfer from epoxy to MWCNT

The Raman spectra of the composite sample before and after the compression test is shown in Figure 4.61, where a shift in G-band between them was observed from 1585 to

1594 cm^{-1}, which confirmed the effective stress transfer from the epoxy to MWCNT, and improved interfacial bonding between them leading to the enhancement of mechanical properties of the composites. Cronin et al. [2004] reported that the vibration in the sp^2 C-C bond was generated by the persuaded strain, which was confirmed from the Raman spectra.

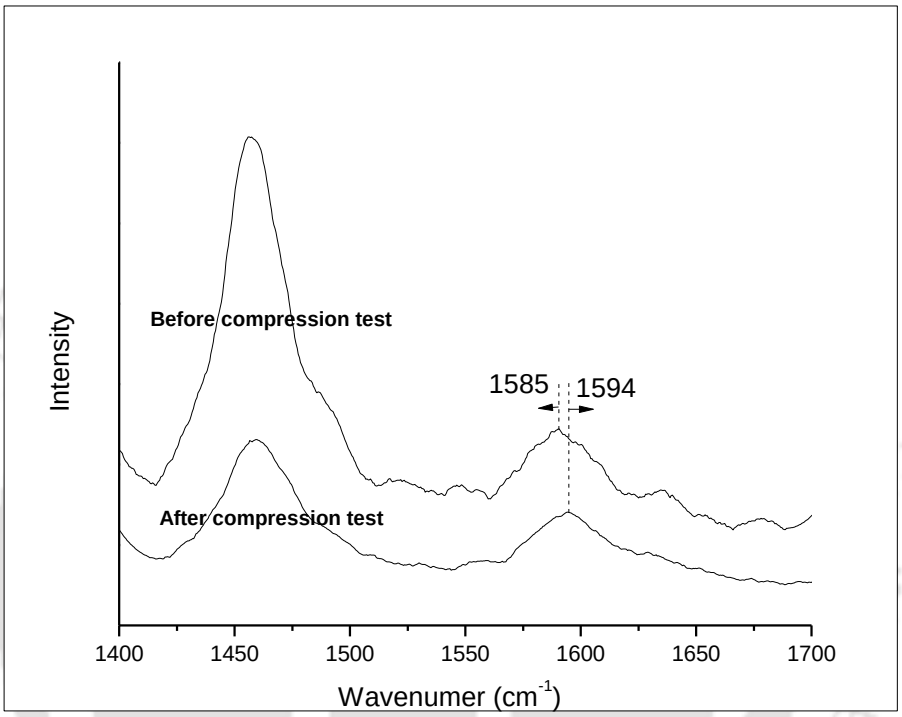

Fig. 4.61 Raman spectra before and after the compression test of Epoxy/MWCNT composite

c) Homogeneous dispersion of MWCNT in epoxy

Fig. 4.62 shows the DC electrical conductivity of epoxy/MWCNT composites, which was measured to confirm the homogeneous dispersion of MWCNT in epoxy, and it helped to increase the mechanical properties of the composites. The electrical conductivity of epoxy/MWCNT at 0.4 wt. % of MWCNT reinforcement was observed to be 2-order more than that of the 0.3 wt. % of MWCNT composite, where the interconnectivity among the network of MWCNT within the composites was confirmed. The above observation was also reported by Vaudreuil et al. [2007]. Moisala et al. [2006] reported that the lower percolation threshold confirmed the homogeneous

dispersion of MWCNT in the matrix. Thus, the enhancement of mechanical properties of composites was observed up to 0.3 wt. % of MWCNT reinforcement. An agglomeration noted beyond which influenced the reduction of mechanical properties of the composites.

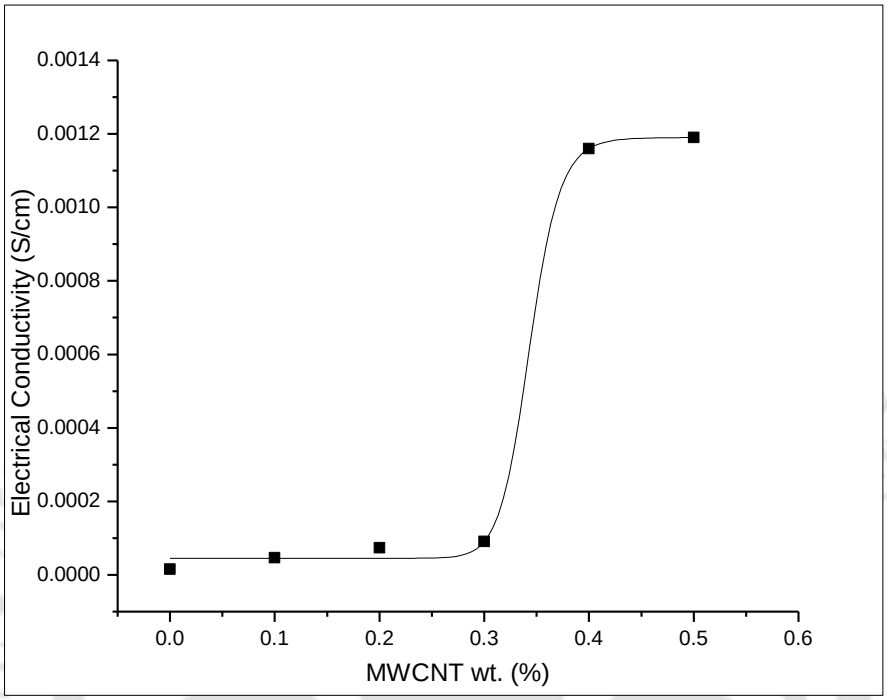

Fig. 4.62 Electrical conductivity of epoxy/MWCNT composites

d) Increased crystallinity of the composites and improved interfacial bonding between the matrix and reinforcement.

Fig. 4.63 shows the relative crystallinity of epoxy/MWCNT composites, which was observed to be increased linearly with MWCNT concentration. The relative crystallinity of pure epoxy was observed to be 18.3 % and it was increased by 10.7, 40.1, 54.5, 83.2 and 88 % for 0.1, 0.2, 0.3, 0.4 and 0.5 wt. % of MWCNT reinforcement, respectively, where the MWCNT acted as a nucleating agent to initiate the formation of new crystallites. From the slope of the curve, it is noted that the rate of increase of relative crystallinity of the composites against MWCNT concentration is found to be high. The same observation was also reported by Zhang et al. [2008] for the increase of crystallinity, which caused the improvement of mechanical properties of the epoxy with MWCNT reinforcement.

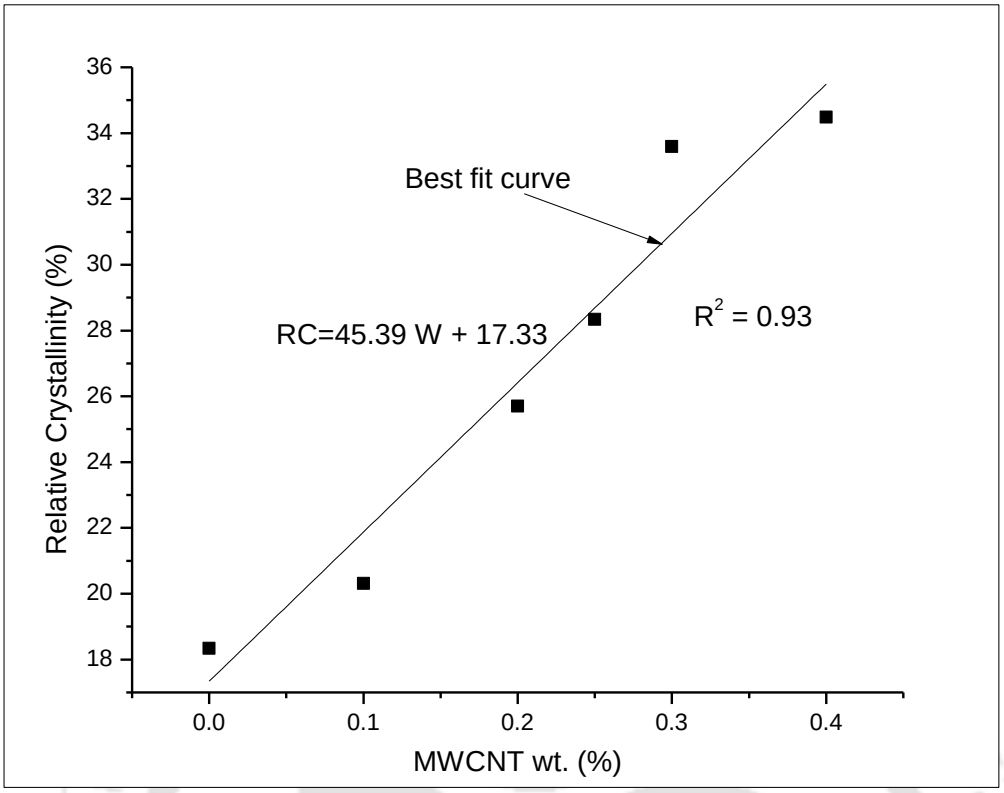

Fig. 4.63 Relative crystallinity of epoxy/MWCNT composites

The interfacial bonding between epoxy and MWCNT was confirmed using the derivative of thermogravimetric curve (DTG) and glass transition temperature (Tg), which helped to increase the mechanical properties of the composites and it was also supported by Jin et al. [2002]. Fig. 4.64a, b and c shows the thermal stability, DTG and Tg of epoxy/MWCNT composites, respectively. It was noticed from Fig. 4.64a that the degradation temperature of epoxy was observed to be increased with the reinforcement of MWCNT, which acted as a hindrance for the degradation of epoxy. From the DTG plot shown in Fig. 4.64b, the delay in thermal degradation of epoxy confirmed its thermal stability by the reinforcement of MWCNT. The degradation temperature of epoxy was found to be 349.5 °C and it was increased to 352.7, 356.1, 359.0, 362.1 and 366.4 °C at 0.1, 0.2, 0.3, 0.4 and 0.5 wt. % of MWCNT reinforcement, respectively. It was noticed from Fig. 4.64c that the Tg of epoxy was increased linearly with MWCNT concentration and it was increased by 4.9, 9.7, 14.5, 19.4 and 24.2 °C at 0.1, 0.2, 03, 0.4 and 0.5 wt. % of MWCNT reinforcement, respectively. As the slope of the linear fitting of Tg was found to be very high, it confirmed the strong influence of MWCNT concentration on the glass transition temperature of the composites, and the strong

interfacial bonding between the epoxy and MWCNT. Thus, the interaction between epoxy and MWCNT was confirmed causing the enhancement of mechanical properties of the composites.

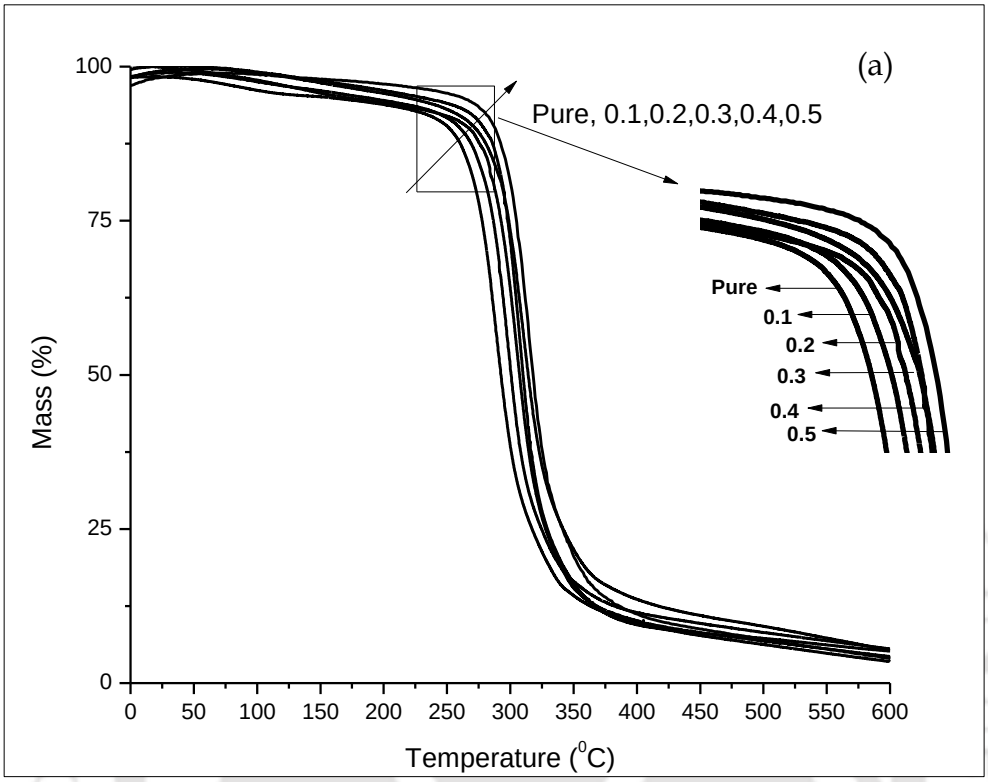

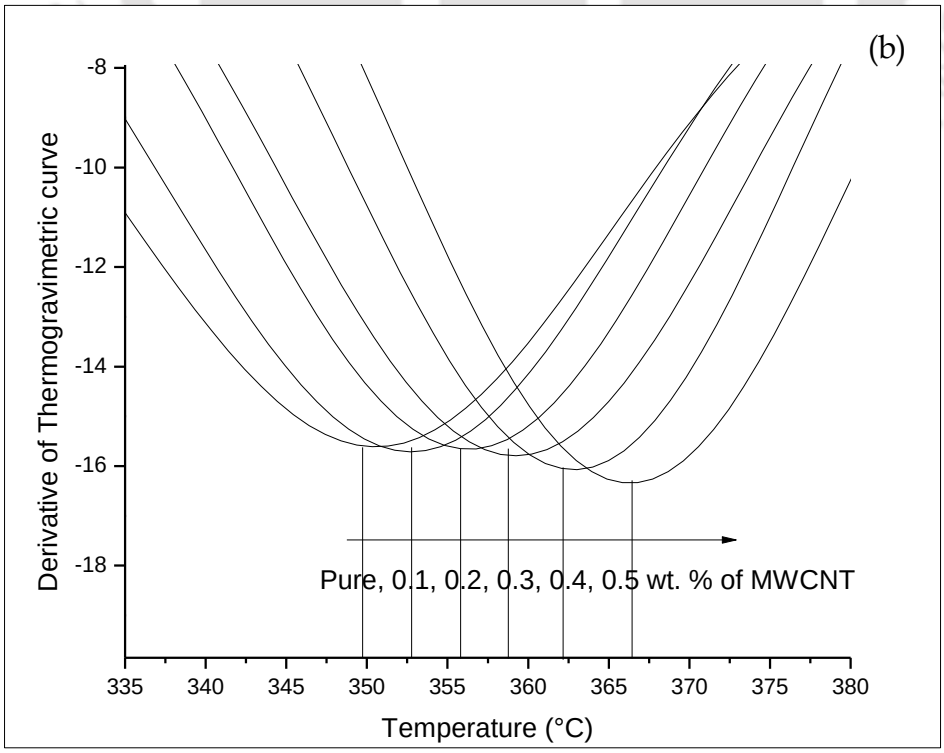

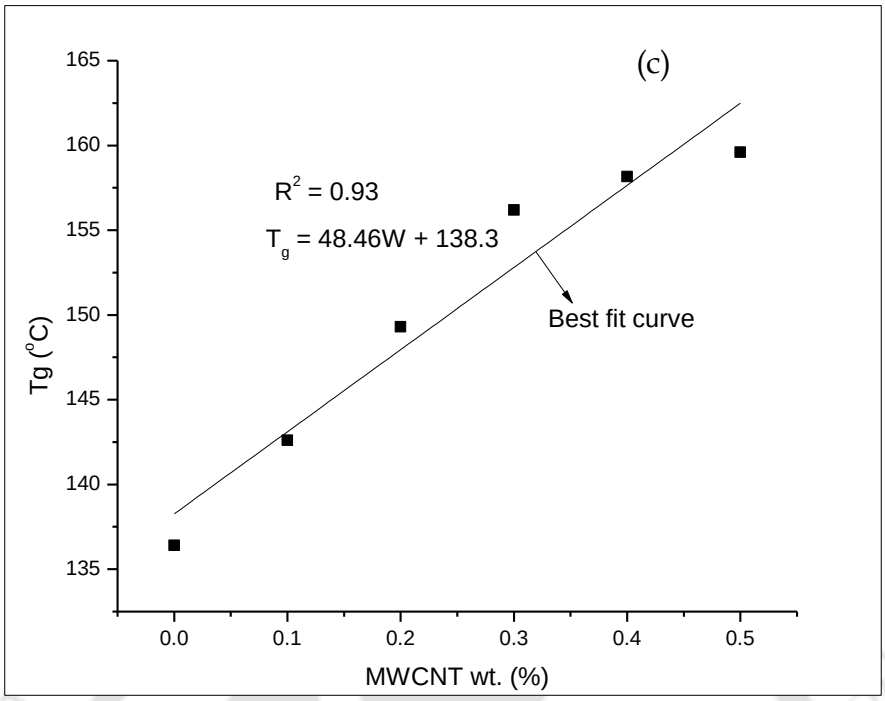

Fig. 4.64 (a) Thermal stability (b) Derivation of a part of TGA curve of epoxy/MWCNT composites and (c) Glass transition temperature of epoxy/MWCNT composites

Though the relative crystallinity and Tg of epoxy were observed to be increased with MWCNT concentration due to improved interaction between them, the mechanical properties of composites were found to be decreased beyond 0.3 wt. % of MWCNT. The reasoning for the same is discussed below in detail.

4.4.2.2 Reasons for the reduction of mechanical properties

The following are the probable reasons for the reduction of mechanical properties of the composites beyond 0.3 wt. % of MWCNT reinforcement.

a) Increase in specific surface area of the chemically treated MWCNT

b) Increase in complex viscosity of epoxy/MWCNT mixture

c) Presence of voids in epoxy/MWCNT composites

The specific surface area of MWCNT before and after the chemical treatment process was found to be 260.9 and 342.24 m^2/g, respectively corresponding to the enhancement of 31.2 %. Thus, the available quantity of epoxy may not be sufficient enough to wet the MWCNT, which led to the formation of more number of micro-voids in the composites. Nieto et al. [2011] also found that the surface area of MWCNT was increased due to its

functionalization by 33.3 %. The same phenomenon in the composites at higher concentration of MWCNT was also reported by Sreekanth et al. [2013].

Fig. 4.65a shows the complex viscosity of epoxy/MWCNT mixture. It was noted that the complex viscosity of epoxy was increased by MWCNT dispersion and it led to the formation of micro-voids beyond the optimum concentration of MWCNT during the preparation of composites. The maximum enhancement of complex viscosity of 0.1, 0.2, 0.3, 0.4 and 0.5 wt. % of MWCNT dispersed epoxy was found to be 19.2, 93.3, 171.5, 231.1 and 289.4 %, respectively compared to that of epoxy at the shear rate of 70 s^{-1}. The complex viscosity of epoxy/MWCNT mixture was observed to be increased drastically at higher concentration of MWCNT, which is expected to increase the shear force required for the epoxy/MWCNT-hardener mixture and it resulted the large number of micro-voids beyond 0.3 wt. % of MWCNT reinforcement. The above observation was also confirmed by Annala et al. [2012].

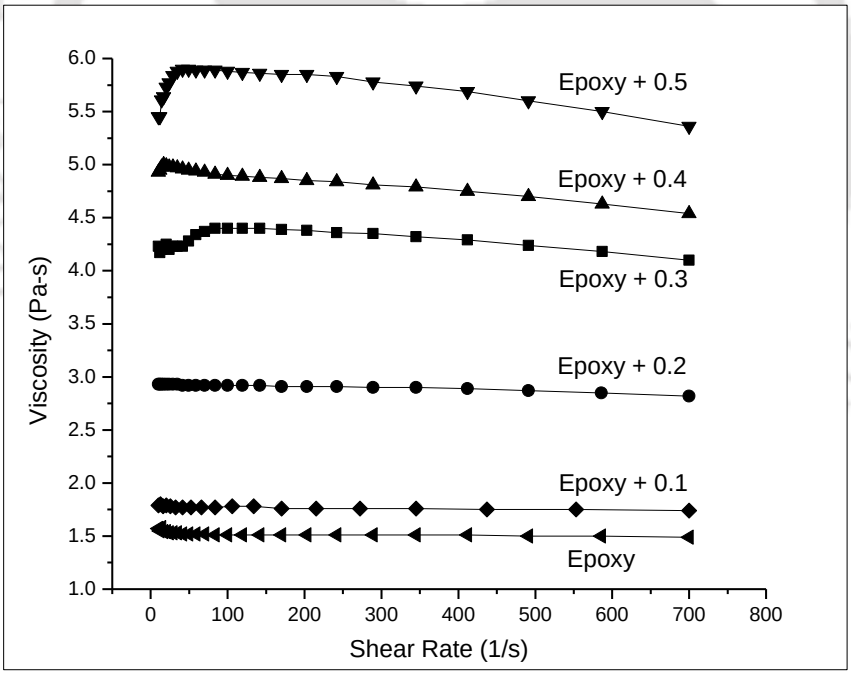

Fig. 4.65 Complex viscosity of epoxy/MWCNT mixture

The micro-voids present in epoxy/MWCNT composites are shown in Fig. 4.66a and b. It was observed that the composite having 0.4 wt. % of epoxy/MWCNT showed the voids in the range of 15 µm, whereas it was noted to be 40 µm in case of 0.5 wt. % of epoxy/MWCNT composite.

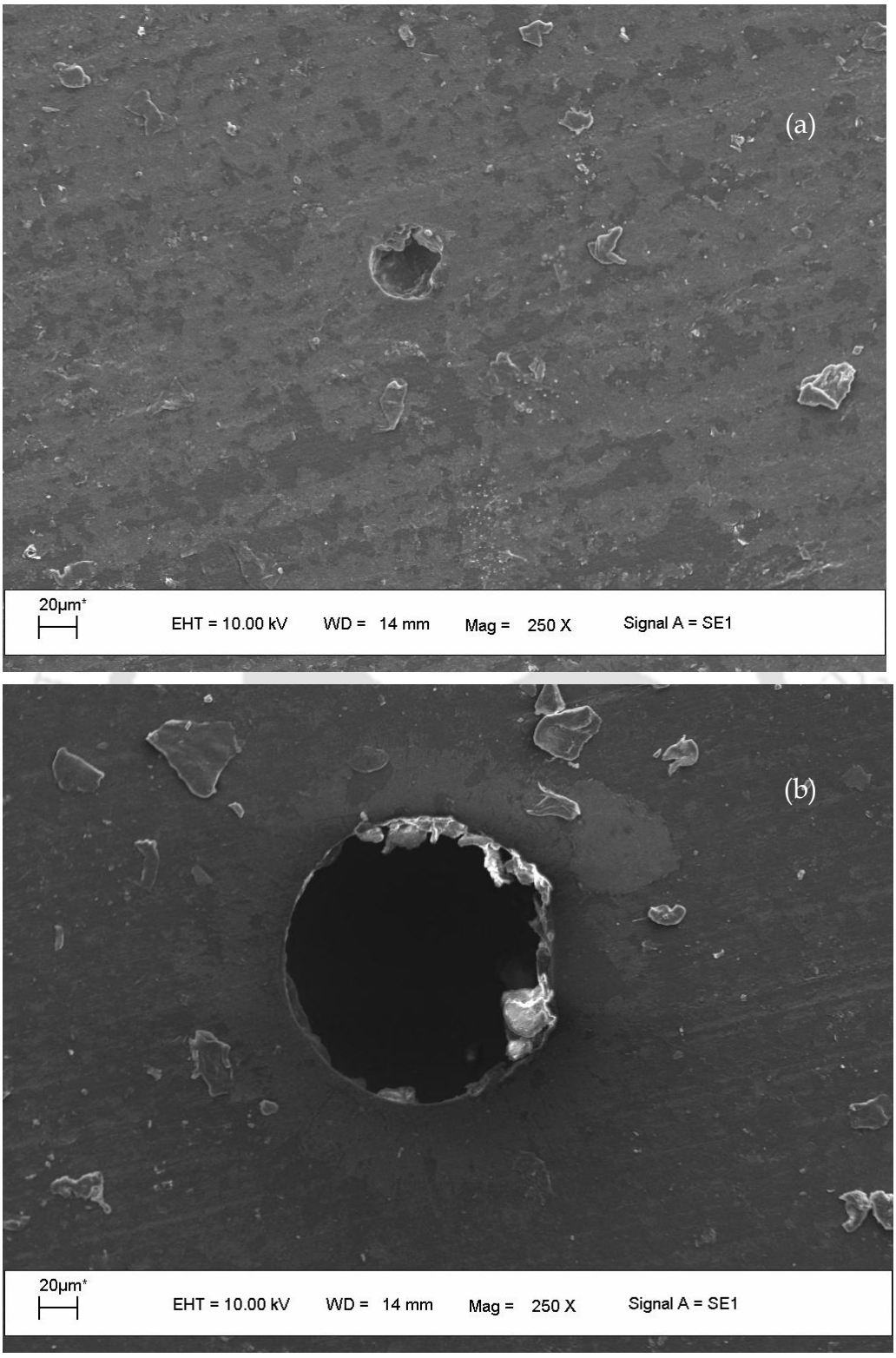

Fig. 4.66 (a) SEM image of 0.4 wt. % and (b) 0.5 wt. % of Epoxy/MWCNT composites

4.4.3 Thermal properties of the Epoxy/MWCNT composites

Fig. 4.67 shows the volumetric specific heat, thermal diffusivity and thermal conductivity of epoxy/MWCNT composites against the concentration of reinforcement. It was noted that the volumetric specific heat was observed to be decreased linearly with an increase of MWCNT concentration. The reduction of volumetric specific heat of 0.1, 0.2, 0.3, 0.4 and 0.5 wt. % of MWCNT reinforced epoxy was found to be 7.6, 14.4, 26.4, 35.5 and 37.2 %, respectively compared to that of unreinforced epoxy. The reduction of volumetric specific heat of epoxy with MWCNT reinforcement is expected to reduce the accumulation of heat in the residual stump, when the said composites are used to make the sockets.

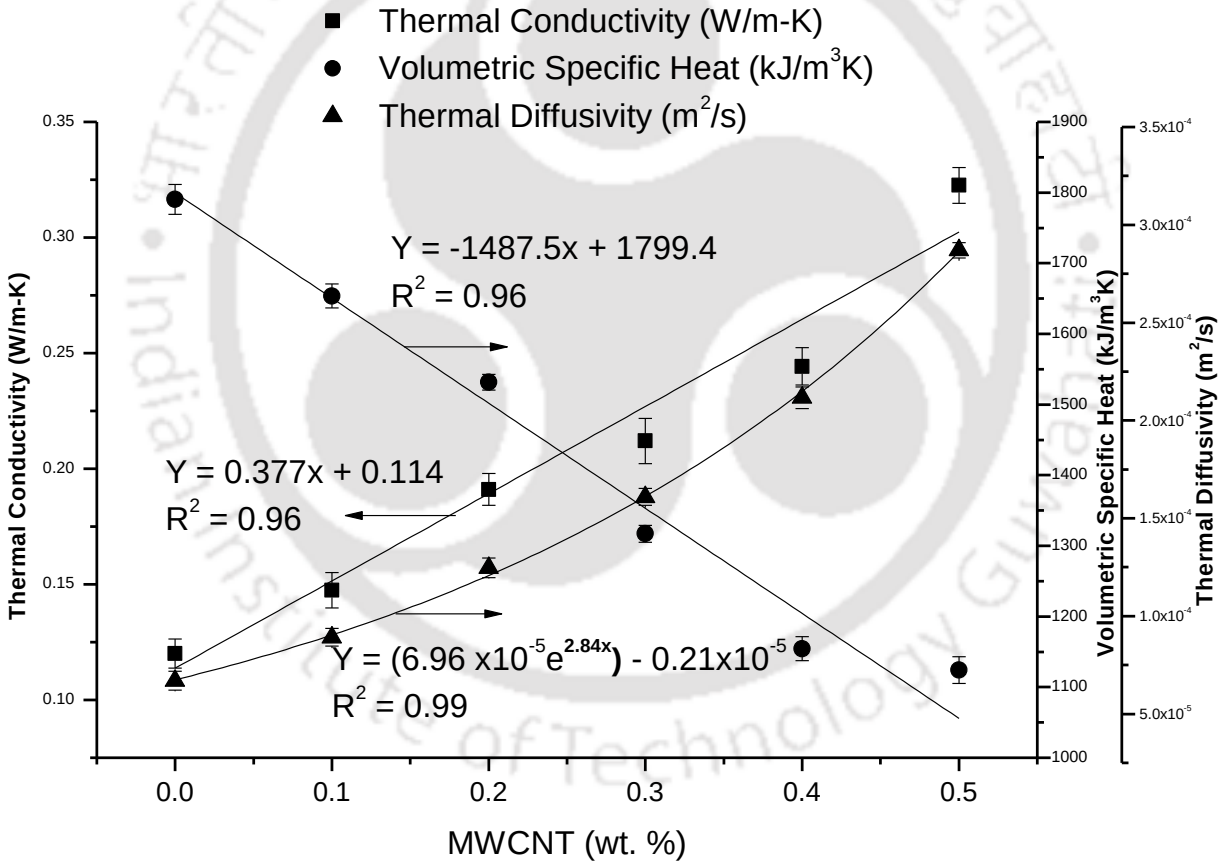

Fig. 4.67 Volumetric specific heat, thermal diffusivity and thermal conductivity of epoxy/MWCNT composites

The thermal diffusivity of epoxy was found to be increased exponentially with an increase of MWCNT concentration, and it is shown in Fig. 4.67. The enhancement of thermal diffusivity of 0.1, 0.2, 0.3, 0.4 and 0.5 wt. % of MWCNT reinforced epoxy was

found to be 33.0, 86.0, 140.2, 215.7 and 328.2 %, respectively, compared to that of unreinforced epoxy. The thermal diffusivity of 0.3 and 0.5 wt. % of epoxy/MWCNT composites was observed to be $1.61\times10^{-4} \pm 4.3\times10^{-6}$ and $2.87\times10^{-4} \pm 3.9\times10^{-6}$ m^2/s, respectively, whereas it was noted to be $0.67 \times 10^{-4} \pm 4.8\times 10^{-6}$ m^2/s for pure epoxy. Hence, the increase in thermal diffusivity of epoxy based composites is expected to enhance the rate of diffusion of heat from the stump to the surrounding via socket.

It was also noted from Fig. 4.67 that the thermal conductivity of epoxy was found to be linearly increased with MWCNT concentration, where the thermal conductivity of 0.1, 0.2, 0.3, 0.4 and 0.5 wt. % of MWCNT reinforced epoxy was found to be increased by 22.9, 59.2, 76.7, 103.6 and 168.8 %, respectively in comparison to that of unreinforced epoxy. Thus, it led to the enhancement of heat transfer characteristics of the socket.

4.4.3.1 Reasons for the improvement of thermal properties of the epoxy/MWCNT composites

The different possible reasons for the improvement of thermal properties of epoxy/MWCNT composites are given below:

a) Inherent thermal properties of MWCNT

b) Increased crystallinity of the composites and

c) Increased interfacial bonding between the matrix and reinforcement

(a) Inherent thermal properties of MWCNT:

Table 4.9 shows the thermal conductivity, thermal diffusivity and volumetric specific heat of epoxy and MWCNT, where the values for the former were obtained experimentally and the same for the latter were referred from Yang et al. [2009]. It was observed that the thermal conductivity of MWCNT was found to be about several orders more than that of the epoxy, which confirmed that the reinforcement of MWCNT in epoxy increased the thermal conductivity of composites. Similarly, the volumetric specific heat of epoxy was found to be more than twice that of MWCNT. The thermal diffusivity of MWCNT was 2-order higher than that of the epoxy. Hence, the reinforcement of MWCNT in epoxy matrix decreased the volumetric specific heat and increased the thermal diffusivity and thermal conductivity of the epoxy/MWCNT

composites. Thus, the inherent thermal properties of MWCNT strongly influenced the thermal properties of the composites.

Table 4. 9 Thermal properties of epoxy and MWCNT

Thermal Properties	MWCNT Yang et al. [2009]	Epoxy (Experimentally)
Thermal Conductivity (W/m-K)	3000	0.12 ± 0.0063
Thermal Diffusivity (m^2/s)	4.3×10^{-3}	$6.7 \pm 0.48 \times 10^{-5}$
Volumetric specific heat (kJ/m^3K)	700	1790.4 ± 21

b) Increased crystallinity of the composites

The conduction between MWCNT and epoxy can be further enhanced with an increase of geometrically regular crystals and strong bonding between them in the composites. The packing of crystalline structure in polymer plays a major role for the enhancement of thermal conductivity by reducing the interfacial thermal resistance between the matrix and reinforcement. In addition to that the increased crystallinity of the composites led to achieve the thermal equilibrium beforehand compared to pure epoxy, which caused the enhancement of thermal diffusivity and reduction of volumetric specific heat of the composites. Fig. 4.63 shows the relative crystallinity of epoxy/MWCNT composites, which was linearly increased with MWCNT concentration. The above discussed mechanism was also supported by Haggenmueller et al. [2007].

c) Increased interfacial bonding between the matrix and reinforcement

The interaction between epoxy and MWCNT was confirmed by the enhancement of thermal stability and Tg of epoxy/MWCNT composites, which are reported in Fig. 4.64a and c, respectively. A good interaction between MWCNT and epoxy is accounted for the decrease in interfacial thermal resistance between them and the reduction of the duration to reach thermal equilibrium leading to enhance the thermal conductivity and thermal diffusivity and the reduction of volumetric specific heat of the epoxy composites. Hence, it is expected to be one of the major reasons for the enhancement of

thermal characteristics of the composites. Moniruzzaman et al. [2006b] also reported that the improvement of thermal stability led to enhance the thermal characteristics of the composites.

From the above discussion, it was observed that the volumetric specific heat of epoxy was found to be reduced with the reinforcement of MWCNT, whereas the thermal conductivity and thermal diffusivity of epoxy were observed to be increased. However, the mechanical properties of epoxy/MWCNT composites were found to be decreased beyond 0.3 wt. % of MWCNT reinforcement. Thus, the 0.3 wt. % of MWCNT was considered for manufacturing the sandwich composites to make the sockets.

4.4.4 Characterization of Epoxy/MWCNT/E-glass woven fabric /stockinet layers sandwich composites

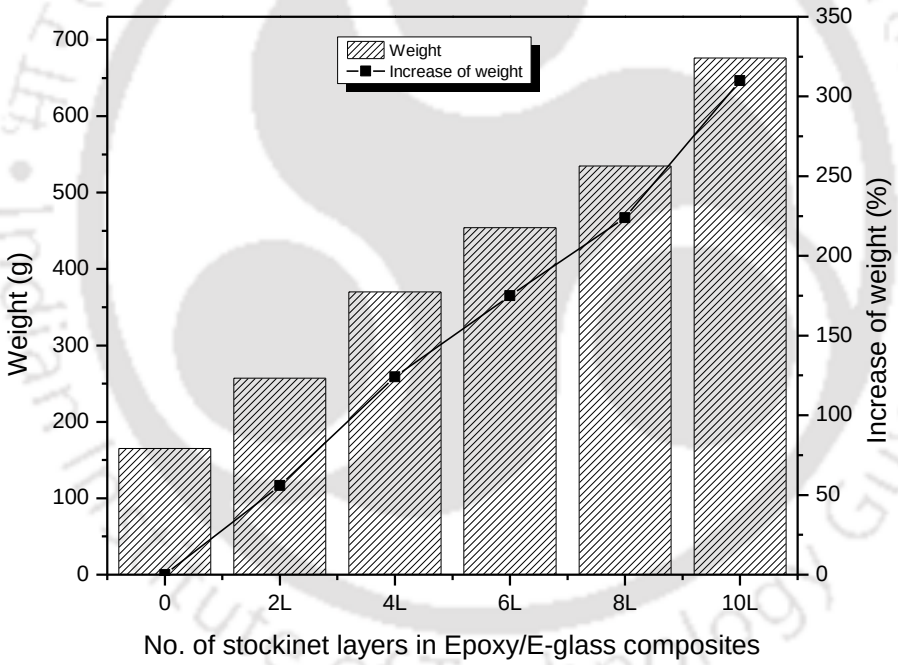

Fig. 4.68 Weight of Epoxy/E-glass composites with different number of stockinet layers and increase in weight with respect to composites without stockinet layer

After selecting the MWCNT concentration based on the mechanical and thermal properties of epoxy, the Epoxy/E-glass woven fabric/stockinet (0-10 layer) (FRP) sandwich composites were fabricated with and without the dispersion of 0.3 wt. % of MWCNT concentration. The weight of the composites was measured for the size of 200 × 200 mm rectangular sheet, which was found to be increased with number of stockinet layers and it is also shown in Fig. 4.68. It was due to the absorption of more quantity of

epoxy resin with an increase of stockinet layers to prepare the void-free composites. The increase in weight of the composites for 2, 4, 6, 8 and 10 layers of stockinet was observed to be 56, 124, 175, 224 and 310 %, respectively, compared to the composites without any stockinet layers. If the weight difference between prosthetic leg and other leg is 100 %, it leads to increase the metabolic cost of the amputee by 12 %, Smith et al. [2013]. Hence, the gain in weight of the socket with number of stockinet layers led to increase the metabolic cost of an amputee. Thus, the thermal and mechanical properties of the sandwich composites were evaluated and the number of stockinet layers was selected in order to reduce the metabolic cost of the amputees.

4.4.4.1 Thermal characterization of Epoxy/MWCNT/E-glass woven fabric/stockinet layers sandwich composites

This section discusses about the variation of thermal properties of the sandwich composites with dispersion of 0.3 wt. % of MWCNT reinforcement. It is observed from the experimental results that the deviation in the thermal properties of sandwich composites was noted to be 3.2 % up to 10 number of stockinet layers. Hence, the average results of thermal properties of different sandwich composites were considered and reported. Fig. 4.69 shows the volumetric specific heat, thermal diffusivity and thermal conductivity of the epoxy based different types of composites. It was noted that thermal properties of epoxy/MWCNT composites and epoxy/glass composites were observed to be very similar. However, the weight reduction of MWCNT composites was 22.4 % compared to FRP composites. It was observed that the reduction of volumetric specific heat of 0.3 wt. % of MWCNT reinforced sandwich composites was found to be 14.6 % compared to that of unreinforced sandwich composites and it helped to increase the socket temperature even with minimum heat stored in the stump zone. It was noticed that the energy required by the pure epoxy socket to increase the temperature by 1 °C was 1790 kJ/m^{3}K, whereas the same was reduced by 28.1, 31.3 and 41.4 % for Epoxy/E-glass, sandwich and 0.3 wt. % of MWCNT reinforced sandwich composites, respectively. As per Arthur et al. [2001], it was reported that the raise in 1 °C temperature inside the socket led to increase the metabolic cost by 10 %. Thus, it is inferred that the temperature raise in the socket of an amputee is anticipated to be

reduced by 14.6 % for the 0.3 wt. % of MWCNT reinforced sandwich composites compared to that of unreinforced sandwich composites, which is expected to reduce the metabolic cost of an amputee.

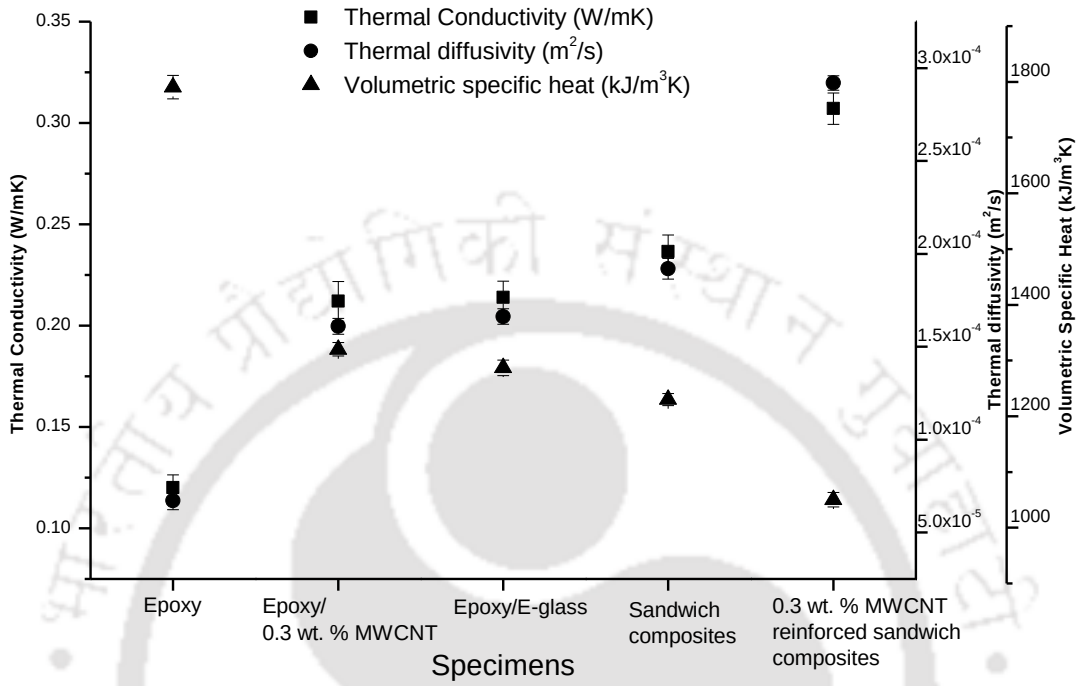

Fig. 4.69 Volumetric specific heat, thermal diffusivity and thermal conductivity of epoxy based different types of composites

The enhancement of thermal diffusivity and thermal conductivity and the reduction of volumetric specific heat of epoxy based different types of composites with respect to epoxy is shown in Fig. 4.70. The thermal diffusivity of Epoxy/E-glass, sandwich and 0.3 wt. % of MWCNT reinforced sandwich composites was found to be enhanced by 148, 186.5 and 335.7 %, respectively compared to pure epoxy, whereas the thermal conductivity for the same was found to be increased by 78.3, 97.2 and 155.9 %, respectively and the specific heat of the composites was decreased by 28.1, 31.3 and 41.4 %, respectively. The increase in thermal diffusivity of the epoxy based socket material is expected to enhance the rate of diffusion of heat from the stump-socket interface to the environment. The enhancement in thermal conductivity of the socket material improves its rate of heat transfer. Reasoning for the same has been already discussed in section 4.4.3.1. It is also noted that the thermal diffusivity and thermal conductivity of sandwich composites reinforced by 0.3 wt. % of MWCNT were found

to be increased by 52 and 29.8 %, respectively, compared to that of unreinforced sandwich composites.

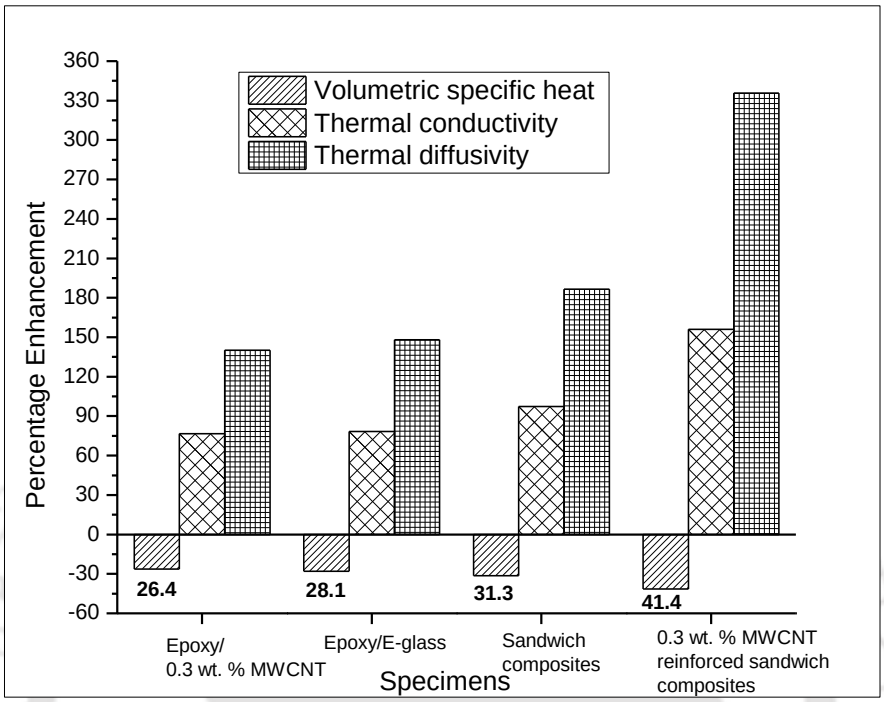

Fig. 4.70 Enhancement of volumetric specific heat, thermal diffusivity and thermal conductivity of epoxy based different types of composites compared to that of pure epoxy

Thus, the accumulation of heat inside the socket is expected to be reduced significantly and the same is transferred effectively with the usage of MWCNT reinforced sandwich composites, which is expected to increase the comfort level of the amputees and decrease their metabolic cost.

4.4.4.2 Mechanical properties of Epoxy/MWCNT/E-glass woven fabric/stockinet layers sandwich composites

Fig. 4.71 and 4.72 shows the flexural properties of Epoxy/E-glass woven fabric/stockinet sandwich composites with and without the dispersion of 0.3 wt. % MWCNT reinforcement. Fig. 4.71 shows the load against compression of the test samples. It was observed that the flexural properties were found to be increased with the number of stockinet layers in epoxy/glass composites, which was further increased with the reinforcement of 0.3 wt. % of MWCNT.

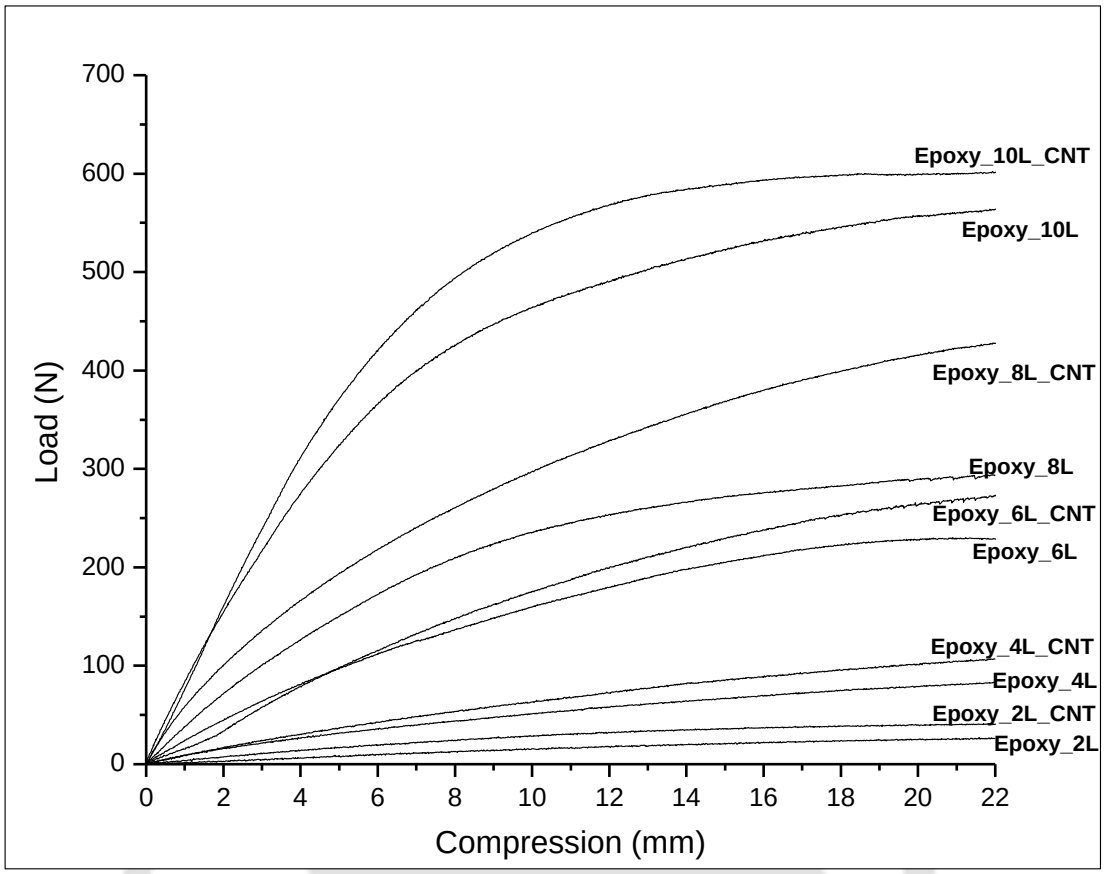

Fig. 4.71 Load vs compression of sandwich composites with and without MWCNT reinforcement

Fig. 4.72a and b shows the flexural strength and flexural modulus of the sandwich composites with and without the MWCNT reinforcement, respectively. It was observed that the increase in flexural strength of sandwich composites with 0.3 wt. % MWCNT reinforcement was observed to be 5.9 and 11.38 ± 1.5 % for 2 and 4-10 layers of stockinet, respectively, in comparison to that of unreinforced respective sandwich composites. The flexural modulus of sandwich composites having 2 to 10 layers of stockinet with MWCNT reinforcement was found to be increased by 4.5 ± 1.4 % compared to that of sandwich composites without MWCNT reinforcement. The reasoning for the enhancement of flexural properties of the sandwich composites with MWCNT reinforcement is the same as discussed in section 4.4.2.1 in addition to good bonding among the stockinet layer, epoxy and MWCNT.

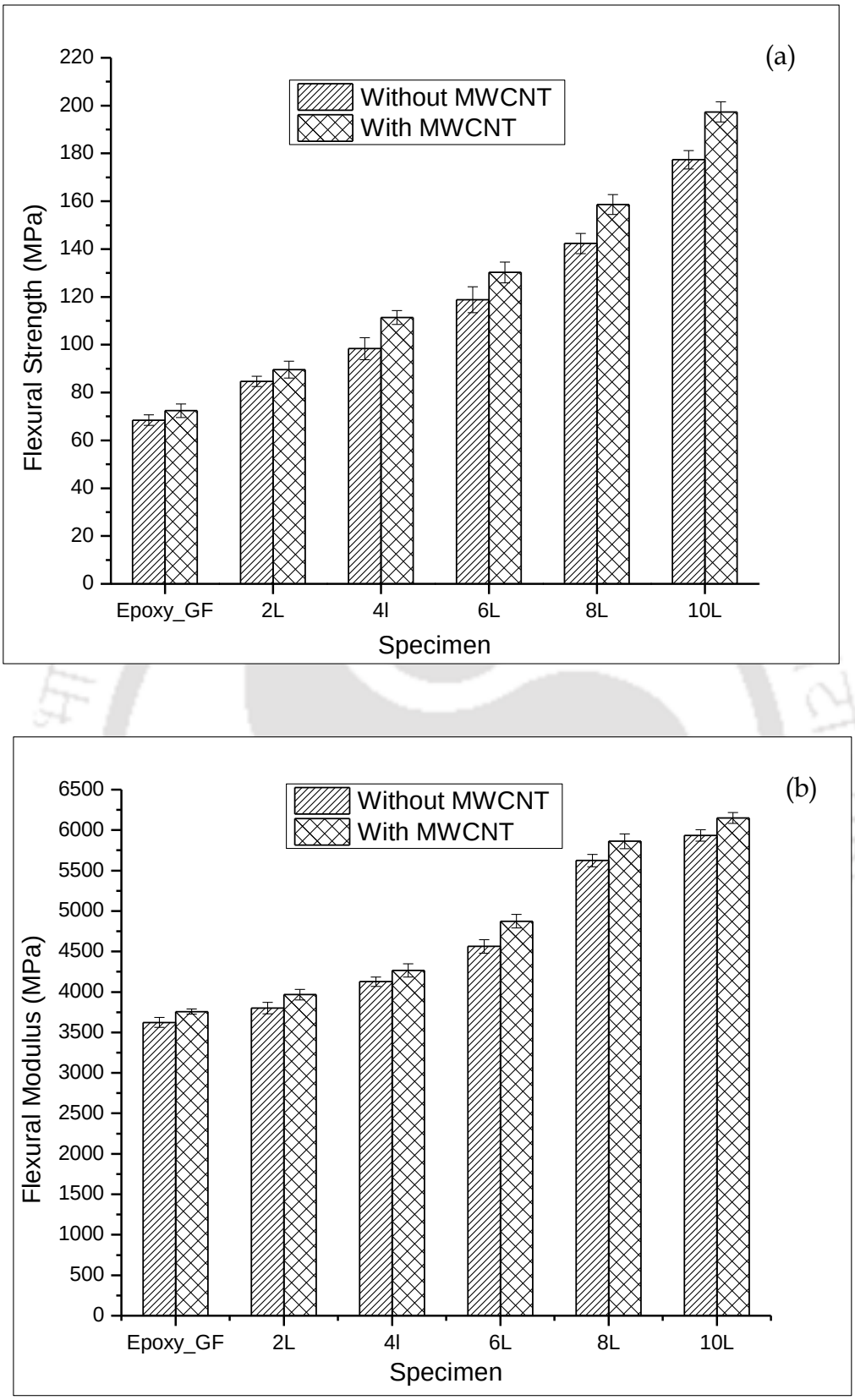

Fig. 4.72 a) Flexural strength and b) flexural modulus of sandwich composites with and without MWCNT reinforcement

4.4.5. Summary of the evaluation of the characteristics of sandwich composites proposed to be used for the socket

The combined effect of thermal diffusivity, volumetric specific heat and thermal conductivity increased the heat transfer characteristics of the trans-femoral socket leading to the reduction of accumulation of heat inside the socket. It was also observed that the increase in mechanical properties of the sandwich composites with the reinforcement of 0.3 wt. % of MWCNT led to reduce 2 layers of stockinet (eg. 4 layers instead of 6 stockinet layer), which decreased the overall weight of the socket. Therefore, the integrated effects of enhanced thermal and mechanical properties of the socket are expected to increase the comfort level of the amputees by decreasing their metabolic cost.

Chapter 5

Conclusions and future scope

5.1 Conclusions

The passive-polymeric-polycentric-prosthetic-knee joint was developed and it was fitted with nine unilateral trans-femoral amputees and the rehabilitation feedback was obtained from seven amputees after six months of its fixation. The health related quality of life and prosthesis function were noticed to be satisfactory by the amputees after the fixation of the developed prosthesis. The gait analysis of the amputees was obtained after the fixation of developed prosthesis and it was found to be comparable with that of near sound leg gait. The PMMA/MWCNT composite was proposed to be the knee joint material to restrict the ultraviolet rays induced degradation. The MWCNT reinforced epoxy based sandwich composite was also developed and proposed to be used as a socket material, which is anticipated to decrease the temperature raise inside the socket system and the metabolic cost of an amputee. The increased performance of the developed knee joint and proposed socket material are expected to make a huge impact in the locomotive disabled people to enhance their quality of life and affordability of the artificial limb. The summary of major results obtained under each sub-heading is given below:

5.1.1 1. Design, development and analysis of the prosthetic knee joint

- The alpha and beta stability of the proposed knee joint were obtained to be 26 and 173 mm, respectively.
- The floor clearance of the newly developed knee joint at 90° flexion was found to be 23 mm.
- The stiffness of extension assist was selected to be 0.5 N/mm based on the maximum flexion angle, flexion duration and walking velocity.

- The polycentric knee joint was fabricated with added features such as extension assist, single axis conversion, integrated adapter and pylon receiver.
- The equation of motion obtained from the dynamic analysis predicts the position of the knee joint against instantaneous time, which was also validated using the newly developed knee joint.

5.1.2 2. Patient trial and rehabilitation feedback after the fixation of the developed knee joint

- The health related quality of life of all the amputees was found to be increased significantly after fixing the polycentric knee joint.
- The flexion-extension movement of the prosthetic leg was confirmed by the amputees without any difficulties.
- The rehabilitation studies confirmed the good functional efficiency of the newly developed polycentric knee joint.
- The biomechanical gait pattern of an amputee was compared with that of the non-disabled healthy volunteer and no significant difference between them was observed.

5.1.3 3. Evaluation of the material proposed to be used for the knee joint

- The mechanical properties of PMMA were observed to be increased to maximum at 0.25 wt. % of MWCNT reinforcement, where the flexural modulus, flexural strength, tensile strength and Young's modulus were observed to be increased by 24.1, 26.3, 32.9 and 41.9 %, respectively compared to that of pure PMMA
- The modulus and strength of the PMMA/MWCNT composites can be predicted using the modified Halpin-Tsai model and Pukanszky model, respectively up to 0.25 wt. % MWCNT reinforcement.
- The tensile strength, Young's modulus and tensile strain of PMMA were found to be reduced by 12.1, 22 and 41.3 %, respectively after 12 months of aging in comparison with un-aged PMMA samples, whereas, the respective reduction

was limited to 3.8, 5 and 16 % for the 0.25 wt. % of MWCNT reinforced PMMA after the same period of aging.

- The reduction of flexural modulus, bending strain and flexural strength of pure PMMA after 12 months of aging was observed to be 8.1, 15.9 and 17.4 %, respectively compared to un-aged PMMA, which were correspondingly limited to 2.2, 6.3 and 7.6 % for 0.25 wt. % of MWCNT reinforced PMMA.
- The decrease in free radical concentration and oxidation index of 0.25 wt. % PMMA/MWCNT composite was found to be 54.3 and 77.8 %, respectively compared to pure PMMA after 12 months of aging.

5.1.4 4. Evaluation of the sandwich composites proposed to be used for the socket

- The reduction of volumetric specific heat was found to be 14.6 % for MWCNT reinforced sandwich composites compared to unreinforced sandwich composites, which is expected to increase the socket temperature with minimum heat stored in it.
- The thermal conductivity and thermal diffusivity of MWCNT reinforced sandwich composites were found to be increased by 29.8 and 52 %, respectively compared to unreinforced sandwich composites, and thus the rate of heat transfer and rate of heat diffusion from the socket are expected to increase significantly.
- The combined effect of thermal diffusivity, volumetric specific heat and thermal conductivity increased the heat transfer characteristics of the trans-femoral socket leading to the reduction of the accumulation of heat inside the socket and the corresponding metabolic cost of an amputee.
- The increase in flexural strength of sandwich composites with 0.3 wt. % MWCNT reinforcement was observed to be 11.38 ± 1.5 % for 4-10 layers of stockinet in comparison to that of unreinforced respective sandwich composites.
- The increase in mechanical and thermal properties of the sandwich composites with the reinforcement of 0.3 wt. % of MWCNT led to the selection of one-step

reduced stockinet layer (eg. 4 layers instead of 6 stockinet layer), and it is expected to significantly reduce the metabolic cost of an amputee.

5.2 Scope of future work

The work presented here opens up several avenues for further development in the artificial limb. The scope of the future work is outlined as follows:

- The injection moulding die can be fabricated after the topology optimization of the proposed knee joint.
- The knee joint may be manufactured with proposed PMMA/MWCNT composite in an injection moulding machine.
- The testing of the developed prosthetic knee joint using ISO 10328 standard can be explored.
- The role of friction in restricting the maximum flexion of the knee joint may be analyzed.
- The more number of patient trials can be explored and rehabilitation feedback should be obtained.
- Deep squat features may be integrated in the proposed knee joint in order to increase the hip and spine stability of the trans-femoral amputees.
- Bone anchored prosthesis technique can be explored with the developed knee joint.
- Link length can be selected based on the slope 6 to further increase the β stability of the knee joint to reduce the probability of buckling.
- The advanced functional materials may be utilized to improve the socket performance to reduce the fixation issues and its weight which influences the metabolic cost of an amputee.
- The temperature at the socket-stump interface should be carried out using the suitable sensor in order to evaluate the performance of the proposed material.
- The gait analysis should be carried out in the biomechanics lab

References

Abdalla M, Dean D, Robinson P, Nyairo E. Cure behavior of epoxy/MWCNT nanocomposites: The effect of nanotube surface modification. Polymer 2008; 49:3310–7.

Abdalla M, Dean D, Theodore M, Fielding J, Nyairo E, Price G. Magnetically processed carbon nanotube/epoxy nanocomposites: Morphology, thermal, and mechanical properties. Polymer 2010; 51:1614–20.

Ackermann M, Cozman FG. Automatic knee flexion in lower limb orthoses. J Brazilian Soc Mech Sci Eng 2009; 31:305–11.

Al-mashhadan NJH. Study of degradation effect on physical properties of methyl orange doped PMMA. Eng & Tech Journal 2011; 29(1):20–32.

Andresen EM, Meyers AR. Health-related quality of life outcomes measures. Arch Phy Med and Rehab 2000; 81(12,2):S30-45.

Andrysek J, Naumann S, Cleghorn WL. Artificial knee joint. US7087090 B2, 2006.

Andrysek J, Naumann S, Cleghorn WL. Design and quantitative evaluation of a stance-phase controlled prosthetic knee joint for children. IEEE Trans Neural Syst Rehabil Eng 2005; 13:437–43.

Andrysek J. Lower-limb prosthetic technologies in the developing world: A review of literature from 1994-2010. Prosthet Orthot Int 2010; 34:378–98.

Annala M, Lahelin M, Seppälä J. Utilization of poly(methyl methacrylate)–carbon nanotube and polystyrene–carbon nanotube in situ polymerized composite as masterbatches for melt mixing. eXPRESS Poly Letters 2012; 6:814–25.

Arthur FT, Zhang M, Boone AD. State-of-the-art research in lower-limb prosthetic biomechanics socket interface: A review. J Rehabil Res Dev 2001; 38:161–74.

Asano Y, Mizoguchi H, Osada M, Kozuki T, Urata J, Izawa T, Nakanishi Y, Okada K, Inaba M. Biomimetic design of musculoskeletal humanoid knee joint with patella and screw-home mechanism. 2011 IEEE Int Conf Robot Biomimetics, ROBIO 2011 2011; 1813–8.

Ash BJ, Schadler LS, Siegel RW. Glass transition behavior of alumina/ polymethylmethacrylate nanocomposites. Mater Lett 2002; 55:83–7.

Asmatulu R, Mahmud G, Hille C, Misak HE. Effects of UV degradation on surface hydrophobicity, crack, and thickness of MWCNT-based nanocomposite coatings. Prog Org Coatings 2011; 72:553–61.

ASTM D1238-10. Standard test method for melt flow rates of thermoplastics by extrusion plastometer. 2012; 1-15.

ASTM D638-10. Standard test method for tensile properties of plastics. 2010; 1-16.

ASTM D695-10. Standard test method for compressive properties of rigid plastics. 2010; 1-11.

ASTM F2625–10. Standard test method for measurement of enthalpy of fusion, percent crystallinity, and melting point of ultra-high-molecular weight polyethylene by means of differential scanning calorimetry. 2010; 1-4.

ASTM G154-12a. Standard practice for operating fluorescent ultraviolet (UV) lamp apparatus for exposure of nonmetallic materials. 2012; 1-12.

Au SK, Berniker M, Herr H. Powered ankle-foot prosthesis to assist level-ground and stair-descent gaits. Neural Net 2008; 21:654–66.

Au SK, Weber J, Herr H. Powered ankle – foot prosthesis improves walking metabolic economy. Robotics, IEEE Transactions 2009; 25(1):51-66.

Behrens SM, Unal R, Hekman EEG, Carloni R, Stramigioli S, Koopman HFJM. Design of a fully-passive transfemoral prosthesis prototype. Proc Annu Int Conf IEEE Eng Med Biol Soc EMBS 2011; 591–4.

Böger L, Sumfleth J, Hedemann H, Schulte K. Improvement of fatigue life by incorporation of nanoparticles in glass fibre reinforced epoxy. Compos Part A Appl Sci Manuf 2010; 41:1419–24.

Bounos G, Andrikopoulos KS, Karachalios TK, Voyiatzis GA. Evaluation of multi-walled carbon nanotube concentrations in polymer nanocomposite by Raman spectroscopy. Carbon 2014; 76:301-9.

Brånemark R, Brånemark PI, Bergh P, Gunterberg B. Osseointegration amputation prostheses - a new concept: background and clinical applications. In: SICOT '96 Amsterdam (CD-ROM). - Amsterdam: Excerpta Medica 1996; S30:125-220.

Burger H, Marincek C, Isakov E. Mobility of persons after traumatic lower limb amputation. Disabil Rehabil 1997b; 19(7):272-7.

Burger H, Marincek C. The life style of young persons after lower limb amputation caused by injury. Prosthet Orthot Int 1997a; 21:35–9.

Burgess EM, Coleman E. The Cushion-Socket Below-Knee Prosthesis. Clin Orthop Relat Res 1960; 16:304–7.

Campbell HE. Artificial polycentric knee joint. US 4064569, 1977.

Camponeschi E, Vance R, Al-Haik M, Garmestani H, Tannenbaum R. Properties of carbon nanotube-polymer composites aligned in a magnetic field. Carbon 2007; 45:2037–46.

Ceaykara T, GuÈven O. UV degradation of poly (methyl methacrylate) and its vinyltriethoxysilane containing copolymers. Polym Degrad Stab 1999; 65:225–9.

Census bureau reports 2010
https://www.census.gov/newsroom/releases/archives/miscellaneous/cb12-134.html

Census India, (2011) http://www.census.gov/

Chapartegui M, Florez S, Elizetxea C, Fernandez M, Santamaria A. Carbon nanotubes accelerate epoxy resin curing. Soc Plast Eng (SPE) 2011; 2011:1-2.

Chapartegui M, Markaide N, Florez S, Elizetxea C, Fernandez M, Santamaría A. Specific rheological and electrical features of carbon nanotube dispersions in an epoxy matrix. Compos Sci Technol 2010; 70:879–84.

Chen CW, Chen CC. Artificial knee joint. US 20110270415 A1, 2011.

Cheng QF, Wang JP, Wen JJ, Liu CH, Jiang KL, Li QQ, Fan SS. Carbon nanotube/epoxy composites fabricated by resin transfer molding. Carbon 2010; 48:260–6.

Cheng YT. Prosthetic knee joint structure. US 7279010 B2, 2007.

Cochrane H, Orsi K, Reilly P. Lower limb amputation prosthetics - a 10 year literature review. Prosthet Orthot Int 2001; 25:21-8.

Colombo G, Filippi S, Rizzi C, Rotini F. A new design paradigm for the development of custom-fit soft sockets for lower limb prostheses. Comput Ind 2010; 61:513–23.

Cronin SB, Swan AK, Unlu MS, Goldberg BB, Dresselhaus MS, Tinkham M. Measuring uniaxial strain in individual single-wall carbon nanotubes: resonance Raman spectra of AFM-modified SWNTs. Phys Rev Lett 2004; 93:1- 4.

Cui W, Du F, Zhao J, Zhang W, Yang Y, Xie X, Mia YW. Improving thermal conductivity while retaining high electrical resistivity of epoxy composites by incorporating silica-coated multi-walled carbon nanotubes. Carbon 2011; 49:495–500.

Cummings D. Prosthetics in the developing world: a review of the literature. Prosthet Orthot Int 1996; 20:51–60.

Current TA, Kogler GF, Barth DG. Static structural testing of trans-tibial composite sockets. Prosthet Orthot Int 1999; 23:113-22.

Dabiri Y, Najarian S, Eslami MR, Zahedi S, Moser D. A powered prosthetic knee joint inspired from musculoskeletal system. Biocybern Biomed Eng 2013; 33:118–24.

Darowicki K, Szocinski M, Schaefer K, Mills DJ. Investigation of morphological and electrical properties of the PMMA coating upon exposure to UV irradiation based on AFM studies. Prog Org Coatings 2011; 71:65–71.

Dassios KG, Musso S, Galiotis C. Compressive behavior of MWCNT/epoxy composite mats. Compos Sci Technol 2012; 72:1027–33.

Datsyuk V, Kalyva M, Papagelis K, Parthenios J, Tasis D, Siokou A, Kallitsis I, Galiotis C. Chemical oxidation of multiwalled carbon nanotubes. Carbon 2008; 46:833–40.

Davis DC, Wilkerson JW, Zhu J, Hadjiev VG. A strategy for improving mechanical properties of a fiber reinforced epoxy composite using functionalized carbon nanotubes. Compos Sci Technol 2011; 71:1089–97.

Delis AL, De CJL, Borges G, De RSS, Dos SI, Rocha DAF. Fusion of electromyographic signals with proprioceptive sensor data in myoelectric pattern recognition for

control of active transfemoral leg prostheses. Proc 31st Annu Int Conf IEEE Eng Med Biol Soc Eng Futur Biomed EMBC 2009; 2009:4755–8.

Demczyk BG, Wang YM, Cumings J, Hetman M, Han W, Zettl A, Ritchie RO. Direct mechanical measurement of the tensile strength and elastic modulus of multiwalled carbon nanotubes. Mat Sci Eng A 2002; 334:173–8.

Deng S, Ye L, Mai YW. Influence of fibre cross-sectional aspect ratio on mechanical properties of glass fibre/epoxy composites I. Tensile and flexure behaviour. Compos Sci Technol 1999; 59:1331–9.

Desmond DM, MacLachlan M. Prevalence and characteristics of phantom limb and residual limb pain in the long term following upper limb amputation. Int J Rehabil Res 2010; 33(3):279-82.

Dillingham TR, Pezzin LE, MacKenzie EJ, Burgess AR. Use and satisfaction with prosthetic devices among persons with trauma-related amputations: a long-term outcome study. Am J Phys Med Rehabil 2001; 80(8):563-71.

Dong C, Davies IJ. Flexural and tensile strengths of unidirectional hybrid epoxy composites reinforced by S-2 glass and T700S carbon fibres. Mater. Des 2013; 22: 41-9.

Dumas, Raphael, Frossard, Laurent, Leblanc R, Catheryne, Beaulieu, Marc P, Rickard B. Hip power analysis in individuals with transfemoral amputation: A different strategy different from stabilisation during gait stance. 25th Congress of the International Society of Biomechanics (ISB), 12-16 July 2015; Glasgow, UK.

Duvinage M, Castermans T, Dutoit T. Control of a lower limb active prosthesis with eye movement sequences. IEEE SSCI 2011 - Symp Ser Comput Intell - CCMB 2011 2011 IEEE Symp Comput Intell Cogn Algorithms, Mind, Brain 2011; 136–42.

Eastman. Ergonomic design for people at work. Vol. 2, by Eastman Kodak Company, Van Nostrand Reinhold, 1986.

Endura Plastic, http://endura.com/material-selection-guide/#12, Accessed 3/4/2015.

Esumi K, Ishigami M, Nakajima, Sawada K, Honda H. Chemical treatment of carbon nanotubes. Carbon 1996; 34:279–81.

Etienne S, Becker C, Ruch D, Grignard B, Cartigny G, Detrembleur C, Calberg C, Jerome R. Effects of incorporation of modified silica nanoparticles on the mechanical and thermal properties of PMMA. J Therm Anal Calorim 2007; 87:101–4.

Eve S, Mohr J. Study of the surface modification of the PMMA by UV-radiation. Procedia Eng 2009; 1:237–40.

Faramand F, Rezaeian T, Narimani R, Dinan HP. Kinematic and dynamic analysis of the gait cycle of above-knee amputee. Scientia Iranica 2006; 13(3):261-71.

Florian HG, Wichmann M, Fiedler B, Schulte K. Influence of different carbon nanotubes on the mechanical properties of epoxy matrix composites – A comparative study. Compos Sci Technol 2005; 65:2300–13.

Freudenstein F. An Analytical approach to the Design of Four-Link Mechanisms. ASME Trans 1954; 76(3):483–92.

Friedmann LW. Amputations and prostheses in primitive cultures. Bulletin of Prosthetics Research 1972; 105–38.

Fu J, Naguib HE. Effect of nanoclay on the mechanical properties of pmma/clay nanocomposite foams. Journal of Cellular Plastics 2006; 42:325-42.

Furse A, Cleghorn W, Andrysek J. Improving the gait performance of nonfluid-based swing-phase control mechanisms in transfemoral prostheses. IEEE Trans Biomed Eng 2011; 58:2352–9.

Gagnon GC, Grise MC, Potvin D. Predisposing factors related to prosthetic-use by people with transtibial and transfemoral amputation. Prosthetics Orthot Int 1998; 10:99–109.

Gailey R, McFarland LV, Cooper RA, Czerniecki J, Gambel JM, Hubbard S, Maynard C, Douglas GS, Raya M, Reiber GE. Unilateral lower-limb loss: prosthetic device use and functional outcomes in service members from Vietnam war and OIF/OEF conflicts. J Rehabil Res Dev 2010; 47:317–31.

Gard SA. Use of quantitative gait analysis for the evaluation of prosthetic walking performance. J Prosthetics Orthot 2006; 18(1S):93-104.

Gerschutz MJ, Haynes ML, Nixon D, Colvin JM. Strength evaluation of prosthetic check sockets, copolymer sockets, and definitive laminated sockets. J Rehabil Res Dev 2012b; 49:405–26.

Gerschutz MJ, Haynes ML, Nixon DM, Colvin JM. Industry wide evaluation of prosthetic socket strength. American Academy of Orthotists & Prosthetists 38th Academy Annual Meeting and Scientific Symposium 2012a; 2012:1-1.

Gerschutz MJ, Haynes ML, Nixon DM, Colvin JM. Tensile strength and impact resistance properties of materials used in prosthetic check sockets, copolymer sockets, and definitive laminated sockets. J Rehabil Res Dev 2011; 48:987–1004.

Gojny FH, Schulte K. Functionalisation effect on the thermo-mechanical behavior of MWCNT/epoxy-composites. Compos Sci Technol 2004; 64:2303–8.

Gonzalez RV, Ayers SR, Minelga E, Downing WL, Fisher JB. Prosthetic knee. WO 2011123119 A1, 2011.

Gowariker VR, Viswanathan NV, Sreedhar J. Polymer Science. New Age International (P) Ltd.; 1986.

Grafinger J. Knee joint prosthesis. US 7597716 B2, 2009.

Gramnas F. Device at a knee joint prosthesis. US 6808540 B1, 2004.

Greene MP. Four-bar linkage knee analysis. Orth and Pros. 1983; 37(1):15-24.

Grigoriadou I, Paraskevopoulos KM, Chrissafis K, Pavlidou E, Stamkopoulos TG, Bikiaris D. Effect of different nanoparticles on HDPE UV stability. Polym Degrad Stab 2011; 96:151–63.

Guadagno L, Vertuccio L, Sorrentino A, Raimondo M, Naddeo C, Vittoria V, Iannuzzo G, Calvi E, Russo S. Mechanical and barrier properties of epoxy resin filled with multi-walled carbon nanotubes. Carbon 2009; 47:2419–30.

Guirao L, Samitier CB, Beatriz C, Costea M, Camos JM, Majo M, Pleguezuelos E. Improvement in walking abilities in transfemoral amputees with a distal weight bearing implant. Prosthet Orthot Int 2016; 6,

Guo Y, Zhang X, Chen W. Three-dimensional finite element simulation of total knee joint in gait cycle. Acta Mech Solida Sin 2009; 22:347–51.

Haddan CC, Thomas A. Status of the above-knee suction socket in the United States. Artif Limbs 1954; 12:29–39.

Hagberg K, Brånemark R, Hägg O. Questionnaire for persons with a transfemoral amputation (Q-TFA): initial validity and reliability of a new outcome measure. J Rehabil Res Dev. 2004; 41(5):695-706.

Hagberg K, Brånemark R. Consequences of nonvascular trans-femoral amputation: a survey of quality of life, prosthetic use and problems. Prosthet Orthot Int. 2001; 25(3):186-94.

Haggenmueller R, Guthy C, Lukes JR, Fischer JE, Winey KI. Single wall carbon nanotube/polyethylene nanocomposites: Thermal and electrical conductivity. Macromol. 2007; 40:2417-21.

Hays RD, Hahn H, Marshall G. Use of the SF-36 and other health-related quality of life measures to assess persons with disabilities. Arch Phys Med Rehabil 2002; 83(12):4-9.

Her SC, Lai CY. Dynamic behavior of composite reinforced with multi-walled carbon nanotubes (MWCNT). Materials 2013; 6:2274-84.

Hitchen S, Ogin SL, Smith P. Effect of fibre length on fatigue of short carbon fibre/epoxy composite. Composites 1995; 26:303–8.

Holden JM, Fernie GR. Extent of artificial limb use following rehabilitation. J Orthop Res 1987; 5(4):562-8.

Hynd D, Hughes SC, Ewins DJ. The development of a long, dual-platform triaxial walkway for the measurement of forces and temporal-spatial Data in the clinical assessment of gait. Journal of Engineering in Medicine 2000; 214(H):193-201.

Irawan P, Soemardi TP, Widjajalaksmi K, Reksoprodjo HS. Tensile and flexural strength of ramie fiber reinforced epoxy composites for socket prosthesis application. Int J Mech Mater Eng 2011; 6:46–50.

Ishai G, Bar A, Susak Z. Effects of alignment variables on thigh axial torque during swing phase in AK amputee gait. Prosthet. Orthot. Int. 1983; 7:41–7.

ISO 10328:2006, Prosthetics structural testing of lower-limb prostheses-requirements and test methods. 2011; 2011:1-136.

ISO 22007-2:2008, Plastics--determination of thermal conductivity and thermal diffusivity -- Part 2: Transient plane heat source (hot disc) method. 2008; 2008:1-164.

Jaegers SM, Arendzen JH, Jongh DHJ. Prosthetic gait of unilateral trans-femoral amputees: a kinematic study. Arch Phys Med Rehabil 1995; 76:736-43.

Jia X, Zhang M, Li X, Lee WCC. A quasi-dynamic nonlinear finite element model to investigate prosthetic interface stresses during walking for trans-tibial amputees. Clin Biomech 2005; 20:630–5.

Jin Z, Pramoda KP, Goh SH, Xu G. Poly(vinylidene fluoride)-assisted melt-blending of multi walled carbon nanotube/poly(methyl methacrylate) composites. Mater Res Bull 2002; 37:271-8.

Jindal P, Sain M, Kumar N. Mechanical characterization of PMMA/MWCNT composites under static and dynamic loading conditions. Mater Today Proc 2015; 2:1364–72.

Jing L, Xiansheng Q. Optimization of bionics knee joint mechanism structure. Int Conf on Computer and Communication Technologies in Agriculture Engineering. 2010; 85-88.

Joshi D, Mishra A, Anand S. ANFIS based knee angle prediction: An approach to design speed adaptive contra lateral controlled AK prosthesis. Applied Soft Computing 2011; 11:4757–65.

Kalanovic VD, Popovic D, Skaug NT. Feedback error learning neural network for trans-femoral prosthesis 2000; 8:71–80.

Kane RJ, Yue W, Mason JJ, Roeder RK. Improved fatigue life of acrylic bone cements reinforced with Zirconia fibers. J Mech Behav Biomed 2010; 3:504–11.

Kapti AO, Yucenur MS. Design and control of an active artificial knee joint. Mech Mach Theory 2006; 41:1477–85.

Karlsson SG, Hannesson S, Olafsson S. Prosthetic Knee. US 20130268092 A1, 2013.

Kim J. Development of an above knee prosthesis using MR damper and leg simulator. IEEE Int Conf on Robotics and Automation 2001; 3686–91.

Kim M, Park Y Bin, Okoli OI, Zhang C. Processing, characterization, and modeling of carbon nanotube-reinforced multiscale composites. Compos Sci Technol 2009; 69:335–42.

Kim MT, Rhee KY, Lee JH, Hui D, Lau AKT. Property enhancement of a carbon fiber/epoxy composite by using carbon nanotubes. Compos Part B Eng 2011; 42:1257–61.

Klute GK, Rowe GI, Mamishev V, Ledoux WR. The thermal conductivity of prosthetic sockets and liners. Prosthet Orthot Int 2007; 31:292–9.

Kotha SP, Li C, McGinn P, Schmid SR, Mason JJ. Improved mechanical properties of acrylic bone cement with short titanium fiber reinforcement. J Mater Sci, Mater Med 2006; 17:1403–9.

Krasheninnikov V, Nordlund K. Irradiation effects in carbon nanotubes. Nucl Instruments Methods Phys Res Sect B Beam Interact with Mater Atoms 2004; 216:355–66.

Kurtz SM. UHMWPE Hand book. Second edition, Paris, Academic press, 2009.

Lambrecht BGA, Kazerooni H. Design of a semi-active knee prosthesis. IEEE Int Conf on Robotics and Automation 2009; 639–45.

Lang TS. A prosthetic knee joint mechanism. EP 1603495 B1, 2013.

Lee JH, Rhee KY, Lee JH. Effects of moisture absorption and surface modification using 3-aminopropyltriethoxysilane on the tensile and fracture characteristics of MWCNT/epoxy nanocomposites. Appl Surf Sci 2010a; 256:7658–67.

Lee JH, Rhee KY, Park SJ. Silane modification of carbon nanotubes and its effects on the material properties of carbon/CNT/epoxy three-phase composites. Compos Part A Appl Sci Manuf 2011; 42:478–83.

Lee JH, Rhee KY, Park SJ. The tensile and thermal properties of modified CNT-reinforced basalt/epoxy composites. Mater Sci Eng A 2010b; 527:6838–43.

Legro MW, Reiber G, Aguila DM, Ajax MJ, Boone DA, Larsen JA, Smith DG, Sangeorzan B. Issues of importance reported by persons with lower limb amputations and prostheses. J Rehabil Res Dev 1999; 36(3):155-63.

Li J, Yang R, Yu J, Liu Y. Natural photo-aging degradation of polypropylene nanocomposites. Polym Degrad Stab 2008; 93:84–9.

Li M, Gu Y, Liu Y, Li Y, Zhang Z. Interfacial improvement of carbon fiber/epoxy composites using a simple process for depositing commercially functionalized carbon nanotubes on the fibers. Carbon 2013; 52:109–21.

Li Q, Zaiser M, Koutsos V. Carbon nanotube/epoxy resin composites using a block copolymer as a dispersing agent. Physica status solidi 2004; 201:89-91.

Littlejohn B, Heeger KM, Wise T, Gettrust E, Lyman M. UV degradation of the optical properties of acrylic for neutrino and dark matter experiments. J Instrument 2009; 4:1-13.

Logakis E, Pandis CH, Pissis P, Pionteck J, Pötschke P. Highly conducting poly(methyl methacrylate)/carbon nanotubes composites: Investigation on their thermal, dynamic-mechanical, electrical and dielectric properties. Compos Sci Technol 2011; 71:854–62.

Lopes P, Corbellini M, Ferreir BL, Almeida N, Fredel M, Fernandes MH, New CR. PMMA–co–EHA glass–filled composites for biomedical applications, mechanical properties and bioactivity. Acta Biomaterialia 2009; 5:356–62.

Lura DJ, Wernke MM, Carey SL, Kahle JT, Miro RM, Highsmith MJ. Differences in knee flexion between the genium and C-Leg microprocessor knees while walking on level ground and ramps. Clin Biomech 2015; 30:175–81.

Mark WS, Hutchinson S, Vidyasagar M. Robot modeling and control, 1st Edition, John Wiley & Sons Inc., New York 1992.

Martel GG, Iler EA. Leg prosthesis, US 4883493, 1985.

Martin D. UV resistance in thin film geomembranes: accelerated and natural weathering studies. Waste Contain Remediat 2005; 40789:1–9.

Masouros SD, Bull AMJ, Amis AA. Biomechanics of the knee joint mini-symposium: soft tissue surgery in the knee. Orthop Trauma 2010; 24:84-91.

McGimpsey G, Bradfo TC. Limb prosthetics services and devices critical unmet need: market analysis white paper, Bioengineering Institute Center for Neuroprosthetics, Worcester Polytechnic Institution 2012.

Mecklenburg M, Mizushima D, Ohtake N, Bauhofer W, Fiedler B, Schulte K. On the manufacturing and electrical and mechanical properties of ultra-high wt.% fraction aligned MWCNT and randomly oriented CNT epoxy composites. Carbon 2015; 91:275–90.

Moisala A, Li Q, Kinloch LA, Windle AH. Thermal and electrical conductivity of single- and multi-walled carbon nanotube-epoxy composite. Compos Sci Technol 2006; 66(10):1285-8.

Moniruzzaman M, Du F, Romero N, Winey KI. Increased flexural modulus and strength in SWNT/epoxy composites by a new fabrication method. Polymer 2006a; 47:293–8.

Moniruzzaman M, Winey KI. Polymer nanocomposites containing carbon nanotubes. Macromol 2006b; 39(16):5194–205.

Mont D. Measuring disability prevalence. Disability & development team, HDNSP The World Bank 2007.

Montazeri A, Montazeri N. Viscoelastic and mechanical properties of multi walled carbon nanotube/epoxy composites with different nanotube content. Mater Des 2011; 32:2301–7.

Narayan N, Sadler J, Thorsell E. Polycentric knee joint prosthesis for extreme affordability. WO 2012119156 A2, 2012.

Nerlich AG, Zink A, Szeimies U, Hagedorn HG. Ancient Egyptian prosthesis of the big toe. The Lancet 2000; 356:2176-9.

Nieto EA, Cadenas MP, Carter J, Anderson JA, Ruiz AG. Preparation and surface functionalization of MWCNTs: study of the composite materials produced by the interaction with an iron phthalocyanine complex. Nanoscale Res Lett 2011; 6:353-7.

NLLIC Staff. Amputation statistics by cause limb loss in the United States. 2008; NLLIC.

Norton KM. A brief history of prosthetics. In Motion 2007; 17(7):1-3.

Oddsson M, Jonsson VF, Lecomte CG. Energy returning prosthetic joint. US 30342 A1, 2010.

Ogawa A, Obinata G, Hase K, Dutta A, Nakagawa M. Design of lower limb prosthesis with contact pressure adjustment by MR fluid. Conf Proc IEEE Eng Med Biol Soc 2008; 2008:330–3.

Omasta M, Paloušek D, Návrat T, Rosický J. Finite element analysis for the evaluation of the structural behaviour, of a prosthesis for trans-tibial amputees. Med Eng Phys 2012; 34:38–45.

Omrani A, Rostami AA, Khostavan S, Vazifeshenas Y. Preparation, characterization and application of advanced isoconversional kinetics to epoxy/1,4-Bis(3-aminopropoxy) butane/MWCNT nanocomposite. Compos Part A Appl Sci Manuf 2012; 43:381–7.

Papaioannou G, Mitrogiannis C, Nianios G, Fiedler G. Assessment of amputee socket–stump–residual bone kinematics during strenuous activities using dynamic roentgen stereogrammetric analysis. J Biomech 2010; 43:871–8.

Park JG, Cheng Q, Lu J, Bao J, Li S, Tian Y, Liang Z, Zhang C, Wang B. Thermal conductivity of MWCNT/epoxy composites: The effects of length, alignment and functionalization. Carbon 2012b; 50:2083–90.

Park JM, Kim PG, Jang JH, Wang Z, Kim JW, Lee WI, Park JG, DeVries KL. Self-sensing and dispersive evaluation of single carbon fiber/carbon nanotube (CNT)-epoxy composites using electro-micromechanical technique and nondestructive acoustic emission. Compos Part B Eng 2008; 39:1170–82.

Park JM, Wang ZJ, Kwon DJ, Gu GY, Lee W, Park JK, DeVries KL. Optimum dispersion conditions and interfacial modification of carbon fiber and CNT-phenolic composites by atmospheric pressure plasma treatment. Compos Part B Eng 2012a; 43:2272–8.

Pat M, Avilés F, Toro P, Yazdani-Pedram M, Cauich-Rodríguez JV. Mechanical properties of PET composites using multiwalled carbon nanotubes functionalized by inorganic and itaconic acids. Express Polym Lett 2012; 6:96–106.

Peigney A, Laurent CH, Flahaut E, Bacsa RR, Rousset A. Specific surface area of carbon nanotubes and bundles of carbon nanotubes. Carbon 2001; 39:507–14.

Peng Y, Hua Y, Lingling C, Yanli G. Intelligent lower limb prosthesis following healthy leg gait based on fuzzy control. Proc 2012 24th Chinese Control Decis Conf CCDC 2012; 2012:3729–31.

Petersen EJ, Lam T, Gorham JM, Scott KC, Long CJ, Stanley D, Sharma R, Liddle JA, Pellegrine B, Nguyen T. Methods to assess the impact of UV irradiation on the surface chemistry and structure of multiwall carbon nanotube epoxy nanocomposites. Carbon 2014; 69:194–205.

Pezzin LE, Dillingham TR, MacKenzie EJ. Rehabilitation and the long-term outcomes of persons with trauma-related amputations. Arch Phys Med Rehabil 2000; 1(3):292-300.

Pfeifer S, Pagel A, Riener R, Vallery H. Actuator with angle-dependent elasticity for biomimetic transfemoral prostheses. Mechatronics, IEEE/ASME Trans 2014; 1–11.

Pillai SK, Ray SS. Epoxy-based carbon nanotubes reinforced composites advances in nanocomposites - synthesis, characterization and industrial applications. Edited by Reddy. B, InTech, 2011; 727-92.

Pradhan NR, Duan H, Liang J, Iannacchione GS. The specific heat and effective thermal conductivity of composite containing single-wall and multi-wall carbon nanotubes. Nanotechnology 2009; 20:1-7.

PSG data book, Design Data: Data Book of Engineers by PSG College-Kalaikathir Achchagam - Coimbatore, 2015.

Puglia D, Valentini L, Armentano I, Kenny JM. Effects of single-walled carbon nanotube incorporation on the cure reaction of epoxy resin and its detection by Raman spectroscopy. Diam Relat Mater 2003; 12:827–32.

Puhalski EM, Taylor DM, Poulin TM. How are transfemoral amputees using their prosthesis in Northwestern Ontario? J Prosthetics Orthot 2008; 20:53–60.

Pukanszky B, Turcsanyi B, Tudos F. Effect of interfacial interaction on the tensile yield stress of polymer composite. In: Ishida H, editor. Interfaces in polymer, ceramic and metal matrix composite, Amsterdam, Elsevier, 1988; 467–77.

Putti V. Historic Artificial Limbs. Paul B. Hoeber, Inc., New York, 1930.

Radcliffe CW. Four-bar linkage prosthetic knee mechanisms: kinematics, alignment and prescription criteria. Prosthet Orthot Int 1994a; 18:159 –73.

Radcliffe CW. Prosthetics. In: Rose J, Gamble JG, editors. Human walking. 2nd ed. Baltimore: Williams & Wilkins; 1994b; 167-99.

Radcliffe CW. The Knud Jansen Lecture: above-knee prosthetics. Prosthet Orthot Int 1977; 1:146–60.

Raggi M, Tura A, Rocchi L, Cutti AG, Orlandini D, Chiari L. Gait analysis through inertial sensors in transfemoral amputees: Step and stride regularity. Gait posture. 2006; 1:S17–8.

Rahman MM, Zainuddin S, Hosur MV, Malone JE, Salam MB, Kumar A, Jeelani S. Improvements in mechanical and thermo-mechanical properties of e-glass/epoxy composites using amino functionalized MWCNTs. Compos Struct 2012; 94:2397–406.

Rosa DS, Angelini JMG, Agnelli JM, Mei LHI. The use of optical microscopy to follow the degradation of isotactic polypropylene (iPP) subjected to natural and accelerated ageing. Polym Test 2005; 24:1022–6.

Royan NRR, Sulong AB, Sahari J, Suherman H. Effect of acid- and ultraviolet/ozonolysis-treated MWCNTs on the electrical and mechanical properties of epoxy nanocomposites as bipolar plate applications. J Nanomater 2013; 2013:1-8

Ruoff RS, Qian D, Liu WK. Mechanical properties of carbon nanotubes: theoretical predictions and experimental measurements. C. R. Physique 2003; 4:993–1008.

Sanders JE, Michae RS, Kathryn JA. Computer-Socket Manufacturing Error: How Much Before It Is Clinically Apparent? J Rehabil Res Dev. 2012; 49:567-82.

Sanders JE, Rogers EL, Sorenson E, Lee GS, Abrahamson DC. CAD/CAM transtibial prosthetic sockets from central fabrication facilities: how accurate are they? J Rehabil Res Dev 2007; 44:395–405.

Segal AD1, Orendurff MS, Klute GK, McDowell ML, Pecoraro JA, Shofer J, Czerniecki JM. Kinematic and kinetic comparisons of transfemoral amputee gait using C-Leg and Mauch SNS prosthetic knees. J Rehabil Res Dev. 2006; 43(7):857-70.

Serbetci K, Korkusuz F, Hasirci N. Thermal and mechanical properties of Hydroxyapatite impregnated acrylic bone cements. Polymer Testing 2004; 23:145–55.

Shandiz MA, Farahmand F, Zohour H. Dynamic simulation of the biped normal and amputee human gait. 12th International Conference on Climbing and Walking Robots and the Support Technologies for Mobile Machines (CLAWAR 2009), September 2009 - Istanbul, Turkey. 2009; (9-11):1113-20.

Shang S, Li L, Yang X, Wei Y. Polymethylmethacrylate-carbon nanotubes composite prepared by microemulsion polymerization for gas sensor. Compos Sci Technol 2009; 69:1156–9.

Shirota C, Simon A, Kuiken TA. Transfemoral amputee recovery strategies following trips to their sound and prosthesis sides throughout swing phase. J Neuroeng Rehabil 2015; 12:79.

Siddiqui N, Khan SU, Kim JK. Experimental torsional shear properties of carbon fiber reinforced epoxy composites containing carbon nanotubes. Compos Struct 2013; 104:230–8.

Siddiqui N, Sham ML, Tang BZ, Munir A, Kim JK. Tensile strength of glass fibres with carbon nanotube-epoxy nanocomposite coating. Compos Part A Appl Sci Manuf 2009; 40:1606–14.

Silva P, Albano C, Perera R. Use of electron paramagnetic resonance to evaluate the behavior of free radicals in irradiated polyolefins. Revista Latinoamericana de Metalurgia y Materiales 2009; 28(2):79–90.

Singh B, Sharma N. Mechanistic implications of plastic degradation. Polym Degrad Stab 2008a; 93:561–84.

Singh BP, Singh D, Mathur RB, Dhami TL. Influence of surface modified MWCNT on the mechanical, electrical and thermal properties of polyimide composite. Nanoscale Res Lett 2008b; 3:444–53.

Smith JD, Martin PE. Effects of prosthetic mass distribution on metabolic costs and walking symmetry. J Appl Biomech 2013; 29:317–28.

Sreekanth PSR, Kanagaraj S. Assessment of bulk and surface properties of medical grade UHMWPE based composite using Nanoindentation and microtensile testing. J Mech Behav Biomed 2013; 18:140-51.

Srikanth I, Kumar S, Kumar A, Ghosal P, Subrahmanyam C. Effect of amino functionalized MWCNT on the crosslink density, fracture toughness of epoxy and mechanical properties of carbon-epoxy composites. Compos Part A Appl Sci Manuf 2012; 43:2083–6.

Srivastava VK, Singh SA. Micro-mechanical model for elastic modulus of multi-walled carbon nanotube/epoxy resin composite. Int J Composite Mat 2012; 2(2):1-6.

Starkova O, Buschhorn ST, Mannov E, Schulte K, Aniskevich. Creep and recovery of epoxy/MWCNT nanocomposites. Compos Part A Appl Sci Manuf 2012; 43:1212–8.

Suárez J, Campo M, Gaztelumendi I, Markaide N, Sánchez M, Ureña A. The influence of mechanical dispersion of MWCNT in epoxy matrix by calendering method: Batch method versus time controlled. Compos Part B Eng 2013; 48:88–94.

Taheri A, Karimi MT. Evaluation of the gait performance of above-knee amputees while walking with 3R20 and 3R15 knee joints. J Res Med Sci 2012; 17(3):258-63.

Tan G, Jiang B, Yang L. A novel immune genetic algorithm-based PID controller design and its application to CIP-I intelligent leg. Third Int Conf on Natural Comput (ICNC 2007) 2007; 2007:1-5.

Tang CP. Lagrangian dynamic formulation of a four-bar mechanism with minimal coordinates 2006; 1–7.

Tanolu M, Ergün Y. Porous nanocomposites prepared from layered clay and PMMA [poly (methyl methacrylate)]. Compos Part A Appl Sci Manuf 2007; 38:318–22.

Taylor D. Lower-limb prosthetics – mechanical testing prosthetic sockets. Proc American Acad Ortho & Prosthet 2005; 2005:1-4.

Theodore M, Hosur M, Thomas J, Jeelani S. Influence of functionalization on properties of MWCNT-epoxy nanocomposites. Mater Sci Eng A 2011; 528:1192–200.

Thompson JW. Knee joint apparatus for a leg prosthesis. US 4451939, 1984.

Thompson JW. Leg prosthesis. US 4090264, 1978.

Thorn MBS, Glaister CL. Functional stability of transfemoral amputee gait using the 3R80 and total knee 2000 prosthetic knee units. J Prosthetics Orthot 2009; 21(1):18-31.

Tura A, Raggi M, Cutti AG, Chiari L. Gait symmetry and regularity in transfemoral amputees assessed by trunk accelerations. J Neuroeng Rehabil 2010; 7:4.

Unal R, Carloni R, Hekman EEG, Stramigioli S, Koopman HFJM. Conceptual design of an energy efficient transfemoral prosthesis. 2010 IEEE/RSJ Int Conf Intell Robot Syst 2010; 343–8.

Unnikrishnan L, Mohanty S, Nayak SK, Ali A. Preparation and characterization of poly (methyl methacrylate)-clay nanocomposites via melt intercalation: Effect of organoclay on thermal, mechanical and flammability properties. Mater Sci Eng A 2011; 528:3943–51.

Vannier MW, Commean PK, Smith KE. Three dimensional lower-limb residua measurement systems error analysis. J Prosthet and Ortho 1997; 9(2):67–76.

Varol HA, Sup F, Goldfarb M. Multiclass real-time intent recognition of a powered lower limb prosthesis. IEEE Trans Biomed Eng. 2010; 57:542–51.

Vaudreuil S, Labzour A, Ray SS, EI MK, Bousmina M. Dispersion characteristics and properties of poly(methyl methacrylate)/multiwalled carbon nanotubes nanocomposites. J. Nanosci. Nanotechnol. 2007; 7:2349-55.

Velez JJO, Zahedi MS. Stabilising knee joint for a lower limb prosthesis. US 0292807 A1, 2010.

Villalpando MEC, Herr H. Agonist-antagonist active knee prosthesis: a preliminary study in level-ground walking. J Rehabil Res Dev 2009; 46:361–73.

Villoria DRG, Miravete A, Cuartero J, Chiminelli, Tolosana N. Mechanical properties of SWNT/epoxy composites using two different curing cycles. Compos Part B Eng 2006; 37:273–7.

Walker CR, Ingram RR, Hullin MG, McCreath SW. Lower limb amputation following injury: a survey of long-term functional outcome. Injury 1994; 25(6):387-92.

Wang GA, Wang CC, Chen CY. The disorderly exfoliated LDHs/PMMA nanocomposites synthesized by in situ bulk polymerization: The effects of LDH-U on thermal and mechanical properties. Polym Degrad Stab 2006; 91:2443–50.

Wang Q, Dai J, Li W, Wei Z, Jiang J. The effects of CNT alignment on electrical conductivity and mechanical properties of SWNT/epoxy nanocomposites. Compos Sci Technol 2008; 68:1644–8.

Ware JE, Kosinski M, Bayliss MS, McHorney C, Rogers WH, Raczek. Comparison of methods for the scoring and statistical analysis of SF-36 health profile and summary measures: summary of results from the medical outcomes study. Med Care 1995; 33:AS264–S279.

Ware JE, Sherbourne CD. The MOS 36-item short-form health survey (SF-36) I. Conceptual framework and item selection. Med Care 1992; 30:473–83.

Waters RL, Perry J, Antonelli D, Hislop H. Energy cost of walking of amputees: the influence of level of amputation. J Bone Joint Surg Am 1976; 58:42–6.

Watts PCP, Fearon PK, Hsu WK, Billingham NC, Kroto HW, Walton DRM. Carbon nanotubes as polymer antioxidants. J. Mater. Chem. 2003; 13:491–5.

Wichmann MHG, Sumfleth J, Gojny FH, Quaresimin M, Fiedler B, Schulte K. Glass-fibre-reinforced composites with enhanced mechanical and electrical properties - Benefits and limitations of a nanoparticle modified matrix. Eng Fract Mech 2006; 73:2346–59.

Wild GE. Prosthetic knee and rotary hydraulic chamber. US 7066964 B2, 2006.

Wilson AB. Limb prosthetics-1972. Robert E. Krieger Publishing Company, Huntington, N.Y., 1972.

Wolf SI, Alimusaj M, Fradet L, Siegel J, Braatz F. Pressure characteristics at the stump/socket interface in transtibial amputees using an adaptive prosthetic foot. Clin Biomech 2009; 24:860–5.

Xie H, Sheng Z, Liu Y. Mechanical optimization design of intelligent bionic leg. 3rd Int Conf on Bioinformatics and Biomedical Engineering 2009; 8–11.

Xie HL, Liang ZZ, Li F, Guo LX. The knee joint design and control of above-knee intelligent bionic leg based on magneto-rheological damper. Int J Autom Comput 2010; 7:277–82.

Yakimovich T, Kofman J, Lemaire ED, Conventional A. Design and evaluation of a stance-control knee-ankle-foot orthosis knee joint. IEEE Trans Neural Syst Rehabil Eng 2006; 14:361–9.

Yang K, Mingyuan G, Yiping G, Xifeng P, Guohong M. Effects of carbon nanotube functionalization on the mechanical and thermal properties of epoxy composite. Carbon 2009; 47:1723 –37.

Yeh MK, Tai NH, Liu JH. Mechanical behavior of phenolic-based composites reinforced with multi-walled carbon nanotubes. Carbon 2006; 44:1-9.

Yokogushi K, Narita H, Uchiyama E, Chiba S, Nosaka T, Yamakoshi K. Biomechanical and clinical evaluation of a newly designed polycentric knee of transfemoral prosthesis. J Rehabil Res Dev 2004; 41:675–82.

Yu MF, Files BS, Arepalli S, Ruoff RS. Tensile loading of ropes of single wall carbon nanotubes and their mechanical properties. Phys. Rev. Lett 2000; 84:5552–5.

Yu N, Zhang ZH, He SY. Fracture toughness and fatigue life of MWCNT/epoxy composites. Mater Sci Eng A 2008; 494:380–4.

Zainuddin S, Fahim A, Arifin T, Hosur MV, Rahman MM, Tyson JD, Jeelani S. Optimization of mechanical and thermo-mechanical properties of epoxy and E-glass/epoxy composites using NH2-MWCNTs, acetone solvent and combined dispersion methods. Compos Struct 2014; 110:39–50.

Zeng J, Saltysiak B, Johnson WS, Schiraldi D, Kumar S. Processing and properties of poly(methyl methacrylate)/carbon nano fiber composites. Compos Part B Eng 2004; 35:173–8.

Zeynalov EB, Friedrich JF. Antioxidative activity of carbon nanotube and nanofiber. Open Mater Sci J 2010; 2:28–34.

Zhang J, Shen L, Shen L, Li A. Gait analysis of powered bionic lower prosthesis. Proc the 2010 IEEE Int Conf on Robotics and Biomimetics December 14-18, 2010, Tianjin, China 2010; 2010:25–9.

Zhang M, Smith ART, Tanner A, Robert VC. Clinical investigation of the pressure and shear stress on the transtibial stump with a prosthesis. Med Eng Phys 1998; 20:188–98.

Zhang S, Minus ML, Zhu L, Wong CP, Kumar S. Polymer transcrystallinity induced by carbon nanotubes. Polymer 2008; 49:1356-64.

Zhang X, Liu Y, Zhang F, Ren J, Sun YL, Yang Q, Huang H. On design and implementation of neural-machine interface for artificial legs. IEEE Trans Ind Informatics 2012; 8:418–29.

Zhao FM, Takeda N. Effect of interfacial adhesion and statistical fiber strength on tensile strength of unidirectional glass fiber / epoxy composites. Part I: experiment results. Compos Part A Appl Sci Manuf 2000; 31:1203–14.

Zhao H, Li RKY. A study on the photo-degradation of zinc oxide (ZnO) filled polypropylene nanocomposites. Polymer 2006; 47:3207–17.Ziegler-Graham K, MacKenzie EJ, Ephraim PL, Travison TG, Brookmeyer R.. Estimating the prevalence of limb loss in the United States: 2005 to 2050. Arch Phy Medi and Rehab 2008; 89(3):422-9.

Outcome of the thesis work

Patents

1. S. Arun, S. Kanagaraj. Injection mouldable polymeric composite based passive polycentric knee joint. US patent Application No. 14/840,052 and Indian Patent Application No. 2761/DEL/2014, dated: 25/09/2014.
2. S. Arun, Mrutyunjay Maharana, S. Kanagaraj, A walking simulator to test walking condition of prosthetic knee joint before fitting to the patient. Indian Patent Application No. 630/DEL/2015, dated: 07/03/2015.

International journals (Published)

1. S. Arun, S. Kanagaraj. Performance enhancement of epoxy based sandwich composites using multiwalled carbon nanotubes for the application of sockets in trans-femoral amputees. Journal of the Mechanical Behavior of Biomedical Materials, 59, 1-10, 2016
2. S. Arun, S. Kanagaraj, Mechanical characterization and validation of Poly (methyl methacrylate)/Multi walled carbon nanotube composite for the polycentric knee joint. Journal of Mechanical Behavior of Biomedical Materials 50, 33-42, 2015.
3. S. Arun, Mrutyunjay Maharana, S. Kanagaraj. Optimizing the processing conditions for the reinforcement of epoxy resin by multi walled carbon nanotubes. Journal of Nanotechnology, Article number 634726, 2013.
4. S. Arun, S. Kanagaraj, Effect of reinforcement and processing methods in PP/MWCNTs nanocomposites, Advanced Materials Research 747, 575-578, 2013.

International journals (under review)

1. S. Arun, S. Kanagaraj, Rehabilitation evaluation of the newly developed polymeric based passive polycentric knee joint.
2. S. Arun, S. Kanagaraj, Improving the longevity of PMMA by restricting the UV rays induced mechanical degradation by multi walled carbon nanotubes.
3. S. Arun, S. Kanagaraj. Design, development and analysis of user friendly and inexpensive passive polycentric knee joint for Trans-femoral amputee.

Book Chapter

1. S Arun, S Kanagaraj. Polymer-Nanotube nanocomposites for trans-femoral socket in Polymer Nanotube and Nanocomposites Edition 2, Edited by Vikas Mittal, Wiley, 187-210, 2014.

Conferences Attended

The following are the conferences attended during the research work

1. Orthotics and Prosthesis Association of India (OPAI), Chennai, Feb 14-16, 2014.
2. ISHMT-ASME Heat and Mass transfer conference, Kharagpur, Dec 28-31, 2013.
3. Multi-Functional Materials and Structures, Bangkok, Thailand, July 14-17, 2013.
4. Advancements in polymeric materials, CIPET, Lucknow, March 1-3, 2013.
5. World congress on International society for prosthetics and orthotics, HICC, Hyderabad, February 4-7, 2013.
6. Twenty first international symposium on processing and fabrication of advanced materials, IIT Guwahati, Guwahati, December 10-13, 2012.

Awards and Honors

- First Place, model exhibition in research conclave- 2016
- Silver award for best innovator - 2015
- The project was one of the top 7 finalists in Samsung Innovation Awards-2015
- First Place, Best Innovation Awards - 2015.
- Gandhian Young Technological Innovation Awards - 2015 by National Innovation Foundation, India, Appreciated under MLM (More from Less for Many) for the development of passive polycentric knee joint
- Project was appended in the Directory of Aids and Assistive Devices, Ministry of Empowerment of Persons with Disabilities, Govt. of India.

ANNEXURE I

CONSENT FORM

Patient Details (Name/Age/Sex/Wt/Ht):

Details of Amputation (Right/Left/AK/BK):

Cause of Amputation:

Cost of Prosthesis (Include last used details):

Cost of Fixation:

	Tick
1) I confirm that I have read and understand the information sheet **SF-36** and **Q-TFA** for the above study. I have had the opportunity to consider the information, ask questions and have had these answered satisfactorily.	☐
2) I understand that my participation is voluntary and that I am free to withdraw at any time without giving any reason, without my medical care or legal rights being affected.	☐
3) I understand that relevant sections of my medical notes and data collected during the study, may be looked at by individuals, regulatory authorities or the person taking part in this research. I give permission for these individuals to have access to my records.	☐
4) I agree to publish all the details and the study related to me in any report or in journal format.	☐
5) I agree to take part in the above study.	☐

Name of Patient: Date: Signature

Name of Person taking consent: Date: Signature

SF-36 QUESTIONNAIRE

(1992 -- Medical Outcomes Trust)

Patient Name: _____ **Date:** _____

1. In general, would you say your health is: (circle one)

   Excellent Very good Good Fair Poor

2. Compared to one year ago, how would you rate your health in general now? (circle one)

   Much better now than one year ago.

   Somewhat better now than one year ago.

   About the same as one year ago.

   Somewhat worse than one year ago.

   Much worse than one year ago.

3. The following items are about activities you might do during a typical day. Does your health now limit you in these activities? If so, how much? (Mark each answer with an **X**)

ACTIVITIES	**Yes, Limited A Lot**	**Yes, Limited A Little**	**No, Not Limited At All**
a. **Vigorous activities,** such as running, lifting heavy objects, participating in strenuous sports			
b. **Moderate activities,** such as moving a table, pushing a vacuum cleaner, bowling, or playing golf			
c. Lifting or carrying groceries			
d. Climbing **several** flights of stairs			
e. Climbing **one** flight of stairs			
f. Bending, kneeling or stooping			
g. Walking **more than a mile**			
h. Walking **several blocks**			
i. Walking **one block**			
j. Bathing or dressing yourself			

4. During the past 4 weeks, have you had any of the following problems with your work or other regular daily activities as a result of your physical health? (Mark each answer with an **X**)

	YES	NO
a. Cut down on the **amount of time** you spent on work or other activites		
b. **Accomplished less** than you would like		
c. Were limited in the **kind** of work or other activities		
d. Had **difficulty** performing the work or other activities (for example, it took extra effort)		

5. During the past 4 weeks, have you had any of the following problems with your work or other regular daily activities as a result of any emotional problems (such as feeling depressed or anxious)? (Mark each answer with an **X**)

	YES	NO
a. Cut down the **amount of time** you spent on work or other activities		
b. **Accomplished less** than you would like		
c. Didn't do work or other activities as **carefully** as usual		

6. During the past 4 weeks, to what extent has your physical health or emotional problems interfered with your normal social activities with family, friends, neighbors or groups? (circle one)

Not at all Slightly Moderately Quite a bit Extremely

7. How much bodily pain have you had during the past 4 weeks? (circle one)

None Very mild Mild Moderate Severe Very severe

8. During the past 4 weeks, how much did pain interfere with your normal work (including both work outside the home and housework)?

Not at all A little bit Moderately Quite a bit Extremely

9. These questions are about how you feel and how things have been with you during the past 4 weeks. For each question, please give the one answer that comes closest to the way you have been feeling. How much of the time during the past 4 weeks – (Mark each answer with an **X**)

	All of the Time	**Most of the Time**	**A Good Bit of the Time**	**Some of the Time**	**A Little of the Time**	**None of the Time**
a. Did you feel full of pep?						
b. Have you been a very nervous person?						
c. Have you felt so down in the dumps that nothing could cheer you up?						
d. Have you felt calm and peaceful?						
e. Did you have a lot of energy?						
f. Have you felt downhearted and blue?						
g. Did you feel worn out?						
h. Have you been a happy person?						
i. Did you feel tired?						

10. During the past 4 weeks, how much of the time has your physical health or emotional problems interfered with your social activities (like visiting with friends, relatives, etc.)? (circle one)

All of the time Most of the time Some of the time A little of the time None of the time

11. How TRUE or FALSE is each of the following statements for you?

	Definitely True	**Mostly True**	**Don't Know**	**Mostly False**	**Definitely False**
a. I seem to get sick a little easier than other people					
b. I am as healthy as anybody I know					
c. I expect my health to get worse					
d. My health is excellent					

QUESTIONNAIRE FOR PERSONS WITH A TRANSFEMORAL AMPUTATION (Q-TFA)

Welcome!
You should answer the questions by entering a cross or a figure in the appropriate box. If you require additional information, please contact your physiotherapist.

EMPLOYMENT SITUATION

Level of employment (please give figures):

Work_____ % Education _____ % Unemployment_____%

Sick leave_____ % Disability pension _____ % Retired _____%

Type of work:_____

If you are in employment, approximately what proportion of your working day is made up of work that is...

	0%	25 %	50 %	75 %	100 %
Sitting	☐	☐	☐	☐	☐
Moving, slight	☐	☐	☐	☐	☐
Moving, considerable	☐	☐	☐	☐	☐

LEVEL OF EDUCATION

☐ Primary School
☐ Secondary School
☐ Exam from University

CIVIL STATUS

☐ Single
☐ Married/Cohabiting

If you have any other points of view you would like to share with us after completing the questionnaire, please write them in your own words on the reverse of this page.

SECTION **A**

YOUR CURRENT PROSTHESIS USAGE

1. **How many days per week, on average, do you wear the prosthesis?**
Number of days:
0 1 2 3 4 5 6 7
☐☐☐☐☐☐☐☐

2. **How many hours per day, on average, do you wear the prosthesis?**

☐ 0 – 3 hours
☐ 4 – 6 hours
☐ 7 – 9 hours
☐ 10 – 12 hours
☐ 13 – 15 hours
☐ more than 15 hours

3. **Approximately what proportion of the time you are at home, on average, do you wear the prosthesis?**
0% **25 %** **50 %** **75 %** **100 %**
☐ ☐ ☐ ☐ ☐

4. **Approximately what proportion of the time you are outdoors, on average, do you wear the prosthesis?**

0% **25 %** **50 %** **75 %** **100 %**
☐ ☐ ☐ ☐ ☐

5. **Approximately what proportion of the time you are at work or place of study, on average, do you wear the prosthesis?**

0% **25 %** **50 %** **75 %** **100 %**
☐ ☐ ☐ ☐ ☐

If you do not work or study, enter a cross here: ☐

6. **Do you normally prefer to wear the prosthesis or not during the following activities?**

	Wear	Do not wear
a) Cooking or similar	☐	☐
b) Cleaning, gardening or similar	☐	☐
c) Driving or travelling by car	☐	☐
d) Socialising in your own home	☐	☐
e) Socialising in public places/other people's homes	☐	☐

7. **What is/are your primary reason/s for choosing not to wear the prosthesis?**
(Feel free to enter more than one cross)

- ☐ It hurts to wear the prosthesis.
- ☐ It is strenuous wearing the prosthesis.
- ☐ I move about too slowly when I am wearing the prosthesis.
- ☐ My hands are not free when I am wearing the prosthesis.
- ☐ I feel that my life is simpler without the prosthesis.
- ☐ I do not like the prosthesis.
- ☐ I have experienced other difficulties that make it hard to wear the prosthesis.
- ☐ Other reason (please specify): _____

If you always choose to wear the prosthesis, cross here: ☐

8. **Over the past three months, have you been forced to refrain entirely from wearing the prosthesis for a whole day or more?**

Yes ☐ Please answer questions 9-11 as well
No ☐ Please proceed to section B, question 12

9. **Please specify the total number of days off and working days (or school days) on which you have been forced to refrain from using the prosthesis over the past three months?**

	1	2-3	4-6	7-15	>15 days
Days off	☐	☐	☐	☐	☐
Working days	☐	☐	☐	☐	☐

10. **Did this entail having to stay home from work or school?**

☐ Yes ☐ No

11. **Which problem/s forced you to refrain entirely from wearing the prosthesis?** (Feel free to enter more than one cross)

- Phantom pain ☐
- The prosthesis did not fit well ☐
- Skin problems ☐
- Pain in the residual limb (stump) ☐
- Fault in the prosthesis/broken prosthesis components ☐
- Other reason (please specify): _____ ☐

SECTION **B**

YOUR CURRENT LEVEL OF FUNCTION WITH THE PROSTHESIS

12. Which walking aid do you normally use when walking in your home wearing the prosthesis?

☐ Walking frame or similar ☐ 2 crutches or 2 sticks ☐ 1 crutch or 1 stick ☐ Nothing ☐ Other

If other, please specify:_____

13. Which walking aid do you normally use when walking outdoors wearing the prosthesis?

☐ Walking frame or similar ☐ 2 crutches or 2 sticks ☐ 1 crutch or 1 stick ☐ Nothing ☐ Other

If other, please specify:_____

14. Approximately what proportion of all your movements from one place to another, when you are wearing the prosthesis, do you make sitting in a wheelchair?

0% ☐ **25%** ☐ **50%** ☐ **75%** ☐ **100%** ☐

15. Can you perform the following movements wearing the prosthesis and with the support of your normal walking aid? Please feel free to try the movement if you are unsure of your answer.

	Yes	**No**	Not tried
a) Walking up and down stairs without a handrail:	☐	☐	☐
b) Walking up a hill:	☐	☐	☐
c) Walking down a hill:	☐	☐	☐
d) Walking over uneven terrain, e.g. on forest trails or fields:	☐	☐	☐
e) Walking quickly over a distance of 50 metres:	☐	☐	☐
f) Walking while carrying a bag of food shopping or light suitcase:	☐	☐	☐

16. **Can you do the following when wearing the prosthesis?** Please feel free to try if you are unsure of your answer.

	Yes	No	Not tried
a) Standing up for 10-15 minutes without support and without discomfort:	☐	☐	☐
b) Walking across the room carrying a tray with both hands:	☐	☐	☐
c) Sitting comfortably in a low armchair or in the back seat of a car:	☐	☐	☐
d) From a seated position, bending down and tying your shoelaces:	☐	☐	☐
e) Easily sitting down on the floor and standing up again:	☐	☐	☐
f) Cycling:	☐	☐	☐

17. **Can you use the following means of transport when wearing the prosthesis?**

	Yes	**No**	Not tried
a) Bus / Tram	☐	☐	☐
b) Aeroplane	☐	☐	☐
c) Train / Underground	☐	☐	☐
d) Car / Taxi	☐	☐	☐

18a. **Over the past three months, how often have you used the prosthesis to continuously walk outdoors any of the distances shown below? (**Enter one cross for each distance)

	Daily	Several times/week	Once/week	Less than once/week	Never
10 m:	☐	☐	☐	☐	☐
50 m:	☐	☐	☐	☐	☐
200 m:	☐	☐	☐	☐	☐
500 m:	☐	☐	☐	☐	☐
2 km:	☐	☐	☐	☐	☐
5 km or more:	☐	☐	☐	☐	☐

18b. Over the past three months, have you ever fallen while wearing the prosthesis?

☐ Yes ☐ No

18c. Please specify the total number of falls caused by reasons related to the prosthesis and those caused by other reasons not related to the prosthesis.

a) Number of falls caused by reasons related to the prosthesis during the last three months:

_____

b) Number of falls caused by other reasons during the last three months:

_____

SECTION **C**

YOUR CURRENT PROBLEMS

19. Over the past four weeks, have you been troubled by any of the following?
Please specify how much trouble you have had and how this trouble has affected your quality of life. Enter a figure between 0 - 4 in the box for trouble and a figure between 0 - 4 in the box for quality of life.

Trouble
0 = No trouble
1 = Slight trouble
2 = Moderate trouble
3 = Considerable trouble
4 = Great deal of trouble

Quality of life
0 = No reduction in quality of life
1 = Slight reduction in quality of life
2 = Moderate reduction in quality of life
3 = Considerable reduction in quality of life
4 = Extreme reduction in quality of life

Trouble regardless of prosthesis usage

	Trouble	**Quality of life**
1a Have you experienced phantom pains?	☐	
1b How has this affected your quality of life?		☐
2a Have you had pain in your residual limb (stump) when not wearing the prosthesis?	☐	
2b How has this affected your quality of life?		☐
3a Have you experienced back pain?	☐	
3b How has this affected your quality of life?		☐
4a Have you had pain in your shoulders?	☐	
4b How has this affected your quality of life?		☐
5a Have you experienced pain in your other leg?	☐	
5b How has this affected your quality of life?		☐
6a Have you been troubled by the appearance of your residual limb (stump)?	☐	
6b How has this affected your quality of life?		☐
7a Have you been troubled by being with other people without your prosthesis?	☐	
7b How has this affected your quality of life?		☐

	Trouble	Quality of life
8a Have you had difficulty using public transport?	☐	
8b How has this affected your quality of life?		☐
9a Have you had difficulty visiting public places such as the cinema, theatre, museum or sports ground?	☐	
9b How has this affected your quality of life?		☐
10a Have you been troubled by not being able to have your hands free when using a walking aid?	☐	
10b How has this affected your quality of life?		☐

Trouble in connection with prosthesis usage

	Trouble	Quality of life
11a Have you had pain in your residual limb (stump) when standing and walking?	☐	
11b How has this affected your quality of life?		☐
12a Have you had difficulty putting on (donning) or removing (doffing) the prosthesis?	☐	
12b How has this affected your quality of life?		☐
13a Have you been unable to rely on the prosthesis being securely fastened?	☐	
13b How has this affected your quality of life?		☐
14a Have you been troubled by noises from the prosthesis' socket?	☐	
14b How has this affected your quality of life?		☐
15a Has the prosthesis made it uncomfortable to sit down?	☐	
15b How has this affected your quality of life?		☐
16a Has the prosthesis made it troublesome to sit on the toilet?	☐	
16b How has this affected your quality of life?		☐
17a Has the prosthesis given rise to sores, chafing or skin irritation?	☐	
17b How has this affected your quality of life?		☐

Trouble
0 = No trouble
1 = Slight trouble
2 = Moderate trouble
3 = Considerable trouble
4 = Great deal of trouble

Quality of life
0 = No reduction in quality of life
1 = Slight reduction in quality of life
2 = Moderate reduction in quality of life
3 = Considerable reduction in quality of life
4 = Extreme reduction in quality of life

	Trouble	Quality of life
18a Have you had trouble maintaining good hygiene on your residual limb (stump)?	☐	
18b How has this affected your quality of life?		☐
19a Has the prosthesis caused increased wear on your clothes?	☐	
19b How has this affected your quality of life?		☐
20a Have you had difficulty directing and keeping control of the prosthesis?	☐	
20b How has this affected your quality of life?		☐
21a Have you been unable to walk quickly?	☐	
21b How has this affected your quality of life?		☐
22a Have you been unable to walk in woods or fields?	☐	
22b How has this affected your quality of life?		☐
23a Have you been troubled by the way you walk (e.g. limping / waddling)?	☐	
23b How has this affected your quality of life?		☐
24a Have you had difficulty feeling what type of surface you are standing/walking on?	☐	
24b How has this affected your quality of life?		☐
25a Does your residual limb (stump) become tired when walking with the prosthesis?	☐	
25b How has this affected your quality of life?		☐
26a Have you been troubled by the prosthesis feeling heavy?	☐	
26b How has this affected your quality of life?		☐
27a Have you been troubled by the appearance of the prosthesis (colour, shape, surface)?	☐	
27b How has this affected your quality of life?		☐
28a Have you been forced to refrain entirely from using the prosthesis?	☐	
28b How has this affected your quality of life?		☐

Trouble
0 = No trouble
1 = Slight trouble
2 = Moderate trouble
3 = Considerable trouble
4 = Great deal of trouble

Quality of life
0 = No reduction in quality of life
1 = Slight reduction in quality of life
2 = Moderate reduction in quality of life
3 = Considerable reduction in quality of life
4 = Extreme reduction in quality of life